



**Fe-based heterogeneous catalysts for the catalytic wet peroxide oxidation of
phenolic compounds for wastewater treatment**

Thesis submitted to The University of Sheffield for the degree of Doctor of Philosophy in
Science

Ghadeer Albalawi

The University of Sheffield

Department of Chemistry

30/10/2023

Thesis Declaration

I, Ghadeer Albalawi, hereby declare that the work presented in this thesis, titled "Fe-based heterogeneous catalysts for the catalytic wet peroxide oxidation of phenolic compounds for wastewater treatment," is entirely my own work, except where otherwise indicated. This research has been carried out under the supervision of Marco Conte. I affirm that:

All sources of information used in this thesis have been properly cited and referenced, and any assistance received in its preparation has been acknowledged.

This thesis has not been previously submitted for any degree or qualification at any university or educational institution.

Wherever I have reproduced the work of others, I have provided proper attribution and citations, and I have not plagiarised any material in this thesis.

I am aware of the academic and ethical standards required by my institution, and I have adhered to these standards throughout the research and writing process.

I also grant University of Sheffield the non-exclusive right to archive, reproduce, and distribute my thesis for academic and research purposes, subject to the policies and regulations of the university.

Ghadeer Albalawi

Foreword

من أدرك الخليج العربي في خمسينات القرن العشرين لا بد وأنه عاش أزمة شح المياه آنذاك، وبالتالي ربما طرقت مسامعه قصيدة الشاعر الكويتي فهد بورسلي مطلعها «ليت هالنفط الغزير ينقلب ماي غدير»، وهي قصيدة معبرة كانت تعكس واقع الحال في بلد تسكن فوق محيط من النفط لكنه يفتقر إلى المياه العذبة بالكميات المناسبة. قائل هذه القصيدة التي نصها هو الآتي:

ليت هالنفط الغزير .. ينقلب ماي غدير
مانبي النفط ومعاشه .. صرنا للعالم طماشة
أهلها ماتوا عطاشة .. ضاع بالطوشة الفقير
من الفجر شایل قربه .. بس يبي لو درب يصب به
نفطها غرق أوروبا .. والظما بها يستدير

فهد راشد ناصر بورسلي

In the 1950s, anyone who experienced the Arabian Gulf must have lived through a water scarcity crisis at that time. Therefore, they might have come across a poem by the Kuwaiti poet Fahad Boursli that begins with the line, "If only this abundant oil could turn into Ghadeer* (the meaning of the name Ghadeer in the Arabic language fresh water). This poem is expressive and reflects the reality of a country situated above an ocean of oil but lacking an adequate supply of fresh water.

The lines from the poem by the Kuwaiti poet Fahad Boursli can be translated as follows:

"If only this abundant oil could turn into Ghadeer (fresh water),

We don't want oil and its wealth; we've become a source of trouble for the world.

Its people died of thirst, lost in the confusion of poverty.

Since the morning, they've been carrying its burden, but it needs a path to be poured into.

Its oil flooded Europe, and the thirst within it continues to swirl."

In these verses, the poet is lamenting the paradox of having vast reserves of oil but facing a severe shortage of fresh water in the region. He expresses the desire for the valuable oil resources to be transformed into the essential resource of water to alleviate the suffering of the people. The poem highlights the socioeconomic and environmental challenges faced by a region rich in oil but lacking in essential resources like water.

Acknowledgments

I would like to express my sincere gratitude to all those who have contributed to the completion of this thesis, titled "Fe-based heterogeneous catalysts for the catalytic wet peroxide oxidation of phenolic compounds for wastewater treatment."

First and foremost, I am deeply indebted to my supervisor, Dr. Marco Conte, for his unwavering support, guidance, and invaluable insights throughout the entire research process. His expertise and mentorship have been instrumental in shaping this work and my academic journey.

I extend my heartfelt appreciation to the faculty members of the Chemistry department at university of Sheffield, for their commitment to fostering an environment of academic excellence and for their constructive feedback during the various stages of this research.

I am thankful to my colleagues and friends who have provided encouragement, shared their knowledge, and offered their assistance when needed. Your camaraderie has made this academic pursuit an enriching experience. Thanks also go to: Dr. Craig Robertson (University of Sheffield) for XRD analysis, Dr. David Morgan (University of Cardiff) for XPS analysis, Ms. Abby Shipley (CBE, University of Sheffield) for textural properties analysis of materials, Heather Grievson and Anna Foster (university of Sheffield) for ICP analysis, Dr. Marco Conte (University of Sheffield) for data analysis for XRD, XPS and textural properties.

I would like to express my sincere gratitude to my sponsor, the University of Tabuk, for their generous support and invaluable assistance. I would also like to thank my family parent and husband for their unwavering support and understanding throughout this journey. Your encouragement and belief in me have been my driving force.

Finally, I dedicate this work, for his soul, my brother Essam.

This thesis represents the culmination of years of hard work, dedication, and the collective efforts of many. While space limitations prevent me from mentioning everyone who has influenced this work, please know that your support and contributions are deeply appreciated.

Thank you all for being a part of this academic endeavour.

Abstract

Water shortages worldwide are exacerbated by wastewater discharge into the environment without adequate treatment, thus requiring developments in water treatment technologies, an area of research that has gained increasing attention in recent years and it is one of the sustainable energy development goals (SDG6) to be achieved by 2030. One of the most promising approaches to tackle and remedy this fundamental environmental issue, we will apply catalysis and the development of new materials to the abatement of toxic pollutants. In this work, we will exploit an emerging catalytic technology known as catalytic wet peroxide oxidation (CWPO) based on Fenton and Fenton-like reactions, to degrade aromatic pollutants in water under mild conditions by targeting phenolic compounds as the representative of pollutants. The scope to develop new iron-activated carbons and zeolites capable of degrading phenol-like compounds to CO₂ and water is to have materials that are applicable for large-scale applications. Also, to be durable as expected for the treatment of large volumes of water, by having materials with a diminished amount of metal leaching in solution and thus to increase the catalyst reusability and diminish the environmental impact.

Fe-supported activated carbon catalysts were prepared by using a wetness impregnation protocol with a Fe loading fixed at 12wt%. In all our catalytic tests the amount of phenol to consume was set at 1 g·L⁻¹ and reaction times for 1 to 4 h. A peculiarity of this study was the pre-treatment of the carbon matrices with HCl and HNO₃ to induce structural changes on Fe centres and in turn on the catalytic activity of these materials. A comparative analysis was done to study the effect of these pre-acid treatments (using HCl and HNO₃). It was observed that Fe/AC catalysts can show high phenol conversion (100%), but the high Fe leaching (up to 50%) affects the stability of the catalysts. Elemental analysis, XPS and XRD methods were employed to provide ground for structure/activity correlations. We found that the active species was Fe₂O₃, and most active catalysts were those with a Fe₂O₃ diameter less than 40 nm whereas those least affected by leaching were those with a diameter greater than 120 nm. Fe leaching though could be reduced to about 12% by the activated carbons doping with S and N. Catalytic activity results show that, the Fe-S-N/AC, prepared by AC pre-treated with HCl and HNO₃, catalysts are the most active and stable catalysts when they were applied for phenolic compound oxidation.

In view of these results, we then extended our investigation in the use of Fe-doped zeolites. Fe-ZSM-5 was prepared by wetness impregnation method and shows a high phenol conversion

(100%), 12% residual intermediates%, and H₂O₂ consumption (100%) under the reaction conditions. However, the Fe-ZSM-5 catalyst suffers poor stability due to high metal leaching losses (> 50%). Fe-ZSM-5 was also synthesized by an innovative wetness impregnation under vacuum method. However, no difference in the catalytic activity between the two catalysts for phenol oxidation by the CWPO reaction at an array of reaction temperatures from 40 to 80 °C.

Based on the extreme catalytic activity of Fe-S-N/AC catalysts, we have applied the same doping protocols for the preparation of zeolites, a novelty in this area. The Fe-S-N-Zeolite-Y catalyst was identified as the most efficient catalyst for this reaction in terms of complete phenol oxidation and mineralization (100% and 0% for phenol conversion and residual intermediates, respectively). The Si:Al molar ratio though was able to influence the final Fe-S-N-Zeolite catalyst performance. However, the materials despite being very active, were affected by high Fe-leaching (ca 50%) Fe leaching at a high level affects the stability of these catalysts. The activity of species besides Fe, like Ag, was also considered and Ag as well as Ag/Fe-doped were synthesised and investigated. A strong synergistic effect from these two metals were identified, and this was irrespective of Si:Al ratios or Zeolite types.

Then this study concluded by expanding the application of the selected heterogeneous catalysts prepared in this project to oxidise phenolic compounds further than phenol. The catalysts: Fe-S-N-ZSM-5, Fe-Ag-ZSM-5, and Fe-S-N/AC derived from pre-acid-treatment of AC by HCl-HNO₃ were identified as the most active when used for the abatement of substrates like: 4-chlorophenol (4CP), 4-bromophenol (4BrP), 3-methoxyphenol (3MOP), 4-cresol (4MP) and 2,4 dimethylphenol (DMP), thus showing the applicability of our methods and materials to an array of compounds which abatement is at the centre of environment application for water purification.

Table of Contents

<i>Thesis Declaration</i>	<i>I</i>
<i>Foreword</i>	<i>II</i>
<i>Acknowledgments</i>	<i>III</i>
<i>Abstract</i>	<i>IV</i>
<i>Abbreviations</i>	<i>4</i>
Chapter 1: Introduction	6
1.1 Overview: water pollution and sustainability	6
1.2 Water pollution by industrial waste	7
1.3 Source of phenol	7
1.3.1 Natural sources.....	8
1.3.2 Sources from human activity.....	9
1.4 The reactivity of phenolic compounds in aquatic environments	11
1.4.1 Microorganism interaction	11
1.4.2 Inorganic compound interactions	11
1.5 The consequences of the toxicity of phenolic compounds on human health	12
1.6 Current methods for removing phenolic compounds from water	12
1.6.1 Physical methods.....	13
1.6.2 Biological methods.....	14
1.6.3 Chemical oxidation processes	15
1.7 The theory of advanced oxidation processes (AOPs)	17
1.7.1 Oxidation principles of AOPs	17
1.8 The comparison of WHPCO with WACO systems	19
1.8.1 Wet air catalytic oxidation processes (WACO)	19
1.8.2 Wet hydrogen peroxide catalytic oxidation processes (WHPCO).....	20
1.9 Perspectives regarding solid catalysts in the WHPO	21
1.9.1 Fenton reagent.....	22
1.9.2 Fenton reaction types	27
1.10 Solid catalysts for Fenton reaction	33
1.10.1 Zeolite catalysts for the CWPO reaction.....	34
1.10.2 Activated carbon for the CWPO reaction.....	39
1.10.3 Pillared clays	42
1.10.4 Metal oxides	43
1.11 Aim of the project	44
1.12 References:	47
Chapter 2: Experimental methods and techniques	58
2.1 Chemical reagents	58

2.1.2 Reagents for catalytic tests	58
2.1.3 Reagents for characterisation of reaction mixtures	59
2.2 Experimental apparatus	59
2.2.1 Equipment for catalyst synthesis	59
2.2.2 Equipment for the catalytic test.....	59
2.2.3 Equipment for the analysis of reaction mixtures	60
2.3 Synthesis of catalysts.....	60
2.3.1 Supported metal catalysts preparation.....	60
2.3.2 Supported metal catalysts- actual preparation procedures.....	63
2.4 Analytical methods for the characterisation of catalysts and reaction mixtures	67
2.4.1 Characterization of catalysts (principle of techniques)	67
2.4.2 Principles of the techniques used for the characterisation of reaction mixtures	73
2.5 Catalytic tests.....	77
2.5.1 Phenolic compounds oxidation by wet hydrogen peroxide catalytic oxidation reaction (WHPCO)..	77
2.5.2 Homogeneous phase control tests	79
2.5.3 Tests of catalyst reusability	80
2.6 Characterization of reaction mixtures by chemical analysis	80
2.6.1 Qualitative determination of phenolic compounds and their intermediates	81
2.6.2 The determination of H ₂ O ₂	82
2.6.3 Determination of metal leaching	85
2.6.4 AC acidity measurements.....	86
2.7 Statistical analysis of data.....	87
2.7.1 Significance testing	87
2.7.2 Statistical methods for normal distributions.....	89
2.8 References:.....	94
<i>Chapter 3: Catalytic wet peroxide oxidation of phenol using catalyst-supported and acid-pre-treated Fe-activated carbon catalysts.....</i>	<i>97</i>
3.1 Fe doping activated carbon catalysts Fe/AC.....	97
3.1.1 Introduction.....	97
3.1.2 Results and discussion.....	106
3.2 S, N and Fe tri-doped activated carbons.....	131
3.2.1 Introduction.....	131
3.2.2 Results and discussion.....	133
3.3 Characterization	161
3.3.1 X-ray diffraction (XRD).....	162
3.3.2 X-ray photoelectron spectroscopy (XPS).....	171
3.3.3 Measurement of porosity.....	173
3.4 Diffusion control tests	174
3.4.1 External diffusion tests:.....	175
B. Using different M:S.....	178
3.5 Conclusion	180
3.6 References.....	184

Chapter 4: Iron-doped zeolites ZSM-5 and Y for phenol oxidation via CWPO	190
4.1 Introduction	190
4.2 Results and Discussion	194
4.2.1 The effects of preparing Fe-ZSM-5 with different iron precursors and ZSM-5 counterions, and study the effect of increasing Fe loading 5wt.% Fe/ZSM-5 and 10 wt%Fe-ZSM-5 on CWPO of phenol	194
4.2.2 Study the effect of different preparation methods by synthesis of Fe-ZSM-5 under vacuum method	201
4.2.3 Adding S and N to Fe-zeolite catalysts	204
4.2.4 Fe-Ag-Zeolites	211
4.3 Characterisation of the catalysts.....	220
4.3.1 X-ray diffraction (XRD).....	220
4.3.2 Porosimetry	224
4.4 Diffusion test	225
4.4.1 External diffusion tests	225
4.5 Conclusion	228
4.6 References	230
Chapter 5: Oxidation of phenolic compounds and homologues	236
5.1 Introduction	236
5.2 Characterization of phenolic compounds	243
5.3 Oxidation of phenolic compounds by selected AC and zeolite based catalysts	244
5.3.1 Chlorophenol (4CP) decomposition	244
5.3.2 Bromophenol (4BrP) decomposition.....	250
5.3.3 Decomposition of 3-methoxy phenol (3MOP).....	254
5.3.4 Cresol (4MP) decomposition	258
5.3.5 Decomposition of 2,4 dimethylphenol (DMP).....	262
5.4 Conclusion	266
5.5 References	268
Chapter 6: Conclusions and future work	274
6.1.1 Supported Fe activated carbons and zeolites for CWPO.....	275
6.1.2 AC and N/S doping and effect of pre-acid treatments.....	275
6.1.3 Fe and Ag- doped zeolites for CWPO.....	278
6.1.4 Extension of catalytic properties of our materials to phenol homologues.....	280
6.2 Future research directions:.....	282
6.3 References:.....	285

Abbreviations

CWPO: Catalytic Wet Peroxide Oxidation

AC: Activated Carbon

AC1: NORIT 1240 GAC

AC2: NORIT SA2

AC3: DARCO G60

XPS: X-ray Photoelectron Spectroscopy

XRD: X-ray Diffraction

HPLC: High-Performance Liquid Chromatography

CMB: Carbon Mass Balance

4CP: 4-Chlorophenol

4BrP: 4-Bromophenol

4MP: Cresol

3MOP: 3-Methoxyphenol

DMP: 2,4 Dimethylphenol

M:S: Metal to Substrate ratio

SDGs: Sustainable Development Goals

EPA: Environmental Protection Agency

pKa: $-\log_{10}$ of acid dissociation constant

AOPs: Advanced Oxidation Processes

UV-vis: Ultraviolet-visible spectroscopy

WHPCO: Wet Hydrogen Peroxide Catalytic Oxidation

WACO: Wet Air Catalytic Oxidation

WAO: Wet Air Oxidation process

COD: Chemical Oxygen Demand

TOC: Total Organic Carbon

IUPAC: International Union of Pure and Applied Chemistry

CIF: Crystallographic Information Files

IZA-SC: provided from the Data-base of Zeolite Structures

BET: Brunauer-Emmett-Teller

BJH: Barrett-Joyner-Halenda

C18: Chain length (octadecyl) of alkyl bonded phase

H-ZSM-5: Zeolite Socony Mobil-5, Hydrogen form

ICP-OES: Inductively Coupled Plasma - Optical Emission Spectroscopy

MFI: Mordenite Framework Inverted (zeolites)

NH₄-ZSM-5: Zeolite Socony Mobil-5, ammonia form

ZSM-5: Zeolite Socony Mobil-5

WI: Wet Impregnation

VI: wet Impregnation under Vacuum

ROS: Reactive Oxygen Species

rpm: revolutions per minute

ppm: parts per million

ppb: parts per billion

IZA: International Zeolite Association

Chapter 1: Introduction

1.1 Overview: water pollution and sustainability

In an era defined by globalization and shared responsibilities, the Sustainable Development Goals (SDGs) emerge as a beacon of collective aspiration and commitment. These goals, set forth by the United Nations, constitute a resounding call to action that crosses borders and ideologies. They encapsulate the profound urgency to transform our world into a realm where poverty is eradicated, the planet is safeguarded, and the prospects of every individual, regardless of location, are elevated. In a historic milestone of global collaboration, the year 2015 witnessed the unanimous adoption of the 17 Sustainable Development Goals (SDGs) by every member state of the United Nations. This pivotal moment marked the inception of a visionary blueprint known as the 2030 Agenda for Sustainable Development a resolute commitment to guide humanity's journey toward a more equitable, resilient, and thriving future. Among these goals, Goal number 6: clean water and sanitation (Figure 1.1) is at the centre of this thesis work. Having access to clean water, and sanitation is essential to human health and wellbeing. These basic services will not be available to billions of people in 2030 only if the current rate of progress is quadrupled. A growing requirement for water has arisen due to rapid population growth, urbanization and increasing water demands in agriculture, industry, and the energy sector. By achieving these goals, we will save about 1 million lives annually, who die due to diseases caused by contaminated water and poor sanitation.¹⁻⁴ Therefore, the objective of this project is the development of novel catalysts able to carry out highly efficient wastewater purification in a durable manner.



Figure 1.1: The 17 Goals of the Sustainable Development Agenda. Goal number 6, clean water and sanitation is at the centre of this thesis work.⁴

1.2 Water pollution by industrial waste

One of the main solutions to minimize waste would be to improve the quality of water through pollution reduction in itself, like enhancing the disposal waste into appropriate treatment facilities, minimizing the discharge of hazardous chemicals and significantly reducing the amount of untreated wastewater. In general, industrial waste water contain harmful organic materials such as phenolic compounds, aromatic substances and intermediates, volatile organic compounds, halogenated species and heavy metals like Pb, Hg, Pb, Cd, Cr, Cu, Ni and Hg.⁵ Due to its toxicity, even at low concentrations, phenol and its substitute derivatives are among the most common organic water pollutants.⁶

The use of phenolic compounds is widespread in a wide range of industries, including petroleum refineries, gas and coke oven industries, pharmaceuticals, explosive manufacture, phenol–formaldehyde resin manufacture, plastic and varnish industries. The presence of phenol in water occurs throughout the manufacturing and production stages of these processes. In wastewater, phenol concentrations usually range from 200 to 1500 mg·L⁻¹. While, the Environmental Protection Agency's maximum for wastewater elimination discharge is 0.5 mg·L⁻¹ for surface water and 1 mg·L⁻¹ for sewerage water.^{7, 8} Phenol and its substitutes are among the most common organic water pollutants due to their toxicity, even at low concentrations. They are poisonous and potentially carcinogenic; even in concentrations of µg·L⁻¹. Phenol is listed as one of 11 among 126 chemicals as hazardous by the United States Environmental Protection Agency (EPA, 2002).⁹

1.3 Source of phenol

Phenolic compounds are organic compounds that contain a hydroxyl group attached to one or more aromatic rings. Among this category the best known is phenol; other names include benzenol, carboic acid, phenylic acid, phenic acid, hydroxybenzene.^{10, 11} Phenol is a colourless crystalline solid with a sickeningly sweet and acrid smell, and it is volatile. Chemical structure is presented in Figure 1.2. and their chemical and physical properties are listed in Table1.1.

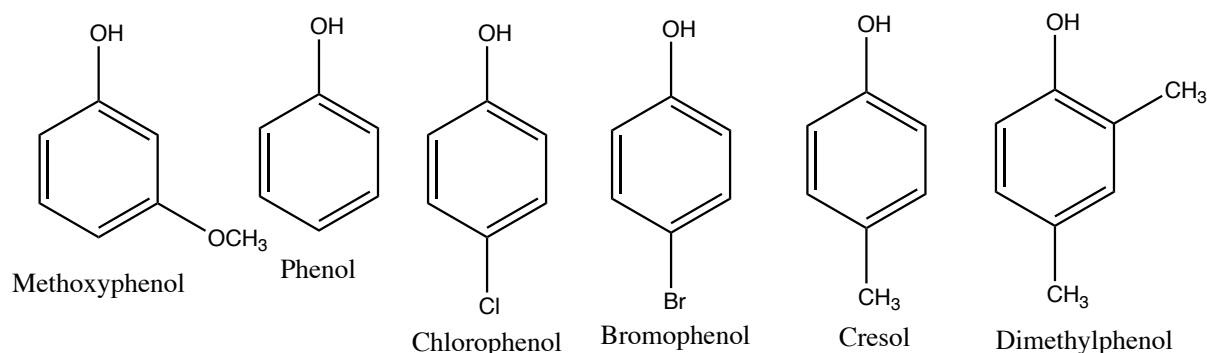


Figure 1.2: Chemical structure of different phenolic compounds.

A common moiety is a hydroxyl group directly bonded to the aromatic ring.

Table 1.1: Physical and chemical properties of phenol.¹²

Molecular formula	C_6H_5OH
Molecular weight	$93 \text{ g}\cdot\text{mol}^{-1}$
Melting point	$40.9 \text{ }^\circ\text{C}$
Boiling point	$181.75 \text{ }^\circ\text{C}$
Solubility in water (at room temperature)	$93 \text{ g}\cdot\text{L}^{-1}$
pKa	9.89
Flammability limits in air	1.7 vol%

The existence of phenolic compounds in water is due to both natural and anthropogenic sources. In nature, these compounds are found in organic matter resulting from dead animals and plants that decompose. Furthermore, aquatic plants synthesize them and microorganisms. The anthropogenic causes of phenolic water pollution come from industries, household, and farming activities. A brief description of these sources will be given in the following paragraphs.

1.3.1 Natural sources

1.3.1.1 Biodegradation of organic matter

The decomposition of deceased plants and animals can produce phenolic compounds in bodies of water, causing organic materials to break down and be washed into water. Various plant varieties produce phenolic compounds, both terrestrial and aquatic. For example: tea (*camellia sinensis*), tea leaves are rich in phenolic compounds, including catechins and flavonoids. These compounds contribute to the flavour and health benefits of tea. Also, grapes (*vitis vinifera*), grapes contain phenolic compounds such as resveratrol, flavonoids, and tannins, which are

important for wine production and have antioxidant properties. Phenolic macromolecules are also found in green and red marine algae.¹³ The internal organs of humans and animals produce phenol, then release it into the environment. Consequently, both humans and animals produce waste products metabolites that contain phenol, which is formed in mammals' gastrointestinal tracts as a result of tyrosine digestion.¹⁴ In addition, phenolic compounds, particularly hydroxybenzoate, is produced by microorganisms from natural substrates.¹⁵ In the presence of glucose and nitrogen, *Debaryomyces hansenii* produce phenolic compounds from ferulic acid. The study, by Max et al. reports about *Debaryomyces hansenii* metabolizing ferulic acid into 4-vinylguaiacol used in the food industry as a flavouring agent.¹⁶

1.3.1.2 Produced from plants

Plants are known to produce phenolic compounds and derivatives in large quantities. The formation of these compounds takes place in chlorophyll under the influence of ultraviolet radiation from the sun, microbial infections, and chemicals (cations, pesticides). Plants produce phenolics from phenylalanine as a precursor. Deamination of phenylalanine to cinnamate is usually catalysed by ammonialysase. Cinnamate is transformed into coumaric acid by hydroxylation through cinnamate-4-hydroxylase; this enzyme was called *Lentinus edodes*, which produced ellagic acid. A precursor for the preparation of stilbenes, flavonoids, furanocoumarines, and other compounds. A group of phenolic compounds catalysed by various enzymes.¹⁷ The above compounds are found in various parts of plants, such as roots, stems, and leaves. In addition, exudates from roots and leaves contain these phenolics, which are then introduced into the soil by exudates. Finally, these compounds drain into nearby bodies of water.

1.3.2 Sources from human activity

1.3.2.1 Waste from industry

Various products used in everyday life contain phenolic compounds. Phenol is commonly used in a wide range of industries, for example for the bulk chemical used (bulk chemicals refer to chemicals that are produced and traded in large quantities, these are typically commodities and are manufactured or processed on a large scale). Examples of bulk chemicals and products that are produced from or contain phenol include bisphenol-A (BPA) which is a major derivative of phenol. It is used in the production of polycarbonate plastics, epoxy resins, and other materials commonly found in consumer products like water bottles, food containers, eyeglass lenses, and dental sealants. Phenolic resins also are synthetic polymers made by condensing

phenol with formaldehyde. They are used as adhesives, coatings, and in the manufacture of melded products such as circuit boards, automotive parts, and countertops. Furthermore, caprolactam is a chemical compound produced from phenol and is used as the primary raw material in the production of nylon 6, a versatile synthetic polymer used in textiles, engineering plastics, and various consumer goods. Among the by-products of this process are alkylphenols, cresols, aniline, and resins.¹⁸ The oil, gas, and coal industries also produced it extensively.¹⁹ The explosives industry, colourants, and fabric factories use phenol in their manufacture. As well, phenolic compounds-such as bisphenol A are essential ingredients for polycarbonate plastics, epoxy resins, and polymer extracts. Additionally, polycaprolactam is used to synthesize nylon-6 (polycaprolactam) and some other fibres (synthetics).²⁰ Phenolic compounds are also found in some pesticides and insecticides. Processes used in various industries, including wood distillation, chlorine decontamination of water bodies, and cookery procedures chlorophenols are also produced during the manufacturing of paper.²¹ Pollution of water bodies is caused by industrial processes discharge effluents that contain phenolic compounds. Additionally, many of these compounds or derivatives are released into the atmosphere through automobile emissions, entering water systems through rain.

1.3.2.2 Waste from agriculture

One of the main causes of water pollution by phenolic compounds is agricultural pesticides, insecticides, and herbicides. In the aquatic environment, phenol and chlorophenols such as 2,4-dichlorophenol and catechols are caused by the biodegradation of some pesticides. As part of these pesticides, 2,4,5-trichlorophenoxyacetic acid, 2,4-dichlorophenoxyacetic acid, and 4-chloro-2-methylphenoxyacetic acid are included.²² Ultimately, breaks down to chlorophenols which contain less chlorine than herbicides, fungicides, and pesticides.²³ These by-products are washed away into water sources.

1.3.2.3 The domestic waste

There are many household chemicals containing phenol, for example disinfectants, antiseptics, and slimicides. Medical and pharmaceutical products can also contain it, for instance lotions, creams, mouthwashes, and mouth sprays that are used for anaesthetic purposes or to treat throat infections. As well as polish, fragrances, soaps, toys, paints and nail paint removers, it has been found in numerous other domestic products. Through drainage systems and basins, household water waste contains traces of aforementioned products that pollute neighbouring water systems.²⁴

1.3.2.4 Waste generated by municipalities

Effluents from municipal waste recycling industries and leachates from landfills are also major sources of phenolic compounds entering water bodies. The *p*-cresols found in municipal waste landfill leachates are thought to originate from the residues of incinerated materials (coal tar or petroleum). Fly ash has also been found to contain 2,4,6-trichlorophenol, 4-*tert*-butylphenol, and bisphenol A in leachates. In landfill leachates, 4-*tert*-octylphenol is mainly derived from combustibles. Several chlorophenols, 4-nonylphenols, and phenols have been found in municipal waste landfills.²⁵ When crude leachates from landfills are discharged into adjoining water bodies along with incineration residues (solid fly ash), phenolic compounds pollute the environment.²⁶

1.4 The reactivity of phenolic compounds in aquatic environments

1.4.1 Microorganism interaction

Non-ionic surfactants have been found to be broken down by certain bacteria within aquatic environments into other, more harmful, phenolic compounds such as alkylphenols. For instance, bacteria degrade nonylphenol polyethoxylate, used in laundry detergents and automotive detergents, creating nonylphenol. The nitrophenol pollutant has been found to form nonylphenoxyacetic acid after microbial degradation, which is even more toxic than the original pollutant. Whenever designing or setting up a degradation process, these experimental observations are very relevant since they should lead to less toxic (or ideally non-toxic) final degradation products and/or effluents. Bacteria can also convert nonylphenol polyethoxylates into other intermediate forms in certain environments. For example; under anaerobic conditions, nonylphenol polyethoxylates are typically transformed into nitrophenols.²⁷ Alternatively, when an aerobic environment is present, an additional conversion of nitrophenol by iso- substitution occurs.²⁸ By reacting with 4-chlorophenoxyacetic acid, 4-chlorophenol is produced. Bacteria degrade pentachlorophenol to produce tetrachlorocatechol, which can be further degraded to produce chlorinated catechols. Moreover, chlorocatechol is a by-product of microbial interactions with chlorobenzenes.¹⁶

1.4.2 Inorganic compound interactions

It is possible for phenol to react with nitrite ions in an aquatic habitat under the ultraviolet radiation from the sun, forming 2-nitrophenol and 4-nitrophenol.²⁹ When nitric ions are available, phenol is converted to nitrophenol. Photolysis of phenol forms hydroquinone along

with charge transfer complexes, while chlorophenol is formed by chlorinating aromatic compounds in water.³⁰

1.5 The consequences of the toxicity of phenolic compounds on human health

The majority of phenolic compounds are able to penetrate the skin very quickly, and in turn be quickly enter the blood stream. They are then metabolized into numerous reactive intermediates, efficiently forming quinone moieties in the tract. Proteins can be covalently bound with quinones, which also have toxic effects on humans.³² Chlorophenols, aminophenols, chlorocatechols, nitrophenols, methylphenols, and other phenolics are toxic to humans.³³ Bisphenol A and some alkylphenols, which alter the development of the mammary gland in animals, have also been found to have endocrine-disrupting effects on humans.³⁴ In addition, delayed puberty in girls can also be attributed to exposure to bisphenol A.³⁵ Drinking water or liquids containing high levels of phenol can cause severe complications in the gastrointestinal tract. Moreover, it can cause muscle tremors and difficulty walking. High-phenol content containing products cause blisters when they come into contact with the skin. Additionally, they cause burns to vital organs like the heart, kidneys, liver, and lungs.¹⁶ Furthermore catechols, which are intermediates generated during phenol degradation, can cause DNA damage by oxidizing rapidly into quinone radicals, which destroys some important proteins of the body.³² More specifically, chlorophenol intoxication leads to mouth and throat burns, necrotic lesions in the mouth, stomach and oesophagus. In the presence of chlorophenol, convulsions, fluctuations in pulse and temperature, as well as feeble muscles, are some of the symptoms of this illness. This may involve malfunction in the lungs, digestive tract, liver, and kidneys.³⁶ Hydroquinone damages chromosomes, while *p*-cresol and 2,4-dimethyl phenol may cause cancer.³⁷ In light of the hazardous effects of phenol and phenol derivatives, it is crucial to develop improved water treatment technologies and implement sustainable water usage methods.

1.6 Current methods for removing phenolic compounds from water

Wastewater generated by a variety of industries requires cost- and time-effective treatments. These can be physical, biological, chemical, or a combination of them. Any methodology will have both benefits and drawbacks depending on a variety of assessment criteria like the chemical point of view, its applicability or economic viability, regardless of the specific context of our research. Here is a brief description of these methods.

1.6.1 Physical methods

Comparatively to chemical and biological methods, these methods are quite commonly used to remove phenol.³⁸ In general, three physical methods are used: adsorption technology, membrane filtration, and nano-filtration. There are a number of advantages of physical processes, such as: simple design, straightforward procedure, relatively high effectiveness to removal, no side effects due to toxic materials, and relatively cheap. These advantages make physical processes one of the possible wastewater treatment methods. Aside from the small amount of chemicals needed, this process is also environmentally friendly. There is high performance in phenol compound removal from wastewater using adsorption techniques. In addition to being simple, it is also in principle eco-friendly.³⁹ Adsorption involves the adsorption of toxic substances on adsorbent materials, typically (solid materials) such as: charcoal and activated carbon. These solid materials must be porous and have a large surface area, be selective for the desirable pollutant, and be hydrophobic. Several factors impact adsorbent performance: the nature of the adsorbent, the construction of the functional groups, and pore volume distribution and surface area. Moreover, their performance is influenced by pH, temperature, polarity degree, the possibility of other elements competing for the adsorbent's surface area, and the concentration of the adsorbate. The properties of the adsorbate, as well affect the adsorption performance, include their solubility in water, hydrophobicity, and amount of molecular weight.⁴⁰ Thus, these factors determine how efficient this technique is.

However, despite these positive aspects there are also a number of drawbacks. Adsorption is generally not highly selective, meaning that it can remove a wide range of pollutants, including both harmful and beneficial substances. This lack of selectivity can lead to the removal of essential nutrients or other compounds that may be present in the wastewater. Adsorption media (such as activated carbon) have a finite adsorption capacity. Once the adsorption sites are saturated with pollutants, the media need to be regenerated or replaced. Regeneration processes can be energy-intensive and may require additional chemicals. In fact, the removal of pollutants by adsorption generates secondary waste in the form of spent adsorbent materials. In many cases, spent adsorbent materials are considered hazardous waste because they contain concentrated pollutants. Disposal involves properly managing and disposing of these materials in compliance with environmental regulations, which can be costly and have environmental implications. Whether the spent adsorbent is disposed of or regenerated, it generates secondary waste from contaminated materials or waste streams. For disposal, this waste may require

specialized handling and disposal methods to prevent environmental contamination. For regeneration, the waste generated can include concentrated pollutant solutions or waste chemicals used in the regeneration process. Proper disposal of these materials can be a challenge, and if not managed correctly, it could lead to additional environmental concerns. Adsorption may not be effective for removing certain types of pollutants, such as dissolved gases or pollutants that are present at very low concentrations.⁴¹ The membrane filtration method can also be used to remove phenol; it can be isolated quickly and with a high degree of selection. However, it has two disadvantages: membrane fouling and incapacity to treat large volumes.⁴² Polymeric membranes have temperature restrictions; their properties cannot be managed at temperatures above 100 °C. In this system, nano-filtration uses membranes whose pores range in size from 1 to 10 nano-meters.⁴³ As an example, NF-97, NF-99, and DSS-HR98PP have the highest phenol removal efficiency. However, it requires high filtration costs, while reverse osmosis requires high pressure.⁴⁴

1.6.2 Biological methods

Biological processes involve oxidation, which transforms contaminants into a simpler and harmless form by the action of microbes or enzymes. Biological oxidation of phenols can be categorized into two types: microbial decomposition and enzymatic oxidation.³⁸ Microbial reactions can take either aerobic (with oxygen) or anaerobic (without oxygen) forms: activated sludge processes and aerated lagoons have been used to treat phenol compounds in wastewater. Most commonly, activated sludge treatment is used.⁴⁵ Activated sludge consists of sludge molecules that are crowded with microorganisms, which are formed in wastewater by growing organisms like bacteria under aeration. Although activated sludge has been used to eliminate phenol the lack of success of these processes has been caused by high concentrations of phenol compounds for a long time.⁴⁶ Wastewater pollution can be treated easily with aerated lagoons (aerated ponds). Using a pond with synthetic aeration the biological oxidation of wastewater improves.⁴⁷ Despite this, Peitz in his study reported that effluent from kraft pulp mills was treated with aerated lagoons, but only 18% of phenol compounds were removed.⁴⁸ In anaerobic reduction, phenols are reduced without oxygen. As for the reduction time, phenol concentration determines the reduction time, a high phenol concentration increases oxidation time significantly.³⁸ An enzyme reduction involves the use of enzymes obtained from a variety of sources. Polyphenol oxidases are the most widely used enzymes. To remove phenol from wastewaters, Jadhav and co-workers applied polyphenol oxidase enzyme extracted from banana

peels. In the case of small concentrations of phenol, complete reduction was achieved after one day and after two days in the case of high concentrations of phenol.⁴⁹

In comparison with the other two main alternatives (physical and chemical treatment) biological treatment is one of the cheapest. Design and maintenance of microorganisms for biodegrading organic contaminants are simple.⁵⁰ The method is economically attractive and can be applied on a large scale. Nevertheless, this method has some disadvantages, such as the need for an ideally suitable environment to contain and conserve microorganisms, low decolorization efficiency, and production of biological sludge and out-of-control degradation products.⁵¹ Biological degradation processes can be relatively slow compared to some chemical oxidation methods. The rate of phenolic compounds removal depends on the growth and metabolic activities of the microorganisms or the enzymatic activity, which might not always be rapid enough to meet stringent treatment requirements. In addition, phenol, as well as intermediate degradation products, can exhibit toxicity to the microorganisms responsible for biodegradation. High phenol concentrations or the accumulation of toxic intermediates can inhibit the microbial activity, slowing down the degradation process. Transitioning from laboratory-scale studies to larger-scale industrial applications can be challenging. Maintaining consistent and controlled conditions at a larger scale can pose difficulties. High initial concentrations of phenol ($1000 \text{ mg}\cdot\text{L}^{-1}$) in wastewater may overwhelm the microbial degradation capacity, leading to reduced efficiency or incomplete removal.⁵²

1.6.3 Chemical oxidation processes

Chemical oxidation process is similar to biological processes in that organic contaminants are destroyed and transformed into simpler compounds. Chemical oxidation has an advantage over biological oxidation because it is generally faster and does not produce solid residues. The use of these technologies, however, has not been widely accepted due to their high capital and operating costs. Additionally, heavy sludge collection creates an elimination issue and the potential for secondary pollution due to severe chemical use. Chemical reagent consumption is a common problem. Industrial wastewater has been treated with a variety of oxidizing agents, including chlorine, chlorine dioxide, ozone, and advanced oxidation processes (AOPs).

1.6.3.1 Oxidation by chlorine and chlorine dioxide

Chlorine is a strong oxidising agent that can effectively oxidise phenolic compounds, breaking them down into less harmful substances. Chlorine oxidation reactions are generally fast, leading to changing them into potentially less toxic materials. Chlorine dosing equipment is

widely available and relatively easy to operate, making it suitable for various treatment facilities. Many dyebaths can be effectively decoloured with chlorine as sodium hypochlorite. In combination with other treatment processes, chlorine can be used at the treatment plant at a low cost.⁵³ Nevertheless, chlorine oxidation can lead to the formation of potentially harmful disinfection by-products (DBPs) if organic precursors are present in the wastewater. Treatment by chlorine generates chlorinated compounds, which can have negative environmental impacts if not appropriately managed. The release of chlorinated substances can harm aquatic ecosystems and human health. The efficiency of chlorine oxidation is pH-dependent, and optimal conditions must be maintained for effective phenol removal. It is corrosive and can damage equipment and infrastructure if not handled properly. Handling and dosing chlorine require careful safety measures due to its toxic and reactive nature. Accordingly, the use of this chemical has decreased.⁵⁴ It is reported that chlorine dioxide generates fewer health and safety concerns than chlorine because it is less reactive than chlorine.⁵³

Chlorine dioxide is a selective oxidizing agent, often targeting specific organic compounds like phenols without forming as many harmful by-products as chlorine. Compared to chlorine, chlorine dioxide generally produces fewer and less harmful disinfection by-products. A wider pH range between pH 4 and pH 10. makes chlorine dioxide more effective in varying wastewater conditions. Chlorine dioxide is less corrosive than chlorine, potentially reducing equipment maintenance requirements.⁵⁵ The production and dosing of chlorine dioxide require specialized equipment, making its implementation more complex than chlorine. Chlorine dioxide can be more expensive to produce and dose compared to chlorine. In summary, both chlorine and chlorine dioxide oxidation methods have their advantages and disadvantages for phenol removal. While effective, the potential formation of harmful by-products and environmental concerns associated with chlorine must be carefully considered. Chlorine dioxide offers some advantages in terms of selectivity, pH tolerance, and reduced by-product formation, but its production and implementation complexity should also be weighed.⁵⁴

1.6.3.2 Ozonolysis process

Ozonation is an effective method for treating wastewater. A large number of organic compounds can be reacted with ozone (O_3), which is a very strong oxidant ($E^\circ = +2.07$ V). Nevertheless, some chemicals, such as chlorinated alkanes, react slowly with ozone. Unlike conventional wastewater treatment methods, this method is capable of treating coloured and organochlorine compounds in wastewater. Furthermore, phenolic pesticides promptly react with ozone.⁵⁶ In spite of this, the short lifetime of ozone and its limited solubility in water at

atmospheric pressure make the process unattractive and expensive. its solubility increases with decreasing temperature and increasing pressure.⁵⁷ Moreover, ozonation has a poor selectivity of the hydroxyl radicals and is mostly used to treat wastewater that contains low amounts of organic compounds.⁵⁸ This issue can be overcome with catalytic ozonation.⁵⁶

1.7 The theory of advanced oxidation processes (AOPs)

1.7.1 Oxidation principles of AOPs

Taking on from ozone oxidation, this leads to a new class of treatments known as: advanced oxidation process (AOP) is an innovative way to degrade organic compounds or convert them into biodegradable ones.⁵⁹ The AOPs are chemical oxidation processes that generate and utilize the hydroxyl radical $\cdot\text{OH}$ as an oxidant. Following fluorine, hydroxyl radicals are the most reactive oxidizing agents commonly used (see Table 1.2).⁶⁰

Table 1.2: The standard redox potential of different oxidants that could be used for water treatment applications, with emphasis to the hydroxyl radical.⁶¹

Oxidant	Oxidation potential (V)
fluorine	3.06
hydroxyl radical	2.80
atomic oxygen	2.42
ozone	2.08
persulfate	2.01
perbromate	1.85
hydrogen peroxide	1.78
perhydroxyl radical	1.70
hypochlorite	1.49
bromate	1.48
chlorine	1.36
dichromate	1.33
chlorine oxide	1.27
permanganate	1.24
oxygen (molecular)	1.23
perchlorate	1.20
bromine	1.09
iodine	0.54

In general, the rates of reaction of $\cdot\text{OH}$ and organic compounds range from $\sim 10^6$ to $10^9 \text{ M}^{-1} \text{ s}^{-1}$.⁶² In comparison to O_3 , its rate is nearly ten times higher.⁶³ Furthermore, AOPs are well-known for

their comprehensive reactions, making them ideal for wastewater treatment and pollution control. Due to their non-selective nature, hydroxyl radicals degrade organic pollutants, including those resistant to conventional oxidation processes like ozonation and chlorination.⁶⁴ •OH radical's mechanism with different materials involves a series of chain reactions resulting in carbon dioxide, water and inorganic salts. As a result, this technique can be considered clean technology.⁶⁵ In AOPs, hydroxyl radicals are produced in a variety of ways, giving it its unique properties. There are three main classes of AOPs, categorized by their oxidants (oxygen O₂, hydrogen peroxide H₂O₂ and O₃). In addition, photocatalytic methods are reported as a fourth type. Although the AOPs are more numerous, they can be combined in more ways, for example using both H₂O₂ and O₂ or O₃, or H₂O₂/light.²⁸ Photocatalysis in heterogeneous systems involves using a narrow-bandgap semiconductor irradiated with UV–Vis light, resulting in the release electrons from their valence band and creating holes.⁶⁶

The performance of AOPs this process can be improved with the use of a catalyst, resulting in a decrease in relative costs that by:⁶

- I. An increase in reaction rate.
- II. Reactors capable of operating in milder conditions.
- III. Minimization of by-products: reduction of harmful by-products, and improved pollution degradation efficiency.
- IV. Enhanced selectivity for the oxidizing agents to alter target chemicals. While different compounds exist in wastewater, when AOPs are used for wastewater pre-treatment, the cost of pre-treatment must be monitored by selectively removing only the desired chemicals (almost not biodegradable, inhibitors and ecotoxic substances).

There are several applications for catalytic AOPs, including the treatment of wastewater from: (i) textile dyeing, (ii) bleaching of Kraft pulp, (iii) petrochemicals, (iv) milling olives, (v) production of acids, and (vi) pyrolysis of wood and cooking plant, although commercial applications are still restricted.⁶

Due to their high reactivity, hydroxyl radicals can interact with a wide range of organic and inorganic reagents. Different AOPs saw different ways to generate hydroxyl radicals from a variety of resources (H₂O, O₂, H₂O₂, O₃). The generation rate of hydroxyl radicals (as well as other radical species like HO₂•) plays a crucial role in determining the reaction conditions and the type of feed that can be processed. Although the photocatalytic method is a fascinating way to treat water, it has its limitations when it comes to feeds with low organic content (less than

100 mg·L⁻¹). Feeding a concentrated stream along with photocatalysts to other AOPs, for instance hydrogen peroxide with iron salts, also known as photo-Fenton processes.⁶⁷

The ozonation method is among the most AOPs widely used, however its solubility in water is limited at atmospheric pressure, it is estimated that 0.7 grams of ozone are soluble in water at atmospheric pressure and 20 degrees Celsius (68 degrees Fahrenheit), as well as its short lifetime. Consequently, this raises the cost of the procedure, furthermore, it can only be applied to diluted solutions, ranging from 1 to 100 milligrams per litre mg·L⁻¹ or parts per million (ppm).⁶⁸ When organic compounds are present in medium to high concentrations in water, for example in agricultural or industrial wastewater, wet air oxidation or wet hydrogen peroxide oxidation is preferred. This discussion will focus on the utilization of solid catalysts in the wet hydrogen peroxide catalytic oxidation (WHPCO) followed by a brief discussion of its advantages and disadvantages compared to wet air catalytic oxidation (WACO).

1.8 The comparison of WHPCO with WACO systems

It does worth to immediately highlight that based on the comparison of WACO and WHPCO methods, no unambiguous conclusion can be drawn. In fact, the comparison of the AOPs techniques is mainly based on the efficiency of removal, while a more accurate comparison would take into account a number of factors, including: (i) the safety of operation (ii) application and management of specific operations (iii) effectiveness in actual waterbodies, (iv) a reduction in post-treatment requirements (to eliminate some remaining substances or metal ions) (v) preventing secondary contamination, (vi) maintaining minimal toxicity of emissions (vii) There is minimal corrosion, plugging, process-control parameters that are sensitive, and (viii) operating costs.⁶

Literature data cannot be used to draw a reliable conclusion regarding the comparison of WACO and WHPCO technologies, nor regarding the comparison of their eco-techno-economics with alternative AOPs processes. In any case, comparing WACO and WHPCO technologies is beneficial in general.

1.8.1 Wet air catalytic oxidation processes (WACO)

The wet air oxidation process (WAO) primarily operates under oxygen pressure (5–200 bar) and at a high temperature (125–320 °C). In general, residence times range from 15 to 120 min, however, longer residence times are necessary for high organic loading or high levels of chemical oxygen demand (COD) elimination (between 75 and 90%). Low-weight oxygenated

substances, including acetic, propionic acids, methanol, ethanol and acetaldehyde, exhibit high resistance to oxidation, thus WAO is often unable to mineralize the waste stream completely. As an example, at temperatures below 300 °C, acetic acid is only partially removed. Under WAO conditions, organic nitrogen compounds can simply change to ammonia. Therefore, WAO is pre-treats liquid wastes which require further treatment of the liquid and gas streams. More than 100 treatment plants are in operation, treating wastewater from petrochemical, chemical, and pharmaceutical industries, as well as sludge left over after wastewater treatment.⁶⁹ Applying catalysts (WACO) allow milder reaction conditions, specifically for increasing the conversion of intermediate products (for example, acetic acid and ammonia) that are usually difficult to convert without a catalyst.^{70, 71}

There are two major drawbacks to WACO technology, aside from metal leaching and deactivation of catalysts, which is a common problem with multi-phase methods using solid catalysts:⁷²

- I. Using high temperatures or pressures consumes a large amount of energy (oxidation of organic materials is exothermic), nevertheless, it is only partly possible to recover the heat of reaction in batch autoclaves.
- II. Cost of the reactor (special materials, such as titanium, must be used in the autoclave reactor, due to corrosion issues caused by low molecular weight acids formed in high concentrations as reaction results. Furthermore, it is common that the actual streams to be treated contain large amounts of ions, such as chlorine, which is oxidized under wet oxidation conditions, resulting in corrosive reaction mediums). In addition, high-pressure reactors require specialized staff and accept all safety procedures required for high-pressure autoclave devices, increasing operational costs. In spite of the, transferring technology from one place to another is difficult due to safety concerns. NO_x, CO, and smelling odour are other problems associated with the handling of dismissed gaseous emissions.

1.8.2 Wet hydrogen peroxide catalytic oxidation processes (WHPCO)

In general, WHPCO operates between 20 and 80 °C and at atmospheric pressure. Therefore, stainless steel or autoclave reactors are not needed and even basins could be used. The formation of foam and smelling odours is not as critical as with WACO processes. There is only one safety issue related to the storage of H₂O₂, although it is not considered a significant

problem, special handling procedures are required. The technology can be transferred from one place to another without requiring specialized staff. In contrast, H_2O_2 is more expensive than air. Even so, in terms of overall costings and health and safety consideration keeping away from high pressures and long reaction times which are required with the O_2 makes WHPCO a preferred and more environmentally friendly abatement method. The storage of oxygen requires controlled pressure or low temperature, and marketing costs cannot be ignored. Conversely, H_2O_2 has gradually become cheaper over time, therefore, its use in environmental protection applications has increased.⁶⁵

In light of these considerations, it appears that WHPCO methods are more desirable than WACO under the following conditions:⁷³ Early pre-treatment of the stream before delivering it to the biological step requires selectively converting harshly biodegradable or hazardous compounds with a relatively low level of total organic carbon (TOC) removal, less than 30% (for example, in the pre-treatment of flow coming from agriculture and food manufacturing). The other case also preflare WHPCO with the treatment of wastewater containing medium to low organic content ($1-30 \text{ g.L}^{-1}$ of TOC) and low levels of suspended solids ($1-100 \text{ m}^3/\text{day}$).⁶

The CWPO can be incorporated into the water purification procedure in several ways:⁷⁴

- I. Improvements should be made to the quality of industrial wastewater effluent. In the last step of wastewater treatment, CWPO can remove residual contaminants like hazardous or refractory materials to produce a high-quality effluent capable of being reused or disposed of safely.
- II. It is important to increase the biodegradability of industrial wastewater. Before the biological process, it is recommended that the CWPO be applied first so the biodegradability of resistant compounds is enhanced, thus making them suitable for biological treatment.
- III. CWPO is most suitable for wastewaters that are non-biodegradable. In the following Through the use of CWPO, the effectiveness and commercial viability of biological processes can be enhanced.

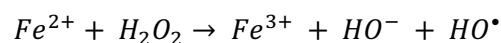
1.9 Perspectives regarding solid catalysts in the WHPO

There is no doubt that hydrogen peroxide is a powerful oxidant which upon decomposition ultimately generate water the greenest of the solvent and by-products; nonetheless, to generate

hydroxyl radicals at the rate that is needed to carry out large scale abatement of pollutants, it needs UV radiation or a catalyst. During the late 19th century, Fenton, when investigating the oxidation of tartaric acid, discovered that Cu and Fe can catalyse the reaction.⁷⁵ Eventually, 40 years later, during the early 1900s, Haber and Weiss indicated hydroxyl radicals were the actual oxidative agents in the Fenton reaction.⁷⁶

1.9.1 Fenton reagent

Fenton's process produces active oxygen species by reacting H₂O₂ with Fe ions, HO[•] radicals capable of oxidising organic and inorganic compounds. The chemist Henry Fenton discovered the reaction and demonstrated that Fe²⁺ salts could activate H₂O₂ to oxidize tartaric acid.⁷⁷ As a result, Fenton reactions have gained a lot of attention for their application in biochemistry, natural water, synthesis and the treatment of hazardous waste. Fenton reactions are considered possible methods of generating oxidation species for chemical waste treatment economically and conveniently. In the Fenton process, the reagents, H₂O₂ and Fe, perform beneficial functions.



1.9.1.1 Hydrogen peroxide

Compared to other oxidants for large scale or bulk oxidation, hydrogen peroxide is safe, limitedly to non-toxic and poses no environmental risk since it breaks down to H₂O and O₂. It is used as the main agent in Fenton reactions, discovered in 1818 by Thenard and was produced when barium peroxide (BaO₂) reacts with nitric acid. As a powerful oxidant, hydrogen peroxide can oxidise across the pH range, with high oxidation potential (+ 2.8 eV at pH = 0 and + 2.0 V at pH = 14) and H₂O as the only by-product.⁷⁸ Inorganic and organic materials are oxidized by hydrogen peroxide when liquid in mild conditions. Industrially, chlorine-containing agents have been replaced by H₂O₂ to bleach materials more efficiently. Furthermore if scaled to its low molecular weight, hydrogen peroxide is an effective oxidizing agent compared to sodium hypochlorite and nitric acid.⁷⁹

1.9.1.2 Chemistry of Fe

Several transition metals can be used as catalysts for Fenton-like reactions, but iron (Fe) is often preferred for several reasons. However, other transition metals like Cu, Mn, Co, Ni and Ti can also be employed depending on the specific application and requirements. Chemically,

iron has the atomic number 26 and it belongs to the first transition series and group 8 of the periodic table. By mass, Fe is among the most abundant elements (ca. 5% of the Earth's) crust as well as contributing to the Earth's core. It can also be found by meteorites in native form. Nowadays, alloys of iron, including steel, stainless steel and special steels, are commonly used in industry because of their low cost and mechanical properties. Therefore, the iron and steel industry are crucial economically since iron is the least expensive metal, costing only a few dollars per pound. It is easy for Fe to react both with oxygen and with water to form dark brown hydrated iron oxides, also known as rust. Adult human bodies contain approximately 4 grams (0.005% of their weight) of iron, mainly in haemoglobin and myoglobin. These proteins play a crucial role during vertebrate metabolism, specifically in the transport of oxygen through the blood and in the storage of oxygen in muscles. To maintain the required levels, the diet must contain a minimum amount of iron. Many important redox enzymes are also based on iron, involved in cellular respiration, oxidation, and reduction.⁸⁰

In chemistry, the most common oxides of iron are Fe^{2+} and Fe^{3+} . Iron has similar properties to other transition metals, such as ruthenium and osmium. Among the elements in its group, iron is the highest reactive element. The compound is pyrophoric upon fine division and readily dissolves in diluted acids. Nevertheless, it reacts with concentrated nitric acid or other oxidizing acids by forming Fe_2O_3 on its surface, which however may form a protective layer, and can react with hydrochloric acid.⁸¹ In industry, the iron compounds produced most frequently are Fe^{2+} sulphate ($\text{FeSO}_4 \cdot 7\text{H}_2\text{O}$) and Fe^{3+} chloride (FeCl_3). The first source provides a readily available source of Fe^{2+} but it is less stable than Mohr's salt ($(\text{NH}_4)_2\text{Fe}(\text{SO}_4)_2 \cdot 6\text{H}_2\text{O}$). It is common for Fe^{2+} compounds to be oxidized to Fe^{3+} compounds in the air.⁸²

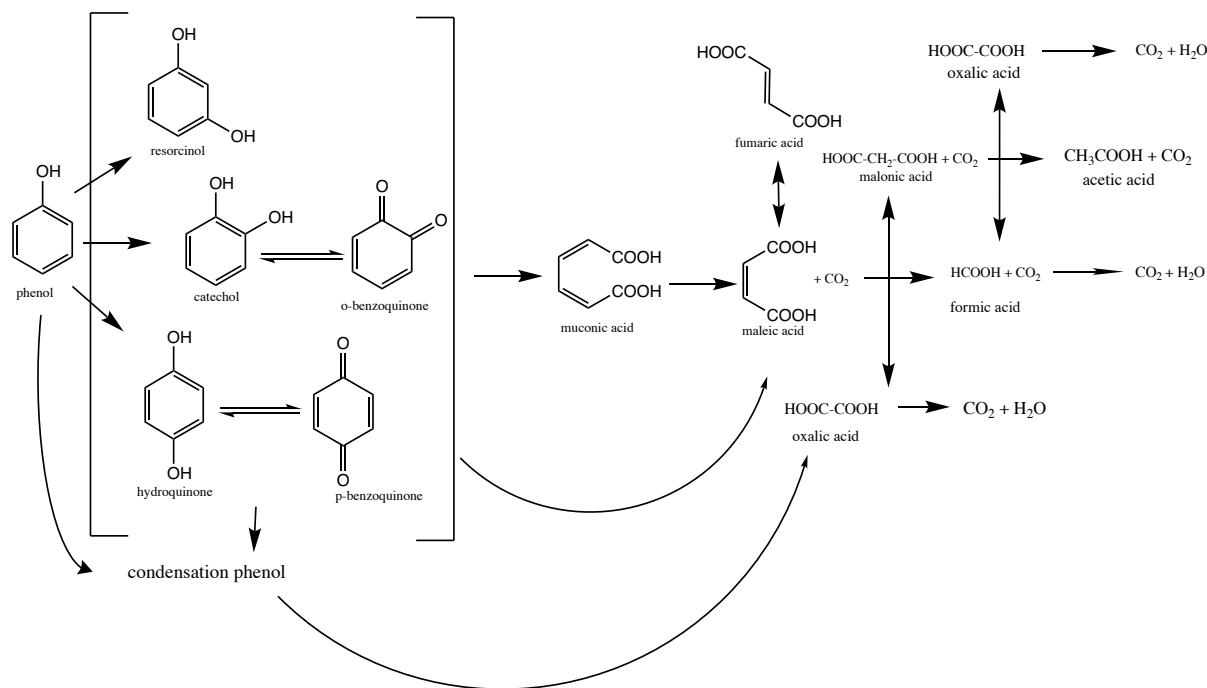
In view of all of these factors, iron is eco-friendly, safe, inexpensive, and abundant. Under the appropriate reaction conditions though Fenton processes can convert organic compounds into CO_2 , H_2O , and inorganic compounds. To accomplish this, excessive chemicals are required, increasing the cost, and typically only partial degradation occurs. The incomplete degradation of pollutants can reduce the toxicity of the pollutants and thus enhance their biodegradability. However, there is, on occasion, the possibility that reactions produce products with the same toxicity or even more than the starting materials.⁸³

1.9.1.3 Phenol reaction mechanisms by Fenton reaction

Although the ability of $\cdot\text{OH}$ radicals to decompose phenol has been widely accepted in recent years, the exact mechanism for oxidation is uncertain because phenol is generally not converted

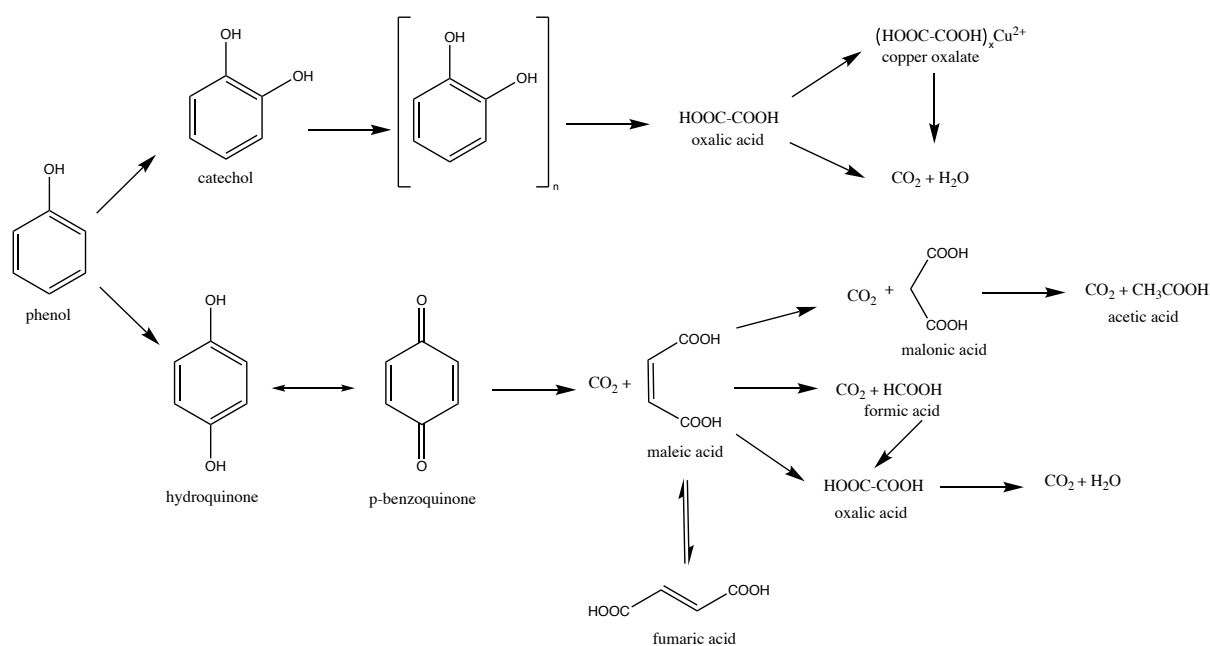
directly into carbon dioxide and water but involves organic intermediaries, for example, aromatics (e.g. hydroquinone) and acids with short chains (e.g. acetic acid). In addition, studies have shown how the pathway of phenol oxidation, in part, is determined by catalysts (e.g. reactive species) and process conditions (e.g. pH), which makes the actual pathway of phenol degradation complicated.⁸⁴

The oxidation of phenol can take place in a variety of ways, with a variety of intermediates.⁸⁵⁻
⁸⁸ There are several reasons for the different reaction pathways described in the literature, including different catalysts Cu,⁸⁵ Fe,⁸⁹ and different oxidant agents H₂O₂,⁸⁵ O₂,⁹⁰ and also reaction conditions like an acidic medium,⁸⁵ or an alkaline medium,⁸⁶ all of which have an impact on the mechanisms involved as well as intermediates produced during oxidation. According to the three illustrated oxidation routes presented in Scheme 1.1, 1.2 and 1.3, intermediates, precursors, and products (e.g. maleic acid, oxalic acid) are different. As an example, the oxidation of phenol with the classical Fenton catalyst (Fe²⁺ salt) as a catalyst is demonstrated in the Scheme 1.1, which indicates that more than ten intermediates were generated through the oxidation of phenol conversion to CO₂ and H₂O. Accordingly, the decomposition of phenol in the Fenton reaction starts with hydroxylation of the aromatic ring to produce dihydroxybenzenes, mostly catechol and hydroquinone, both in redox equilibrium with benzoquinones—afterwards, opening the ring of the aromatic intermediates ends with the formation of muconic acid and maleic acid. Ultimately, the intermediates undergo oxidation to acetic acid, formic acid and oxalic acid; consequently, the pH decreases. In these acids, formic acid decomposes to CO₂ and H₂O, while oxalic acid exhibits great resistance to decomposition. Ultimately, the products of this oxidation process are acetic acid and carbon dioxide.



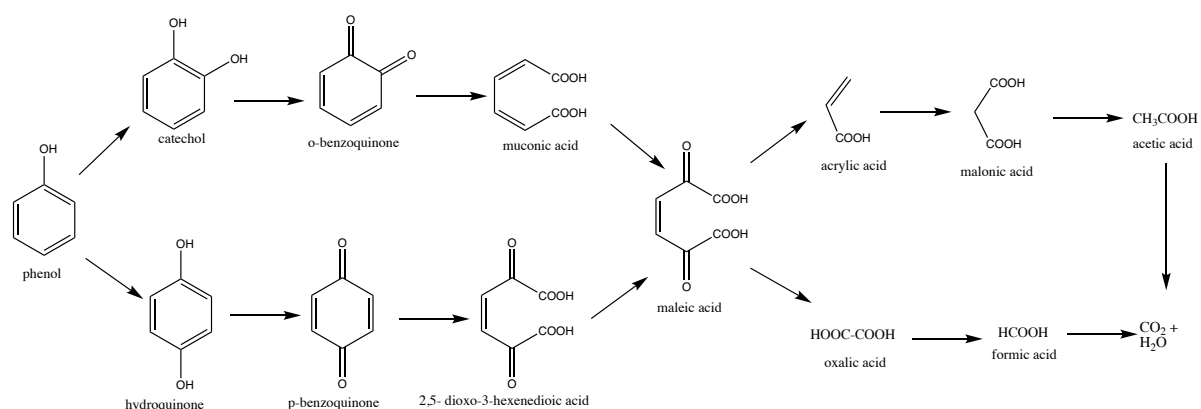
Scheme 1.1: The pathway for the decomposition of phenol using a homogeneous Fe²⁺ catalyst and H₂O₂ as an oxidant. Hydroxyl radicals ($\bullet\text{OH}$) attack the phenol molecule, leading to the oxidation of phenol and the formation of intermediate products. The hydroxyl radicals abstract hydrogen atoms from the phenol molecule, resulting in the formation of phenoxyl radicals ($\bullet\text{C}_6\text{H}_5\text{O}\bullet$). The phenoxyl radicals ($\bullet\text{C}_6\text{H}_5\text{O}\bullet$) can undergo additional reactions, such as further oxidation and cleavage of the phenolic ring. These reactions result in the formation of smaller, less toxic organic compounds and, ultimately, carbon dioxide (CO₂) and water (H₂O).⁸⁹

An oxidation pathway dependent on a Cu-supported catalyst appears in Scheme 1.2, as phenol oxidizes to catechol and hydroquinone, and these intermediates follow different pathways. Catechol formation results in a polymerization byproduct and oxalic acid. In the oxidation reaction, oxalic acid is oxidized to CO₂ or forms Cu oxalate, which is also responsible for the leaching of metals in aqueous solutions.^{91, 92} Other important intermediates, quinones, contributes to forming several acids, among them maleic, fumaric, acetic, formic, malonic and oxalic acids. Furthermore, studies have shown that phenol oxidations under acidic,⁸⁵ as well as basic conditions,⁸⁶ differ significantly with the use of copper catalysts in the same reaction conditions excluding pH.



Scheme 1.2: The pathway of phenol oxidation in water using a Cu-supported catalyst.⁸⁵

There is also another possible phenol oxidation mechanism using noble metal catalysts such as Ru, Pt and Rh as shown in Scheme 1.3. Maleic acid formation plays a crucial role, serving as a link between the degradation of C6 organic molecules and the generation of shorter organic acids (C1, C2 and C3). In contrast to the two examples given in Scheme 1.1 and Scheme 1.2, the oxidation pathway predicts that all intermediates are capable of further oxidation, and CO₂ is the end product under ideal reaction conditions, which include an effective catalyst.



Scheme 1.3: Accepted pathway for the decomposition of phenol in water using noble metal catalysts, like: Pt, Pd and Au.⁸⁷

Even so, it is evident that, despite their differences, all the reaction routes proposed up to this point include the hydroxylation of phenol to hydroquinone and catechol as a first step in two independent reactions, then the conversion of the dihydroxyl benzenes to benzoquinones. At the same time, the quinone-like intermediates will be broken down further to short-chain acids like acetic acid and formic acid and finally to CO₂ and water. In the oxidation process, details ranging from the ring-splitting of quinone compounds to the production of different acids are heavily influenced by the reaction conditions. In addition, it is commonly accepted that the end product of phenol oxidation includes acids that resist degradation, including acetic acid, formic acid and CO₂. In general, a thorough understanding of the reaction route for phenol oxidation, especially intermediate identification, is essential for improving the selectivity of less toxic byproducts like CO₂ and acids and decreasing the toxicity in the reaction solution because some of the intermediates such as hydroquinone and *p*-benzoquinone have even higher toxicity than the initial reactant.^{93, 94}

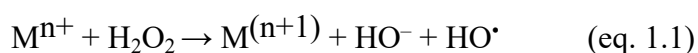
1.9.2 Fenton reaction types

There are two types of Fenton reactions: homogeneous and heterogeneous reactions. Due to their importance and the need to distinguish them, more details are provided in the next sections.

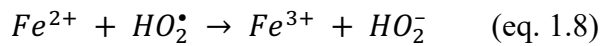
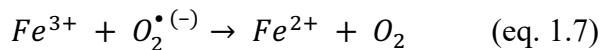
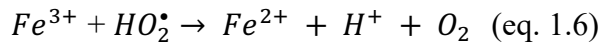
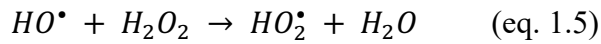
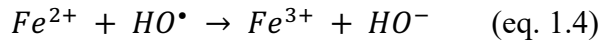
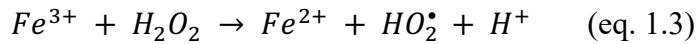
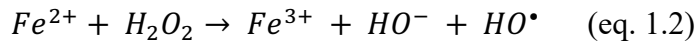
1.9.2.1 The homogeneous Fenton reaction

A homogeneous Fenton reaction occurs when all the Fenton reagents have been present in the solution phase. Precipitation of some insoluble species and metal hydroxides is also possible as part of the reaction although it is not an essential part of the process itself. There are four main reagents involved in homogeneous Fenton reactions: H₂O₂, Fe²⁺, Fe³⁺, light (UV) and inorganic or organic species.⁹⁵

Fenton's reaction can be summarized as follows:



M is a transition metal such as Fe or Cu, H₂O₂ is most likely to decompose in acid homogeneous aqueous solution produces hydroxypropyl (HO₂[•]/O₂^{•(-)}) and hydroxyl radicals [•]OH. In solution, the [•]OH radical reacts with all organic compounds. Regeneration of metal may occur in a variety of ways following are the major recognized schemes for Fe²⁺:⁹⁶



In the homogeneous Fenton reactions, if the reaction starts with Fe^{3+}/H_2O_2 rather than Fe^{2+}/H_2O_2 , it will be slower, as Fe^{3+} needs to be reduced to Fe^{2+} before hydroxyl radicals can be produced. In the literature, this type of reaction is called a Fenton-like reaction. Theoretically, it can be distinguished from Fenton's process. However, Fe^{2+} and Fe^{3+} ions are eventually present simultaneously in the chain reaction, regardless of the initial oxidation state and the starting material.⁹⁷

According to the reaction sequence above, the Fenton reaction depends on H_2O_2 concentration and Fe, and the pH value significantly influences the reaction. Ideally, the pH level should be around 3.5, as it is near this pH level that the reaction rate reaches its maximum. Additionally, at high pH values, iron precipitates as $Fe(OH)_3$, leading to a preference for hydrogen to be decomposed into oxygen and water. A further drawback of homogeneous iron salts in WHPCO reactions is that, in many cases, substances in the feed solution and the products of the reaction bind to the Fe ions, inhibiting their activity and accelerating H_2O_2 side reactions. Therefore, the efficiency of H_2O_2 utilization will decrease, and the reaction rate will become slower. As a means of controlling this negative effect, progressive dosages are used for both H_2O_2 and Fe in the reaction. Using ligands does not solve the issue of iron remaining in solutions after treatment.

1.9.2.2 The heterogeneous Fenton processes

According to our previous discussion, a major disadvantage to using homogeneous Fenton processes for wastewater treatment is that, after the reaction is over, Fe must be extracted from the water, a process that could be carried out easily on a large scale using a higher pH to

precipitate $\text{Fe}(\text{OH})_3$, which required further adjustment to neutral, which increased the process' overall cost. Due to this issue, heterogeneous Fenton processes are used, in which, Fe supported in a solid state and can be recovered after water treatment. Homogeneous Fenton reactions have an additional drawback, which requires a pH between 2-4 during water treatment. As a result of overcoming these challenges, supported Fenton catalysts are becoming more popular.

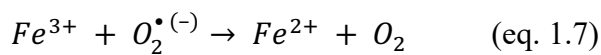
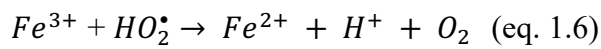
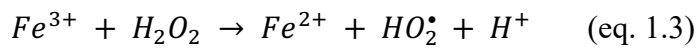
The use of solid catalysts can eliminate or reduce deficiencies by:

- (i) Enhancing the reaction rate, adsorption of organic compounds on solid surfaces increases reactivity; thereby, increasing radical species concentration near the catalyst's surface can improve – the concentration of radical species is crucial to the performance of the reaction.
- (ii) Managing effective local pH (in microporous systems, local pH within the pores may differ from the pH of the bulk solution) and preventing precipitation of iron hydroxide (in response to an electric field, for instance, within zeolite channels).
- (iii) Protecting active sites (such as Fe and Cu) from complex formation and deactivation (assuming the active sites lie within channels of zeolite and not easily accessible by larger compounds in solution).
- (iv) Allows selective attack of desired molecules (thereby improving the effectiveness of H_2O_2). It is still to be explored in the literature, but it is essential selectively removing certain compounds.

An additional reason to use solid catalysts, albeit unstudied, is suggested in relation to equations (2) – (8) indicating the role of the redox $\text{Fe}^{3+}/\text{Fe}^{2+}$ or $\text{Cu}^{2+}/\text{Cu}^+$ cycle in Fenton mechanism, stating in view of the stability of the reduced oxidation state it would be desirable to start with Fe^{2+} or Cu^+ ions directly involved in producing HO^\bullet (eq 2).⁹⁸ It is possible to stabilize the reduced transition metal oxidation states by stabilizing highly dispersed Fe or Cu ions in appropriate microporous supports. Zecchina has reported that Fe^{2+} ions could be stabilized by interacting with the ZSM-5 zeolite framework.⁹⁸

Figure 1.3a illustrates the differences between homogeneous and heterogeneous Fenton catalysts from the efficiency perspective. A comparison is made between homogeneous (Fe^{3+} -salt) and heterogeneous catalysts (Fe-ZSM-5) in Total Organic Carbon (TOC) removal over oxidation of *p*-cumaric acid. The removal of TOC, mg C L^{-1} (mg of carbon per L) is a reliable indication of *p*-cumaric acid conversion due to the rapid and comparable reaction rates in

homogeneous and heterogeneous processes. A clear result shows that TOC conversion occurs within 1 h of the reaction (corresponding to 5 mmol H₂O₂ added). The TOC conversion for the homogeneous Fenton catalyst is stopped, unlike the heterogeneous Fenton catalyst (Fe-ZSM-5). In contrast, the homogeneous reaction's initial rate tends to be higher than the heterogeneous reactions. Consequently, this occurs due to the complexation of Fe ions in solution with the reaction products (oxalic acid) and/or the reduction in the rate of Fe²⁺ generation (eq 1.3, 1.6 and 1.7).



As shown in Figure 1.3a, H₂O₂ is sequentially added to increase its utilization efficiency. A linear relationship between TOC removal and H₂O₂ addition is expected under conditions where H₂O₂ remains constant. The gradual decrease in the slope indicates a decrease in H₂O₂ efficiency, dropping from 90-95% (initially) to less than 50% after several hours. There is a slower slope in the homogeneous reaction in comparison with the heterogeneous reaction one hour later (approximately 5 mmol of H₂O₂ added) indicating that homogeneous systems use H₂O₂ less efficiently.⁶ WHPCO reactions rely on H₂O₂ efficiency. Despite this, little thought was given to the possibility that the solid catalyst might cause H₂O₂ to decompose into H₂O and O₂.

It is important to under lien though that the efficiency of using H₂O₂ is mainly determined by the reaction parameters, in particular, the amount of H₂O₂ added and the ratio between catalyst amount and volume of solution, due to the competition between HO[•] formation and organic compound attack, as illustrated in Figure 1.3b. Using either an extremely low catalyst/solution ratio or an extremely high addition rate of H₂O₂. In these cases, there will be a significant drop in H₂O₂ efficiency, resulting in a reduction in TOC removal.^{6, 99} Thus, choosing the right conditions is crucial to success. Using heterogeneous Fenton-type catalysts for wastewater treatment requires experimental and correct reactor design.

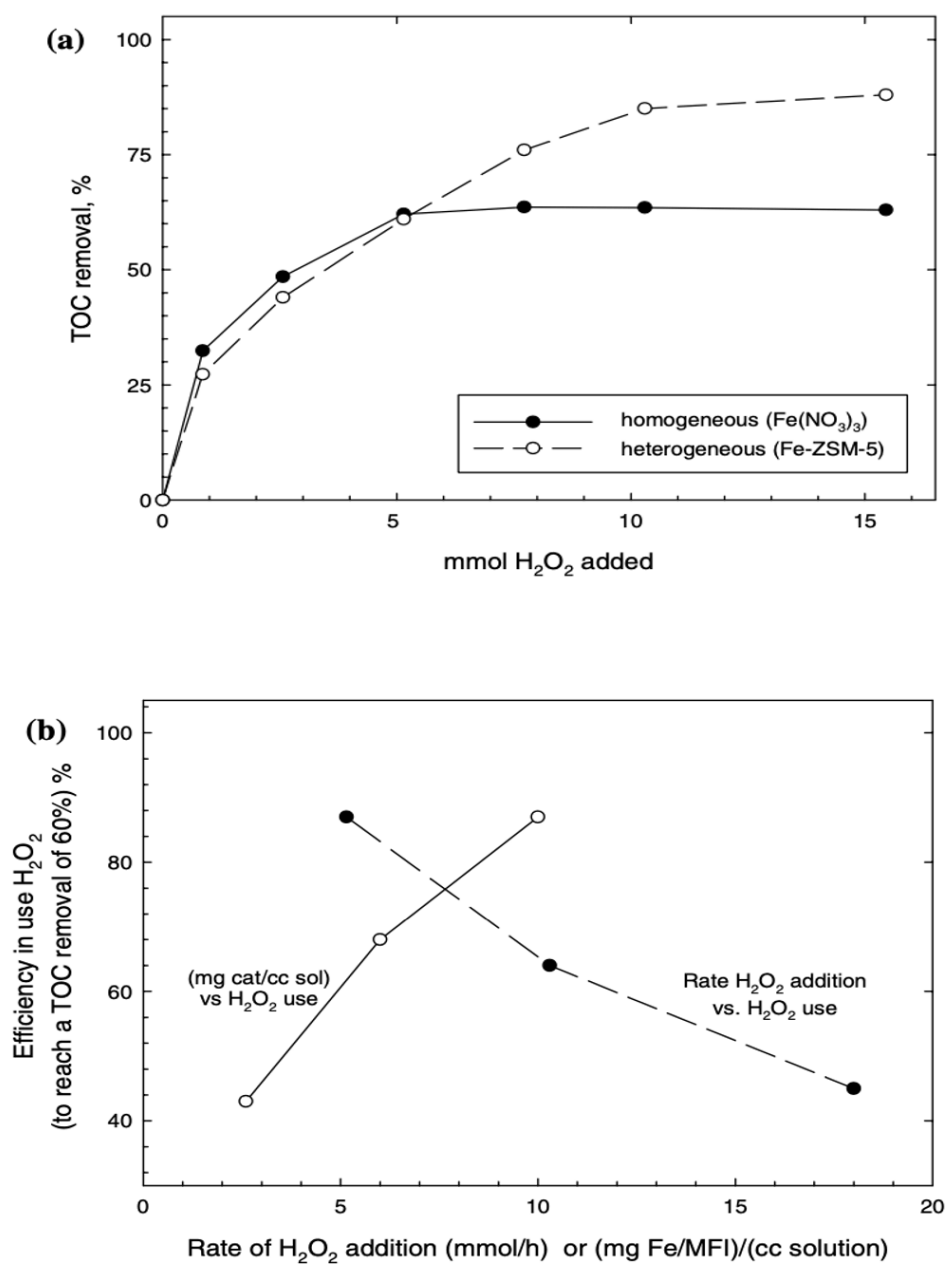


Figure 1.3: (a) Comparison of homogeneous catalysts ($\text{Fe}(\text{NO}_3)_3$ salt) with heterogeneous catalysts (Fe-ZSM-5) Fenton-type, based on the WHPCO removal of TOC from p-coumaric acid. Using the given parameters: 70 °C, pH = 4.8, H_2O_2 addition rate = 5.15 mmol·h⁻¹, the volume of solution for p-coumaric acid = 100mL (TOC initial = 330 mg C L⁻¹), Fe-ZSM-5 (1g) with 1.2% iron loading or a similar molar amount of iron ions (iron-nitrate).

(b) using H_2O_2 addition rate (mmol·h⁻¹) to determine the efficiency of H_2O_2 to achieve 60% of TOC elimination. In addition, the catalyst/solution ratio (mg catalyst/cc solution). With permission.

In WHPCO processes, extending the pH range of the applicability of the degradation method may be possible with solid catalysts. In the homogeneous process, at a narrow pH value, the maximum activity was observed. Compared to the homogeneous process, catalytic activity

showed less sensitivity to the pH parameter. Using pH levels lower than 2.5 or above 5.5 is possible, in contrast to the homogeneous process. Therefore, solid, heterogeneous, specifically Fenton catalysts, can provide a wider pH range.¹⁰⁰ Then again, there is a major challenge to heterogeneous Fenton systems. Ideally, Fenton catalysts would not leach iron, but most of heterogeneous catalysts show evidence that iron is leached during reaction. As a result, this problem accounts for the decrease in efficiency over time and results in metal ion pollution.⁵⁷ This project specifically aims to tackle and ideally solve this issue.

In the design of heterogeneous catalysts, the nature of the active species, or metal active center, is always the primary consideration. Meanwhile, in the CWPO process, multiple oxidation states of metal are required to produce hydroxyl radicals from H₂O₂. Fe (a key component in the Fenton reagent), which can activate H₂O₂ (see Eq.2), controls the efficiency of pollutant degradation in CWPO through the formation of hydroxyl radicals. In addition, metal species (referred to as Fenton-like reagents in the presence of H₂O₂ in aqueous solution) can also be active species due to their ability to decompose H₂O₂ to generate free radicals (Figure 1.4).¹⁰¹

Many common active species, including Ag,¹⁰² Au,¹⁰³ Ru,¹⁰⁴ Pt,¹⁰⁵ Ce,¹⁰⁶ Cr,¹⁰⁷ Mn,¹⁰⁸ and Cu,¹⁰⁹ can decompose H₂O₂ to radicals, individually or in combination have been reported.¹¹⁰ However, precious metal catalysts (like Ag, Au, Pt) are susceptible to poisoning during oxidation, in addition to their high cost, limiting their use.¹¹¹ Therefore, earth-abundant transition metals and their oxides have been the focus of recent research because of their high activity and stability, economic cost and mining availability, and resistance to deactivation. The literature confirms that phenol can be completely removed from water by many non-precious metal catalysts, including Cu, Fe, Mn, Co, and Ni. In the phenol oxidation process, all of these catalysts demonstrated high activity. In particular, copper and iron-based catalysts are more active and often used in Fenton oxidation due to their higher ability to generate hydroxyl radicals.⁸⁴ Fe is often considered superior to Cu as a catalyst for Fenton-like reactions because Iron is considered more environmentally friendly than copper, which can be toxic to aquatic life in elevated concentrations. The EPA has established an action level of 1.3 mg.L⁻¹ for copper in drinking water.¹¹² This is not a regulatory limit but rather a level at which water utilities must take action to control copper corrosion in distribution systems to prevent copper levels from exceeding this value at consumers' taps. In contrast, Fe is an essential nutrient for humans and most living organisms. The use of iron-based catalysts in Fenton reactions is often preferred in environmental remediation and wastewater treatment to minimize the potential for adverse ecological impacts. Furthermore, Fe is more abundant and cost-effective than Cu,

making it a practical choice for large-scale applications in water treatment and pollutant removal.

An important factor that determines catalytic activity is the support type. In this regard, a comprehensive discussion of using zeolites and activated carbon compared to others as solid catalysts for the Fenton reaction is presented.

1.10 Solid catalysts for Fenton reaction

Heterogeneous catalysis relies on supports because, without them, supported species may sinter and aggregate into bulks, resulting in low dispersion causing reduced catalytic performance, as schematised in Figure 1.4. At the same time, using support for dispersing the metal increases the surface area and extends the lifetime of the catalyst. Furthermore, metal-support interactions can be enhanced, thus impacting catalyst efficiency.¹¹³ Therefore, selecting suitable support plays an important role in catalyst design.

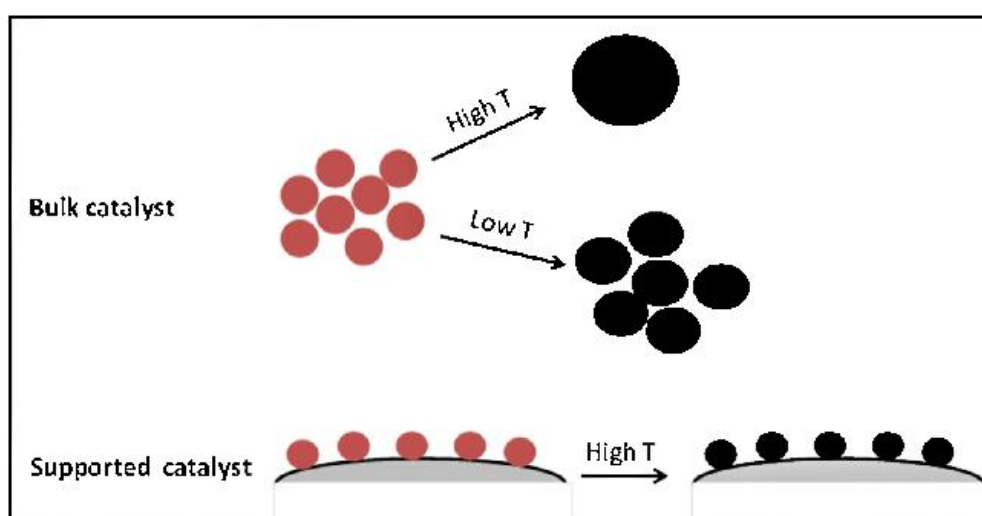


Figure 1.4: A schematic illustration showing how temperature affects catalyst particle size. Since the red points and black points represent metal ions and metal oxides respectively, their growth indicates aggregation of metal oxides.¹¹⁴ With permission.

Additionally, an effective catalyst support needs to meet a number of criteria.¹¹⁵ Physical and mechanical resistance is required to maintain their performance under high temperatures, pressures, and stresses over time. The catalyst should interact sufficiently with the active

species to guarantee the best physical dispersion and mechanical stability. However, generally speaking it should not react in a way that results in the catalyst losing its effectiveness or by promoting undesired parallel reactions. Nonetheless, it is advantageous if the support can enhance the desired reaction, for example, by imposing geometrical constraints, like in zeolites, by supplying acid centres of different nature, or by stabilizing one metal oxidation state over another. Other factors to be considered are the textural properties like porosity and surface area of the support should be sufficient to facilitate a facile reaction. The pores in the support should be minimally resistant to diffusion. If possible, it would be beneficial if the support was relatively inexpensive as well.

Generally speaking, though, despite the existence of tens of support articles in literature, relatively few of them meet all of these criteria simultaneously. There are different types of catalyst support, including zeolites,^{116, 117} activated carbon,^{118, 119} pillared clays,^{78, 120} and metal oxides,^{121, 122} they are used in practice for the heterogeneous Fenton reaction. Zeolites are well known for their unique properties, which include large surface areas, controllability of the number and strength of acid sites, high adsorption capacities, and selective adsorption of organic compounds that are smaller in size. Several studies have shown that iron-containing zeolites exhibit strong catalytic activity in the oxidation of phenol.¹²³

1.10.1 Zeolite catalysts for the CWPO reaction

1.10.1.1 Structure

Zeolite, first identified in 1756, was coined by the Swedish scientist Axel Fredrik Cronstedt to define stilbite, the first categorized zeolite mineral. 'Zeolite' is a Greek word composed of 'zeo', which means 'to boil', and 'lithos', referring to 'a stone'.¹²⁴ Essentially, this refers to zeolites' ability to release and absorb water according to the temperature and humidity of their surroundings.⁸⁴ Zeolites consist of microporous aluminosilicate frameworks, ultimately forming crystals, which consist of intertwined silica $[\text{SiO}_4]^{4-}$ and alumina $[\text{AlO}_4]^{5-}$ connected by oxygen atom bridges, resulting in a three-dimensional structure with equally sized pores ($0.3 < \text{diameter} < 1.2 \text{ nm}$ for the micro-pour range).¹²⁵ Even though silicon tetrahedra possess a neutral charge, Al tetrahedra possess a negative charge within the zeolite framework, which is subsequently balanced through cations outside the framework, such as K^+ , Mg^{2+} , Na^+ and NH_4^+ , in addition to H^+ . In zeolites, the proton shows strong Brønsted acidity, comparable to the acidity of 100% H_2SO_4 (Figure 1.5).¹²⁶

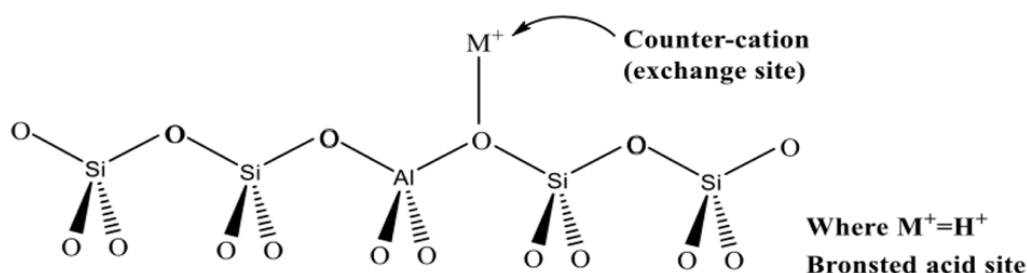
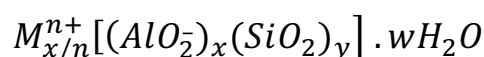


Figure 1.5: The structure of the zeolite and the formation process of the Brønsted acidity due to adding Al into the framework.¹²⁶

According to the International Union of Pure and Applied Chemistry (IUPAC), materials have the following pore sizes:

- Microporous (with a diameter less than 2 nm).
- Mesoporous (diameters of 2-50 nm).
- Macroporous (diameter greater than 50 nm).

Zeolites can cover all of these ranges depending on the micropore dimension, zeolites can be classified as small, medium, and large based on the number of oxygen atoms 8, 10 and 12, respectively. Different pore sizes show different properties of zeolite. Zeolite frameworks of various pore structures and densities can be produced by optimizing reaction conditions regarding the reaction temperature, Si:Al (or alternatively $SiO_2:Al_2O_3$) ratio, and template type. Chemically, zeolites can be described as follows:



Assuming that M represents the exchangeable cation typically belonging to Group I or II (like Na^+ , K^+ , Ca^{2+} , H^+), however, other metal, organic, and non-metal cations can also balance the negative charge created by Al, (n) represents the valence of the cation, (w) is the quantity of

water per unit cell, $(x + y)$ represents the number of tetrahedra per unit cell, and x/y is the framework silicon/aluminium ratio simply Si:Al or in the alternative, the $\text{SiO}_2:\text{Al}_2\text{O}_3$ ratio, which should be greater than 1 or 2 respectively.¹²⁷

By modifying the Si:Al ratio of the zeolite, certain properties can be altered, including hydrophilicity, acidity, and density. Due to their adjustable properties, they can be used for a variety of industrial applications, for example, remediation systems for the environment, water and wastewater treatment, soil remediation, and air filtration.¹²⁸ Additionally, adsorption properties in zeolites can be used to remove heavy metal cations such as Cd, Pb, Ni, Mn, Zn, Fe and Cu.¹²⁹ Most commonly, they are used in heterogeneous catalysts as well as ion exchange materials for decontaminating wastewater and water.¹³⁰ The term molecular sieve is also used to describe zeolites. Some minerals occur naturally (identified by a framework of codes to distinguish them, e.g. CHA, FAU, MOR). Meanwhile, most frameworks are synthesized (for example, MFI, BEA, and LTA). In this project two types of zeolites have been used, ZSM-5, framework code: MFI and Zeolite-Y their framework FAU. Currently, over 200 unique zeolite frameworks are identified, while over 40 natural zeolite types exist, according to the International Zeolite Association (IZA).¹³¹

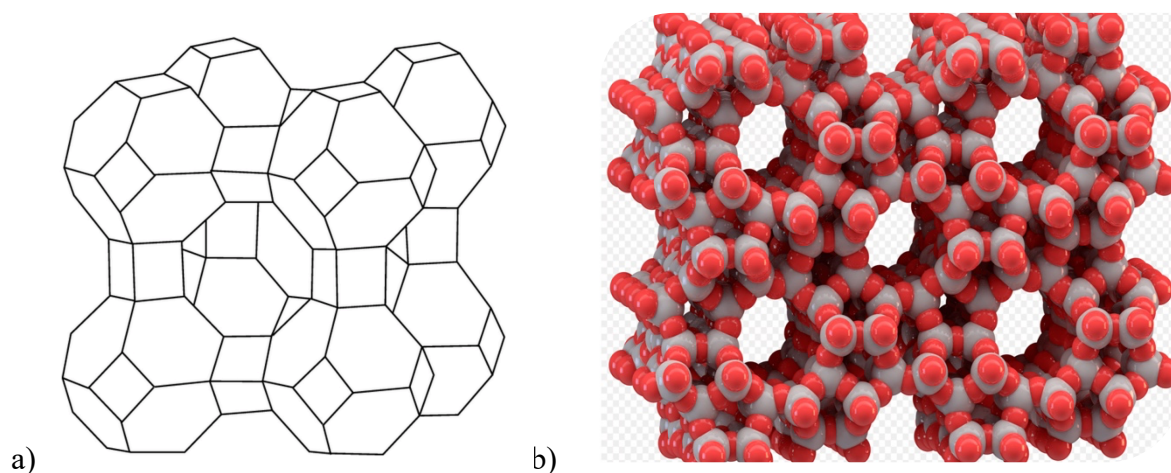


Figure 1.6: The framework of a) zeolite-Y and b) ZSM-5.¹³¹

1.10.1.2 General properties of zeolites

In the first place, zeolites have a large surface area. Fundamentally, increasing the surface area of solid catalysts while reducing metal particle size leads to improved catalytic performance.¹³² Moreover, the surface area of the catalyst corresponds to the production of catalysts when an adsorbent serves as the catalyst support substrate. Due to the fact that it provides a larger surface area per unit mass of catalyst.¹³³ According to Satterfield, zeolites have a surface area that is roughly 500-800 m².g⁻¹.¹³⁴ Vermuelen reported the amount of surface area between 600 to 700 m².g⁻¹.¹³³ The porous structure of zeolites makes them ideal for applications like catalysis and adsorption.¹³⁵ Shape-selective pores control the access of reactants and products by exerting steric influence as well as an orientation effect to reagents, products or intermediates and in turn on the reaction. As well as changing the geometry of the pore structure, it is also possible to fine-tune zeolites by modifying the structure's composition by modifying the Si:Al ratio and cation composition by ion exchange of cations. Zeolites' specific properties are, in part, responsible for their catalytic properties, and modifying their composition and structure makes it possible for different properties to be obtained. The various types of zeolites, including natural and synthetic, have been investigated in the CWPO of phenol.¹³⁶ For instance, zeolites with different frameworks and pore sizes were investigated for their ability to degrade phenol.¹³⁷ Depending on their pore size, zeolites can be categorized as microporous as described above (pores smaller than 2 nm) and mesoporous (pores between 2 and 50 nm) zeolites; these include ZSM-5 (pore diameter of 5.4–5.6 Å, that is, 0.54–0.56 nm) zeolites, as well as SBA-15 (pore size of 5-15 nm) respectively.

In chemical reactions, pore size and distribution of catalyst or support can have a significant impact. Aside from this, the pore structure allows for more surface area for the active sites to disperse uniformly, whereas the metal dispersion is somewhat dependent on the reaction rate. In addition, pore size distribution also affects reaction selectivity. Microporous catalysts may be useful for selectively reacting with small molecules mixed with larger molecules because larger molecules are incapable of passing through the micro-pores. Conversely, macro porous catalysts would be more suitable for large reactant molecules. As an example, Calleja examined different iron-supported zeolites in the CWPO of phenol under the same reaction conditions, including Fe-SBA-15, amorphous SiO₂-Fe₂O₃ mixed oxide and Fe-Silicalite-1.

According to these literature data, the Fe₂O₃-supported mesostructured SBA-15 catalyst achieved the best results, eliminating aromatic compounds completely 100% with TOC decreases of 70% within 10 minutes.¹³⁶ This could be explained by the larger pore size, making

organic matter more accessible to iron sites. As well, Vakaj studied the performance and stability of Cu-Y5 and Cu-ZSM-5 zeolites in the oxidation of phenol using hydrogen peroxide. A study found that Cu-Y5 catalyst activity gives 99% phenol conversion at 60 °C, which was more efficient than that of Cu-ZSM-5 produces 66% phenol conversion at 60 °C) due to its ability to catalyse phenol oxidation more effectively, which is because molecules in the Cu-Y5 catalyst have a lower resistance to diffusion/mass transfer.¹³⁸

Moreover, different ratios of Si:Al in zeolite catalysts, in the form of $\text{SiO}_2:\text{Al}_2\text{O}_3$ or Si:Al, have been investigated extensively. Accordingly, silicon is mostly responsible for maintaining the molecular sieve framework since it makes up most of the framework. Meanwhile, alumina offers acid sites, so varying the Si:Al ratio can result in different results. The acidity of zeolites is one of their key properties, making them useful for catalysis. A wide range of Si:Al ratios have been investigated in zeolites, including pure silica zeolites since they are always more thermally stable. Among them, Chen evaluated the three catalysts, Fe-ZSM-5-1 (Si:Al of 181), Fe-ZSM-5-2 (Si:Al of 37), Fe-ZSM-5-3 (Si:Al of 21,) which were synthesized by incipient-wet impregnation and used as a catalyst in the CWPO reaction of cresol at 30 °C. As a result, among these three catalysts, Fe-zeolites showed the following catalytic activities: Fe-ZSM-5-3 > Fe-ZSM-5-2 > Fe-ZSM-5-1, which suggests an important role for Si:Al ratio in cresol degradation. According to the authors, the difference is explained by the lower Si:Al ratio of the zeolite accelerating HO^\bullet generation.¹³⁹ In addition, Cihanoğlu examined the degradation of acetic acid over catalysts using H_2O_2 at 60 °C. In his study, Fe-ZSM-5 zeolite catalysts with various Si:Al ratios (12.4-42.0) were synthesized using an ion exchange process. The different Si:Al ratios of the zeolite catalyst affected all properties, including the iron content, Brønsted acidity and catalytic activity. Besides cresol and acetic acid, formic acid decomposition was also influenced by the Si:Al ratio of zeolite.¹⁴⁰ Based on Taran's findings, Cu-ZSM-5 zeolites (Si:Al ratio of 17, 30 and 45) produced by ion exchange exhibited different performances in formic acid elimination. Optimal catalytic activity occurs with catalysts based on zeolite with a Si:Al ratio of 30, while the lowest activity occurs with a Si:Al ratio of 17.¹⁴¹

As a result, zeolites have attracted considerable attention, particularly in the field of heterogeneous catalysts. This is due to their unique properties. Zeolite Y, as an example, plays an important role in heterogeneous catalysis, such as fluid catalytic cracking.¹⁴² Additionally, ZSM-5 shows promise for wet oxidation of phenol by H_2O_2 in Fenton reactions.^{109, 143}

ZSM-5 and Zeolite Y are commercially available, making them easily accessible for researchers. This availability facilitates experimentation and testing in various applications. In addition, ZSM-5 and Zeolite Y exhibit versatile properties that make them suitable for a broad range of applications. Both ZSM-5 and Zeolite Y are known for their catalytic activity. They have been extensively studied for their use as catalysts in various chemical reactions, including those in petrochemical and refining industries. These zeolites are acidic, making them effective catalysts in acid-catalysed reactions. This characteristic is valuable in processes such as cracking and isomerization. ZSM-5, in particular, is known for its shape-selective catalysis, which means it can discriminate between molecules based on their size and shape.

1.10.2 Activated carbon for the CWPO reaction

1.10.2.1 Structure

Another class of materials that can be used as a support for our catalysts for the abatement of phenol is activated carbon. Charcoal, the predecessor of modern activated carbon, was the first adsorbent to purify water. Scheele first discovered the adsorptive properties of charcoal in 1773 for the treatment of gases, which led to the first systematic account of charcoal's adsorptive power in liquids. During the following years, from 1789 to 1790, Lowitz developed the charcoal technique for removing bad taste and odour from water. For introducing activated carbon to the world, the credit belongs to a Swedish chemist, von Ostrejko; in 1900 and 1901, he was granted two patents concerning the chemical and thermal (or physical) activation of carbon, first with metal chlorides and then with carbon dioxide and steam.¹⁴⁴

Activated carbon can be manufactured in two ways: through chemical and physical processes. For example, carbon burn-off improves the primary pore structure of the precursor material, resulting in the gasification of the carbon material and forming a porous graphitic network containing oxide groups. During the chemical activation of carbon, raw elements are activated between 600 and 800 °C. As an activator, H₃PO₄ or ZnCl₂ could be added before heating the raw material. In contrast, physically activated carbon is derived from the thermal decomposition of a carbonaceous precursor at temperatures between 600 and 800 °C while steam and/or CO₂ are present.¹³²

The term activated carbon (here abbreviated as AC) refers to carbon-based materials containing pore structures. Carbonaceous materials produce AC, including wood, coal, lignite, and coconut shells. AC has a high surface area, large porosity, well-developed internal pore

structure composed of micro-, meso- and macropores, as well as a wide spectrum of functional groups present on its surface, making it an extremely versatile material with numerous applications in many areas, but primarily in the field of environmental science.¹⁴⁵ A typical AC structure contains oxygen, hydrogen, sulphur, and nitrogen as functional groups or chemically bonded atoms. Several functional groups in the carbon structure generally account for the catalytic activity, including carboxyl, carbonyl, phenols, lactones, and quinones. A carbon surface's functional groups are mainly the result of the activation process, the precursor(s), the thermal treatment, and the post-chemical treatment. Surface functional groups can be modified through thermal or chemical treatments to enhance AC performance in removing specific contaminants.¹⁴⁶ Specific considerations on these groups will be done in chapter 3, section 3.1.1.

1.10.2.2 General properties of activated carbon

The CWAO has recently introduced activated carbon-based catalysts with promising results.¹⁴⁷ ¹⁴⁸ in particular, AC has been widely used as a solid catalyst support of the CWPO oxidation reaction for phenol.^{118, 149-151} The most distinguishing attributes of activated carbons (AC) are their large surface area and porosity, compared to other supports such as Al₂O₃, TiO₂, and CeO₂, in addition to oxygen groups on their surfaces, which may play a role in catalysis.¹⁵² AC has an exceptionally high surface area, typically 800 to 1200 m²·g⁻¹.¹⁵³ This large surface area provides ample sites for catalytic reactions, allowing for better contact between reactants and catalysts. In addition, AC is highly porous, with a complex network of micropores and mesopores. Pore volume distribution typically ranges between (0.9-1.3 mL·g⁻¹).¹⁵⁴ This porosity enhances its adsorption capacity and can help trap and concentrate reactants near the catalytic sites, improving reaction efficiency. The surface of AC can be modified to introduce various functional groups, such as -COOH, -OH, or -NH₂, enhancing its catalytic activity and selectivity for specific reactions. Also, the ability to be stable in both acidic and basic conditions is another crucial factor.¹⁵⁵ AC has strong adsorption properties can benefit certain catalytic processes, especially those involving gas-phase reactions. It can adsorb reactants and products, helping to shift the reaction equilibrium and improve yield.

Despite carbon's reputation as an inert material compared to other catalyst supports though, heteroatoms on its surface create active sites, making it not as inert as expected (O, H, N). In the preparation of catalysts, oxygen-containing groups are of particular interest. According to the literature, surface functional groups influence AC-supported catalyst activity.^{132, 152, 156}

Furthermore, it is relatively inexpensive compared to other support materials, making it an attractive choice for industrial applications. AC is environmentally friendly and can be easily regenerated and reused, reducing waste and environmental impact. By burning carbon support, they can recover metal active particles, though at the cost of re-introducing CO₂ to the environment. The performance of AC can be modified, and often improved by using different chemical treatment methods.¹⁵⁷ It is possible to change the physical and chemical properties of AC through various methods.¹⁵⁸ Literature reports describe different methods for modifying AC surfaces.¹⁵⁹⁻¹⁶² For example, oxidation treatment of AC is primarily used to produce surfaces rich in oxygen-containing surface groups, increases the acidity, reduces mineral content, and enhances hydrophilicity. Indeed, these oxygen surface functional groups may be beneficial to our case to prevent metal active species leaching, which is the main issue associated with the heterogeneous catalyst. The most widely studied acids are nitric acid and sulfuric acid.¹⁶³

Surface chemistry modifications resulted in significant changes in loading capacity and catalytic efficiency.¹⁶⁴ To reduce the mineral matter content of activated carbons, non-oxidant acids such as HCl and HF are frequently used.^{165, 166} According to the amount and nature of minerals and their distribution within the carbon matrix, the demineralization step alters the sample's surface area and porosity because the minerals block a part of the pores. Nevertheless, acid treatment may modify the surface area and porosity of the sample independent of changes induced by mineral removal. This is a method extensively used in this thesis work (see chapter 3, sections 3.1.1).

The study conducted by Rey and his team reported that the CWPO of phenol has been tested using different activated carbon-supported Fe catalysts. The porous structure and surface composition of these catalysts have influenced their performance in CWPO in terms of oxygen groups and Fe distribution. In comparison to catalysts with an internal or external distribution of Fe, those with a more uniform distribution displayed higher oxidation activity. In less than 2 hours, the best catalyst achieved complete phenol conversion and almost 80% mineralization.¹¹⁸ Another study by Messele report that iron-supported activated carbon catalysts enhanced the catalytic activity towards phenol degradation. It is possible to convert phenol above 95 % using this catalyst for 120 minutes of reaction with stoichiometric hydrogen peroxide. The Fe load strongly affects phenol conversion and TOC removal. Moreover, the recycling and subsequent reutilization of the catalyst resulted in nearly the exact phenol conversion as with fresh catalysts.¹⁶⁷ To expand the scope of this synthesized catalyst, further

studies are needed with done in this work. As a drawback though, they may already naturally contain traces of metals (alkali especially). As a result, there is the possibility that some batches of carbon will behave differently, which means some may work well for one application, but another might behave differently. That is in some cases a limited reproducibility due to inconsistencies in the carbon precursor structure.¹³²

1.10.3 Pillared clays

In wastewater treatment, pillared clay minerals, or pillared interlayered clays (PILCs), have found a number of applications in the literature as heterogeneous catalysts.^{26 168, 169} Barrault found that 80% of phenol was converted through 120 minutes of use of Al/Fe-PILCs in CWPO for phenol elimination from wastewater.¹⁰⁰ Clays are considered eco-friendly solid catalysts and they have many benefits, they are largely available, cheap, simple to recover, and highly ion exchangeable. although with a limited surface area of 134 - 362 m².g⁻¹.¹⁷⁰ Pillaring agents, such as Aluminum polycations (e.g. Al₃O clusters) Pillaring with aluminum polycations can improve the thermal stability, acidity, and catalytic activity of clay minerals. These materials are catalysts in hydrocracking, isomerization, and other petrochemical processes. Pillared clays with zirconium oxide nanoparticles (ZrO₂) exhibit enhanced adsorption properties and are used to remove heavy metals and organic contaminants from wastewater, can be used to improve natural clay minerals has emerged as a promising method for opening clay layers, producing high resistance and thermal stability, and increasing the porosity and surface area.²⁶ During the pillaring process, inorganic particles are incorporated into clay minerals in the interlayer region, resulting in oxides strongly bonded between layers. Al, Fe, Zr, Cr and Ti are inorganic pillaring agents (hydroxyl polycations) extensively studied.¹⁷¹ However, a major disadvantage of employing PILCs is that they can be attacked by using high levels of H₂O₂, and they suffer from a low batch-to-batch reproducibility Because of this, commercialization at the industrial scale has been limited so far.

Furthermore, pillared clays typically have lower acidity and catalytic activity compared to zeolites, which are known for their strong acid sites.¹⁷² This limitation can affect their performance in acid-catalysed reactions. As in our case, the acidity of the zeolite can influence the reaction pathway, kinetics, and selectivity. Hence, the acidity of Fe-ZSM-5, for example, provides active sites on the catalyst's surface. These acid sites can facilitate the activation of H₂O₂ molecules, leading to the generation of ·OH. In addition, the acidity of Fe-ZSM-5 can influence the reaction pathway for phenol oxidation. Depending on the strength and distribution of acid sites, different reaction pathways may be favoured. For instance, strong acid sites may

promote the formation of hydroxyl radicals, while milder acid sites may facilitate the formation of other intermediates. The specific pathway can impact the selectivity of the reaction, determining which by-products are formed. The strength and density of acid sites can affect the reaction kinetics. Catalysts with a higher acidity may exhibit faster reaction rates due to more efficient H₂O₂ activation and phenol adsorption. This can impact the overall efficiency of the catalytic process. The other drawback is that Pillared clays can be sensitive to reaction conditions, such as temperature and pressure, limiting their applicability in certain catalytic processes.

Zeolites, on the other hand, are often more robust under varying conditions. Regarding diffusion limitations, the pillaring process can sometimes lead to mesopores and macropores in the clay structure, resulting in diffusion limitations for reactants and products. Zeolites, with their well-defined microporous structure, generally have limited diffusion effects. While pillared clays can have tenable pore sizes to some extent, they may not offer the same precise control over pore size distribution as zeolites.¹⁷³ Zeolites are known for their uniform and well-defined pore structures. Further, Pillared clays can be prone to catalyst deactivation due to factors like pore blockage or coke formation. Zeolites, instead depending on the specific type, may exhibit better resistance to deactivation.¹⁷⁴

In view of all these factors, pillared clays will not be considered any further in this thesis work, though it was important to present a perspective of the materials that can be potentially used for our projects and, as such, describe them by weighing their pros and cons.

1.10.4 Metal oxides

In many reactions, notably heterogeneous catalysts, metal oxides are widely used either as catalysts, both in bulk or nanoparticulate over a support, or as a support themselves.¹⁷⁵ Metal oxide has also been used as a catalyst in CWPO of phenol in several studies.¹⁷⁶⁻¹⁷⁸ This because metal oxides, if belonging to earth abundant materials, are relatively less expensive than noble metals, and their catalytic activity often relies on the mobility of oxygen atoms within their structures. This property is known as "oxygen mobility," and it plays a crucial role in several catalytic processes.¹⁷⁹ Metal oxides with oxygen mobility are used in a wide range of catalytic reactions, including the oxidation of hydrocarbons,¹⁸⁰ water-gas shift reactions,¹⁸¹ catalytic combustion,¹⁸² and various redox reactions,¹⁸³. In these reactions, oxygen mobility enables the efficient transfer of oxygen species between the catalyst and reactants. Metal oxides consist of metal cations (positively charged ions) and oxygen anions (negatively charged ions). Oxygen

mobility creates vacancies. locations within the crystal lattice where oxygen atoms are missing. These vacancies can occur due to the reduction of the metal oxide or as a result of catalytic reactions. Oxygen mobility allows for redox (reduction-oxidation) reactions to take place on the catalyst's surface. In catalytic processes, reactant molecules can adsorb onto the metal oxide surface, and oxygen atoms from the oxide lattice can migrate to the surface to participate in reactions.¹⁸⁴ This oxygen migration facilitates the transfer of electrons between reactants, enabling the conversion of reactants into products by enhancing the adsorption and activation of reactant molecules. During the catalytic reaction, oxygen atoms can migrate from oxygen vacancies to the reacting species and then return to oxygen vacancies when the reaction is complete. This cyclic process allows the metal oxide to act as a catalyst,¹⁸⁵ with an overall process though that is often temperature-dependent. In our case, we expected to form Fe₂O₃ and FeO due to the wetness impregnation catalyst's preparation method.

1.11 Aim of the project

In this project, zeolites and activated carbon will be used as support for active iron species to carry out the decomposition of phenolic compounds using a catalytic wet hydrogen peroxide oxidation (CWPO). This is to obtain materials capable of mineralizing phenol and phenolic compounds up to CO₂ and water under mild conditions (endogenous pressure and T around 80 °C) and, notably obtaining materials capable of retaining Fe over the catalyst surface and, in turn, having durable and reusable catalysts.

During the past few years, activated carbon (AC) has become more popular as a catalyst support material because of its unique properties, including its stability in acidic and basic media. Moreover, AC is easily used to stabilise precious or heavy metals,¹⁸¹ due to its high thermal stability, low cost, and wide availability, as well as its porosity, which allows Fe centres, radical species, and substrates to be brought into proximity. Having the latter property is crucial for maximizing the performance of Fenton systems. Additionally, they exhibit both hydrophilic and hydrophobic features.^{144, 182} These properties might prove helpful in systems like ours, where there is an organic substrate (partially hydrophobic) and a water medium (hydrophilic). The drawback of activated carbon as catalyst support, though, is the existence of minerals formed during its preparation or derived from its sources (e.g. coal, coconut shell, wood). Furthermore, activated carbons often contain a high level of ash (the presence of ash is a property of activated carbon). High levels of ash reduce the effectiveness of AC, which must be washed before catalytic application.^{53, 183, 184} Non-oxidant acids such as HCl and HF are

commonly used to reduce the mineral content of activated carbon.^{158, 185} In this work, HCl has been used.

When preparing catalysts, oxygen-bearing groups are crucial for depositing heavy metals. Catalysts supported on AC exhibit significant activity depending on their surface functional groups.^{127, 186, 187} A carbon surface's acidic and essential characteristics determine its surface chemistry, which can be altered by treating it with oxidizing agents. Oxidation of activated carbons with HNO₃ oxidant acid is expected to result in generating a large number of surface functional groups such as carbonyl, carboxyl, and nitrate groups.¹⁵⁷ This may enhance the Iron binding and increase the wettability of AC which is more advantageous to the reaction in water media, which will enhance the catalyst's durability and effectiveness. Surface chemistry and porosity can also be affected, in addition to removing metals.¹⁸⁸⁻¹⁹⁰

For this reason, Fe/AC catalysts prepared via three different types of AC (NORIT 1240; SA2; DARCO, G60) to understand the changes in surface chemistry that occur as a result of pre-acid treatments with HCl and HNO₃, as well as their extended effect on catalytic activity for phenol oxidation.

Several recent studies have demonstrated that N and S doping enhances Fe/AC catalyst stability and catalytic activity.¹⁹¹⁻¹⁹³ N and S atoms may enhance catalytic activity by increasing Fe²⁺ on the iron oxide surface, thereby preventing Fe leaching.¹⁹¹ Doping N or S can generate complexes with Fe species and form new active sites on the carbon surface. These sites influence acidity, hydrophilicity, and electron transfer properties. Consequently, this work modified Fe/AC catalysts by doping S and N. Wet impregnation methods to prepare Fe-S-N/AC catalysts using three different kinds of AC (NORIT 1240, SA2, G60) under raw-AC and pre-treated by acids.

Then, we moved from activated carbon as catalyst support for Fe species to zeolites. Both are well-known supports and widely used in water treatment.^{138, 194-196} In general, the most attractive properties of zeolite are having a high surface area, a high adsorption capacity, shape-selective properties, and strong acidity containing both Brønsted and Lewis acid sites. Further, it is adjustable in terms of hydrophobicity and hydrophilicity by different Si:Al molar ratios. It is believed that zeolites, which include transition metals, are the most efficient CWPO catalysts. In recent years, considerable research has been carried out on Fe-containing ZSM-5 catalysts that are very active at a wide pH range for oxidising organic pollutants using peroxide.

In Fenton reactions, ZSM-5 is a promising catalyst for wet oxidation of phenolic compounds by H_2O_2 .

The primary problem with these catalysts arises from the leaching of the Fe active phase during the oxidation process. As a solution to this problem, and since heterogeneous catalysts have different catalytic properties depending on the particular technique used to prepare them, the project will study preparation methods of Fe-ZSM-5: incipient wetness impregnation and vacuum wetness impregnation technique. The effects of the preparation method and different variables including different zeolite types (ZSM-5 and Zeolite-Y) and different Si:Al molar ratios (80, 50 and 23) on catalytic performance will be discussed with the aim of obtaining higher stability and catalytic activity for phenolic compounds oxidation. Ultimately, in order to expand applications for these catalysts, they were applied to the oxidation of five different phenolic compounds.

Furthermore, a characterization of the catalysts will be carried out with the aim to identify structure activity correlations with respect to: (i) phenol conversion, (ii) extent of H_2O_2 decomposition, (iii) mineralization to CO_2 and H_2O , and importantly (iv) Fe leaching. In this project using various techniques, such as XRD for crystal structure, XPS to determine the oxidation state of supported metal ions and BET for the surface area as well as elemental analysis which is valuable for studying the changes in catalyst composition and structure during preparation and the reaction.

1.12 References:

1. T. Hák, S. Janoušková and B. Moldan, *Ecological indicators*, 2016, **60**, 565-573.
2. S. FUND, Available at this link: <https://www.un.org/sustainabledevelopment/inequality>, 2015 (accessed September 2023).
3. J. G. Hering, S. Maag and J. L. Schnoor, *Journal*, 2016, **50**, 6122-6123.
4. S. Affairs, *The Sustainable Development Goals: Report 2022*, UN, 2022.
5. M. Soto-Hernández, M. P. Tenango and R. García-Mateos, *Phenolic compounds: natural sources, importance and applications*, BoD–Books on Demand, 2017.
6. S. Perathoner and G. Centi, *Topics in Catalysis*, 2005, **33**, 207-224.
7. I. G. García, J. B. Venceslada, P. J. Pena and E. R. Gómez, *Water Research*, 1997, **31**, 2005-2011.
8. N. Jusoh and F. Razali, *J. Teknol*, 2008, **48**, 51-60.
9. A. Mohd, *International Journal of Environmental Analytical Chemistry*, 2022, **102**, 1362-1384.
10. C. I. Nair, K. Jayachandran and S. Shashidhar, *African journal of biotechnology*, 2008, **7**, 25.
11. R. Gingell, J. O'Donoghue, R. J. Staab, I. W. Daly, B. K. Bernard, A. Ranpuria, E. J. Wilkinson, D. Woltering, P. A. Johns and S. B. Montgomery, *Patty's Toxicology*, 2001.
12. G. Busca, S. Berardinelli, C. Resini and L. Arrighi, *Journal of hazardous materials*, 2008, **160**, 265-288.
13. R. S. Davidson, *Journal of Photochemistry and Photobiology B: Biology*, 1996, **33**, 3-25.
14. Y. Tsuruta, S. Watanabe and H. Inoue, *Analytical biochemistry*, 1996, **243**, 86-91.
15. A. Toms and J. M. Wood, *Biochemistry*, 1970, **9**, 337-343.
16. W. W. Anku, M. A. Mamo and P. P. Govender, *Phenolic compounds-natural sources, importance and applications*, 2017, 419-443.
17. O. Daniel, M. S. Meier, J. Schlatter and P. Frischknecht, *Environmental Health Perspectives*, 1999, **107**, 109-114.
18. A. Careghini, A. F. Mastorgio, S. Saponaro and E. Sezenna, *Environmental Science and Pollution Research*, 2015, **22**, 5711-5741.
19. R. M. Bruce, J. Santodonato and M. W. Neal, *Toxicology and Industrial Health*, 1987, **3**, 535-568.

20. M. J. O'Neil, *The Merck index: an encyclopedia of chemicals, drugs, and biologicals*, RSC Publishing, 2013, **74**, 339.
21. J. Paasivirta, K. Heinola, T. Humppi, A. Karjalainen, J. Knuutinen, K. Mäntykoski, R. Paukku, T. Piilola, K. Surma-Aho and J. Tarhanen, *Chemosphere*, 1985, **14**, 469-491.
22. A. McBain, E. Senior, A. Paterson, C. Du Plessis and I. Watson-Craik, *South African Journal of Science*, 1996, **92**, 426-430.
23. M. M. Laine and K. S. Jorgensen, *Applied and Environmental Microbiology*, 1996, **62**, 1507-1513.
24. J. Ahmed, A. Thakur and A. Goyal, *Industrial wastewater and its toxic effects*, 2021, 1-14.
25. Y. Kurata, Y. Ono and Y. Ono, *Journal of material cycles and waste management*, 2008, **10**, 144-152.
26. J. Baloyi, T. Ntho and J. Moma, *RSC advances*, 2018, **8**, 5197-5211.
27. J. Montgomery-Brown and M. Reinhard, *Environmental engineering science*, 2003, **20**, 471-486.
28. H.-P. E. Kohler, F. L. Gabriel and W. Giger, *Chimia*, 2008, **62**, 358-358.
29. P. Patnaik and J. N. Khoury, *Water Research*, 2004, **38**, 206-210.
30. L. C. Kinney and V. R. Ivanuski, *Photolysis mechanisms for pollution abatement*, Federal Water Pollution Control Administration, 1969, **13**.
31. P. Operations, *Design of wastewater treatment facilities major systems*, Environmental Protection Agency, Office of Water Program Operations, 1979.
32. N. Schweigert, A. J. Zehnder and R. I. Eggen, *Environmental microbiology*, 2001, **3**, 81-91.
33. N. Schweigert, R. W. Hunziker, B. I. Escher and R. I. Eggen, *Environmental Toxicology and Chemistry: An International Journal*, 2001, **20**, 239-247.
34. M. Muñoz-de-Toro, C. M. Markey, P. R. Wadia, E. H. Luque, B. S. Rubin, C. Sonnenschein and A. M. Soto, *Endocrinology*, 2005, **146**, 4138-4147.
35. F. S. Vom Saal and C. Hughes, *Environmental health perspectives*, 2005, **113**, 926-933.
36. N. Schweigert, S. Belkin, P. Leong-Morgenthaler, A. J. Zehnder and R. I. Eggen, *Environmental and molecular mutagenesis*, 1999, **33**, 202-210.
37. L. Zhang, Y. Wang, N. Shang and M. T. Smith, *Leukemia research*, 1998, **22**, 105-113.

38. S. Lakshmi, M. Harshitha, G. Vaishali, S. Keerthana and R. Muthappa, *International Journal of Science, Engineering and Technology Research*, 2016, **5**, 2488-2496.
39. Z. Aksu and J. Yener, *Waste management*, 2001, **21**, 695-702.
40. A. Bhatnagar and A. Minocha, *Conventional and non-conventional adsorbents for removal of pollutants from water - A review*, 2006, **13**, 203-217.
41. L. Qalyoubi, A. Al-Othman and S. Al-Asheh, *Case Studies in Chemical and Environmental Engineering*, 2021, **3**, 100-102.
42. D. Karisma, G. Febrianto and D. Mangindaan, Removal of dyes from textile wastewater by using nanofiltration polyetherimide membrane, 2017, **109**.
43. A. Bódalo, E. Gómez, A. Hidalgo, M. Gómez, M. Murcia and I. López, *Desalination*, 2009, **245**, 680-686.
44. A. Mnif, D. Tabassi, M. Ben Sik Ali and B. Hamrouni, *Environmental Progress & Sustainable Energy*, 2015, **34**, 982-989.
45. P. Modak, *The textile industry and the environment, United Nations Environment Programme, Industry and Environment, Technical, Report*, 1994, **16**.
46. K. Watanabe, S. Hino and N. Takahashi, *Journal of fermentation and bioengineering*, 1996, **82**, 522-524.
47. E. J. Middlebrooks, *Wastewater stabilization lagoon desing, performance and upgrading*, Collier Macmillan, 1982.
48. C. Peitz and C. R. Xavier, *Revista Facultad de Ingeniería Universidad de Antioquia*, 2019, **92**, 60-69.
49. U. Jadhav, S. Salve, R. Dhawale, M. Padul, V. Dawkar, A. Chougale, T. Waghmode, A. Salve and M. Patil, *Textiles and Light Industrial Science and Technology*, 2013, **2**, 27-35.
50. Z. Aksu, *Application of biosorption for the removal of organic pollutants: a review, Process biochemistry*, 2005, **40**, 997-1026.
51. H. Xu, B. Yang, Y. Liu, F. Li, C. Shen, C. Ma, Q. Tian, X. Song and W. Sand, *World Journal of Microbiology and Biotechnology*, 2018, **34**, 1-9.
52. R. Amorati and L. Valgimigli, *Free radical research*, 2015, **49**, 633-649.
53. P. Cooper, *Colour in dyehouse effluent*, Society of dyers and colourists, 1995.
54. J. E. Wajon, D. H. Rosenblatt and E. P. Burrows, *Environmental Science & Technology*, 1982, **16**, 396-402.
55. M.-Y. Xu, Y.-L. Lin, T.-Y. Zhang, C.-Y. Hu, Y.-L. Tang, J. Deng and B. Xu, *Journal of Hazardous Materials*, 2022, **436**, 129195.

56. S. Masten and S. Davies, *Sci. Technol. Wol*, 1994, **28**.
57. G. Centi, S. Perathoner, T. Torre and M. G. Verduna, *Catalysis Today*, 2000, **55**, 61-69.
58. S. J. Masten and S. H. Davies, *Environmental science & technology*, 1994, **28**, 180A-185A.
59. J. J. Rueda Márquez, I. Levchuk and M. Sillanpää, *Catalysts*, 2018, **8**, 673.
60. O. Legrini, E. Oliveros and A. Braun, *Chemical reviews*, 1993, **93**, 671-698.
61. S. C. Ameta and R. Ameta, *Advanced oxidation processes for wastewater treatment: emerging green chemical technology*, Academic press, 2018.
62. F. Ross and A. B. Ross, *Selected specific rates of reactions of transients from water in aqueous solution. III. Hydroxyl radical and perhydroxyl radical and their radical ions*, Notre Dame Univ., IN (USA). Radiation Lab., 1977.
63. R. Andreozzi, V. Caprio, A. Insola and R. Marotta, *Catalysis today*, 1999, **53**, 51-59.
64. P. Gikas and G. Tchobanoglous, *Journal of environmental management*, 2009, **90**, 144-152.
65. P. R. Gogate and A. B. Pandit, *Advances in environmental research*, 2004, **8**, 501-551.
66. M. R. Hoffmann, S. T. Martin, W. Choi and D. W. Bahnemann, *Chemical reviews*, 1995, **95**, 69-96.
67. C. A. Murray and S. A. Parsons, *Chemosphere*, 2004, **54**, 1017-1023.
68. F. Wang, D. W. Smith and M. G. El-Din, *Journal of Environmental Engineering and Science*, 2003, **2**, 413-427.
69. M. Iwamoto, in *Studies in Surface Science and Catalysis*, Elsevier, 2000, **130**, 23-47.
70. J.-C. Béziat, M. Besson, P. Gallezot and S. Durécu, *Journal of Catalysis*, 1999, **182**, 129-135.
71. L. Oliviero, J. Barbier Jr and D. Duprez, *Applied Catalysis B: Environmental*, 2003, **40**, 163-184.
72. G. Centi and S. Perathoner, *Use of solid catalysts in promoting water treatment and remediation technologies*, Royal Society of Chemistry Publishing Cambridge, UK, 2005.
73. C. Zheng, L. Zhao, X. Zhou, Z. Fu and A. Li, *Water treatment*, 2013, **11**, 250-286.
74. M. Neamțu, C. Catrinescu and A. Kettrup, *Applied Catalysis B: Environmental*, 2004, **51**, 149-157.
75. H. J. H. Fenton, *Journal of the Chemical Society, Transactions*, 1894, **65**, 899-910.

76. F. Haber and J. Weiss, *Proceedings of the Royal Society of London. Series A-Mathematical and Physical Sciences*, 1934, **147**, 332-351.
77. V. Sarria, S. Kenfack, O. Guillod and C. Pulgarin, *Journal of Photochemistry and Photobiology A: Chemistry*, 2003, **159**, 89-99.
78. C. Molina, J. Zazo, J. Casas and J. Rodriguez, *Water Science and Technology*, 2010, **61**, 2161-2168.
79. M. S. Yalfani, S. Contreras, F. Medina and J. Sueiras, *Chemical communications*, 2008, **33**, 3885-3887.
80. A. Vitamin, *Archived from the original on April*, 2021, **27**.
81. N. N. Greenwood and A. Earnshaw, *Chemistry of the Elements*, Elsevier, 2012.
82. A. F. Holleman, *Lehrbuch der anorganischen Chemie*, Walter de Gruyter GmbH & Co KG, 2019.
83. J. Barrault, C. Bouchoule, K. Echachoui, N. Frini-Srasra, M. Trabelsi and F. Bergaya, *Applied Catalysis B: Environmental*, 1998, **15**, 269-274.
84. C. Zhou, PhD thesis, University of Sheffield, 2021.
85. A. Santos, P. Yustos, A. Quintanilla, S. Rodriguez and F. Garcia-Ochoa, *Applied Catalysis B: Environmental*, 2002, **39**, 97-113.
86. A. Santos, P. Yustos, A. Quintanilla and F. Garcia-Ochoa, *Applied Catalysis B: Environmental*, 2004, **53**, 181-194.
87. L. Liotta, M. Gruttadauria, G. Di Carlo, G. Perrini and V. Librando, *Journal of hazardous materials*, 2009, **162**, 588-606.
88. A. Alejandre, F. Medina, A. Fortuny, P. Salagre and J. Sueiras, *Applied Catalysis B: Environmental*, 1998, **16**, 53-67.
89. J. Zazo, J. Casas, A. Mohedano, M. Gilarranz and J. Rodriguez, *Environmental science & technology*, 2005, **39**, 9295-9302.
90. A. Quintanilla, J. Casas, A. Mohedano and J. Rodríguez, *Applied Catalysis B: Environmental*, 2006, **67**, 206-216.
91. S. O. Lee, T. Tran, Y. Y. Park, S. J. Kim and M. J. Kim, *International Journal of Mineral Processing*, 2006, **80**, 144-152.
92. M. Taxiarchou, D. Papias, I. Douni, I. Paspaliaris and A. Kontopoulos, *Hydrometallurgy*, 1997, **46**, 215-227.
93. A. Santos, P. Yustos, A. Quintanilla, F. Garcia-Ochoa, J. Casas and J. Rodriguez, *Environmental science & technology*, 2004, **38**, 133-138.

94. A. Santos, P. Yustos, S. Gomis, G. Ruiz and F. Garcia-Ochoa, *Chemical engineering science*, 2006, **61**, 2457-2467.
95. E. E. Kiss, J. G. Ranogajec, R. P. Marinković-Nedućin and T. J. Vulić, *Reaction Kinetics and Catalysis Letters*, 2003, **80**, 255-260.
96. A. Y. Sychev and V. Isak, *Russian Chemical Reviews*, 1995, **64**, 1105.
97. J. Sotelo, G. Ovejero, F. Martinez, J. Melero and A. Milieni, *Applied Catalysis B: Environmental*, 2004, **47**, 281-294.
98. G. Berlier, G. Spoto, G. Ricchiardi, S. Bordiga, C. Lamberti and A. Zecchina, *Journal of Molecular Catalysis A: Chemical*, 2002, **182**, 359-366.
99. M. V. Bagal and P. R. Gogate, *Ultrasonics sonochemistry*, 2014, **21**, 1-14.
100. J. Carriazo, E. Guelou, J. Barrault, J. Tatibouët and S. Moreno, *Applied Clay Science*, 2003, **22**, 303-308.
101. A. Shokri and M. S. Fard, *Environmental Challenges*, 2022, **7**, 100534.
102. E. Aneggi, A. Trovarelli and D. Goi, *Journal of environmental chemical engineering*, 2017, **5**, 1159-1165.
103. C. S. Rodrigues, R. M. Silva, S. A. Carabineiro, F. J. Maldonado-Hódar and L. M. Madeira, *Catalysts*, 2019, **9**, 478.
104. T. Hammedi, M. Triki, Z. Ksibi, A. Ghorbel and F. Medina, *Journal of Sol-Gel Science and Technology*, 2015, **76**, 679-685.
105. M. J. Kim, M. W. Lee and K.-Y. Lee, *Applied Surface Science*, 2021, **541**, 148409.
106. V. Subbaramaiah, V. C. Srivastava and I. D. Mall, *Journal of Hazardous Materials*, 2013, **248**, 355-363.
107. M. Hachemaoui, C. B. Molina, C. Belver, J. Bedia, A. Mokhtar, R. Hamacha and B. Boukoussa, *Catalysts*, 2021, **11**, 219.
108. Q. Zhang, Y. Peng, F. Deng, M. Wang and D. Chen, *Separation and Purification Technology*, 2020, **246**, 116890.
109. O. P. Taran, A. N. Zagoruiko, A. B. Ayusheev, S. A. Yashnik, R. V. Prihod'ko, Z. R. Ismagilov, V. V. Goncharuk and V. N. Parmon, *Chemical Engineering Journal*, 2015, **282**, 108-115.
110. J. Carriazo, E. Guélou, J. Barrault, J.-M. Tatibouët, R. Molina and S. Moreno, *Water research*, 2005, **39**, 3891-3899.
111. S. G. Peera, T. Maiyalagan, C. Liu, S. Ashmath, T. G. Lee, Z. Jiang and S. Mao, *International Journal of Hydrogen Energy*, 2021, **46**, 3056-3089.

112. S. D. Buchanan, R. A. Diseker, T. Sinks, D. R. Olson, J. Daniel and T. Flodman, *International Journal of Occupational and Environmental Health*, 1999, **5**, 256-261.
113. X. Zhang, A. Li, Z. Jiang and Q. Zhang, *Journal of hazardous materials*, 2006, **137**, 1115-1122.
114. S. L. González-Cortés and F. E. Imbert, *Applied Catalysis A: General*, 2013, **452**, 117-131.
115. H. Schobert, *Chemistry of fossil fuels and biofuels*, Cambridge University Press, 2013.
116. K. Fajerwerg and H. Debellefontaine, *Applied Catalysis B: Environmental*, 1996, **10**, L229-L235.
117. D. He, H. Zhang and Y. Yan, *Royal Society open science*, 2018, **5**, 172364.
118. A. Rey, M. Faraldos, J. Casas, J. Zazo, A. Bahamonde and J. Rodríguez, *Applied Catalysis B: Environmental*, 2009, **86**, 69-77.
119. R.-M. Liou and S.-H. Chen, *Journal of Hazardous Materials*, 2009, **172**, 498-506.
120. S. Zhou, C. Zhang, R. Xu, C. Gu, Z. Song and M. Xu, *Water Science and Technology*, 2016, **73**, 1025-1032.
121. G. Ovejero, A. Rodríguez, A. Vallet, P. Gómez and J. García, *Water Science and Technology*, 2011, **63**, 2381-2387.
122. S. R. Pouran, A. A. A. Raman and W. M. A. W. Daud, *Journal of Cleaner Production*, 2014, **64**, 24-35.
123. M. Aleksić, H. Kušić, N. Koprivanac, D. Leszczynska and A. L. Božić, *Desalination*, 2010, **257**, 22-29.
124. A. Behnam, G. Buck, F. Capacci, A. Checa, F. Di Benedetto, A. Eisenhauer, R. Giere, H. Gies, E. Griesshaber and R. Gunder, *Highlights in Applied Mineralogy*, Walter de Gruyter GmbH & Co KG, 2017.
125. C. S. Cundy and P. A. Cox, *Chemical reviews*, 2003, **103**, 663-702.
126. J. F. Haw, J. B. Nicholas, T. Xu, L. W. Beck and D. B. Ferguson, *Accounts of chemical research*, 1996, **29**, 259-267.
127. A. Tiwari and S. Titinchi, *Advanced catalytic materials*, John Wiley & Sons, 2015.
128. Z. Ghasemi, I. Sourinejad, H. Kazemian and S. Rohani, *Reviews in Aquaculture*, 2018, **10**, 75-95.
129. H. Kazemian and M. MALAH, *Iranian Journal of Chemistry and Chemical Engineering.*, 2006, **25**, 91-94.
130. A. Corma, *Chemical reviews*, 1997, **97**, 2373-2420.

131. S. Salehi and M. Anbia, *Journal of Physics and Chemistry of Solids*, 2017, **110**, 116-128.
132. E. Auer, A. Freund, J. Pietsch and T. Tacke, *Applied Catalysis A: General*, 1998, **173**, 259-271.
133. R. K. Vyas and S. Kumar, *CSIR*, 2004, **11**, 704-709.
134. C. Satterfield and J. Wilkens, *Industrial and Engineering Chemistry Process Design and Development*, 1980, **19**, 154-160.
135. R. Carvalho, F. Lemos, M. Lemos, J. Cabral and F. R. Ribeiro, *Journal of Molecular Catalysis A: Chemical*, 2006, **248**, 48-52.
136. G. Calleja, J. A. Melero, F. Martinez and R. Molina, *Water Research*, 2005, **39**, 1741-1750.
137. J.-Y. Kim, J. Moon, J. H. Lee, X. Jin and J. W. Choi, *Fuel*, 2020, **279**, 118484.
138. K. Valkaj, O. Wittine, K. Margeta, T. Granato, A. Katović and S. Zrnčević, *Polish Journal of Chemical Technology*, 2011, **13**, 28-36.
139. N. Li, F. Tan, W. Chen, M. Dai, F. Wang, S. Shen, W. Tang, J. Li, Y. Yu and W. Cao, *The Lancet Respiratory Medicine*, 2022, **10**, 378-391.
140. A. Cihanoğlu, G. Gündüz and M. Dükkancı, *Applied Catalysis B: Environmental*, 2015, **165**, 687-699.
141. O. P. Taran, S. A. Yashnik, A. B. Ayusheev, A. S. Piskun, R. V. Prihod'ko, Z. R. Ismagilov, V. V. Goncharuk and V. N. Parmon, *Applied Catalysis B: Environmental*, 2013, **140**, 506-515.
142. J. Weitkamp, *Solid state ionics*, 2000, **131**, 175-188.
143. Y. Yan, S. Jiang, H. Zhang and X. Zhang, *Chemical Engineering Journal*, 2015, **259**, 243-251.
144. H. Sontheimer, J. C. Crittenden and R. S. Summers, *Activated carbon for water treatment*, American Water Works Association, 1988.
145. J. Cookson, P. Cheremishinoff and F. Ellerbusch, *Michigan: Ann Arbor Science Publishers*, 1978.
146. A. Bhatnagar, W. Hogland, M. Marques and M. Sillanpää, *Chemical Engineering Journal*, 2013, **219**, 499-511.
147. V. Tukač and J. Hanika, *Collection of Czechoslovak chemical communications*, 1996, **61**, 1010-1017.
148. F. Stüber, J. Font, A. Fortuny, C. Bengoa, A. Eftaxias and A. Fabregat, *Topics in Catalysis*, 2005, **33**, 3-50.

149. J. Zazo, J. Casas, A. Mohedano and J. Rodríguez, *Applied Catalysis B: Environmental*, 2006, **65**, 261-268.
150. M. Santiago, F. Stüber, A. Fortuny, A. Fabregat and J. Font, *Carbon*, 2005, **43**, 2134-2145.
151. A. Quintanilla, J. Casas and J. Rodriguez, *Applied Catalysis B: Environmental*, 2010, **93**, 339-345.
152. F. Rodriguez-Reinoso, *Carbon*, 1998, **36**, 159-175.
153. W. Reimerink, *ChemInform*, 1999, **30**, no-no.
154. A. B. Stiles, *Catalyst supports and supported catalysts*, OSTI. GOV, United States, 1987.
155. A. E. Aksoylu, M. M. A. Freitas and J. L. Figueiredo, *Applied Catalysis A: General*, 2000, **192**, 29-42.
156. A. Aksoylu, J. Faria, M. Pereira, J. Figueiredo, P. Serp, J.-C. Hierso, R. Feurer, Y. Kihn and P. Kalck, *Applied Catalysis A: General*, 2003, **243**, 357-365.
157. L. Monser and N. Adhoum, *Separation and purification technology*, 2002, **26**, 137-146.
158. P. Pietrowski, I. Ludwiczak and J. Tyczkowski, *Materials Science*, 2012, **18**, 158-162.
159. J. Lee, J. Kim and T. Hyeon, *Advanced materials*, 2006, **18**, 2073-2094.
160. C. Y. Yin, M. K. Aroua and W. M. A. W. Daud, *Separation and purification technology*, 2007, **52**, 403-415.
161. J. Rivera-Utrilla, M. Sánchez-Polo, V. Gómez-Serrano, P. Álvarez, M. Alvim-Ferraz and J. Dias, *Journal of hazardous materials*, 2011, **187**, 1-23.
162. M. S. Shafeeyan, W. M. A. W. Daud, A. Houshmand and A. Shamiri, *Journal of Analytical and Applied Pyrolysis*, 2010, **89**, 143-151.
163. W. Shen, Z. Li and Y. Liu, *Recent Patents on Chemical Engineering*, 2008, **1**, 27-40.
164. P. Vinke, M. Van der Eijk, M. Verbree, A. Voskamp and H. Van Bekkum, *Carbon*, 1994, **32**, 675-686.
165. C. Moreno-Castilla, F. Carrasco-Marin, F. Maldonado-Hodar and J. Rivera-Utrilla, *Carbon*, 1998, **36**, 145-151.
166. M. López-Ramón, C. Moreno-Castilla, J. Rivera-Utrilla and R. Hidalgo-Alvarez, *Carbon*, 1993, **31**, 815-819.
167. S. Messele, F. Stüber, C. Bengoa, A. Fortuny, A. Fabregat and J. Font, *Procedia Engineering*, 2012, **42**, 1373-1377.

168. V. Guimaraes, A. R. Teixeira, M. S. Lucas, A. M. Silva and J. A. Peres, *Separation and Purification Technology*, 2019, **228**, 115768.
169. M. A. De León, J. Castiglioni, J. Bussi and M. Sergio, *Catalysis Today*, 2008, **133**, 600-605.
170. M. J. Rezende, M. S. Pereira, G. F. Santos, G. O. Aroeira, T. C. Albuquerque Jr, P. A. Suarez and A. C. Pinto, *Journal of the Brazilian Chemical Society*, 2012, **23**, 1209-1215.
171. F. Bergaya, M. Jaber and J. F. Lambert, *Rubber-Clay Nanocomposites: Science, Technology, and Applications*, 2011, 1-44.
172. Y. M. Sani, W. M. A. W. Daud and A. A. Aziz, *Applied Catalysis A: General*, 2014, **470**, 140-161.
173. A. Gil, S. Korili and M. Vicente, *Catalysis Reviews*, 2008, **50**, 153-221.
174. F. L. Bleken, K. Barbera, F. Bonino, U. Olsbye, K. P. Lillerud, S. Bordiga, P. Beato, T. V. Janssens and S. Svelle, *Journal of catalysis*, 2013, **307**, 62-73.
175. M. A. Peña and J. Fierro, *Chemical reviews*, 2001, **101**, 1981-2018.
176. N. Inchaurredo, P. Massa, R. Fenoglio, J. Font and P. Haure, *Chemical Engineering Journal*, 2012, **198**, 426-434.
177. S. Yang, W. Zhu, J. Wang and Z. Chen, *Journal of Hazardous Materials*, 2008, **153**, 1248-1253.
178. L. Zhang, F. Li, D. Evans and X. Duan, *Industrial & engineering chemistry research*, 2010, **49**, 5959-5968.
179. B. Solsona, I. Vázquez, T. Garcia, T. E. Davies and S. H. Taylor, *Catalysis letters*, 2007, **116**, 116-121.
180. S. Park, R. J. Gorte and J. M. Vohs, *Applied Catalysis A: General*, 2000, **200**, 55-61.
181. Y. Li, Q. Fu and M. Flytzani-Stephanopoulos, *Applied Catalysis B: Environmental*, 2000, **27**, 179-191.
182. M. Alifanti, J. Kirchnerova, B. Delmon and D. Klvana, *Applied Catalysis A: General*, 2004, **262**, 167-176.
183. S. Yusuf, L. M. Neal and F. Li, *ACS Catalysis*, 2017, **7**, 5163-5173.
184. L. Zeng, Z. Cheng, J. A. Fan, L.-S. Fan and J. Gong, *Nature Reviews Chemistry*, 2018, **2**, 349-364.
185. A. Ruiz Puigdollers, P. Schlexer, S. Tosoni and G. Pacchioni, *Acs Catalysis*, 2017, **7**, 6493-6513.

186. H. Wang, H. Jiang, L. Kuang and M. Zhang, *The Journal of Supercritical Fluids*, 2014, **92**, 84-92.
187. G. Busca, *Physical Chemistry Chemical Physics*, 1999, **1**, 723-736.
188. T. Biemelt, K. Wegner, J. Teichert, M. Lohe, J. Martin, J. Grothe and S. Kaskel, *Applied Catalysis B: Environmental*, 2016, **184**, 208-215.
189. W. Wallace, PhD thesis, Cardiff University, 2019.
190. A. Quintanilla, A. Fraile, J. Casas and J. Rodríguez, *Journal of Hazardous Materials*, 2007, **146**, 582-588.
191. M. Timofeeva, S. T. Khankhasaeva, E. Talsi, V. Panchenko, A. Golovin, E. T. Dashinamzhilova and S. Tsybulya, *Applied Catalysis B: Environmental*, 2009, **90**, 618-627.
192. K.-H. Kim, J.-R. Kim and S.-K. Ihm, *Journal of hazardous materials*, 2009, **167**, 1158-1162.
193. G. Ovejero, J. L. Sotelo, F. Martínez, J. A. Melero and L. Gordo, *Industrial & engineering chemistry research*, 2001, **40**, 3921-3928.
194. S. S. Sable, A. Georgi, S. Contreras and F. Medina, *Water-Energy Nexus*, 2021, **4**, 95-102.
195. O. P. Taran, A. N. Zagoruiko, S. A. Yashnik, A. B. Ayusheev, A. V. Pestunov, I. P. Prosvirin, R. V. Prihod'ko, V. V. Goncharuk and V. N. Parmon, *Journal of Environmental Chemical Engineering*, 2018, **6**, 2551-2560.
196. Y. Yan, S. Jiang and H. Zhang, *Separation and Purification Technology*, 2014, **133**, 365-374.

Chapter 2: Experimental methods and techniques

This section will provide experimental details about the materials used for: catalyst preparation, catalytic tests and analysis. Also, it will explain the catalysts synthesis method used in this thesis work. In addition, it will summarise the principle for the main instrumental methods used for characterising reaction mixtures (determination of reagent's concentration and their intermediates) and instruments used to detect the metal leaching. In addition, private principles for techniques used for catalyst characterisation were synthesised during this project.

2.1 Chemical reagents

2.1.1 Reagents for catalysts preparation

Chemicals and materials utilised for the synthesis of the catalysts were: iron (III) nitrate nonahydrate ($\text{Fe}(\text{NO}_3)_3 \cdot 9\text{H}_2\text{O}$, 99+%, Acros), iron(II) sulfate heptahydrate ($\text{FeSO}_4 \cdot 7\text{H}_2\text{O}$, 99+%, Acros), ammonium iron (II) sulfate hydrate ($(\text{NH}_4)_2\text{Fe}(\text{SO}_4)_2(\text{H}_2\text{O})_6$, 99.99%, Alfa Aesar), iron (III) oxide, 99.98%, Sigma Aldrich), silver (I) nitrate (AgNO_3 , $\geq 99.8\%$, Sigma Aldrich), silver (I) oxide (Ag_2O , 99%, Honeywell), silver (I) acetate ($\text{AgC}_2\text{H}_3\text{O}_2$, 99%, SLS), zeolite ZSM-5 ammonium ($425 \text{ m}^2 \cdot \text{g}^{-1}$, 23:1 $\text{SiO}_2:\text{Al}_2\text{O}_3$, Alfa Aesar), zeolite ZSM-5 ammonium ($425 \text{ m}^2 \cdot \text{g}^{-1}$, 50:1 $\text{SiO}_2:\text{Al}_2\text{O}_3$, Alfa Aesar), zeolite ZSM-5 ammonium ($425 \text{ m}^2 \cdot \text{g}^{-1}$, 80:1 $\text{SiO}_2:\text{Al}_2\text{O}_3$, Alfa Aesar), zeolite Y hydrogen ($730 \text{ m}^2 \cdot \text{g}^{-1}$, 5.1:1 $\text{SiO}_2:\text{Al}_2\text{O}_3$, Alfa Aesar), activated charcoal: NORIT GAC 1240 (12 – 40 mesh, Acros), NORIT SA 2, (Acros), DARCO G60 (Acros), hydrochloride acid (HCl , 12M, VMR International), nitric acid (HNO_3 , 14M, VMR International).

2.1.2 Reagents for catalytic tests

The materials and chemicals used for catalytic tests were: phenol ($\text{C}_6\text{H}_5\text{OH}$, $\geq 99\%$, Sigma Alorich), 2,6-dimethylphenol ($(\text{CH}_3)_2\text{C}_6\text{H}_3\text{OH}$, $\geq 99.5\%$, Sigma Alorich), *m*-cresol ($\text{CH}_3\text{C}_6\text{H}_4(\text{OH})$, Fluorochem), 3-methoxyphenol ($\text{C}_7\text{H}_8\text{O}_2$, 97%, Alfa Aesar), 4-chlorophenol ($\text{C}_6\text{H}_4\text{ClOH}$, $\geq 99\%$, Sigma Alorich), 4-bromophenol ($\text{C}_6\text{H}_4\text{BrOH}$, Fluorochem), hydrogen peroxide (H_2O_2 , 30% (w/w), VMR International).

2.1.3 Reagents for characterisation of reaction mixtures

The following chromatographic standards were used: phenol (C_6H_5OH , $\geq 99\%$, Sigma Aldrich), 2,6-dimethylphenol ($(CH_3)_2C_6H_3OH$, $\geq 99.5\%$, Sigma Aldrich), m-cresol ($CH_3C_6H_4(OH)$, fluorochem), 3-methoxyphenol ($C_7H_8O_2$, 97%, Alfa Aesar), 4-chlorophenol (C_6H_4ClOH , $\geq 99\%$, Sigma Aldrich), 4-bromophenol (C_6H_4BrOH , Fluorochem), hydroquinone ($C_6H_6O_2$, 99.5%, Acros), p-benzoquinone ($C_6H_4O_2$, $\geq 99.5\%$, Sigma Aldrich), catechol ($C_6H_6O_2$, 99+%, Acros), oxalic acid dihydrate ($C_2H_2O_4 \cdot 2H_2O$, $\geq 99.0\%$, Sigma Aldrich), acetic acid ($C_2H_4O_2$, 100%, VMR International), formic acid (CH_2O_2 , 99%, Acros), malonic acid ($C_3H_4O_4$, $\geq 99.95\%$, Sigma Aldrich), maleic acid ($C_4H_4O_4$, $\geq 99.0\%$, Sigma Aldrich), fumaric acid ($C_4H_4O_4$, 99+%, Acros).

For determination of H_2O_2 concentration: potassium permanganate ($KMnO_4$, 99-100.5%, Fluka), sodium oxalate ($Na_2C_2O_4$, $\geq 99.5\%$, Honeywell), potassium iodide (KI, 99%, Acros), sodium thiosulfate ($Na_2S_2O_3$, 99%, Fisher), starch (Alfa Aesar), sulfuric acid (H_2SO_4 $\geq 97.5\%$, Sigma Aldrich).

For determination of activated carbon's acidity: hydrochloride acid (HCl, 35%, VMR International), sodium hydroxide (NaOH, $\geq 98\%$, VWR international).

For the analysis by high-performance liquid chromatography (HPLC): the mobile phase was orthophosphoric acid (H_3PO_4 , 85%, VWR International), acetonitrile (C_2H_3N , HPLC grade, Fisher).

2.2 Experimental apparatus

2.2.1 Equipment for catalyst synthesis

The equipment used for catalysts preparation was: hot stirrer plate (Asynt), centrifuge (SCIOLOGEX D1008 Mini-Centrifuges), drying oven (Genlab Mino 30/F/DIG), muffle oven (Carbolite CWF 11/14), tubular furnace (Carbolite MTF 12/38/250), universal digital oven (UN30, Memmert), RE100-Pro Rotary evaporator.

2.2.2 Equipment for the catalytic test

The tools used for the catalytic test were: a hot stirrer plate (Asynt), an Alumina block (diameter of 16 cm, custom-made) it is a multi-sample holder (four) for testing various materials, and a glass batch reactor (volume of 100 mL, custom-made) which was equipped with a young tap to allow both reagent addition and closing the system.

2.2.3 Equipment for the analysis of reaction mixtures

The instruments used for analysis are a centrifuge (SCIOGEX D1008 Mini-Centrifuges) to separate the catalyst from the solution and solution recovery, HPLC (Shimadzu Prominence Liquid Chromatograph) with a C18 column (Waters XBridge C18, 4.6×250 mm) include a UV detector (Shimadzu CBM-20A) to determine the concentration of reagents and their intermediates, ICP-OES (Agilent 4500 spectrometer) for determination of metal leaching.

2.3 Synthesis of catalysts

2.3.1 Supported metal catalysts preparation

The catalytic properties of heterogeneous catalysts' activity, selectivity and stability may strongly depend on the preparation method used to synthesise the catalyst.¹ For this purpose, the active phase (the metal) must be dispersed sufficiently to yield a large specific surface area and, as a result, maximum specific activity. A highly porous and thermostable support (with a large surface area and suitable mechanical strength) is usually used to deposit the active metal component on its surface to achieve this goal. This material is capable of dispersing the metal and increasing its thermal stability, thus increasing the life of the catalyst.²

A. Blending of the metal precursor

There are many ways to blend the metal precursor on the support, such as deposition precipitation, sol immobilisation and impregnation; this study will mainly focus on the impregnation method, which can divide into (i) wetness impregnation and (ii) incipient wetness impregnation.²

- **Impregnation methods (WI)**

This catalyst preparation method involves mixing a metal salt precursor dissolved in a solution (often water) with solid catalyst support. After an appropriate mixing time, the resulting slurry is aged for a short time, approximately 1 h, dried and finally calcined. According to the volume of added solution, two types of impregnations have been reported: (i) incipient wetness or dry impregnation; and (ii) wet impregnation.^{3, 4}

- **Incipient Wetness impregnation**

This procedure uses equivalent amounts of the volume of metal precursor solution to fill the volume of the pores of the support. Therefore, this technique is also called 'dry impregnation'. This process uses a pore-filling method suitable for fewer additive loadings. A volume equal to the support's pore size is used to introduce the desired quantities of constituents. Upon

drying and calcinating, a stable catalyst is obtained. This technique is appropriate for depositing species that weakly interact (weak interactions) with the surface and for depositing particles with excellent adsorption sites, weak interactions (e.g., Co/SiO₂) with the support.⁵ It will be challenging for small metal precursor particles to redistribute on the surface if they are adsorbing inside the pores, for example, with a Pd/C catalyst. As the surface oxygen group concentration increased, the Pd dispersion increased. The catalytic activity, however, did not improve proportionally, probably because Pd particles were distributed more uniformly inside the smaller pores.⁶

- **Wet Impregnation**

In this variant, an excess volume of solution is used compared to the volume of the pores in the support. The resulting slurry is stirred for a set period of time; then, it is filtered and dried. A significant interaction between the precursor and the support is required for this method's strong interactions (e.g., Co/Al₂O₃) with the support instead of incipient wetness impregnation.⁵ So, the concentration of metal precursors within or on the support is determined by the concentration of the solution, its pore volume, and adsorption sites.² It is possible to decrease the surface area through this process. Due to the larger volume of impregnating solution, less active metal may be deposited into the support. As a result, usually, the impregnated metals aren't deposited uniformly on the support surface because of this inner deposition process.

Because the impregnation process, compared to other protocols, is relatively simple and cheap, waste in the synthesis process is kept to a minimum, and its robustness, by changing from one experimentalist to another, is well known. Even so, being largely dominated by gradient effects, it gets uncontrolled, and the impregnated material will not be deposited uniformly on the support. Besides, during the drying step, precursors may travel to the pore's tip, emphasising non-uniformity. Furthermore, it results in the formation of large metal particles through agglomeration.⁷ Despite some severe disadvantages, this method is still widely used.⁸

B. Drying step

To evaporate the solvent and promote the deposition of a metal centre over or within the support, slurries leading to heterogeneous catalysts are usually dried between 80 °C and 200 °C. Several parameters can affect the final catalyst's morphology or oxidation state, such as the heating rate, optimum temperature, duration and kind of atmosphere.² This should be taken

into account when choosing it. With prolonged drying, the solvent is evaporated, allowing the salt dispersion to reach deeper pore liquids by penetrating the surface.

This will lead to a high solution concentration in the internal consistency (only applies to porous or reasonably porous materials). As a result of precipitation, the metal precursor is primarily found in the pores' inner walls. On the other hand, higher drying rates will create temperature gradients, pushing the solution to the surface of the particles, where it precipitates. It is necessary to dry the solution more frequently than to homogenise it to achieve uniform dispersion. The porous system complicates the process.²

C. Calcination

During this stage, a previously deposited active species onto or within support is heated in an air atmosphere (either statically or underflow) at comparatively high temperatures (typically > 500 °C). During the calcination step, metal precursors are decomposed into metal oxides, and water, gases, and counterions such as NH_4^+ or NO_3^- , common in many metal precursors, are eliminated as NO_x . In addition to decomposition, calcination may cause unwanted sintering of metal precursors or oxides and their reaction with supports. As a consequence, this step often requires lots of trial and error to find the optimal conditions.²

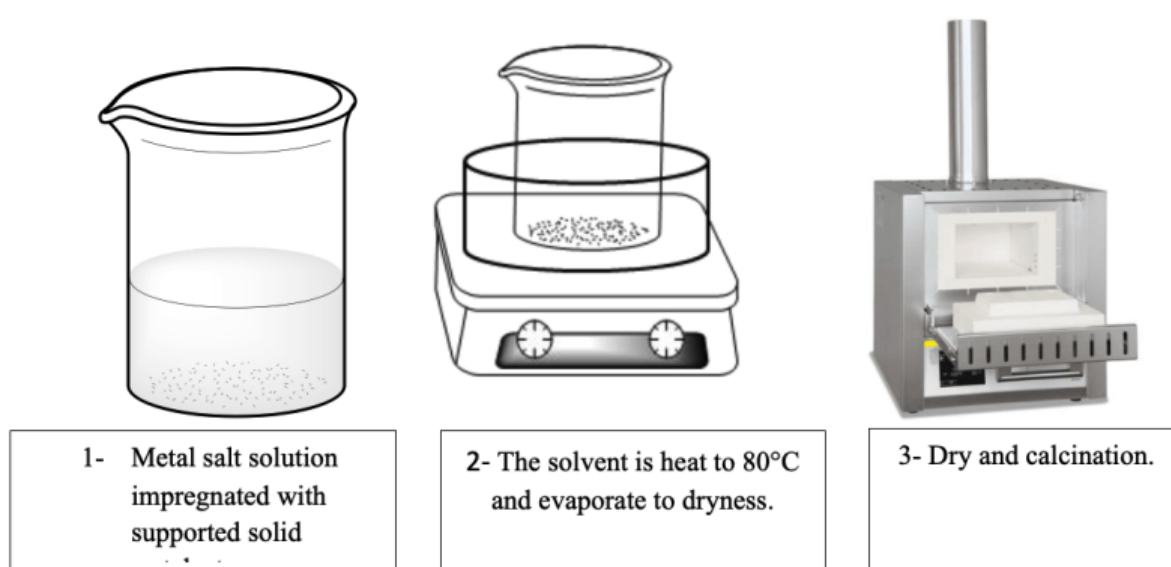


Figure 2.1: The Schematic shows three steps for preparing a metal-supported catalyst using wet impregnation.

2.3.2 Supported metal catalysts- actual preparation procedures

In this project, iron (Fe), silver (Ag), sulfur (S) and nitrogen (N) metals were used to dope solid porous materials, either zeolites or activated carbon (AC). NH₄-ZSM-5 with different SiO₂:Al₂O₃ ratios (1:23, 1:50 and 1:80) and Zeolite Y in its acidic, hydrogen form with a 5.1:1 SiO₂:Al₂O₃ have been used.⁹⁻¹²

For the activated carbons, three different kinds of ACs were used as support: NORIT GAC 1240, NORIT SA 2 and DARCO G60, either considering an array of various pre-treatments or not like washings or activations with HCl, HNO₃, or both.¹³⁻¹⁶

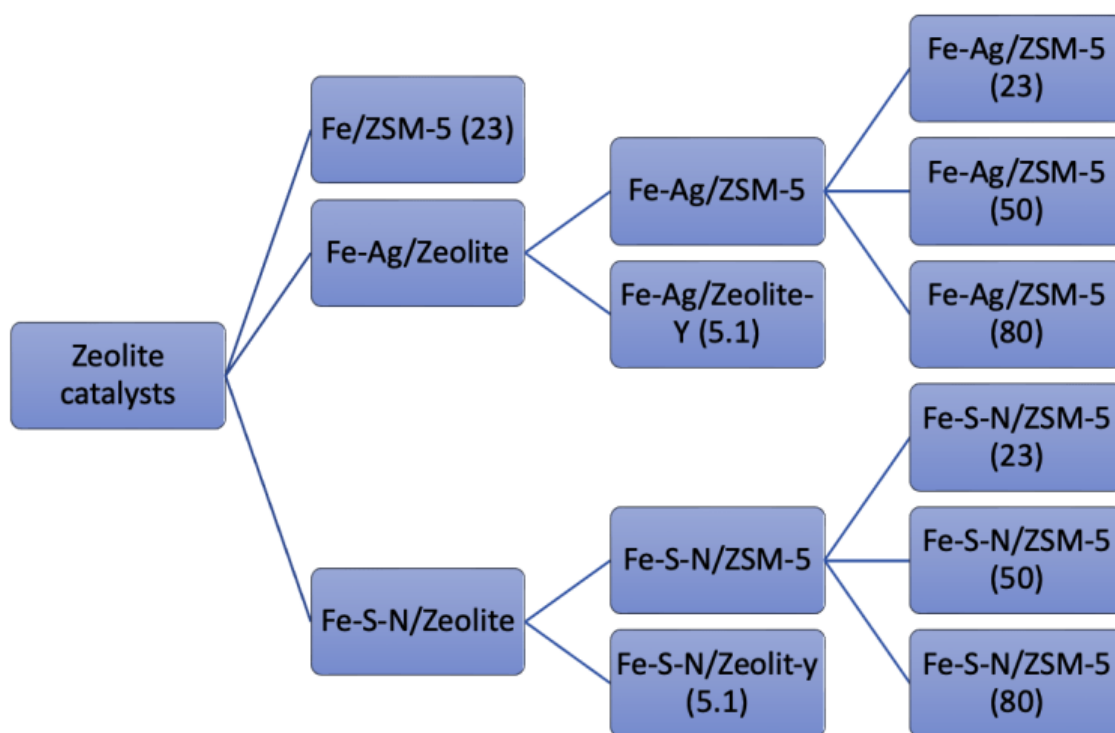


Figure 2.2: Schematic diagram summarizing the zeolite catalysts that were synthesized in this study. A wetness impregnation protocol was used to synthesise all catalysts in this scheme. Fe loading is 1 wt% for Fe/ZSM-5 and Fe-S-N/Zeolite catalysts, while Fe-Ag/Zeolite is 0.5 wt%.

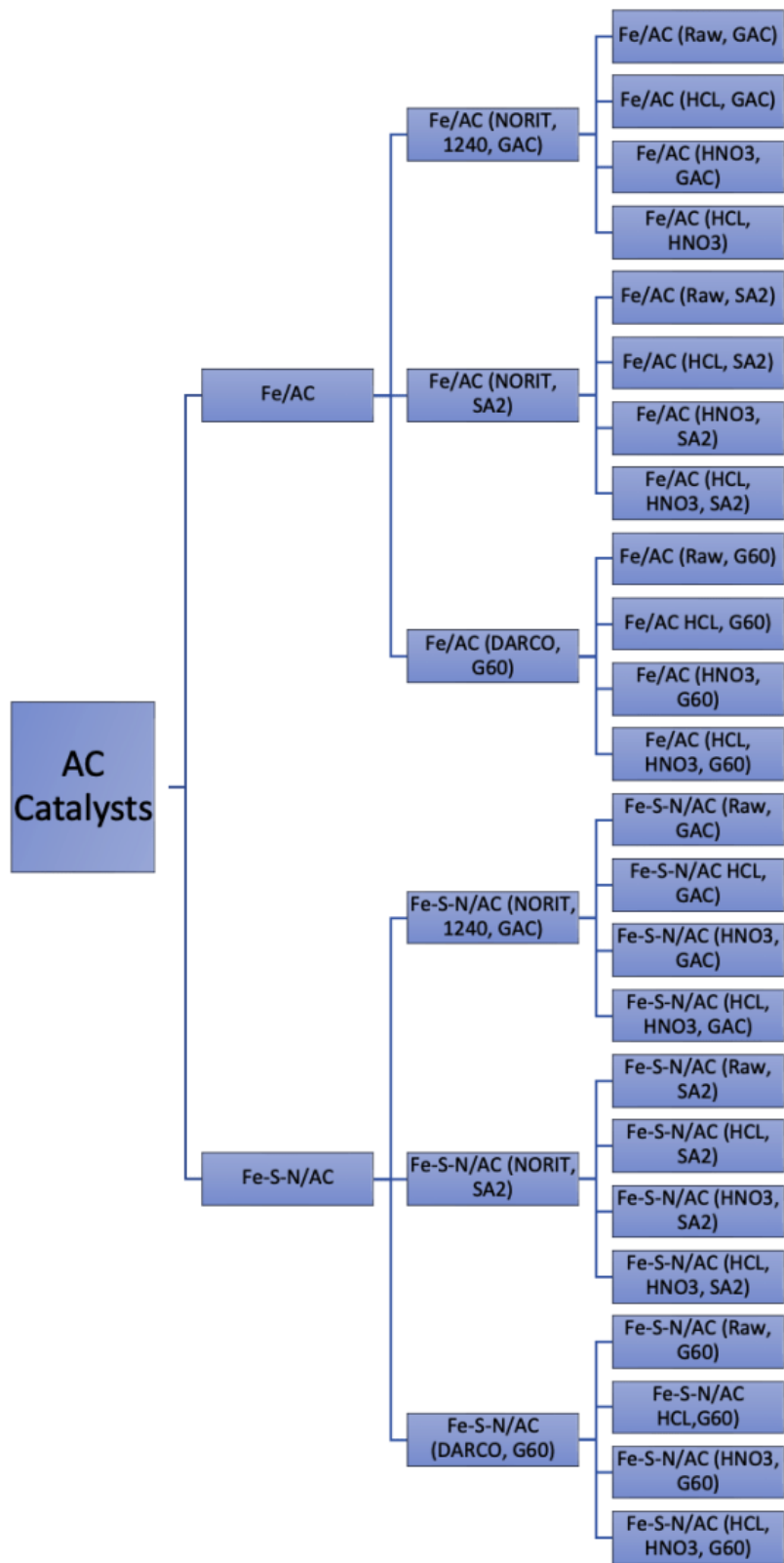


Figure 2.3: Schematic diagram summarising the activated carbon catalysts prepared in this study. All catalysts are synthesised using wet impregnation protocol using three different kinds of AC (NORIT, 1240, GAC, NORIT, SA2 and DARCO, G60) at different conditions. Fe/AC and Fe-S-N/AC catalysts have a Fe expecting to load 12 wt%.

A. Fe/AC

Fe/AC catalysts loadings of 12wt% of Fe were synthesised via an incipient wetness impregnation technique with different kinds of activated carbon (NORIT GAC 1240, NORIT SA2, DARCO G60) at various conditions (AC as it, AC washed with HCl, AC treated with HNO₃ and AC treated with both HCl and HNO₃) as shown above in Figure 2.3. A solution was prepared by dissolving 2 g of Fe(NO₃)₃·9H₂O in deionised water (25 mL). After adding AC (2 g) to a metal precursor solution, the resulting slurry was slowly heated and evaporated to dryness by using an oil bath at 80 °C.

After drying at 120 °C for 16 hours, the material/catalysts were thermally treated in a tubular furnace in the presence of 10 mL·min⁻¹ N₂ flow up to a temperature of 650 °C for 3h with a ramping rate of 20 °C·min⁻¹

I. Pre-treatment of AC with HCl

To eliminate Na, Fe, and Cu, which are known contaminants, from the AC, the carbon matrices were treated with diluted aqueous HCl (1 mol·L⁻¹) for 5h at 70 °C to remove them.¹⁷ After filtering and washing the carbon with distilled water (2 L of water per 1 g of AC), it was dried for 24 h at 120 °C in an oven.¹⁶

II. Pre-treatment of AC with HNO₃

The AC was treated with (0.5 mol·L⁻¹) HNO₃ for 10 h at room temperature (for each flask, 1 g of AC and 100 mL of (0.5M) HNO₃ solution was added). Then, the AC was washed with distilled water till pH neutrality of the supernatant solution (3 L of water per 1 g of AC) and dried in the GC oven at 110 °C for 24 h.¹³

III. Pre-treatment of AC with HCl and HNO₃

The same procedure described in the two above paragraphs was used for the simultaneous use of HCl and HNO₃ as pre-treatments for AC, initially with HCl and then after drying with HNO₃.

B. Fe-S-N/AC

Incipient wetness impregnation was used to synthesise N, S, and Fe-tri-doped AC catalysts with Fe expected to load 12wt%. Fe-S-N/AC catalysts were prepared with three types of AC under different conditions (raw AC, AC washed with HCl, AC treated with HNO₃, and AC washed with both HCl and HNO₃). Two iron precursors have been used: 0.1 mol·L⁻¹ of Fe(NO₃)₃·9H₂O (1 g) and 0.1 mol·L⁻¹ of (NH₄)₂Fe(SO₄)₂·6H₂O (0.98 g) was added into 2 g of AC; these dissolved in 25 mL of distilled water. As a next step, the slurry was heated to 80 °C

and evaporated to dryness; then, it was dried at 110 °C for 16 h in a gas chromatography (GC) oven. The catalyst was thermally treated in the tubular furnace at 650 °C for 3 h (temperature ramp 20 °C.min⁻¹) in the presence of N₂ flow.

C. Fe-ZSM-5

The catalyst was prepared by dissolving 0.1446 g of Fe (NO₃)₃.9H₂O in 25 mL of deionised water and mixing it vigorously with 1.98 g of NH₄-ZSM-5 and H-ZSM-5 powder. Using 80 °C as a heat source, the resulting slurry was evaporated until dry. It was then dried thoroughly at 120 °C for 16 h and then calcined at 550 °C for 4 h in a muffle oven (temperature ramp 20 °C·min⁻¹).

I. Pre-treatment of zeolite

To obtain H-ZSM-5, an NH₄-ZSM-5 zeolite precursor was calcined for 4 h in a muffle oven operating in static air at 550 °C (temperature ramp of 20 °C.min⁻¹).

II. Fe-ZSM-5 (under vacuum)

Fe-ZSM5 with 1 wt% Fe loading was prepared by mixing 0.1446 g of Fe (NO₃)₃.9H₂O with 1.98 g of NH₄-ZSM-5 dissolved in 25 mL of deionised water. The water was then dried in a rotary evaporator (10 min) under a mild vacuum at 80 °C and in an oven for 16 h at 120 °C overnight. After that, calcination is carried out for 4 h at 550 °C (temperature ramping 20 °C·min⁻¹). This technique expects high Fe dispersion.¹⁸

D. Fe-S-N-Zeolites (ZSM-5 (23,50 and 80), Zeolite-Y)

Three different Fe-S-N-ZSM-5 catalysts were prepared using the wet impregnation method: SiO₂:Al₂O₃ molar ratio is 23, 50, and 80, and Fe-S-N-Zeolite-Y (5.1:1 SiO₂:Al₂O₃). An ammonium iron (II) sulphate hydrate of 0.16 g, 1.98 g of zeolite, and 25 ml of deionised water mixed, drying at 80 °C, followed by 16 h at 120 °C, and calcination at 550 °C, temperature ramping 20 °C.min⁻¹ for 4 h.

E. Ag-ZSM-5

To prepare 1 wt% Ag-ZSM-5 (SiO₂:Al₂O₃ molar ratio is 23), 0.036 g of AgNO₃ was added to 1.98 g of NH₄-ZSM-5 dissolved in 25 mL of deionised water and mixed under vigorous stirring. The resulting slurry was heated to 80 °C and evaporated to dryness. The solid was then completely dried at 120 °C for 16 h and calcined in a muffle oven with a temperature held at 550 °C for 4 h (temperature ramp 20 °C·min⁻¹).

F. Fe-Ag- Zeolites (ZSM-5 (23,50 and 80), Zeolite-Y)

The typical preparation of Fe-Ag-ZSM-5 catalysts consists of three different Fe loadings of 0.5, 1 and 2wt%, prepared by an incipient wet impregnation using NH₄-ZSM-5 at various SiO₂:Al₂O₃ ratio (23, 50 and 80), also 0.5wt% Fe-Ag-Zeolite-Y (5.1:1 SiO₂:Al₂O₃).

Fe-Ag-ZSM-5-WI catalysts with 0.5wt% Ag and 0.5wt% Fe loading were prepared by dissolving 0.07 g of Fe(NO₃)₃.9H₂O in 25 mL of deionised water and adding 0.0157 g of AgNO₃ under vigorous stirring to 1.98 g of NH₄-ZSM-5, SiO₂:Al₂O₃ ratio 23, 50 and 80 powder. Heat the slurry to 80 °C and evaporate until it is dry. After drying at 120 °C for 16 h, the solid was calcined in a muffle oven at 550 °C for 4 h (temperature ramp 20 °C·min⁻¹).

To synthesise the Fe-Ag-ZSM-5-WI catalyst with 1wt% Fe and 1wt% Ag, 0.144 g of Fe(NO₃)₃.9H₂O and 0.036 g of AgNO₃ were mixed with 1.98 g NH₄-ZSM-5, SiO₂:Al₂O₃ ratio 1:23, in 25 mL of deionised water. After this, the slurry was heated to 80 °C and evaporated to dryness. Afterwards, the solid was dried at 120 °C for 16 h and calcined at 550 °C for 4 h (temperature ramp 20 °C·min⁻¹).

To prepare Fe-Ag-ZSM-5-WI (using NH₄-ZSM-5, SiO₂:Al₂O₃ ratio 1:23) catalyst with 2 wt% Fe and Ag, a mixture of 0.28 g of Fe(NO₃)₃.9H₂O and 0.073 g of AgNO₃ in 25 mL of deionised water containing 1.98 g of NH₄-ZSM-5 (23) dissolved in the mixture. Then, it was heated to 80 °C and evaporated until dry. Following complete drying at 120 °C for 16 h, the solid was calcined at 550 °C for 4 h (temperature ramp of 20 °C·min⁻¹).

2.4 Analytical methods for the characterisation of catalysts and reaction mixtures

2.4.1 Characterization of catalysts (principle of techniques)

A. X-ray powder diffraction (XRPD)

X-ray powder diffraction (XRPD) is a non-destructive method for determining a material's composition or crystal structure.¹⁹ X-ray diffraction patterns are used to measure the arrangement of atoms in a unit cell, their positions, and their spacing angles because of the relation between wavelength and atomic size.²⁰

Crystallised structures consist of regular and repeated arrangements of atoms. A unit cell is the smallest repeating element in a crystal. The length of the three axes (*a*, *b*, *c*) and the angles between them (*α*, *β*, *γ*) describe the size and shape of the unit cell (Figure 2.4).²¹

When an X-ray hits an atom in a solid, the electrons part of the material scatters the X-rays. Depending on the position of the atoms, constructive or destructive wave interference may occur.²² If the atomic structure of the solid is ordered, constructive interference occurs and may be detected. Crystallographic diffraction patterns are strongly correlated with periodic atomic structures. Short repeated distances lead to diffraction at high angles, while long repeated distances cause diffraction at small angles.²² Unit cells determinations for shape and size are done using diffraction peak positions, while atomic positions and atomic numbers are determined by diffraction peak intensities.²³ The diffraction of monochromatic X-rays from a single crystal was explained and measured by William Bragg.²⁴ In Bragg's analysis (Figure 2.5), layers or atomic planes produced reflections when incident light or X-rays impinged on the planes of atoms.²⁵ At the lattice plane, the incident beam makes an equal angle with the diffracted beam. Bragg's diffraction is satisfied if n is equal to the path difference lengths. By scanning a sample from two angles and converting the diffraction peaks to d -spacings, crystalline materials can be identified by their unique d -spacings.

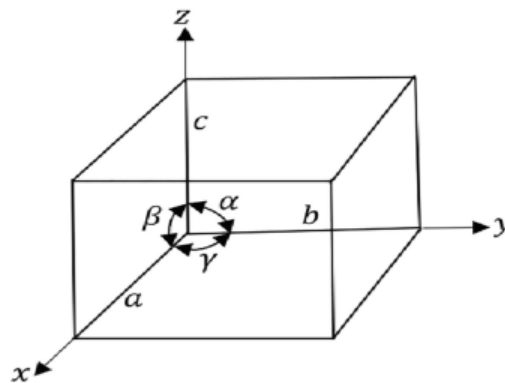


Figure 2.4: Vector of three-dimensional units. Unit cells are defined by length and angle between the three axes (a, b, c).²⁶ With permission.

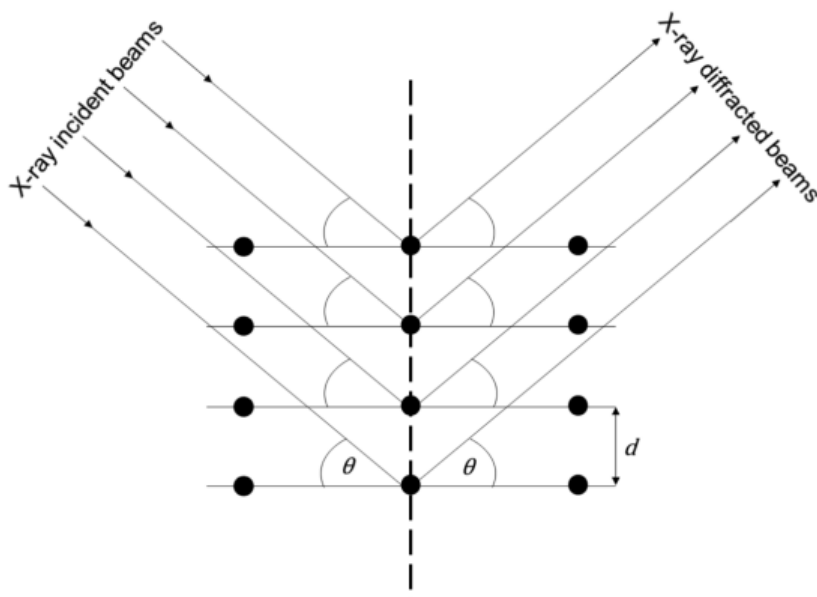


Figure 2.5: Diffraction from reflection according to Bragg's Law. To determine inter-layer spacing, d takes the angle between the incident beams and the normal lattice.²⁴ With permission.

X-ray powder diffraction (XRPD) patterns were collected by using a Bruker D8 Advance diffractometer that was equipped with a LynxEye detector. The specimens were placed onto a sample holder composed of amorphous silicon. The apparatus was operated at a voltage of 40 kV and a current of 40 mA, with the $\text{CuK}\alpha$ radiation (wavelength of 1.5406 Å) selected as the X-ray source. The samples underwent analysis within the 2θ range of 5–80°, with a scan period of 70 minutes. Analysis of the patterns was carried out with X-Pert Pro software.

The evaluation of the agreement between experimental and simulated X-ray powder diffraction (XRPD) patterns was carried out using a χ^2 -test,²⁷ employing Rietveld refinement²⁸ as a full-pattern fitting algorithm. The initial atomic coordinate values for the fit were acquired using crystallographic information files (CIF) provided from the Data-base of Zeolite Structures (IZA-SC).²⁹

Using the Scherrer equation to determine the particle size of supported metal oxides is common practice in place of XRD methods.¹⁰¹⁻¹⁰³ In the Scherrer equation, which is used to estimate the average crystallite size of a material from X-ray diffraction data. **2-theta (2θ):** This represents the diffraction angle. In X-ray diffraction experiments, X-rays are directed at a crystalline material, and when they interact with the crystal lattice, they are diffracted at various angles. The 2θ angle is the angle between the incident X-ray beam and the diffracted X-ray beam. It is

a key parameter in X-ray diffraction experiments and is used to determine the diffraction pattern of a material. **FWHM (Full Width at Half Maximum)**: This refers to the width of a diffraction peak at half of its maximum intensity. In an X-ray diffraction pattern, crystalline materials produce diffraction peaks at specific 2θ angles. The FWHM is a measure of how broad or narrow these peaks are. A narrower FWHM indicates a more well-defined and crystalline material, while a broader FWHM suggests a more disordered or amorphous material. **Inst B (Instrumental Broadening)**: This term accounts for the broadening of the diffraction peaks due to limitations of the X-ray diffraction instrument itself. Instrumental broadening can occur due to imperfections in the X-ray source, detector, or other components of the X-ray diffractometer. It is important to account for instrumental broadening when using the Scherrer equation to calculate crystallite size because it affects the measured FWHM. **d Å (Average Crystal Size)**: This is the parameter we were trying to calculate using the Scherrer equation. It represents the average size of the crystalline domains within the material. The Scherrer equation relates the FWHM of a diffraction peak, the wavelength of the X-rays used, the 2θ angle, and the average crystal size. The Scherrer equation is as follows:

$$dA = \frac{k \cdot \lambda}{B \cdot \cos \theta}$$

Where:

- dA is the average crystal size (in nanometers).
- K is the Scherrer constant, typically around 0.9.
- λ is the wavelength of the X-rays used.
- B is the FWHM of the diffraction peak (corrected for instrumental broadening).
- θ is the diffraction angle (2θ).

B. X-ray photoelectron spectroscopy (XPS)

One of the most widely used surface analysis techniques is X-ray photoelectron spectroscopy (XPS), which provides both elemental and chemical state information. The photon energy from an X-ray beam can dislodge electrons up to the surface of a sample and cause them to be excited (photoelectrons). Occasionally, these electrons can escape the host material, as shown in Figure 2.6.

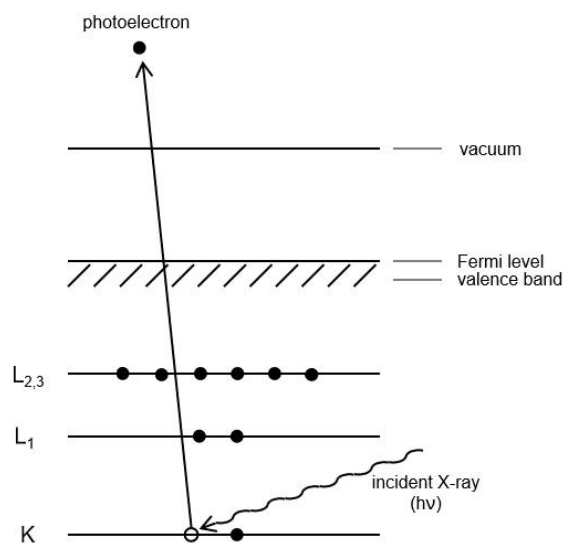


Figure 2.6: An XPS surface analysis diagram shows the photoemission process.³⁰ A molecule or an atom can release an electron when it absorbs an X-ray photon. Electrons' kinetic energy (E_k) is a valid indicator of surface elements and chemical states (E_k).

Einstein's photoelectric equation (Eq. 2.1)^{30,31} describes the relationship between photoelectron kinetic energy (E_k) and electron binding energy (E_b). Alternatively, E_b reflects the type and valence of the elements in the sample.

$$E_k = h\nu - E_b - \phi \quad (\text{Eq. 2.1})$$

There are five terms in this equation: E_k is the kinetic energy of emitted electron; E_b is the binding energy of the emitted electron; h is Planck's constant; ν is the frequency of incident X-ray, and ϕ is the work function of the spectrometer.

Some practical applications of this technique are:³²

- I. Determine the presence of elements at the surface level except for hydrogen and helium.
- II. Determine the oxidation state of elements.
- III. The local environment (e.g. ligands) next to a metal centre chemical bonds.
- IV. Provide information on the composition of a material at a nano-meter depth.

The photoelectron is immediately scattered and absorbed by the sample's atoms if the photoemission process occurs within the bulk of the material. Conversely, only photoelectrons originating at the top of the surface can escape from the model without being scattered or absorbed. Therefore, XPS usually has an analysis depth of less than 10 nm.

X-ray photoelectron spectroscopy (XPS) analysis was carried out using a Kratos Axis Ultra DLD spectrometer. The spectrometer employed a monochromatized Al K α X-ray source with a power output of 120 W. For survey scans, an analyser pass energy of 160 eV was utilised, while for detailed elemental scans, a pass energy of 40 eV was employed. The binding energies are standardised with respect to the C(1s) binding energy of carbon, which is conventionally assigned a value of 284.7 eV.³³

C. Brunauer-Emmett-Teller (BET)

The Brunauer-Emmett-Teller (BET) builds on Langmuir's theory,³⁴ is a model for measuring surface area and pore size is widely used for characterising micro- and mesoporous materials. BET theory describes how a gas adsorbs on adsorbent surfaces, and from the amount of gas, it is possible to extrapolate the surface area of a material or the characteristics of its porosity.

A monolayer adsorption of gas molecules is assumed to be ideal under Langmuir's theory. In contrast, the BET theory assumes multilayer adsorption and equilibrium between all layers (and no interaction between them). As a result, the Langmuir equation applies to every layer. The BET isotherm can be expressed as follows Eq. 2.2.^{34, 35}

$$\frac{\frac{P}{P_0}}{n \left(1 - \frac{P}{P_0}\right)} = \frac{1}{n_m C} + \frac{C - 1}{n_m C} \left(\frac{P}{P_0}\right) \quad (\text{Eq. 2.2})$$

According to the equation above, n represents the specific amount of adsorbates at the relative pressure P/P₀, P and P₀ are the equilibrium and saturation pressures of the adsorbates at the adsorption temperature, n_m is the monolayer capacity (the amount of the adsorbate necessary to occupy all of the adsorption sites) of the adsorbed gas, and C is the BET constant. It is a function of the enthalpies of adoption and liquefaction of the gas under consideration. As such, C can be used to determine the shape, pore size and pore volume of an isotherm in the BET range.³⁶⁻³⁸

The BET analysis was performed using a Micromeritics 3Flex Gas Sorption System. The sample was degassed at 180 °C for 24 h before examination, and the adoption step was carried out by using N₂ as a gas probe at its liquefaction temperature of 77K.

2.4.2 Principles of the techniques used for the characterisation of reaction mixtures

A. High-performance liquid chromatography (HPLC)

In analytical chemistry, high-performance liquid chromatography separates (or resolves), and in turn, can identify and quantify the compounds that are part of a mixture. In this method, a liquid solvent containing a sample mixture is pumped through a column containing a solid adsorbent using pumps. Different compounds interact differently with the stationary phase. Therefore, each analyte or compound, by spending a different amount of time bound to a stationary phase, will result in a different elution time needed to reach the end of a chromatographic column (also known as retention time), resulting in a separation process as the components exit the column. An HPLC instrument with some primary features is shown in Figure 2.7: reservoirs for storing the mobile phase; a pump for pushing it through the chromatographic column; an injector for injecting the sample; a packed column for resolving the sample into constituents; and a detector for detecting eluent coming from the column. Every component of this system will be discussed.³⁹

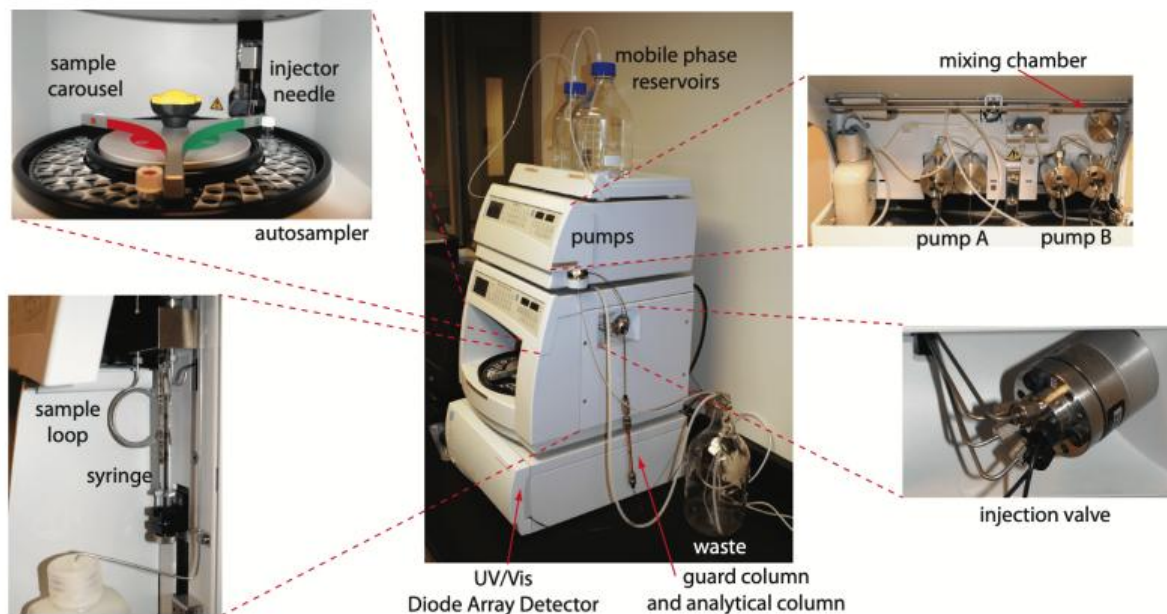


Figure 2.7: Displays the pump used to move the mobile phase and the plumbing used to inject the sample into the mobile phase of high-performance liquid chromatography. An autosampler is included with this instrument. Manually injected samples are injected through loop injection valves with a different type of flow control.³⁹

Two columns may be present in an HPLC: an analytical column (always present) to separate the sample and a guard column positioned before the analytical column to protect it against contamination.³⁹ HPLC columns are usually stainless-steel tubes with an internal radius of 2.1 to 4.6 mm and a length of 30 to 300 mm. There are generally 3–10 μm porous silica units in the column that have irregular or spherical shapes. The efficiency of a column can range from $4 \cdot 10^4$ to $6 \cdot 10^5$ theoretical plates/m (Number of Theoretical Plates N). This is a mathematical relationship that can be calculated using the following equation 2.3:^{39, 40}

$$N = 5.545 \left(\frac{t_R}{w_h} \right)^2 \quad (\text{Eq. 2.3})$$

Analytical columns are limited in their lifetime by two factors. The interaction of primary solutes with the stationary phase irretrievably reduces the column's efficiency by reducing its ability to segregate its components. The analytical column could also be blocked by particulate substances introduced with the sample. So, the mixture before analysis is centrifuged to separate the catalyst. This constraint is mitigated by placing the guard column before the

analytical column. The packing and stationary phases of guard columns are the same as those of analytical columns, but they are smaller and less expensive. This column is typically 7.5 mm long and costs one-tenth as much as an analytical column. A guard column is also frequently substituted.⁴¹ The guard columns used in the analysis are Phenomenex Security Guard Gemini-NX C18 (4 mm × 3 mm id).

A liquid film is used in liquid-liquid chromatography to plate a stationary phase, typically 3 to 10 μm of silica particles. A loss, or even a partial loss, of the stationary phase, can lead to a shorter column lifetime since the stationary phase partially dissolves in the mobile phase; it may dissolve or be eluted from the column over time. Because of this, silica particles are covalently bound to the stationary phase. A bond between stationary phases and silica particles is formed by the reaction between the silica particles and an organochlorosilane with the general formula $\text{Si}(\text{CH}_3)_2\text{RCl}$, where R stands for an alkyl group or substituted alkyl. The alkyl group (or groups) bound to an organosilane determines stationary phases; for example, polar phases are determined by R. A common HPLC method utilises polar stationary and nonpolar mobile phases, referred to as reversed-phase chromatography in this study. The most widely used non-polar stationary phases are organochlorosilanes where R is an *n*-octyl (C8) or *n*-octyl decyl (C18) hydrocarbon chain.

In this analysis, a C18 column was used with 5 μm, 4.6 mm × 250 mm length. In reversed-phase separations, a buffered solution is applied to a polar mobile phase or other polar solvents; in this study, acetonitrile and 1% orthophosphoric acid solution with a ratio of 30%/70% (V/V) were used as a mobile phase with a flow rate of 1 mL·min⁻¹. Due to the hydrolysis potential of silica substrate in eluted solutions, the pH of the mobile phase must be lower than 7.5. In reversed-phase chromatography, polar compounds, such as benzoic acid, will not interact with the stationary phase surface, so they stay in the mobile phase for a long time. This will result in faster elution. Contrary to this, substances like *p*-ethyl phenyl methanol with alkyl chains and high hydrophobicity will interact strongly with the stationary phase, leading to increased retention time and subsequent elution. Solvents are typically stored in 1–4 reservoirs on standard HPLC equipment. During this study, two reservoirs were used, one for distilled water and the other for the mobile phase. In most cases, one or more pumps are needed to drag the solvent from its reservoirs.⁴²

The loop injector is used to inject samples. Sample loops ranging in size from 0.5 μL to 5 mL are exposed to the atmosphere as they are separated from the mobile phase. The loop volume

used in this study was 5 μL . Syringes of many folds larger than the sample loop are used to fill the loop and remove different samples via the waste line. Following sample loading, the injector is moved to the injected spot, guiding the mobile phase through the sample loop to the column.³⁹ Various detectors are used to examine HPLC separations; spectroscopic detectors are the most common ones.⁴³

In our case, a sophisticated HPLC detector utilised the analyte's UV/Vis absorption spectrum (centered to a wavelength of a maximum or relative maximum of absorption). Monochromators are included in these detectors. Flow cells range in volume from 1 to 10 μL and path length from 0.2 to 1 cm. The chromatogram of a UV/Vis detector represents absorbance as a function of elution time. One important constraint is associated with employing absorbance as a parameter to assess concentrations: the mobile phase need not absorb at the desired wavelength.³⁹

B. Inductively coupled plasma optical emission spectroscopy (ICP-OES)

The ICP/OES procedure is one of the most powerful and popular methods for determining multiple elements in various samples (liquids and solids). The plasma produced by argon streams is a highly energetic, electrically neutral gas comprising ions, electrons, and neutral particles.⁴⁴ ICP-OES uses a high-frequency inductively coupled plasma as a light source. As a consequence, it involves the spontaneous emission of photons from atoms and ions that have been excited by radiofrequency (RF) discharges. An RF-induced argon plasma is used to atomise the sample solution; once atomised, the sample is dried, vaporised, and energised at high temperatures (over 6000 K) through collisional excitation.⁴⁵ In a plasma, collisional excitation promotes analyte atoms from the ground state to the excited state.

Through photon emission, excited atomic and ionic species may relax to the ground state. Quantized energy levels within atoms or ions determine photons' characteristic energies. A qualitative analysis of the elements from which the photons originated can be carried out by measuring the wavelength of the emitted photons. Quantitative analysis is based on the number of photons directly proportional to the concentration of the sample component.⁴⁶

The detection of iron metal leaching from the catalysts in the solution mixtures was tested by ICP-OES using an Agilent 4500 instrument via an appropriate calibration curve and by directly using our reaction mixtures as samples for ICP analyses.

2.5 Catalytic tests

A custom-designed reaction setup was used to heat the reaction mixture for catalytic tests (see section 2.2.2).

2.5.1 Phenolic compounds oxidation by wet hydrogen peroxide catalytic oxidation reaction (WHPCO)

Stock solutions containing phenol, 2,3 dimethyl phenol DMP, 3-methoxy phenol, *m*-cresol, 4-chlorophenol and 4-bromophenol were prepared by dissolving the desired amount of standard in deionised water and stored in volumetric flasks. The catalytic tests for phenolic compounds oxidation were carried out in a custom-made 100 mL stoppered glass batch reactor at a desired temperature and stirring rate under atmospheric pressure. The catalyst (M:S 1:100) and an aqueous reagent solution of 50 mL were placed in the glass reactor, which was heated via an Asynt stirrer-hotplate with a heating rate of 200 °C·min⁻¹ via an aluminium block at atmospheric pressure.

A stoichiometric amount of H₂O₂ to achieve complete mineralisation of the organic substrate to CO₂ and H₂O was added to the solution already containing a catalyst after stabilisation of the temperature at 80 °C. Ice baths were used to quench the reaction after the reaction to ensure a constant and reproducible reaction time. During the kinetic test, samples were removed from the reactor every 30 minutes in the first hour and every 1 hour in the last three hours. For analysis, the supernatant solution was collected from the centrifuged reaction mixture after separating it from the suspended solid catalyst.

Typically, a certain amount of solid catalyst (30 mg of 1wt% Fe/ZSM-5-WI or 1 wt% Fe-S-N/Zeolite, 60 mg of 0.5 wt% Fe-Ag-Zeolite and 3 mg of 12 wt% Fe-S-N/AC or 12 wt% Fe/AC catalysts with M:S ratio of 1:100) and 50 mL of **phenol** (1000 mg·L⁻¹) was placed into the reactor and heated to 80 °C (set temperature from calibration 85 °C) 844 µL of H₂O₂ (30% (w/w) with a stoichiometric mole ratio of phenol and H₂O₂ of 1:14 was added into the reaction mixture to start the reaction after the set temperature stabilising at 85 °C for 10 min. The reaction was conducted for 4 h under the continuous stirring rate of 500 rpm and then quenched with an ice-water bath.

For the complete oxidation of phenol to CO₂ and H₂O, the stoichiometric ratio of phenol to H₂O₂ was set at 1:14.



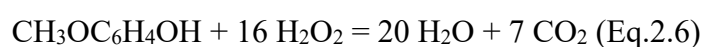
In a typical experiment, a certain amount of solid catalyst (20 mg of 1wt% Fe/ZSM-5-WI or 1 wt% Fe-S-N/Zeolite 50 mg of 0.5 wt % Fe-Ag-Zeolite and 2 mg of 12 wt% Fe-S-N/AC or 12 wt% Fe/AC catalysts, M:S ratio of 1:100) and 50 mL of **2,3 dimethylphenol DMP** ($1000 \text{ mg}\cdot\text{L}^{-1}$) was added into the reactor and heated to $80 \text{ }^\circ\text{C}$, $908 \text{ }\mu\text{L}$ of H_2O_2 (30% (w/w) with a stoichiometric ratio of DMP and H_2O_2 of 1:20 was added into the reaction mixture to start the reaction after the set temperature stabilising at $85 \text{ }^\circ\text{C}$ for 10 min. The reaction was conducted for 4 h under the continuous stirring rate of 500 rpm and then quenched with an ice-water bath.

A stoichiometric ratio of DMP to H_2O_2 was set at 1:20 for the complete oxidation of DMP to CO_2 and H_2O , as shown in Eq. 2.5.



According to a typical experiment, a certain amount of solid catalyst (30 mg of 1wt% Fe/ZSM-5-WI or 1 wt% Fe-S-N/Zeolite, 60 mg of 0.5 wt % Fe-Ag-Zeolite and 3 mg of 12 wt% Fe-S-N/AC or 12 wt% Fe/AC catalysts with M:S ratio of 1:100) and 50 mL of **3-methoxyphenol** ($1500 \text{ mg}\cdot\text{L}^{-1}$) were placed into the reactor and heated to $80 \text{ }^\circ\text{C}$, $1090 \text{ }\mu\text{L}$ of H_2O_2 (30% (w/w) with a stoichiometric ratio of 3-methoxyphenol and H_2O_2 of 1:16 was added into the reaction mixture to start the reaction after the set temperature stabilising at $85 \text{ }^\circ\text{C}$ for 10 min. The reaction was conducted for 4 h under the constant stirring rate of 500 rpm and then quenched with an ice-water bath.

A stoichiometric ratio of 3-methoxyphenol to H_2O_2 was set at 1:16 for the complete oxidation of 3-methoxyphenol to CO_2 and H_2O , as shown in Eq. 2.6.



Typically, a precise amount of solid catalyst (25 mg of 1 wt% Fe/ZSM-5-WI or 1 wt% Fe-S-N/Zeolite, 50 mg of 0.5 wt % Fe-Ag-Zeolite and 2.5 mg of 12 wt% Fe-S-N/AC or 12 wt% Fe/AC catalysts with M:S ratio of 1:100) and 50 mL of ***m*-cresol** ($1000 \text{ mg}\cdot\text{L}^{-1}$) were placed into the reactor and heated to $80 \text{ }^\circ\text{C}$, $888 \text{ }\mu\text{L}$ of H_2O_2 (30% (w/w) with a stoichiometric ratio of *m*-cresol and H_2O_2 of 1:17 was added into the reaction mixture to start the reaction after the set temperature stabilising at $85 \text{ }^\circ\text{C}$ for 10 min. The reaction was conducted for 4 h under the constant stirring rate of 500 rpm and then quenched with an ice-water bath.

A stoichiometric ratio of *m*-cresol to H₂O₂ was set as 1:17 for the complete oxidation of *m*-cresol to CO₂ and H₂O, as shown in Eq. 2.7.



In a typical experiment, a specific amount of solid catalyst (20 mg of 1wt% Fe/ZSM-5-WI or 1 wt% Fe-S-N/Zeolite, 40 mg of 0.5 wt% Fe-Ag-Zeolite and 2 mg of 12 wt% Fe-S-N/AC or 12 wt% Fe/AC catalysts with M:S ratio of 1:100) and 50 mL of **4-chlorophenol** (1000 mg·L⁻¹) were placed into the reactor and heated to 80 °C, 1181μL of H₂O₂ (30% (w/w) with a stoichiometric ratio of 4-chlorophenol and H₂O₂ of 1:27 was added into the reaction mixture to start the reaction after the set temperature stabilising at 85 °C for 10 min. The reaction was conducted for 4 h under the continuous stirring rate of 500 rpm and then quenched with an ice-water bath.

A stoichiometric ratio of 4-chlorophenol to H₂O₂ was set as 1:27 for the complete oxidation of 4-chlorophenol to CO₂ and H₂O, as shown in Eq. 2.8.



According to a typical experiment, a clear amount of solid catalyst (20 mg of 1wt% Fe/ZSM-5-WI or 1 wt% Fe-S-N/Zeolite, 40 mg of 0.5 wt% Fe-Ag-Zeolite and 2 mg of 12 wt% Fe-S-N/AC or 12 wt% Fe/AC catalysts with M:S ratio of 1:100) and 50 mL of **4-bromophenol** (1300 mg·L⁻¹) were placed into the reactor and heated to 80 °C, 1135 μL of H₂O₂ (30% (w/w) with a stoichiometric ratio of 4-bromophenol and H₂O₂ of 1:27 was added into the reaction mixture to start the reaction after the set temperature stabilising at 85 °C for 10 min. The reaction was conducted for 4 h under the continuous stirring rate of 500 rpm and then quenched with an ice-water bath.

A stoichiometric ratio of 4-bromophenol to H₂O₂ was set as 1:27 for the complete oxidation of 4-bromophenol to CO₂ and H₂O, as shown in Eq. 2.9.



2.5.2 Homogeneous phase control tests

Control tests, by using a homogeneous catalyst, the catalytic test determine whether leached metal contributes to the catalytic reaction (zeolite and activated carbon). 50 mL of the mixture solution containing 1 g·L⁻¹ of reagent and metal ions (such as Ag⁺ from AgNO₃ and Fe³⁺ from

Fe(NO₃)₃) with concentrations corresponding to leached metal was prepared and heated to 80 °C. To start the reaction, H₂O₂ was added to the solution after stabilising it for 10 minutes. It compared the catalytic results obtained with heterogeneous catalysts to those obtained with a homogeneous catalyst.

2.5.3 Tests of catalyst reusability

The reusability of the catalyst was tested by successive catalyst reactions by recovering the catalyst after each run and reusing it without regeneration. Following the first reaction cycle, the catalyst was filtered and washed with deionised water (2 L per 1 g of catalyst) and dried at 120 °C overnight. The recovered catalyst was weighed before being used in the next run of the catalytic test. To ensure that no catalyst was lost, the exact amount of catalyst was used. Until the last reaction run (fourth run) the same process was repeated.

2.6 Characterization of reaction mixtures by chemical analysis

In CWPO of phenolic compounds, the catalytic performance of a catalyst was mainly determined by the conversion of phenolic compounds, the distribution of intermediates, the consumption of H₂O₂, and the metal leaching loss. Based on HPLC results, phenolic compound conversion and intermediate distribution were calculated.⁴⁷ The formulas for calculating these values are given in this part:

The phenolic compounds conversion ($X_{\text{phenolic compound, \%}}$) was calculated as:

$$X_{\text{phenolic compound, \%}} = \frac{C_{0, \text{phenolic compound}} - C_{f, \text{phenolic compound}}}{C_{0, \text{phenolic compound}}} \times 100\% \quad (\text{Eq. 2.10})$$

Where $C_{0, \text{phenolic compound}}$ (mol·L⁻¹) represents the concentration at the initial time (time 0) and $C_{f, \text{phenolic compound}}$ (mol·L⁻¹) is the final concentration, at the end reaction time, of the phenolic compound in the reaction mixture.¹³

The mass carbon balance (CMB) was calculated as follows:

$$\text{The CMB, \%} = \frac{\sum n_{f,i} \times N_{c,i}}{n_{0, \text{phenolic compound}} \times N_{c, \text{phenolic compound}}} \times 100\% \quad (\text{Eq. 2.11})$$

Where $n_{f,i}$ is the moles of intermediates (includes phenolic compound) remained in the reaction mixture after reaction, $N_{c,i}$ is the number of C atoms in each intermediate (contains phenolic

compound) molecule, $n_{0, \text{phenolic compound}}$ is the number of moles of initial phenolic compound in water, $N_{\text{C, phenolic compound}}$ is the number of C atoms in the phenolic compound molecule.¹³

The H₂O₂ consumption ($X_{\text{H}_2\text{O}_2, \%}$) was calculated by:

$$X_{\text{H}_2\text{O}_2, \%} = \frac{C_{0, \text{H}_2\text{O}_2} - C_{f, \text{H}_2\text{O}_2}}{C_{0, \text{H}_2\text{O}_2}} \times 100\% \quad (\text{Eq. 2.12})$$

Where $C_{0, \text{H}_2\text{O}_2}$ (mol·L⁻¹) and $C_{f, \text{H}_2\text{O}_2}$ (mol·L⁻¹) represent the initial and final concentration of H₂O₂ in the reaction mixture. The initial and final concentration of H₂O₂ in the reaction mixture was determined by iodometry titration.¹³

The metal leaching loss ($X_{\text{leaching}, \%}$) was calculated as follows:

$$X_{\text{leaching}, \%} = \frac{C_{\text{metal, leached}}}{C_{\text{metal, total}}} \times 100\% \quad (\text{Eq. 2.13})$$

Where $C_{\text{metal, leached}}$ (mg·L⁻¹) and $C_{\text{metal, total}}$ (mg·L⁻¹) represent the metal concentration detected in the reaction mixture after the reaction and the total concentration of metal used in the response, respectively. The metal concentration in the reaction mixture was determined using ICP-OES.

2.6.1 Qualitative determination of phenolic compounds and their intermediates

Due to the similar properties among tens of potential products during the phenol oxidation and, at the same time, the relatively low concentration of some components, qualitative and quantitative analysis of the reaction mixture is challenging. Due to its ability to determine all potential products, HPLC was used as the primary technique for intermediate analysis in this project.

In the HPLC analysis conditions, the sample mixture, after filtering, was analysed with a UV detector using a Waters XBridge C18 column as the stationary phase and orthophosphoric acid (0.1% (v/v)) as a dual mobile phase. The flow rate was set at 1 mL·min⁻¹, and a gradient elution program was as follows: isocratic acetonitrile 2% in water from 0 to 5 min, 2% of acetonitrile at 5 min to 70% at 20 min that to clean the column, 2% of acetonitrile from 20.1 min - 30 min. A volume of 5 µL samples were injected into the sampling system and analysed with a UV detector at different wavelengths (phenol 270 nm; DMP 271 nm; *m*-cresol 273 nm; 3-

methoxyphenol 274 nm; 4-chlorophenol; and 4-bromophenol 281 nm, other intermediates 200 nm).

- **An analysis of phenol and its intermediates**

To determine the amount of phenol and intermediates in the reaction mixture, five steps were followed. Based on current literature, created a list of all the possible intermediates involved in phenol oxidation, ii) Prepared standard solutions mimicking a reaction mixture expected to be used to determine phenol and the expected intermediates, iii) Analyse the effectiveness of the method in the characterization of actual reaction mixtures, iv) Use an external standard method, quantify the concentration of phenol and all intermediates mentioned in the reaction mixture, and v) Use carbon mass balance (CMB) in water, verify that the analysis method is consistent.

- **Using HPLC to analyse phenol and intermediates in standard solutions**

HPLC, commonly used to separate, identify, and quantify mixture components, can be used to quantify phenol and its intermediates. Accordingly, the mobile phase components interact slightly differently with the stationary phase (the solvent carries the sample through the column). There is a slight difference in how the stationary phase interacts with it (the immobile phase retains the sample component). Consequently, each component will take a different amount of time to flow out of the column if the column is filled with different components. The retention time (t_R) is the amount of time between the injection of the sample and the peak maximum, as calculated by equation 2.14.

$$t_R = t_R' + t_M \quad (\text{Eq.2.14})$$

Thus, the retention time is the total time the solute spends in the stationary phase (t_R') and in the mobile phase (t_M).

The HPLC chromatogram of the standard solution is shown in figure 2.8. As can be seen, the separation of phenol and the expected intermediates occurred under the analysis condition (see figure 2.8). Based on the HPLC chromatogram, retention times can be used to identify each known standard compound in the mixture solution.

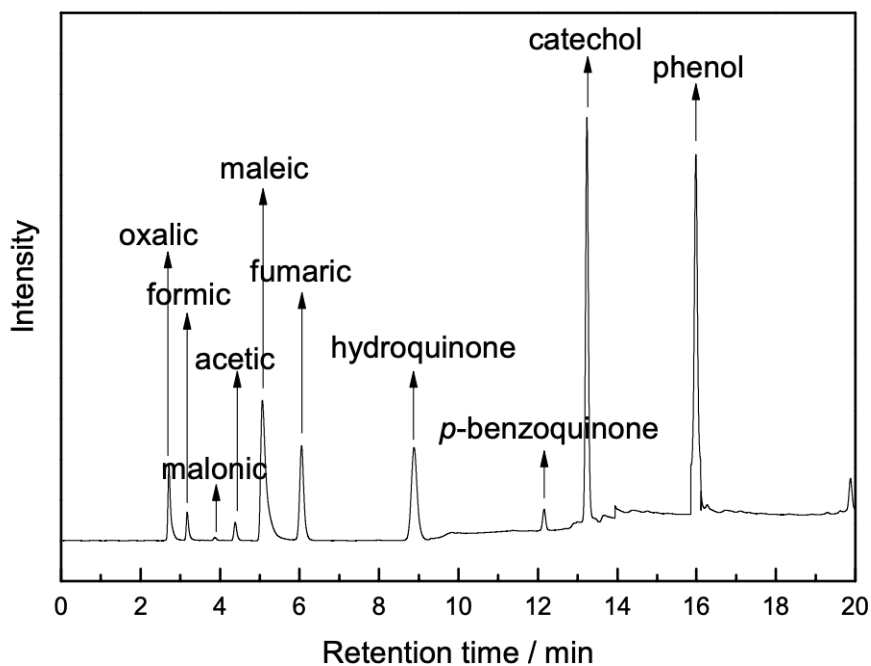


Figure 2.8: HPLC chromatogram of mixed standard solution (analysis condition: H_3PO_4 solution (0.1% (v/v)) and acetonitrile as dual mobile phases with acetonitrile percentage of 2% from 0-5 min, 2%- 70% from 5-20 min, 2 % from 20.1-30 min, injection volume 5 μL , wavelength 200 nm).

The elution order of those compounds is (shown in table 2.1): oxalic acid (2.6 ± 0.1 min), formic acid (3.1 ± 0.1 min), malonic acid (3.8 ± 0.1 min), acetic acid (4.4 ± 0.1 min), maleic acid (5.1 ± 0.1 min), fumaric acid (6.1 ± 0.1 min), hydroquinone (8.9 ± 0.2 min), p-benzoquinone (12.1 ± 0.1 min), catechol (13.2 ± 0.1 min) and phenol (16.0 ± 0.1 min).

Based on table 2.1, phenol and all the expected intermediates can be separated per sample in just 20 minutes, demonstrating a highly efficient analysis method.

Table 2.1: Retention times of phenol and expected intermediates in mixed standards solution (reaction condition: 0.1 g 1% Fe/ZSM-5-WI, 50 mL of 1 g·L⁻¹ phenol, phenol: H₂O₂=1: 14, 80 °C, 40 min, 500 rpm).

Component	Retention time in mixed standards solution / min	Retention time in actual reaction mixture / min
Oxalic acid	2.6 ± 0.1	2.6 ± 0.1
H ₂ O ₂	--	2.7 ± 0.1
Formic acid	3.1 ± 0.1	3.1 ± 0.1
Malonic acid	3.8 ± 0.1	3.8 ± 0.1
Acetic acid	4.4 ± 0.1	4.4 ± 0.1
Maleic acid	5.1 ± 0.1	5.1 ± 0.1
Fumaric acid	6.1 ± 0.1	6.1 ± 0.1
hydroquinone	8.9 ± 0.2	8.9 ± 0.2
<i>p</i> -benzoquinone	12.2 ± 0.1	12.2 ± 0.1
Catechol	13.2 ± 0.1	13.2 ± 0.1

2.6.2 The determination of H₂O₂

In the laboratory, iodometry is usually the ultimate calibration method for H₂O₂ standards, so it was decided to use it instead of one of the alternatives.⁴⁸⁻⁵⁰ Although the method is not quite as accurate as permanganate titration, it is less susceptible to interference from organic compounds. In addition, it is more appropriate for measuring levels of H₂O₂ mg·L⁻¹.⁵¹ It is more appropriate to perform iodometry titration in this reaction system; the typical titration procedure is as follows.

A diluted reaction solution of 5 mL (with a dilution ratio of 100), 5 mL KI (100 g·L⁻¹), and 1 mL H₂SO₄ was pipetted into the flask; the mixture was allowed to sit for 10 minutes in a dark until a yellow solution was obtained.⁵² The sample solution was titrated with Na₂S₂O₃ (2 mM) till the solution became pale yellow. 1 mL starch solution (10 g·L⁻¹) was added to indicate the colour change (from pale yellow to blue). More Na₂S₂O₃ (2 mM) was added till the blue colour disappeared (Figure 2.9). The volume (V₄) of Na₂S₂O₃ solution at the end point of titration was recorded, and then calculate the concentration of H₂O₂ followed the formula (Eq. 2.15):

$$C_{H_2O_2} = \frac{1}{2} \times \frac{C_{Na_2S_2O_3} \times V_4}{V_{H_2O_2}} \times D_2 = 10 \times C_{Na_2S_2O_3} \times V_4 \quad (\text{Eq. 2.15})$$

Where $C_{Na_2S_2O_3}$ ($\text{mol} \cdot \text{L}^{-1}$) and V_4 (mL) represent the concentration and the volume of $Na_2S_2O_3$ solution, while $V_{H_2O_2}$ (mL) and D_2 ($=100$) are volumes and the dilution ratio of H_2O_2 solution (or reaction mixture).

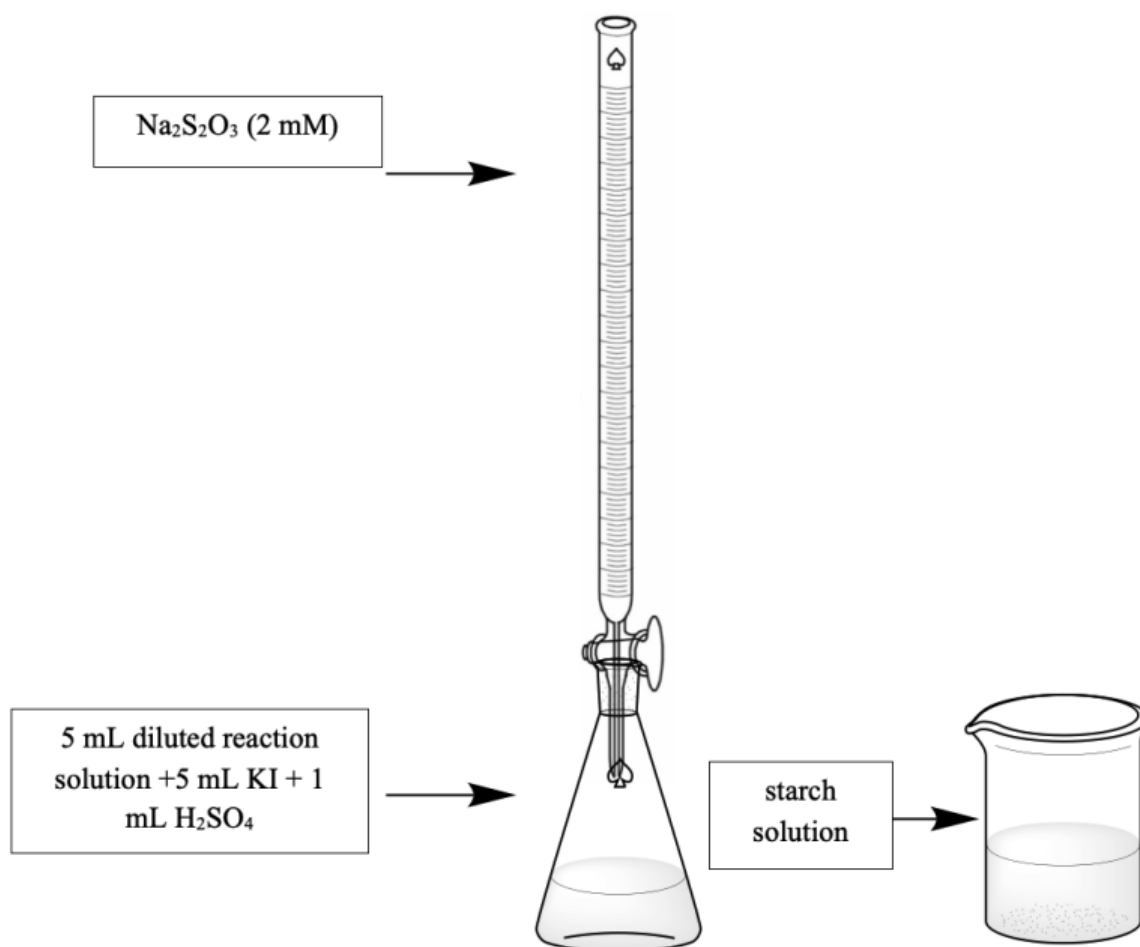


Figure 2.9: The reaction scheme of H_2O_2 determination by iodometry titration.

2.6.3 Determination of metal leaching

ICP-OES was used to test the metal leaching of the catalyst during the reaction by a calibration dilution method of standards prepared from stock solutions containing 1000 parts per million (ppm) of metal standards, calibrated to 10 parts per billion (ppb). A calibration graph was used

to calculate the concentrations of metal ions in the samples. After the reaction, a sample of the reaction mixture (5 mL) was taken for the leaching tests.

2.6.4 AC acidity measurements

In carbon materials, the surface chemistry is determined by their surface's acidic and essential nature. The total surface acidity and basicity of the surfaces were determined by titrating them with NaOH and HCl.⁵³ According to Boehm (1966) and Fabish and Schleifer (1984), titration using alkalimetric procedures. The activated carbon sample (5 g) was dried in a vacuum oven at 120 °C for 24 h before titration. In a series of test tubes containing a given amount of activated carbon, 25 ml of NaOH (0.1 N) solution was added. The sample was mixed at 100 rpm and 25 °C for 24 h. The supernatant was then withdrawn from the test tubes and back-titrated with HCl (0.1 N).⁵⁴

The mean of acid-base back titration will measure the acidity of AC in (mmol.g⁻¹). Typically, 100 mg of AC is stirred with 10 mL of standardised NaOH with a concentration of 0.13 M at 40 °C overnight. The solutions were washed with 10 mL of deionised water and filtrated; the filtrate was titrated with 0.128 M of standardised HCl using methyl orange as an indicator.

To calculate the acid sites in mol per gram:

$$\text{The acid sites mol. g}^{-1} = \frac{n_{\text{reacted NaOH}}}{\text{mass of AC in g}} \times 1000 \text{ (Eq. 2.16)}$$

Where $n_{\text{reacted, NaOH}}$ is the number of moles of reacted NaOH that can be calculated as:

$$n_{\text{reacted NaOH}} = n_{i, \text{NaOH}} - n_{\text{HCl, back}} \text{ (Eq. 2.17)}$$

As *the* $n_{i, \text{NaOH}}$ is the initial concentration in mol of NaOH ($\frac{C \times V}{100}$), $n_{\text{Back, HCl}}$ is the

concentration of HCl in mol ($\frac{C \times V}{100}$)

The second way has been used to determine the acidity of AC was by using a pH meter calibration measurement.

2.7 Statistical analysis of data

2.7.1 Significance testing

The validity of significance testing has recently gained much interest.⁵⁵ It is, therefore, appropriate to report this section to emphasise the importance of ensuring that the data and research questions are compatible. Statistical analysis should be interpreted in accordance with the data and not taken to mean more than it implies.⁵⁶ As part of the analytical chemistry process, significance testing is often used in conjunction with exploratory data analysis (Is there a reason to suspect that the two analytical methods are different when applied to the same sample?) or inferential data analysis (Is there any reason to assume that these two independent measurements are related?). In these questions, a statistically significant result generally leads to the design of additional experiments that can make suggestions or clarify cause-and-effect relationships more clearly. A significance test is the first step toward a better understanding of an analytical problem, but it does not provide the final answer.

A. The Construction of a Significance Test

The aim of a significance test is to identify if the difference between two or more results is significant and that it cannot be justified by indeterminate errors. A significance test is created by stating the problem in terms of yes or no answers. A null hypothesis and an alternative hypothesis describe the two potential answers to the yes or no question.

The null hypothesis, H_0 , is that indeterminate errors are sufficient to explain any differences between the results. The alternative hypothesis, H_A , assumes that the differences in results are too significant to be explained by random error. Tests the null hypothesis, which is either retained or rejected. If it rejects the null hypothesis, then it must agree with the alternative hypothesis and conclude that the difference is significant. Null hypotheses are retained rather than accepted when they are not rejected. Null hypotheses are retained whenever the evidence is insufficient to prove that they are incorrect. Null hypotheses cannot be proven true due to how significance tests are conducted.

Once the alternative and null hypotheses have been outlined, in the second step, a significance level is determined for the analysis. The significance level is a measure of the probability that the null hypothesis will be incorrectly rejected or a measure of the confidence level in the null hypothesis. A significance level is expressed in the former case as a percentage (e.g., 95%), whereas in the latter, as α , where α is defined as

$$\alpha = 1 - \frac{\text{confidence level (\%)}}{100} \quad (\text{Eq 2. 18})$$

Thus, for a 95% confidence level, α is 0.05.

The third step is to calculate the test statistic and compare it to a critical value. The test statistic's critical value provides a limit between values that leads to rejecting or retaining the null hypothesis. Calculating the test statistic depends on the comparison. Finally, it is either to retain the null hypothesis or reject it and accept the alternative hypothesis.

B. One-Tailed and Two-Tailed Significance Tests

For example, it might want to determine whether a new analytical method is accurate. This method could be used to analyse a Standard Reference Material that contains a known concentration of analyte, μ . By analysing the standard several times, a mean value, \bar{X} , is obtained for the concentration of the analyte. Null hypothesis: There is no difference between \bar{X} and μ

$$H_0 : \bar{X} = \mu \quad (\text{Eq 2.19})$$

The null hypothesis is retained if the significance test is conducted at $\alpha = 0.05$, and a 95% confidence interval around \bar{X} contains μ if the alternative hypothesis is

$$H_A : \bar{X} \neq \mu \quad (\text{Eq 2.20})$$

The null hypothesis is rejected, and the alternative hypothesis is accepted if \bar{x} lies in the shaded areas at either end of the distribution curve of the sample (Figure 2.10 a). Shaded areas account for 2.5% of the probability distribution curve, totalling 5%. This is a two-tailed significance test since it rejects the null hypothesis for values of \bar{x} at either end of the probability distribution curve for the sample. It could write the alternative hypothesis in two different ways

$$H_A : \bar{X} > \mu \quad (\text{Eq 2.21})$$

$$H_A : \bar{X} < \mu \quad (\text{Eq 2.22})$$

In Figure 2.10 b or Figure 2.10 c, reject the null hypothesis if \bar{x} falls within the shaded areas. For each case, the shaded area corresponds to 5% of the area under the probability distribution curve. One-tailed significance tests are illustrated in these examples.

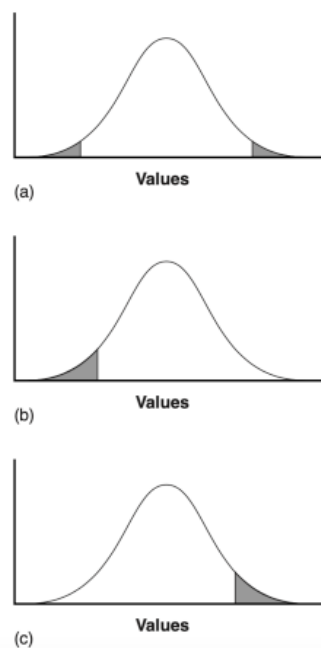


Figure 2.10: Examples of (a) two-tailed and (b, c) one-tailed significance tests of X and n . The probability distribution curves, called normal distributions, depending on the sample's mean and standard deviation. For a $\alpha = 0.05$, the shaded areas cover 5% of the curve's area. If n falls within the shaded areas, it rejects the null hypothesis and accepts the alternative hypothesis. The null hypothesis is retained if the value of n falls within the unshaded area of the curve.

A two-tailed significance test with a fixed confidence level is more conservative since rejecting the null hypothesis requires a larger difference between the parameters. When comparing two parameters, it is reasonable to expect one to be larger (or smaller). As an example, when evaluating the accuracy of a new analytical method. In most cases, it is appropriate to use a two-tailed significance test.

2.7.2 Statistical methods for normal distributions

A normal distribution is the most common distribution for results. Constructing and evaluating significance tests on normal distribution curves is simple because the area between their limits is well-defined.

A. Comparing \bar{X} to μ

Analysing a sample containing a known amount of analyte, n , is one way of validating a new analytical method. A significance test is used to compare \bar{X} to μ , the average amount of analyte in the sample, to judge the method's accuracy. According to the null hypothesis, the difference between \bar{X} and μ can be explained by indeterminate errors that affect the calculation of \bar{X} . An alternative hypothesis is that the difference between \bar{X} and μ is too large to be explained by indeterminate errors.

The equation for the test (experimental) statistic, t_{exp} , is derived from the confidence interval for μ

$$\mu = \bar{X} \pm \frac{t_{exp} s}{\sqrt{n}} \quad (Eq\ 2.23)$$

Rearranging equation

$$t_{exp} = \frac{|\mu - \bar{x}| \times \sqrt{n}}{s} \quad (Eq\ 2.24)$$

When μ is either at the right or left edge of the sample's confidence interval, it gives the value of t_{exp} . The null hypothesis is retained or rejected by comparing the value of t_{exp} to its critical value, $t(\alpha, \nu)$, where α is the confidence level, $t(\alpha, \nu)$ is the number of degrees of freedom for the sample. A critical value $t(\alpha, \nu)$ defines the maximum confidence interval that can be accounted for by indeterminate errors. If $t_{exp} > t(\alpha, \nu)$, then the sample's confidence interval is significantly larger than that explained by indeterminate errors. The null hypothesis is rejected in this case, and the alternative hypothesis is accepted. If $t_{exp} \leq t(\alpha, \nu)$, a null hypothesis retains a confidence interval lower than the indeterminate error.

This significance test, is known as a **t-test** of \bar{X} to μ . The t-test compares two mean values to see if there is a large difference between them that cannot be explained by indeterminate error.

B. Comparing S^2 to σ^2

If it analyses a particular sample regularly, it may be able to establish an expected variance, σ^2 , for the analysis. A few replicate analyses of a single sample give a sample variance, S^2 , whose value is differences may or may not be significant from σ^2 .

The statistical comparison of S^2 to σ^2 , indicates whether the analysis is under "statistical control." The null hypothesis is that S^2 and σ^2 , are identical, and the alternative hypothesis is

that they are not identical. The test statistic for evaluating the null hypothesis is called an **F-test**, and is given as either

$$F_{exp} = \frac{s^2}{\sigma^2} \text{ if } (s^2 > \sigma^2) \text{ or } F_{exp} = \frac{\sigma^2}{s^2} \text{ if } (\sigma^2 > s^2) \quad (\text{Eq 2.25})$$

Based on when S^2 is greater or smaller than σ^2 . The value of F_{exp} is determined by ensuring its value is above or equal to 1.

Assuming the null hypothesis is true, then F_{exp} should equal one; despite this, due to indeterminate errors, F_{exp} usually is much higher than one. A critical value, $F(\alpha, \nu_{num}, \nu_{den})$, is the largest value of F_{exp} that it can give to indeterminate error based on its significance level, α , and the degrees of freedom for the variance in its numerator, ν_{den} and the variance in the denominator, ν_{den} . The degrees of freedom for σ^2 is $n-1$, where n is the number of replications to calculate variance, and the degrees of freedom for σ^2 is defined as infinity, ∞ . Critical values of F for $\alpha = 0.05$ are listed in Appendix 5 for both one-tailed and two-tailed F -tests. So, **F-test:** Statistical test for comparing two variances to see if their difference is too large to be explained by indeterminate error.

C. Comparing two sample variances

The F -test can be modified to compare variances for two samples, A and B, by rewriting the equation as

$$F_{exp} = \frac{S_A^2}{S_B^2} \quad (\text{Eq 2.26})$$

where A and B are defined such that S_A^2 is greater than or equal to S_B^2 .

D. Comparing two sample means

Three factors influence the results of analysis: the method, the sample, and the analyst. It is possible to study the influence of these factors by conducting two experiments where only one factor is changed. For example, the same analyst can compare two methods by applying them to the same sample and examining their means. Similarly, two analysts or samples can be compared.

According to the source of the data, significance testing for comparing two mean values can be divided into two categories. An unpaired data set is one derived from the analysis of several samples taken from the same source. Data pairs are encountered when analysing samples from different sources.

Unpaired Data Consider two samples, A and B, for which the mean values, \bar{X}_A and \bar{X}_B , and standard deviations, s_A and s_B , are known. For both samples, confidence intervals for μ_A and μ_B can be calculated.

$$\mu_A = \bar{X}_A \pm \frac{ts_A}{\sqrt{n_A}} \quad (\text{Eq 2.27})$$

$$\mu_B = \bar{X}_B \pm \frac{ts_B}{\sqrt{n_B}} \quad (\text{Eq 2.28})$$

Where n_A and n_B are the number of trials replicated on samples A and B. Comparing the means is based on a null hypothesis that \bar{X}_A and \bar{X}_B are identical and an alternative hypothesis that the means are significantly different.

A test statistic is derived by letting μ_A equal μ_B ,

$$\bar{X}_A \pm \frac{ts_A}{\sqrt{n_A}} = \bar{X}_B \pm \frac{ts_B}{\sqrt{n_B}} \quad (\text{Eq 2.29})$$

Solving for $|\bar{X}_A - \bar{X}_B|$ and using a propagation of uncertainty, gives

$$|\bar{X}_A - \bar{X}_B| = t \times \sqrt{\frac{s_A^2}{n_A} + \frac{s_B^2}{n_B}} \quad (\text{Eq 2.30})$$

Finally, solving for t , which we replace with t_{exp} , leaves us with

$$t_{\text{exp}} = \frac{|\bar{X}_A - \bar{X}_B|}{\sqrt{\left(\frac{s_A^2}{n_A} + \frac{s_B^2}{n_B}\right)}} \quad (\text{Eq 2.31})$$

The value of t_{exp} is compared with a critical value, $t(\alpha, \nu)$, based on the significance level, α , the degrees of freedom in the sample, ν , and whether the significance test is one-tailed or two-tailed.^{57, 58}

2.8 References:

1. C. Perego and P. Villa, *Catalysis Today*, 1997, **34**, 281-305.
2. F. Pinna, *Catalysis Today*, 1998, **41**, 129-137.
3. J. R. Sietsma, A. J. van Dillen, P. E. de Jongh and K. P. de Jong, in *Studies in surface science and catalysis*, Elsevier, 2006, **162**, 95-102.
4. J. Haber, J. Block and B. Delmon, *Pure and applied Chemistry*, 1995, **67**, 1257-1306.
5. G. Jacobs, Y. Ji, B. H. Davis, D. Cronauer, A. J. Kropf and C. L. Marshall, *Applied Catalysis A: General*, 2007, **333**, 177-191.
6. D. J. Suh, P. Tae-Jin and I. Son-Ki, *Carbon*, 1993, **31**, 427-435.
7. P. Yan, J. Mensah, A. Adesina, E. Kennedy and M. Stockenhuber, *Applied Catalysis B: Environmental*, 2020, **267**, 118690.
8. F.-W. Chang, M.-S. Kuo, M.-T. Tsay and M.-C. Hsieh, *Applied Catalysis A: General*, 2003, **247**, 309-320.
9. A. Ribera, I. Arends, S. De Vries, J. Pérez-Ramirez and R. Sheldon, *Journal of Catalysis*, 2000, **195**, 287-297.
10. M. M. Mohamed, I. O. Ali and N. Eissa, *Microporous and Mesoporous Materials*, 2005, **87**, 93-102.
11. Y. Yan, S. Jiang and H. Zhang, *Separation and Purification Technology*, 2014, **133**, 365-374.
12. R. Long and R. T. Yang, *Catalysis Letters*, 2001, **74**, 201-205.
13. G. Yang, S. Mo, B. Xing, J. Dong, X. Song, X. Liu and J. Yuan, *Environmental Pollution*, 2020, **258**, 113687.
14. A. Rey, M. Faraldos, J. Casas, J. Zazo, A. Bahamonde and J. Rodríguez, *Applied Catalysis B: Environmental*, 2009, **86**, 69-77.
15. H. Qin, R. Xiao and J. Chen, *Science of the Total Environment*, 2018, **626**, 1414-1420.
16. M. Conte, A. F. Carley, C. Heirene, D. J. Willock, P. Johnston, A. A. Herzing, C. J. Kiely and G. J. Hutchings, *Journal of catalysis*, 2007, **250**, 231-239.
17. A. E. Aksoylu, M. M. A. Freitas and J. L. Figueiredo, *Applied Catalysis A: General*, 2000, **192**, 29-42.
18. A. Rahman and S. Jonnalagadda, *Catalysis letters*, 2008, **123**, 264-268.
19. T. Guma, P. Madakson, D. Yawas and S. Aku, *Int. J. Mod. Eng. Res*, 2012, **2**, 4387-4395.

20. N. Pappas, *American Journal of Physiology-Gastrointestinal and Liver Physiology*, 2006, **2**, 285-292.
21. R. Sharma, D. Bisen, U. Shukla and B. Sharma, *Recent research in science and technology*, 2012, **4**, 77-79.
22. B. Fultz and J. M. Howe, *Transmission electron microscopy and diffractometry of materials*, Springer Science & Business Media, 2012.
23. Y. Zhang, R. Colella, S. Kycia and A. Goldman, *Acta Crystallographica Section A: Foundations of Crystallography*, 2002, **58**, 385-390.
24. E. Ameh, *The international journal of advanced manufacturing technology*, 2019, **105**, 3289-3302.
25. D. S. Sivia, *Elementary scattering theory: for X-ray and neutron users*, Oxford University Press, 2011.
26. M. Razeghi, *Proceedings of the IEEE*, 2002, **90**, 1006-1014.
27. F. Sánchez-Bajo and F. Cumbreira, *Journal of applied crystallography*, 1999, **32**, 730-735.
28. R. Hill and L. Cranswick, *Journal of applied crystallography*, 1994, **27**, 802-844.
29. R. F. Lobo, *Handbook of zeolite science and technology*, 2003, 92-124.
30. J. F. Watts, *Surface science techniques*, 1994, **45**.
31. J. Chastain and R. C. King Jr, *Perkin-Elmer Corporation*, 1992, **40**, 221.
32. J. D. Andrade, *Surface and Interfacial Aspects of Biomedical Polymers: Volume 1 Surface Chemistry and Physics*, 1985, 105-195.
33. M. Conte, A. F. Carley and G. J. Hutchings, *Catalysis Letters*, 2008, **124**, 165-167.
34. F. Ambroz, T. J. Macdonald, V. Martis and I. P. Parkin, *Small methods*, 2018, **2**, 1800173.
35. D. Do, H. Do and D. Nicholson, *Chemical engineering science*, 2010, **65**, 3331-3340.
36. D. M. Antonelli and J. Y. Ying, *Chemistry of materials*, 1996, **8**, 874-881.
37. Z. Konya, V. Puentes, I. Kiricsi, J. Zhu, J. Ager, M. Ko and H. Frei, *Chem. Mater.*, 2003, **15**, 1242-1248.
38. A. Janssen, A. Koster and K. De Jong, *The Journal of Physical Chemistry B*, 2002, **106**, 11905-11909.
39. H. David, *Journal of the American College of Cardiology*, 2019, **8**, 1044-53..
40. C. Horváth, *High-performance liquid chromatography: advances and perspectives*, 2013.
41. C. A. Rimmer, *Analytical and Bioanalytical Chemistry*, 2011, **399**, 1809-1810.

42. S. Lindsay, *High performance liquid chromatography*, John Wiley & Sons, 1992.
43. S. A. Korhammer and A. Bernreuther, *Fresenius' journal of analytical chemistry*, 1996, **354**, 131-135.
44. C. G. Novaes, M. A. Bezerra, E. G. P. da Silva, A. M. P. dos Santos, I. L. da Silva Romao and J. H. S. Neto, *Microchemical journal*, 2016, **128**, 331-346.
45. J. A. Broekaert, *Analytical atomic spectrometry with flames and plasmas*, John Wiley & Sons, 2006.
46. X. Hou and B. T. Jones, *Journal*, 2000, **2000**, 9468-9485.
47. C. Zhou, PhD thesis, University of Sheffield, 2021.
48. C. Ricciuti, J. Coleman and C. Willits, *Analytical chemistry*, 1955, **27**, 405-407.
49. I. Kolthoff and B. R. Stenger, *Journal of American Chemical*, 1957.
50. R. J. Kieber and G. Helz, *Analytical Chemistry*, 1986, **58**, 2312-2315.
51. N. V. Klassen, D. Marchington and H. C. McGowan, *Analytical Chemistry*, 1994, **66**, 2921-2925.
52. W. J. Shen, Y. Ichihashi, M. Okumura and Y. Matsumura, *Catalysis letters*, 2000, **64**, 23-25.
53. C. Moreno-Castilla, M. Ferro-Garcia, J. Joly, I. Bautista-Toledo, F. Carrasco-Marin and J. Rivera-Utrilla, *Langmuir*, 1995, **11**, 4386-4392.
54. C. Moreno-Castilla, F. Carrasco-Marín and A. Mueden, *Carbon*, 1997, **35**, 1619-1626.
55. R. Nuzzo, *Nature*, 2014, **506**, 150.
56. J. T. Leek and R. D. Peng, *Science*, 2015, **347**, 1314-1315.
57. D. Harvey, *Modern analytical chemistry*, McGraw-Hill New York, 2000.
58. E. R. Ziegel, *Technometrics*, 2004, **46**, 498.

Chapter 3: Catalytic wet peroxide oxidation of phenol using catalyst-supported and acid-pre-treated Fe-activated carbon catalysts

3.1 Fe doping activated carbon catalysts Fe/AC

3.1.1 Introduction

The Fenton reaction is a highly convenient, economical, and effective way of treating phenolic compounds in wastewater.¹⁻³ In the Fenton process, $\text{Fe}^{2+}/\text{Fe}^{3+}$ species can be used under acidic conditions (below pH 2.5/3, H_2O_2 can decompose, and Fe^{3+} can be inhibited/destabilised) as a catalyst to generate $\cdot\text{OH}$ radicals, thus removing high pollutants.⁴ However, the direct use of Fe salt is made difficult because of the non-straightforward recovery from effluents resulting in the formation of iron sludge, and as such, its use in wastewater treatment is limited.⁵⁻⁷ Therefore, much research has been devoted to iron being immobilised on supports to overcome these problems to turn it into a heterogenous catalyst, resulting in catalytic wet peroxide oxidation CWPO.⁸ Furthermore, CWPO can be carried out under mild conditions without using complex equipment.⁹ In CWPO, catalyst support improves the dispersion of Fe, prevents sintering, and increases chemical and thermal stability, leading to enhanced pollution degradation by a longer catalyst lifetime and recovery.¹⁰ Catalysts for the CWPO process are often based on bonding Fe onto porous surfaces, such as activated carbon,¹¹ carbon xerogel,¹² alumina,¹³ pillared clays or zeolites,¹⁴ and TiO_2 .¹⁵

In recent years, activated carbon (AC) has gained popularity as a catalyst support material due to its unique properties, such as stability in both acidic and basic media, the ease of stabilising precious or heavy metals when supported on AC,⁹ and its high thermal resistance, the cheap cost and at the same time large availability, and importantly its porosity so that it can bring Fe centres, radical species and substrates all at close range. The latter is an essential property for the exploitation of Fenton systems. In addition, they have both hydrophilic and hydrophobic properties.^{16, 17}, which might be useful in systems like ours where we have an organic substrate (partially hydrophobic) and a water media (hydrophilic). One of the drawbacks of activated carbons as catalyst support, though, is the presence of minerals during the preparation process or arising from its sources (e.g. coal, coconut shell, wood). As well as the fact that many activated carbons contain high levels of ash (ash is one of the properties of activated carbon. Higher ash in the activated carbon reduces its effectiveness), especially those made from coal, and such need to be washed before any catalytic application.^{18 19 20}

Carbon is considered an inert material compared to other catalyst supports (it should be noted, though, that the inertness or not is also reaction dependent), but its surface is not as inert as expected because of the presence of heteroatoms, which may serve as both active sites for a reaction or conveniently as ‘anchoring’ sites when doping the carbon with a metal. As such, the surface chemistry of carbon materials is fundamentally dependent on the heterogeneity of the surface composition.²¹ The term heteroatom refers to an atom other than carbon in a parent matrix, such as O, N, H, S, and P. Activation methods and precursors determine the nature and amount of these elements.²²⁻²⁴ It has been proposed that heteroatoms can generate surfaces with acidic or basic properties by combining surface functionalities with delocalised electrons in aromatic carbon.

Quite importantly, among all these hetero-species, the primary one is mostly oxygen which leads to oxygen-containing functional groups.²⁵⁻²⁷ These are generally located on the external surfaces or edge regions of the carbon and plays a major role in controlling carbon’s chemical nature. In these specific outer positions, oxygen concentrations play a significant role in determining the adsorption capabilities of carbon due to their primary use as adsorption sites. Researchers have found that many groups containing oxygen atoms are located on carbon surfaces, including carboxylic, chromene, lactone, phenol, quinone, pyrone, carbonyl and ethers. Surface acidity is usually attributed to functional groups containing carboxylic groups (Figure 3.1).²⁸⁻³¹ There are also anhydrides, lactones, and phenolic hydroxyls present on the surface.

If nitrogen species are considered instead, activated carbon is characterised by two features: (i) delocalised electrons within fused aromatic structures and (ii) nitrogen-enriched functionalities that can bind protons.³²⁻³⁴ It has also been demonstrated that certain functional groups containing oxygen, such as chromene, ketone, and pyrone, contribute to the acidity/basicity of carbon (Figure 3.1), with oxygen generally contributing to acidity and mostly a Bronsted like acidity. In this case, the oxygen atom, with lone pairs of electrons, can serve as a site for proton acceptance, (an acid, according to Lewis, is a substance with a vacant orbital capable of accepting electron pairs while Bronsted defines an acid as donating a proton or H^+ to another compound and forming a conjugate base. As a result, Bronsted acids donate H^+ , while Bronsted bases accept H^+ and compounds that donate electrons are Lewis bases, while compounds that accept electrons are Lewis acids) and nitrogen to basicity. However, extensive studies have revealed that the basicity of activated carbons is derived from delocalised electrons. That is, π -electrons in carbon layers behave like Lewis basic sites. A survey conducted by Leon y Leon

et al. showed that oxygen-free activated carbon surfaces could adsorb protons efficiently from aqueous media.³⁵ Those sites on the basal plane of carbon crystallites which are electron-rich, account for the excellent adsorption properties, which are highly needed by the charged metals in this case, indicating the good choice of activated carbon as a support. Therefore, these regions are Lewis basic.³⁶ Nitrogen groups usually induce basic character so that they can improve interactions between carbon surfaces and acidic species by dipole-dipole interactions, hydrogen bonding, and covalent bonding.^{37, 38}

In catalyst preparation, like in our case, where we aim to deposit heavy metals as dopants, oxygen-bearing groups play a crucial role. According to the related literature, surface functional groups have a significant impact on the activity of AC-supported catalysts.³⁹⁻⁴² A few studies have proposed that the surface chemistry of the support affects the precursor/support interaction and, consequently, the reducibility of the catalyst.⁴²

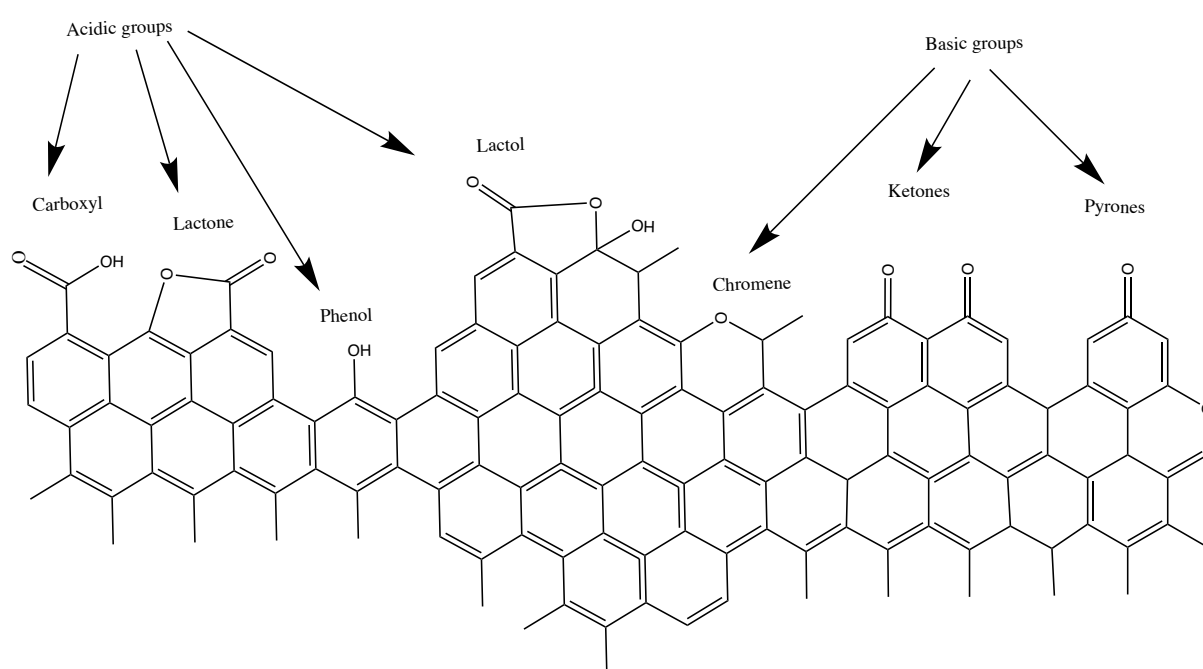


Figure 3.1: Typical representation for an acidic and basic surface functionality is observed on the carbon basal plane.⁴³

As mentioned, carbon surfaces' acidic and essential characteristics determine their surface chemistry, which can be changed by treating an AC with oxidising agents (but not directly using molecular oxygen; otherwise, this would burn the carbon). These treatments produce oxygen surface complexes containing seven types of surface groups that can be formed on AC,

including carboxylic acid, lactone, phenol, carbonyl, anhydride, and ether and quinone groups,⁴⁴ (Figure 3.2). That makes the carbon material more hydrophilic and acidic, lowering the pH of their point of zero charges (the pH of point zero charges (PZC) is the pH value where the components of surface charge equal zero under certain conditions, including temperature, pressure, and components of the aqueous solution. However, it does not mean there are no charges on the surface of PZC, as there are equally positive and negative charges) increasing their surface charge density.^{33, 45-54} In addition, changes in surface chemistry resulted in significant improvements in loading capacity and catalytic activity.²⁷ Various oxidising agents can be used in aqueous solutions to form oxygen surface complexes, such as nitric acid, hydrogen peroxide, and ammonium peroxydisulfate.⁵⁵ It has been reported that not all of these ACs behave in the same manner.^{51, 52}

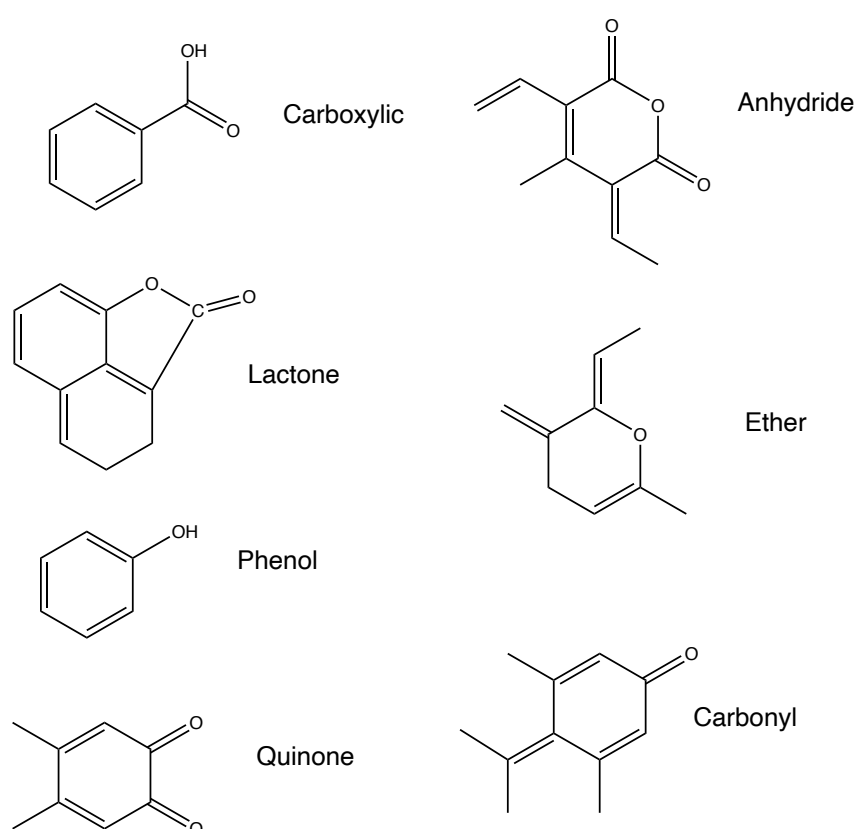


Figure 3.2: Types of groups expected to be formed by oxidation treatment of AC.

Activated carbons are commonly treated with non-oxidant acids such as HCl and HF to reduce their mineral content.^{56 57} The demineralisation process can change the surface area and pore texture of the sample depending on the amount and nature of the mineral matter and its distribution within the carbon matrix. In addition, surface area and porosity may be modified by acid treatment independently of the change introduced by mineral removal. Also, it has been reported that this treatment causes a relative increase in single-bonded oxygen functional groups such as phenols, ethers, and lactones. A possible reaction is illustrated in Figure 3.3.⁵⁸

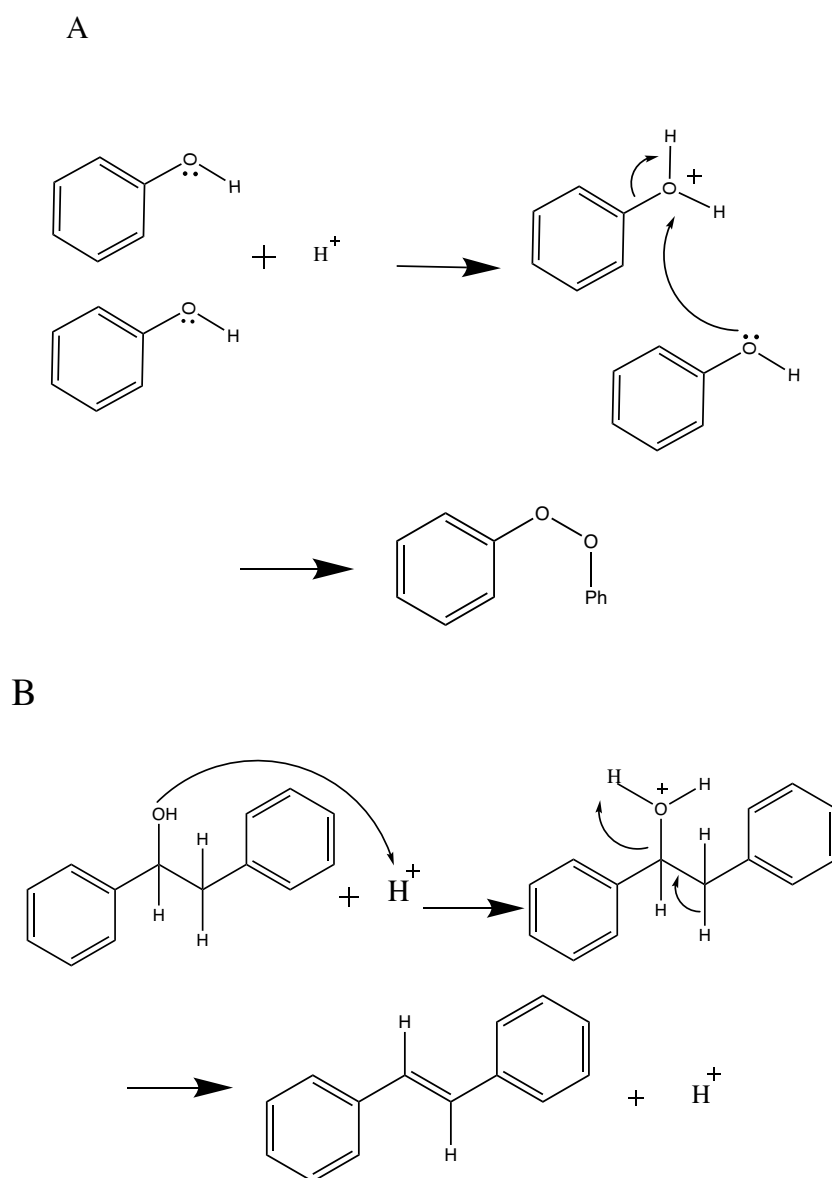


Figure 3.3: Possible reactions that could occur on the surface of AC after washing with HCl. There are two possible reactions: the first (A) is ether formation; the second (B) is dehydration.⁵⁹ Note: The aromatic groups are considered independent for easy drawing, but they should be considered merged and part of the carbon matrix.

On the other hand, the oxidation of activated carbons with oxidant acids, such as HNO_3 , is expected to significantly damage the matrix itself, resulting in generating a large number of surface functional groups such as carbonyl, carboxyl, and nitrate groups.⁵³ This can promote the binding of Fe as well as increase the wettability of AC which is preferable to the reaction in water media, so these will contribute to a more durable and effective catalyst. Besides removing metals, it can change the surface chemistry and affect the surface area and porosity.^{47, 60-62} Oxidation of activated carbon surfaces is particularly susceptible to aliphatic side chains. These are illustrated in Figure 3.4.⁵⁸

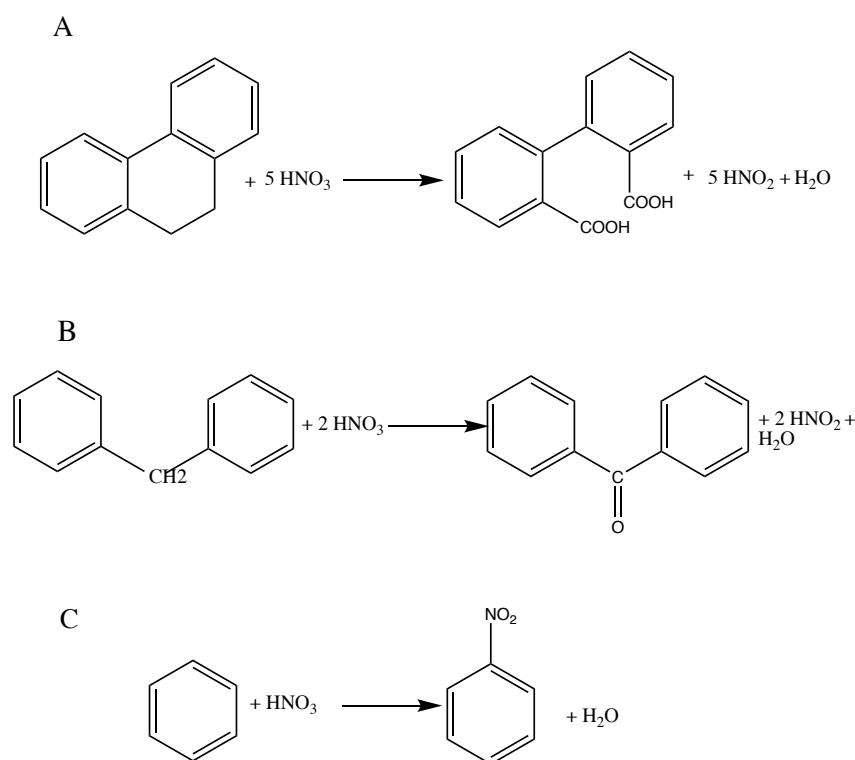


Figure 3.4: Possible reactions that could occur on the surface of AC after washing/treatment with HNO_3 . The oxidation by HNO_3 generates many surface functional groups, such as carbonyl (A), carboxyl (B), and nitrate groups (C).⁵⁸

Even though there are many reports involving the partial oxidation of AC for the formation of oxygenated functional groups, conclusions are usually challenging to draw due to the differences in carbon types and oxidising agents used, as well as different oxidation

conditions.⁶³⁻⁶⁸ As an example, Kuzin and his team reported no changes in adsorption capacity when AC was oxidised with HNO₃, but their other studies reported an increase in pore volume (probably due to some pore walls collapsing).⁶⁹ Others reported a decrease in the micropore volume (probably because of brittle properties).⁶³ Depending on the structural and surface properties of AC, they can be oxidised differently under the same conditions. Therefore, to gain a deeper understanding of the changes occurring in the surface chemistry of AC by the pre-acid treatments with HCl and HNO₃ and their extended effect on the catalytic activity with varying degrees of activation, three different kinds of AC (NORIT 1240 GAC; SA2; DARCO, G60) been used and labelled as GAC, SA2 and G60 respectively.

GAC is derived from various raw materials, such as bituminous coal, lignite coal, coconut shells, wood, peat, sawdust, and nut shells.⁷⁰ The carbon materials consist of small, irregularly ordered layers (like graphene, which is oriented parallel to the particle surface).³⁶ The process of activating carbon particles involves high-temperature steam (between 900 °C and 1100 °C) and chemical treatment (in chemical activation, raw material is mixed with an activating agent, such as phosphoric acid, which increases cellulose's volume and opens up its structure. A paste of raw material and phosphoric acid dries and carbonizes, usually in a rotary furnace. A relatively low temperature of 400 °C to 500 °C is used for this process). As a result of thermal activation, the internal porosity increases and the layered stacks separate, resulting in an increase in surface area. There are a variety of pore sizes in the internal porosity, including micropores (< 2 nm in diameter), mesopores (2-50 nm), and macropores (> 50 nm in diameter) which affect the diffusional access of contaminants and reagents during oxidation.

Carbon activation affects the formation of functional groups on graphene plane edges in the GAC. In terms of oxygen content and acidic surface oxide (ASO), these functional groups can be divided into four types: carboxyls, lactones, phenols, and carbonyls.³⁶ These groups are oxygen-rich, have a high cation exchange capacity, and are non-reactive with H₂O₂.⁷¹ GAC's surface polarity is increased by ASOs, causing its carbon surface affinity to decrease. A basic surface oxide (BSO) functional group, such as one with pyrone or chromene structure (Figure 3.1), has a low oxygen content, a high anion exchange capacity, and is reactive with H₂O₂. Surface chemistry, contaminant adsorption, and H₂O₂ reactivity are influenced by the distribution of ASOs and BSOs in GAC.^{51, 69, 72}

The raw materials used to produce GAC can differ significantly in their metal content, including iron and manganese. Pre-acid treatment by HCl and HNO₃ of the GAC reduces the

inner metal content (especially alkali metals) and ash. In addition, as a result of these processes, the final GAC product can exhibit a variety of physical and chemical properties, such as particle size (mesh size), pH,⁷³ metals content, surface area, pore volume, pore size distribution, and surface functionality. It's been reported that GACs were manufactured for water treatment applications, derived from various raw materials, and activated and processed under various conditions.⁷⁴ There are 31 kinds of GACs commercially available. GAC has been used with this study; their mesh size is 12 to 40, been activated via steam, raw materials bituminous coal and has $0.5 \text{ g}\cdot\text{mL}^{-1}$ apparent density,⁷⁴ and the surface area (BET) reported to be up to $1400 \text{ m}^2\cdot\text{g}^{-1}$.⁷⁵

SA2 is well reported to use for water treatment applications.⁷⁶⁻⁷⁸ SA2 is obtained from peat rich in organic carbon. In addition, it does not contain any substances that can harm the environment, and it cannot be dissolved in water. Their apparent density is $0.46 \text{ g}\cdot\text{mL}^{-1}$, and the surface area (BET) is $950 \text{ m}^2\cdot\text{g}^{-1}$, particle size is 20-140 μm and contains 9% ash.⁷⁶

G60 raw materials, Bitumen coal tar, amorphous black granules or fine powders. The specific surface area is $600 \text{ m}^2\cdot\text{g}^{-1}$; the density is $0.7 \text{ g}\cdot\text{mL}^{-1}$. Particle size is 100-325 mesh, contains 3.5% ash and is not soluble in water, the pH is 6-8.⁷⁹ Raw materials used in this strain include charcoal, fruit shells, and high-quality coal. Raw materials are crushed, sieved, activated, and rinsed through physical and chemical methods for raw materials. Porous and loose substances with strong adsorption capacity are produced through processes such as drying and screening. According to their physical and chemical properties, they can be used for water applications.⁸⁰

Three sets of Fe/AC catalysts were prepared by an incipient wet impregnation method using three different kinds of AC: GAC, SA2, G60 and by considering both raw and pre-treated activated carbon by acid washing and the insertion of heteroatoms like N and S, as discussed in Chapter 2. In all catalysts, Fe loading was kept fixed at 12 wt%.

The working hypotheses of the acid pre-treatments are

- 1- **Acid-washing by HCl.** Three effects of washing the AC with HCl are expected: (i) the AC not be structurally affected (but for the removal of alkali metal species) as

HCl doesn't have any parodically oxidising properties. (ii) ether groups may form, as according to scheme B in Figure 3.3 and 3.4. If this is the case, a water molecule will be released, and some loss of oxygen may occur, which is, however, dependent from the extent of any etherification, which, however, is not expected to be dominant. Then (iii) possibility is a dehydration reaction (as in scheme B Figure 3.3). According to the scheme, this will lead to the release of a water molecule that will be washed away and, in turn, loss of oxygen, and the same considerations for the formation of ether apply.

However, washing with HCl is essential for removing metal contaminants from an AC. In addition, treating with HCl will then provide a blank/background, thus making it more reproducible. The latter is an important factor in catalyst development. In terms of catalytic activity (the CWPO reaction for phenol), HCl should not lead to any significant effect; and with regard to the O content was expected to decrease slightly or any changes not be detected by analysis of the elemental content.

- 2- **Acid washing by HNO₃.** Given that HNO₃ has some oxidising properties, we would expect to increase the formation of oxygen surface groups like hydroxyl, ketone and acid. In addition, some double bonds may form by dehydration. Consequently, the increase in the O bonds will increase AC's hydrophilicity, which should increase its catalytic activity by promoting interactions with the reaction media, as well as change O's quality to lead to functional groups capable of being better binders with Fe and thus preventing or limiting Fe leaching. And in turn, lead to a catalyst that is both more active and more durable. This change was expected to be detected by increasing the O contents by elemental analysis. In addition, the dehydration reaction led to material with more crystalline, which may be detected by XRD. Furthermore, both dehydration and increased oxygen content could also be detected by XPS analysis.
- 3- **Combining HCl-HNO₃.** A Fe/AC catalyst prepared by using both these acids as a form of pre-treatment should then lead to more reproducible, active and durable catalysts, as these should be free from inner contaminants, more hydrophilic and less prone to leaching, respectively.

Elemental analysis, XPS and XRD were used to gather quantitative information for the bulk and surface of heteroatoms and carbon content, as well as to identify if any changes in the

amorphous state of carbon could have occurred after these treatments. The catalytic activity for phenol degradation, the ability of H₂O₂ decomposition, carbon mass balance CMB (residual intermediates) and Fe leaching were tested over the catalysts.

3.1.2 Results and discussion

A comprehensive analysis of catalyst activity implies more than just the conversion of the target reactant and is an essential parameter for assessing a catalyst's performance in a chemical reaction. Besides phenol conversion, other parameters, such as H₂O₂ consumption, residual intermediates and Fe leaching, are all investigated and quantified within this PhD experimental and data analysis work. Furthermore, in order to accurately account for the evolution of phenol removal over different catalysts, the adsorption capacity of AC and the oxidation of H₂O₂ were also considered. In addition, the contribution of pure adsorption with AC and oxidation with H₂O₂ alone to the removal of phenol was also evaluated.

3.1.2.1 Catalytic test for the CWPO using Fe/AC catalysts prepared by raw-AC

A. Control tests for the evaluation of the adsorption ability of three types of raw-AC
Carbon materials' adsorption capacity depends on their pore structure and surface chemistry.⁸¹ The phenol removal, by considering: no iron doping and only raw-AC (GAC; SA2; G60) over a 4 h, was investigated (Figure 3.5). The results indicate that phenol removal increases by increasing the amount of the AC, but Fe-doped and H₂O₂ are required for high phenol conversion. This implies that both Fe and H₂O₂ are needed to carry out the oxidation process and that the apparent decrease in phenol, when only AC is present, is due to some adsorption of phenol by the carbon itself.

Regarding this adsorption effect, though, this should not be seen as entirely detrimental. Actually, it proves that carbon can promote a proximity effect by bringing the organic substrate and the reactive free radicals to a close distance, thus promoting the decomposition process. Although the adsorption of phenol to the carbon surface is beneficial to promote a proximity effect between phenol, the active metal centre, and •OH radicals to increase the rate of the reaction (the latter is very important as the free mean path in aqueous solution is just a few angstroms),⁸² it is important to note that strong adsorption is detrimental as this may preclude phenol from reacting in analogy to expected trends as for the Sabatier's principle.⁸³

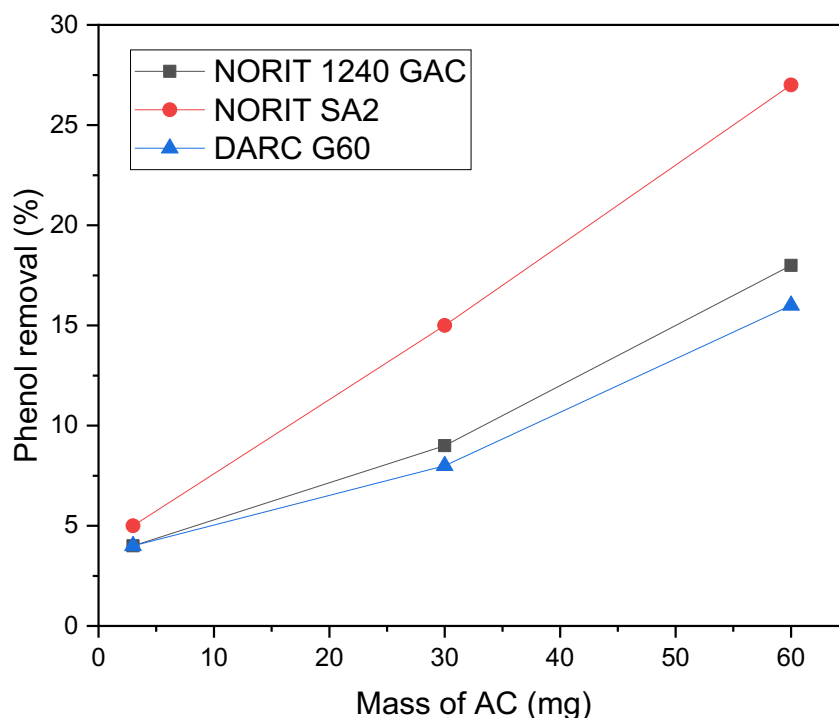


Figure 3.5: Control test using raw- AC (GAC, SA2, G60) without iron doping to determine the phenol removal by adsorption of the AC, initial phenol concentration of $1 \text{ g}\cdot\text{L}^{-1}$, reaction temperature of $80 \text{ }^\circ\text{C}$ for 4 h.

The largest amount of phenol removal was for the SA2, when using 60 mg of the AC. We estimated the phenol removal by absorption of raw-AC to be about 5% for all raw-AC's catalysts at all reactions when 3 mg of catalysts were used, and this has been accounted as a correction factor for the tests in the presence of Fe and H_2O_2 . The catalytic tests were conducted in a batch reactor with an initial phenol concentration of $1 \text{ g}\cdot\text{L}^{-1}$ and a reaction temperature of $80 \text{ }^\circ\text{C}$.

B. Control test to evaluate the phenol removal by adsorption ability of raw-AC in the presence of H_2O_2

The phenol removal was assessed by considering: no iron doping, only raw-AC (GAC, SA2, G60) and adding H_2O_2 . This was done with the aim to assess phenol oxidation and the possible generation of reactive free radicals without a catalyst. The tests were conducted in a batch

reactor with an initial phenol concentration of $1 \text{ g}\cdot\text{L}^{-1}$, a phenol: H_2O_2 molar ratio of 1:14, a reaction temperature of $80 \text{ }^\circ\text{C}$ and a reaction time was 4 h (Figure 3.6).

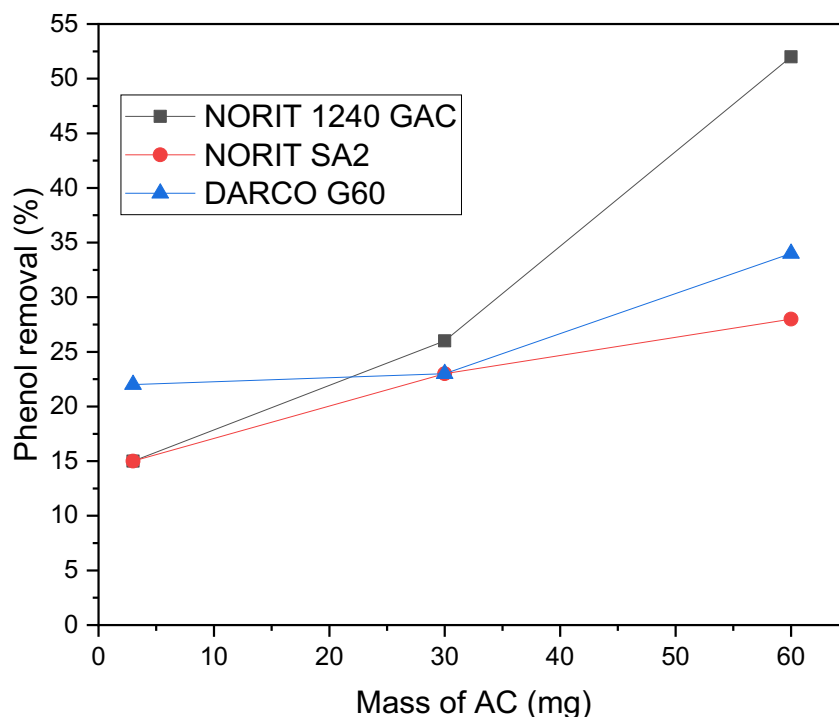


Figure 3.6: Control test using AC and H_2O_2 without Fe doping to determine the phenol removal by adsorption of the AC (GAC, SA2, G60) and the oxidation of H_2O_2 , phenol: H_2O_2 molar ratio of 1:14 and a reaction temperature of $80 \text{ }^\circ\text{C}$ for 4 h.

The results indicate that phenol removal increases by increasing the amount of the AC and adding the oxidising agent H_2O_2 which can be explained as the AC has residual metals in their framework,^{84, 85} including Fe, so these metals could play a catalytic role with H_2O_2 increasing the phenol oxidation. Still, doping Fe in AC is essential for full phenol conversion.

C. Elemental analysis for raw-AC

The three types of AC were submitted for elemental analysis as they were received without any modification of pre-treatment to determine the amount of O. This is to assess the change that could occur on the surface of AC because of the pre-acid treatments. As shown in Figure 3.7, the results show that GAC has the highest O mol%, followed by SA2, and G60 has the lowest.

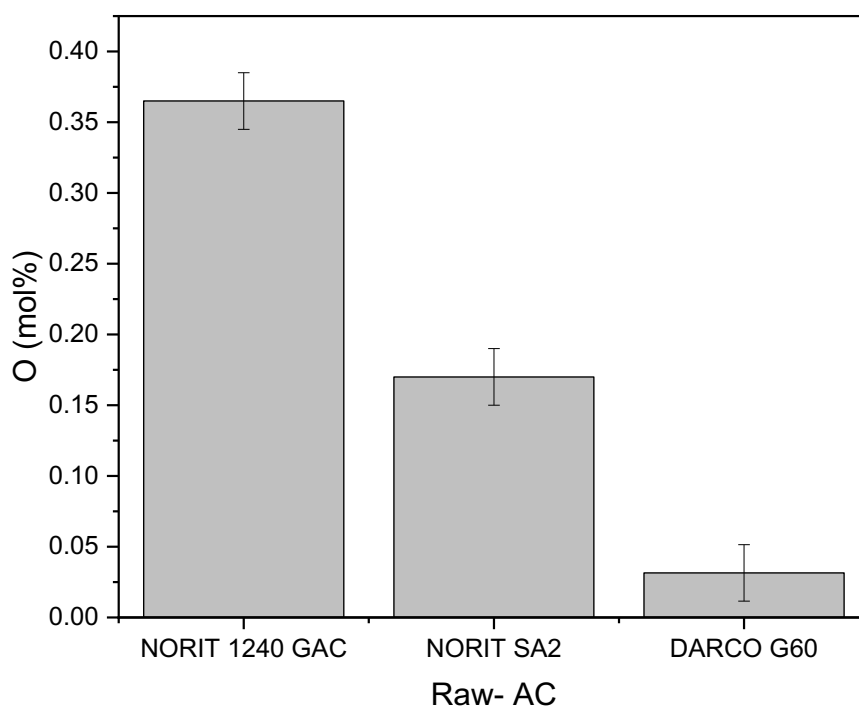


Figure 3.7: Elemental analysis results by mol% for O in the raw-AC (GAC, SA2, G60).

Based on these data, GAC has the highest oxygen content, which in turn should also make it the most hydrophilic, and, according to one of our working hypotheses (see section 3.1.1), inherently more active because of a better interaction with the reaction medium. In fact, if the amount of carbon is sufficiently high, this effect can be detected (Figure 3.6), and this carbon is indeed the most active (though due to the presence of residual metals in this matrix). As the latter is not reproducible, this also explains why the trend is not neat for the other AC at lower carbon amounts.

D. Catalytic activity, metal leaching and H₂O₂ consumption results for metal-doped raw-AC

Phenol conversion reaching 100% indicates that all the phenol has been transformed into other products, suggesting an efficient catalytic process. The high phenol conversion across all catalysts (100%) implies that the catalysts are effective in facilitating the breakdown of phenol into other compounds. Residual intermediates% is only 20% and 13% with GAC and SA2 catalysts (Figure 3.8). Meanwhile, with Fe/AC catalysts prepared by G60, residual

intermediates % was relatively high, about 40%. With catalysts from GAC, SA2 and G60, the consumption of H₂O₂ was 75%, 76% and 60%, respectively. These results of H₂O₂ consumption are compatible with the phenol conversion and residual intermediates; in the case of GAC and SA2, phenol conversion reaches 100% and 20, 13% residual intermediates at the same. The H₂O₂ consumption time comes to 75 – 76% ±5, so 20% is left from H₂O₂, which matches the residual intermediates. All catalysts, however, exhibited high Fe leaching% (the leaching is a relative leaching% with respect to the total Fe content), which is the main challenge associated with heterogeneous catalysts. In this project, catalysts are being developed to solve the problem. The first step was to wash the AC with HCl and then dope the Fe. To assess the effect of this treatment, the catalyst was tested for phenol oxidation, as will show in the next part.

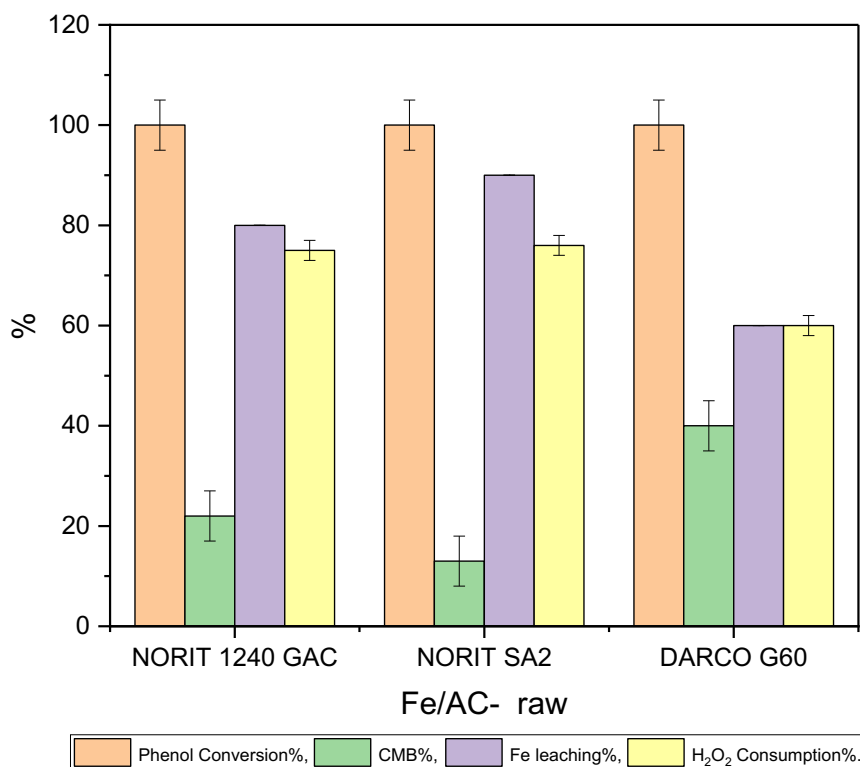


Figure 3.8: Catalytic activity, in terms of phenol conversion, CMB, Fe leaching and H₂O₂ consumption result for phenol oxidation by CWPO, using three types of Fe/AC catalysts (GAC, SA2, G60). All catalysts have 12wt% Fe loading (the leaching is a relative leaching% with respect to the total Fe content), 4 h reaction time at 80 °C and 1:100 M:S.

Carbon mass balance (CMB% in our case) basically refers to stoichiometric considerations; it's a measure of carbon content in water and is the result of the sum of organic compounds remaining in solution (see the experimental chapter 2, section 2.6). Low CMB% means high mineralization of phenol (Mineralization of phenol refers to the process by which phenol, is broken down and converted into simpler inorganic substances, and formation of CO₂ and H₂O).

E. Elemental analysis for Fe/AC by raw-AC

Comparing the results in Figure 3.9 with the elemental analysis of raw-AC without iron doping in Figure 3.7, find that O mol% is consistent for GAC. However, it is observed that SA2 and G60 increase their O mol% content from 0.17 and 0.05 mol to 0.3 and 0.2 mol for SA2 and G60, respectively. We speculate this is a consequence of the catalyst preparation process that ultimately involves the formation of Fe_xO_y species (most likely Fe₂O₃ see section 3.3.1) as the active phase.

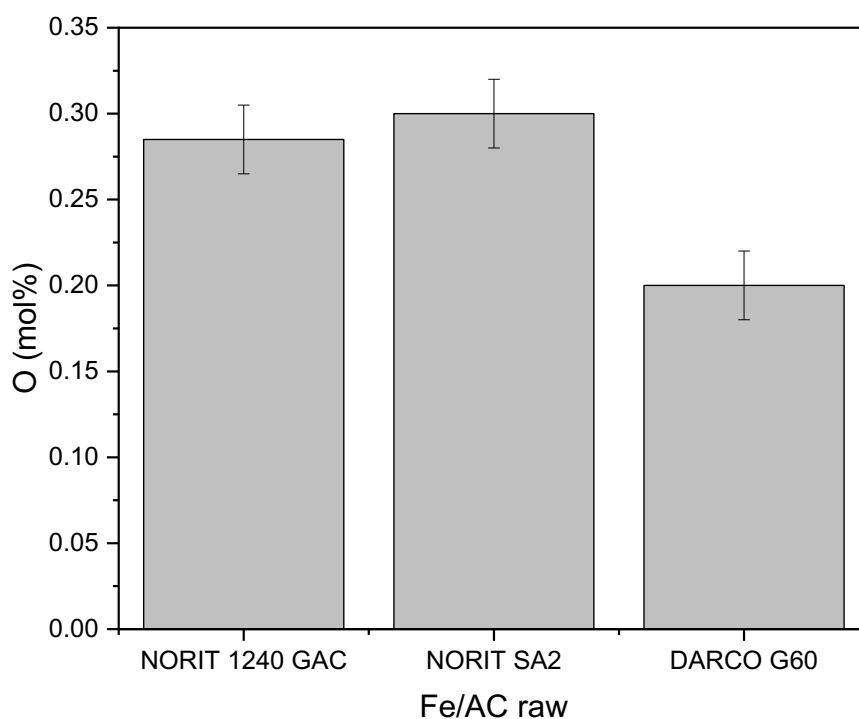


Figure 3.9: Elemental analysis results reported in mol% for O content in the Fe/AC by raw-AC (GAC, SA2, G60).

3.1.2.2 Catalytic test for the CWPO using Fe/AC catalysts prepared by AC washed by HCl

As mentioned above, the purpose of HCl treatment is to wash out the metal contaminants (mostly alkali metals) within AC, though this can induce the formation of some groups or some dehydration (see hypothesis 1, section 3.1.1 introduction). To study the impact of the HCl washing process on the surface and catalytic activity of AC, three types of AC (GAC, SA2, G60) were washed by HCl before doping with Fe. These three sets of catalysts, Fe/AC, HCl-AC, were applied for phenol conversion by CWPO.

A. Control test to evaluate the adsorption ability of three types of AC washed with HCl-AC

The phenol removal by considering: no iron doping, only HCl-AC (GAC, SA2, G60) to assess phenol adsorption by the HCl-ACs without iron doping. The same experimental conditions as in section 3.1.2.1 (A).

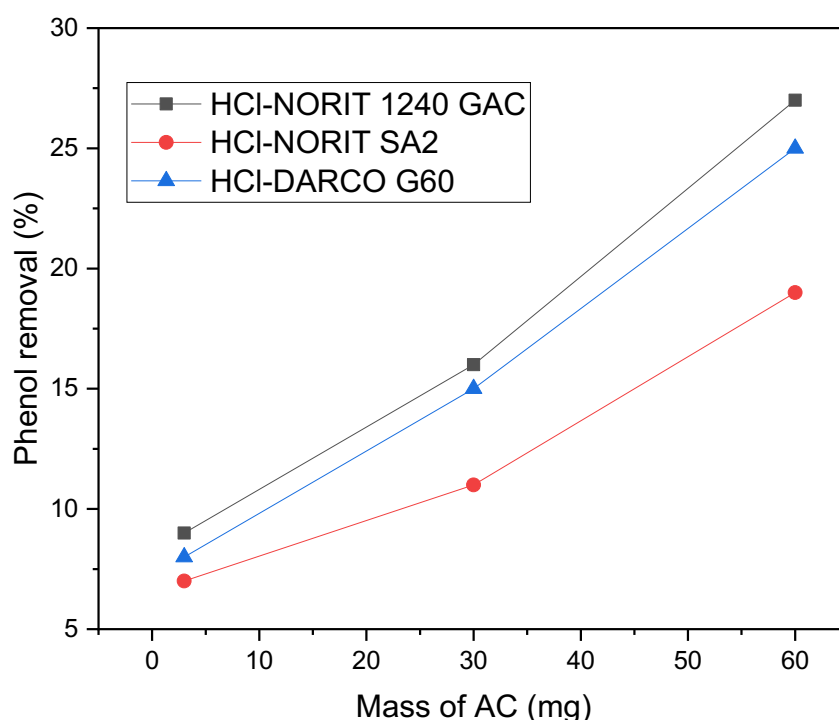


Figure 3.10: Control test using HCl-AC (GAC, SA2, G60) washed from iron to determine the phenol removal by adsorption of the AC, initial phenol concentration of $1 \text{ g}\cdot\text{L}^{-1}$, reaction temperature of $80 \text{ }^\circ\text{C}$ for 4 h.

Comparing these results in Figure 3.10 with Figure 3.5 (raw-AC), the phenol adsorption generally increases with HCl-ACs. Removing residual metals from the AC framework might free up adsorption sites for phenol in the AC, increasing the adsorption capacity. There is no significant difference between the three kinds of AC at 3 mg of AC (M:S, 1:100). Increasing the amount of AC increases the adsorption of phenol.

B. Control test to evaluate the phenol removal by adsorption ability of HCl-AC in the presence of H₂O₂

The phenol removal by considering: no iron doping, only HCl-AC (GAC, SA2, G60) and adding H₂O₂ to assess phenol oxidation without iron doping. The same experimental conditions as in section 3.1.2.1 (B).

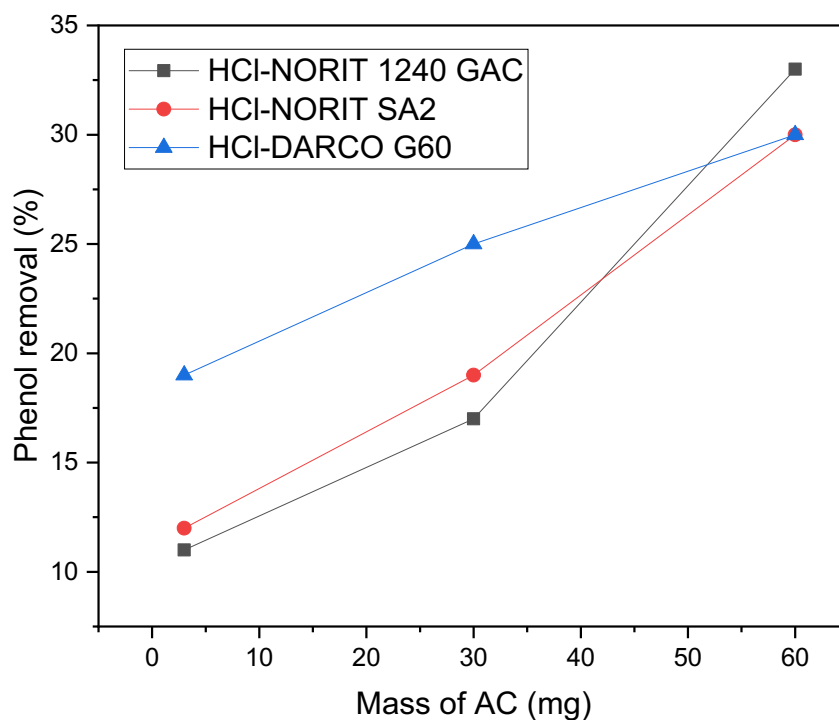


Figure 3.11: Control test using AC washed with HCl and H₂O₂ no iron doping to determine the phenol removal by adsorption of the AC-HCl (GAC, SA2, G60), and the oxidation of H₂O₂, phenol:H₂O₂ molar ratio of 1:14 and a reaction temperature of 80 °C for 4 h.

Based on the results in Figure 3.11, increasing the amount of the AC and adding H₂O₂ increases phenol removal, which is explained by the fact that the AC contains many metals, including

Fe, so these metals could act as catalysts, with H_2O_2 increasing phenol oxidation. A comparison of HCl-AC with raw-AC phenol removal in the presence of H_2O_2 (Figure 3.6) shows a decrease due to the reduction of minerals capable of acting as active species with H_2O_2 in the HCl-AC.

C. Elemental analysis for HCl-AC

The data in Figure 3.12 show that the O mol% slightly decreases for the GAC after washing with HCl. While SA2 and G60 pre-treated by HCl have a steady amount of O content compared with the AC without pre-treatment Figure 3.7.

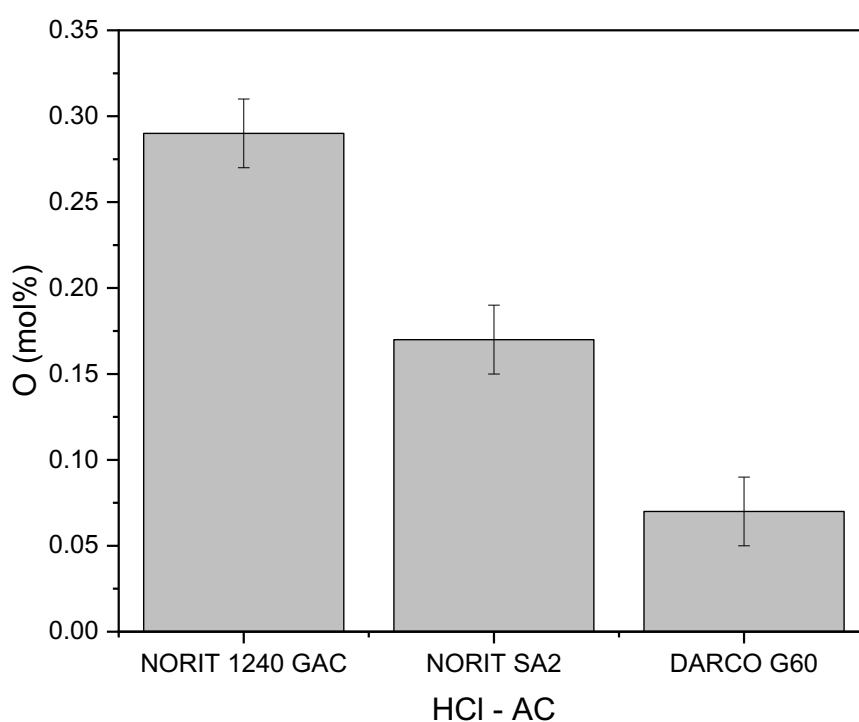


Figure 3.12: Elemental analysis results by mol% for O in the HCl-AC (GAC, SA2, G60).

This means that our HCl treatment does not induce any significant ether or dehydration reactions (at least at the bulk level), and it serves only as a medium to have a metal-free background in activated carbon. This is important. It matches one of our working hypotheses and expectations, and it will help to discriminate between effects induced by HNO_3 or pre-treatments with HCl and HNO_3 , thus providing a good base for quantitative comparisons.

D. Catalytic activity, metal leaching and H₂O₂ consumption results for metal-doped HCl-AC

Applying Fe/AC, HCl-AC catalysts for phenol oxidation by CWPO shows that pre-acid treatment of AC by HCl led to a dramatic drop in the catalytic activity. For all Fe/AC prepared by HCl-AC, phenol oxidation is 55, 66 and 50% with GAC, SA2 and G60, respectively. Furthermore, residual intermediates % is unchanged at 100% with all catalysts, thus meaning that although there is a consumption of phenol, this doesn't proceed to mineralization to CO₂ and H₂O, but it stops to longer chain intermediates (from previous studies within the group, malonic acid).⁸⁶ Fe leaching decreases as a consequence of a residual metal removal process by HCl wash. The H₂O₂ consumption validated the phenol oxidation results; since the stoichiometric amount of phenol to H₂O₂ was used 1:14, the consumption of H₂O₂ was 34%, 32% and 23% for GAC, SA2 and G60, respectively. The phenol conversion is in the range of 60%, but residual intermediates un change at 100% which is compatible with the H₂O₂ consumption results. That means there was a small amount of [•]OH that probably attacked phenol but did not reach the full oxidation, so there was no mineralization in these reactions.

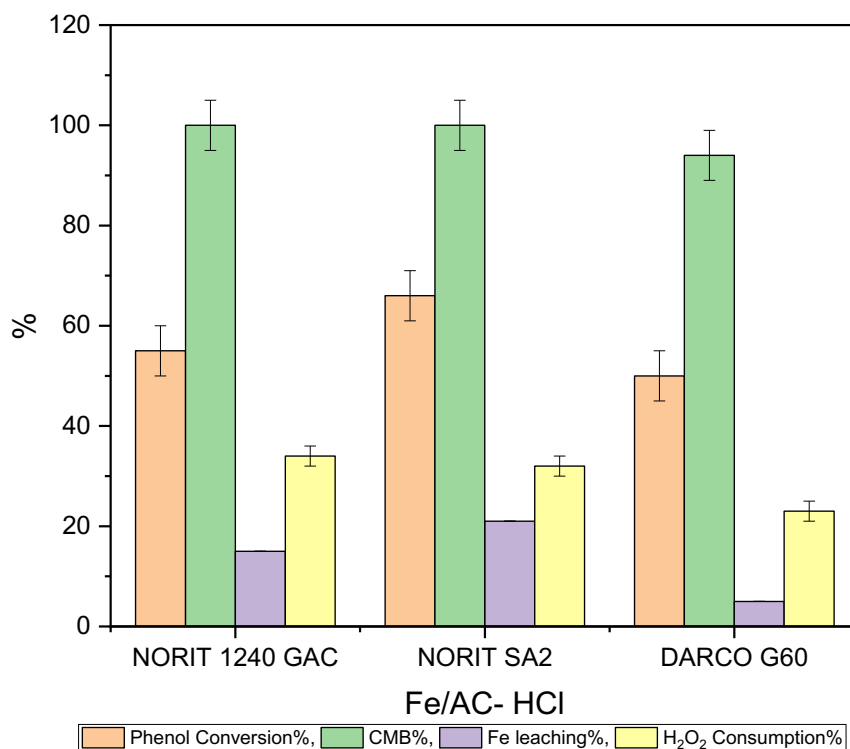


Figure 3.13: Catalytic activity, in terms of phenol conversion, CMB, Fe leaching and H₂O₂ consumption result for phenol oxidation by CWPO, using three types of Fe/AC catalysts prepared by AC-HCl (GAC, SA2, G60). All catalysts have 12 wt% Fe loading (the leaching is a relative leaching% with respect to the total Fe content), 4 h reaction time at 80 °C and 1:100 M:S.

If taken as a whole (Figures 3.12, 3.13), these results support our first working hypothesis (section 3.1.1) that HCl pre-treatment of AC is an initial process to eliminate elements and ash from AC but does not chemically affect the AC. So, to affect the surface of AC chemically could be done by using an oxidation acid like HNO₃, which is expected to significantly increase the oxygen surface groups increasing the catalytic activity, which will be discussed in the next section.

E. Elemental analysis for Fe/AC by HCl-AC

The data in Figure 3.14 show that Fe/AC, HCl-AC for GAC and G60 have a steady amount of oxygen content compared with the Fe/AC, raw-AC Figure 3.9. For SA2, the O mol% decreased as a result of the dehydration process. Due to the heat treatments, O mol% increased slightly after doping Fe. In other words, the treatment with HCl does not affect the O content, and the increased O amount compared to the raw material is due to the Fe deposition process.

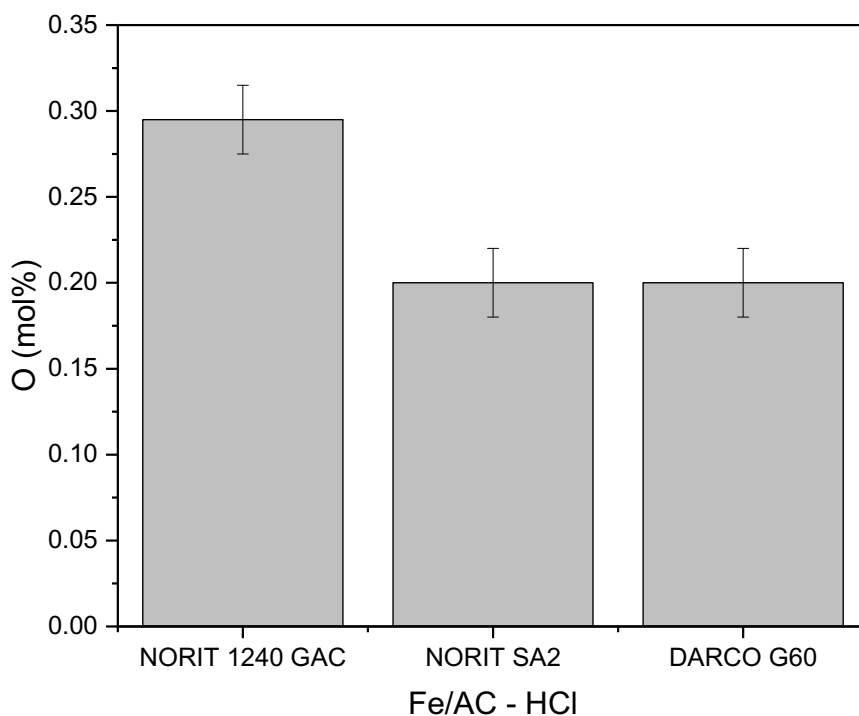


Figure 3.14: Elemental analysis results reported in mol% for O content in the Fe/AC by HCl-AC.

3.1.2.3 Catalytic test for the CWPO using Fe/AC catalysts prepared by AC washed by HNO₃

As described in section 3.1.1, HNO₃ treatment generates many surface functional groups, such as carbonyl, carboxyl and nitrate; it is also possible to form some double bonds. As a result, the expectation would be that an increase in the O bonds will increase AC's hydrophilicity and catalytic activity, and change O's quality to better binders with Fe, preventing Fe from leaching.

A. Control test to evaluate the adsorption ability of three types of HNO₃- AC

The effect of the HNO₃ treatment on carbon surface area is not apparent. Gomez-Serrano *et al.* observed a slight increase in surface area, while Mazet *et al.* observed a significant increase.⁵⁸ The phenol removal by considering: no iron doping, only HNO₃-AC (GAC, SA2, G60) to assess phenol adsorption by the HNO₃-ACs without iron doping. The same experimental conditions as in section 3.1.2.1 (A).

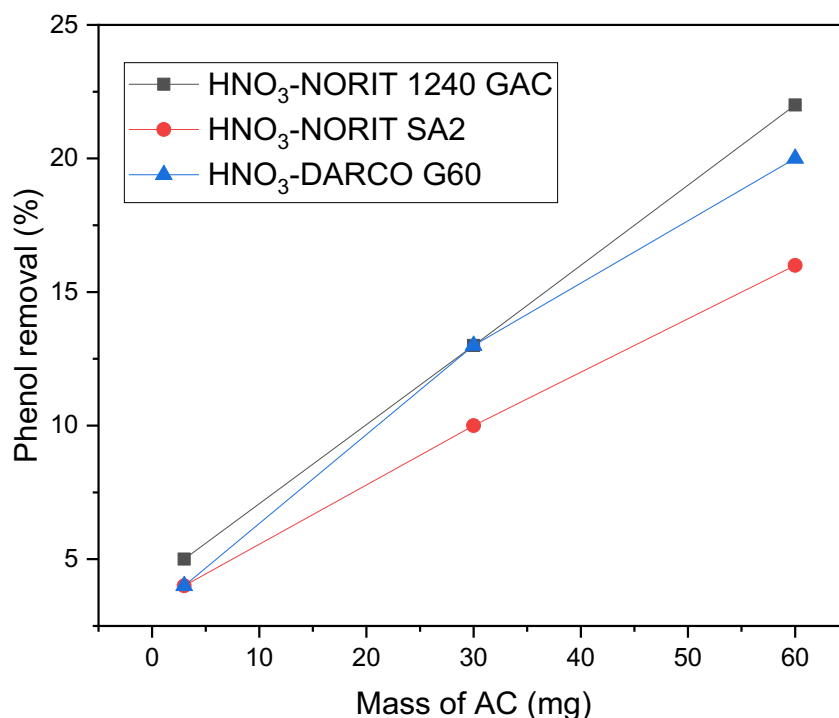


Figure 3.15: Control test using HNO₃-AC (GAC, SA2, G60) no iron doping to determine the phenol removal by adsorption of the AC, initial phenol concentration of 1 g·L⁻¹, reaction temperature of 80 °C for 4 h.

Comparing these results in Figure 3.15 with Figure 3.5 (raw-AC), there is no significant difference (considering the experimental error of 5%) using 3 mg of HNO₃-AC in phenol adsorption after oxidation by HNO₃. The three kinds of AC at 3 mg of AC (M:S, 1:100) have 5% adsorbed phenol. However, with 30 and 60 mg of HNO₃ - AC, the phenol adsorption was slightly decreased compared with the raw-AC. This slight decrease could be explained by treating AC with HNO₃ in two ways the carbon may lose some porosity, resulting in a reduction of surface area.⁵³

B. Control test to evaluate the phenol removal by adsorption ability of HNO₃-AC in the presence of H₂O₂

The phenol removal by considering: no iron doping, only HNO₃-AC (GAC, SA2, G60) and adding H₂O₂ to assess phenol oxidation without iron doping. The same experimental conditions

as in section 3.1.2.1 (B). Based on the results of Figure 3.16, increasing the amount of the AC and adding H₂O₂ increases phenol removal, which is explained by the fact that the AC contains many metals including Fe, Al, K, Li, Ca, Ni, Cu, Cr, Co, Na,⁸⁷ so that these metals could act as catalysts towards H₂O₂ decomposition to [•]OH free radicals and in turn with H₂O₂ increasing phenol oxidation.

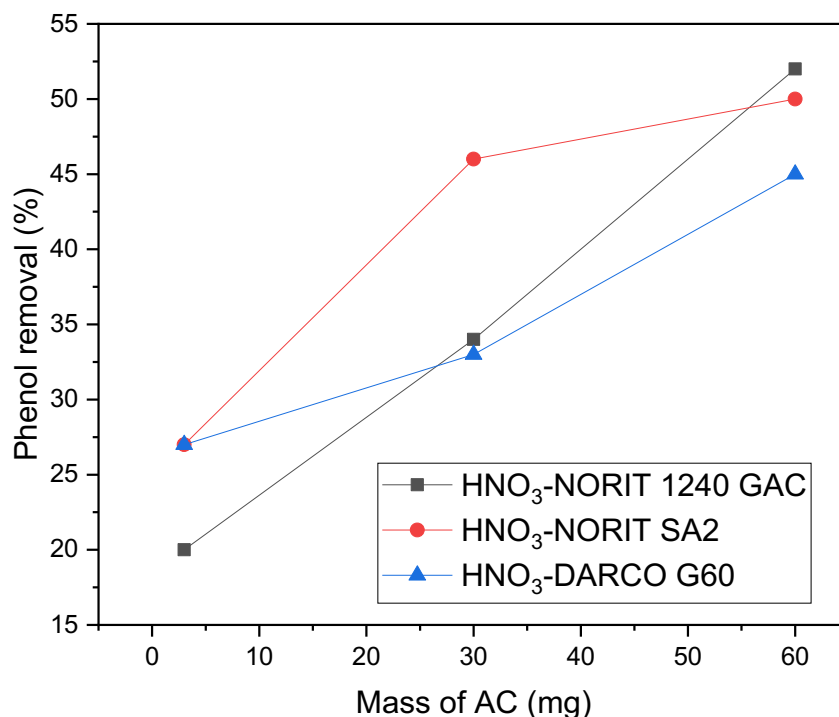


Figure 3.16: Control test using AC treated with HNO₃ and H₂O₂ no iron doping to determine the phenol removal by adsorption of the AC- HNO₃ (GAC, SA2, G60), and the oxidation of H₂O₂, phenol:H₂O₂ molar ratio of 1:14 and a reaction temperature of 80 °C for 4 h.

A comparison of HNO₃-AC with raw-AC phenol removal in H₂O₂ (Figure 3.6) shows increased phenol removal for all HNO₃-AC. As mentioned previously, this treatment is expected to increase the O surface functional group leading to an increase in the affinity of the support for the reaction media, H₂O₂, the substrate with a small but appreciable dipole moment (ca 1.4 D) and, in turn, catalytic activity.

C. Elemental analysis for HNO₃-AC

Surprisingly though, the O mol% for the GAC (Figure 3.17) didn't increase after washing with HNO₃, if compared to Figure 3.7 regarding the raw carbon materials. In particular, for GAC, there is actually a decrease in O mol% (from 0.35 to 0.16), whereas, for SA2, it is nearly the same (from 0.16 to 0.15) and for G60, a slight increase (from 0.05 to 0.07). These results are in part unexpected and could be interpreted as such: for GAC, the acid treatment with HNO₃ promotes there and dehydration (that would lead to a lower O content); for SA2, there is practically no tangible effect; for G60, however, some oxidation is occurring. So, with HNO₃ oxidation, different AC behaved differently, and all in all, in some cases opposite to our expectations.

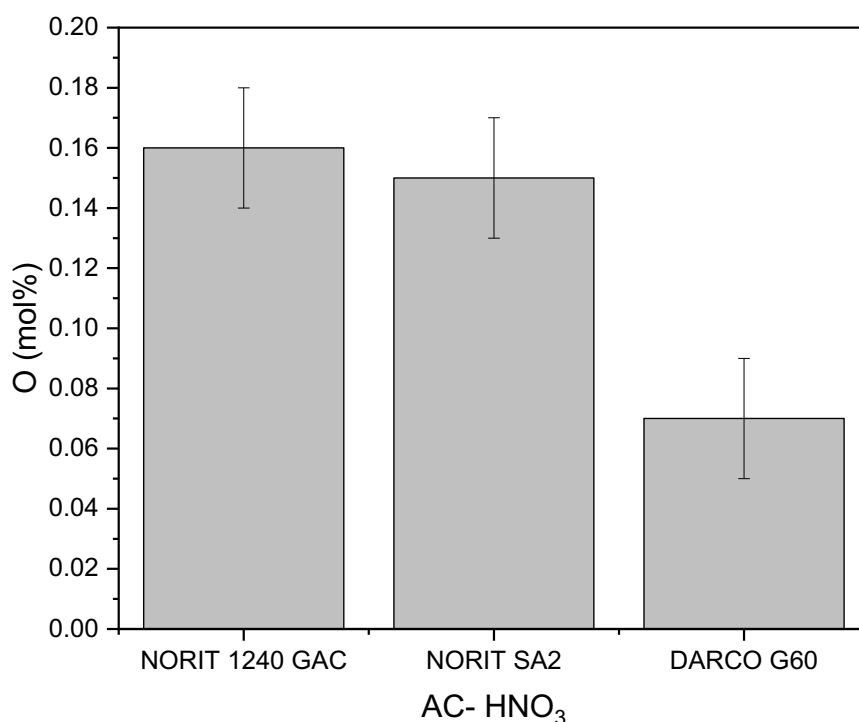


Figure 3.17: Elemental analysis results by mol% for O in the HNO₃-AC (GAC, SA2, G60).

D. Catalytic activity, metal leaching and H₂O₂ consumption results for metal-doped HNO₃-AC

The use of Fe/AC, HNO₃-AC catalysts for phenol oxidation by CWPO shows that a pre-treatment of AC by HNO₃ increases the catalytic activity. Phenol conversion for all catalysts is 100%; however, this is also the upper limit for the conversion, an assessment of the residual

intermediates% (Figure 3.8) Fe/AC by raw-AC, and in turn, the mineralization to CO₂ and H₂O is a better indicator, in this case, of the catalytic performance. residual intermediates% is 10, 17 and 19% for GAC, SA2 and G60, respectively. Comparing the residual intermediates% results when using Fe/AC by raw-AC, there is an increase of catalytic activity (mineralization) by the HNO₃ pre-treatment. With catalysts from GAC the consumption of H₂O₂ was 65% and 71% for SA2 and G60 catalysts, compared with (Figure 3.8) Fe/AC by raw-AC showing there was no significant difference in the H₂O₂ consumption considering the experimental error 5%. Noteworthy though, these results indicated that the HNO₃ treatment increased the efficiency toward the [•]OH increasing the mineralization. Fe leaching in the range of 60% for all catalysts was slightly decreased from 80% compared with raw catalysts.

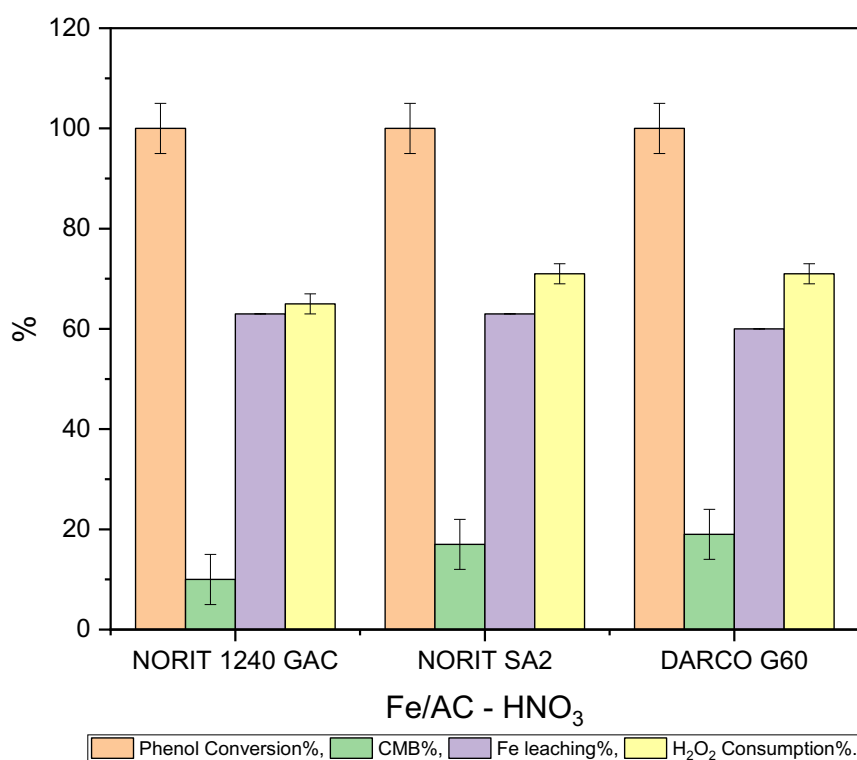


Figure 3.18: Catalytic activity, in terms of phenol conversion, CMB, Fe leaching and H₂O₂ consumption result for phenol oxidation by CWPO, using three types of Fe/AC catalysts prepared by AC-HNO₃ (GAC, SA2, G60). All catalysts have 12wt% Fe loading (the leaching is a relative leaching% with respect to the total Fe content), 4 h reaction time at 80 °C and 1:100 M:S.

E. Elemental analysis for Fe/AC by HNO₃-AC

The data in Figure 3.19 show that by comparing Fe/AC, HNO₃-AC and Fe/AC, raw-AC Figure 3.9, there were no significant differences in the O mol% for all catalysts prepared by different AC. These results could be that oxidation via HNO₃ is expected to increase oxygen content significantly; however, the conditions used to carry out the selective oxidation of carbon centres process may play a crucial role. Based on these results, the conditions used during the pre-acid treatment were insufficient to increase the O mol% as desired. However, from the residual intermediates% reported in Figure 3.18 there is an increase in the catalytic activity compared with Fe/AC, raw-AC Figure 3.8. also, iron leaching slightly decreased. It appears that AC surface properties were affected by the HNO₃.

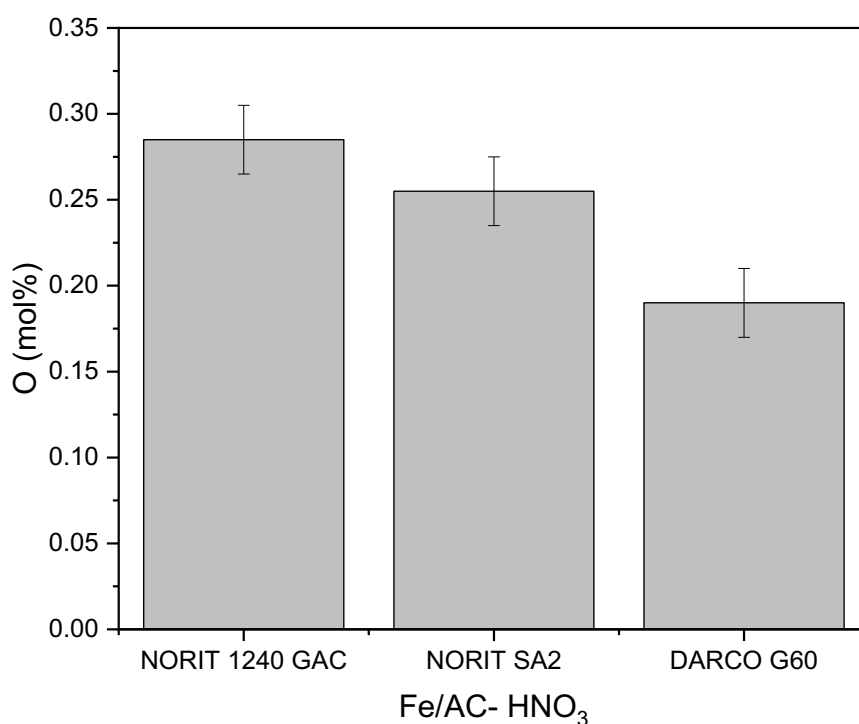


Figure 3.19: Elemental analysis results reported in mol% for O content in the Fe/AC by HNO₃-AC.

Still, Fe leaching is very high for all the catalysts, about 60%. To solve Fe leaching simultaneously and increase the catalytic activity (high phenol conversion and low residual intermediates%), the following sets of catalysts were then prepared with sequential acid pre-treatments by using both HCl and HNO₃.

3.1.2.4 Catalytic test for the CWPO using Fe/AC catalysts prepared by AC pre-acid treatment by both HCl and HNO₃

The combination of both treatments, firstly washing the AC with HCl to have a stable background and then followed by HNO₃ to increase the hydrophilicity and probably durability of the catalysts, was carried out. In addition, it was anticipated that the elemental analysis could detect increases in the O mol%. To evaluate the effect of HCl-HNO₃ treatments on the surface and catalytic activity of AC, three types of AC (GAC, SA2, G60) were washed with HCl and then oxidized by HNO₃ before doping Fe. These three sets of catalysts, Fe/AC, HCl-HNO₃-AC, were applied for phenol conversion by CWPO.

A. Control test to evaluate the adsorption ability of three types of HCl-HNO₃- AC

Control tests for the degradation of phenol by considering: no iron doping, only HCl-HNO₃-AC (GAC, SA2, G60) with no Fe, were preliminarily carried out to assess phenol adsorption and any residual activity. The same experimental conditions as in section 3.1.2.1 (A).

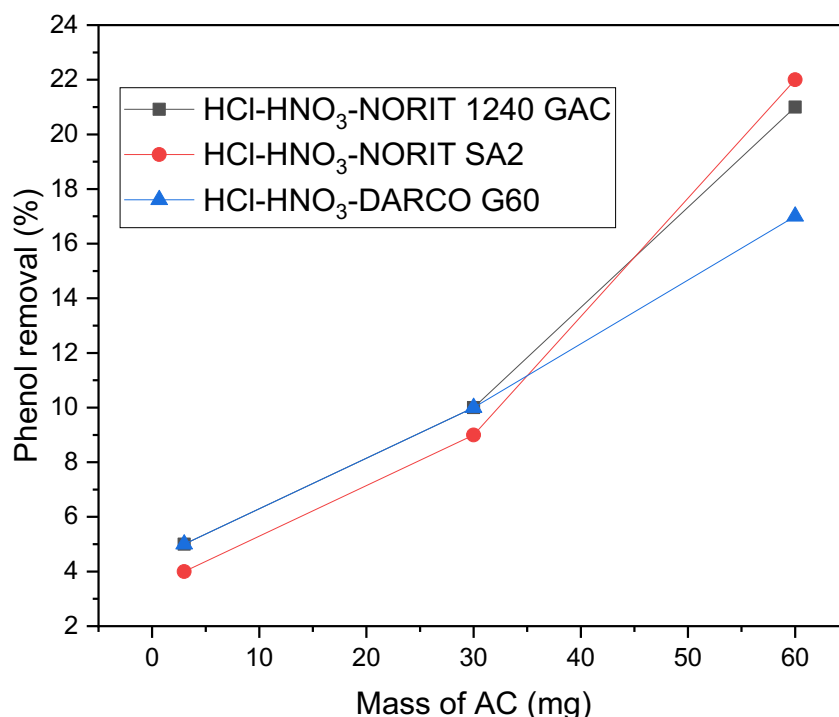


Figure 3.20: Control test using HCl-HNO₃-AC (GAC, SA2, G60) without iron doping to determine the phenol removal by adsorption of the AC, initial phenol concentration of 1 g·L⁻¹, reaction temperature of 80 °C for 4 h.

Comparing these results, Figure 3.20, with Figure 3.5 (raw-AC), there is no difference in phenol adsorption after pre-acid treatments by HCl and HNO₃. The three kinds of AC at 3 mg of AC (M:S, 1:100) have about 5% adsorbed phenol. However, with 30 and 60 mg of HCl-HNO₃-AC, the phenol adsorption was slightly decreased compared with the raw-AC. It was reported that inorganic acids such as HCl and HNO₃ have small molecular weights that may prevent they are being adsorbed by organic functional groups in carbons. Therefore they may not significantly change the surface area of ACs.⁵⁸

B. Control test to evaluate the phenol removal by adsorption ability of HCl-HNO₃-AC in the presence of H₂O₂

The phenol removal by considering: no iron doping, only HCl-HNO₃-AC (GAC, SA2, G60) and adding H₂O₂ to assess phenol oxidation without iron doping. The same experimental conditions as in section 3.1.2.1 (B).

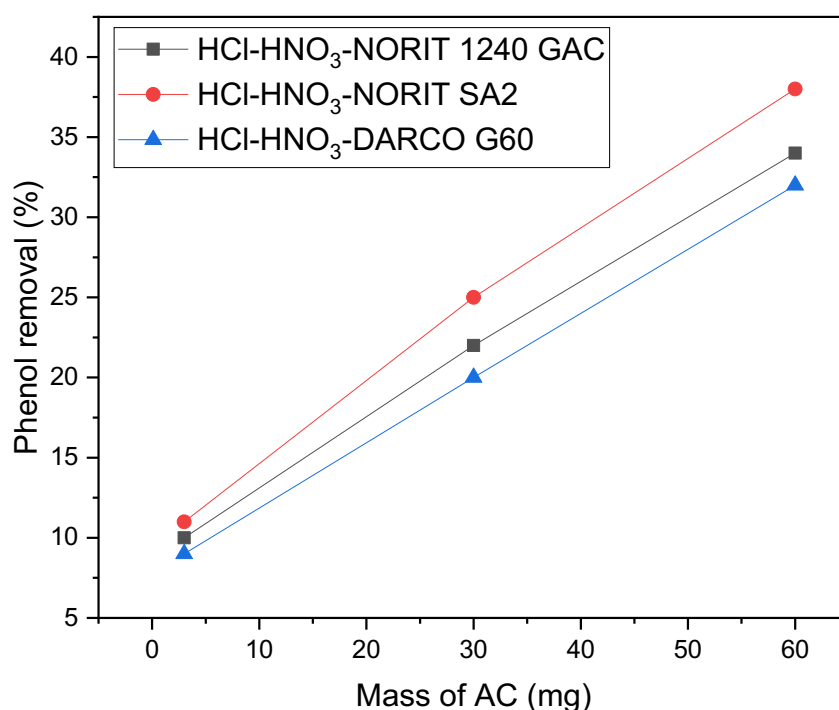


Figure 3.21: Control test using HCl-HNO₃ – AC (GAC, SA2, G60) in the presence of H₂O₂ without iron doping to determine the phenol removal by adsorption and the oxidation of H₂O₂, phenol:H₂O₂ molar ratio of 1:14 and a reaction temperature of 80 °C for 4 h.

Based on the results, increasing the amount of the AC and adding H_2O_2 increases phenol removal. A comparison of HCl- HNO_3 -AC with raw-AC phenol removal in H_2O_2 (Figure 3.6) shows a decrease of phenol removal using 3 mg (M:S, 1:100) for all ACs. As mentioned previously, this treatment was expected to increase the O surface functional group leading to an increase in the affinity of H_2O_2 and catalytic activity. The decrease that happened may be because the raw-AC is expected to have many metals increasing the oxidation of phenol in the presence of H_2O_2 . These pre-acid treatments were expected to decrease these residual metals contents dramatically.

C. Elemental analysis HCl- HNO_3 -AC

The data in Figure 3.22 show that was comparing Fe/AC, HCl- HNO_3 -AC, and Fe/AC, raw-AC Figure 3.7, different types of AC behave differently. For GAC, O mol% was decreased due to the HCl washing process, which was expected to drop the O mol%. However, HNO_3 oxidation was supposed to increase oxygen surface content; but, the conditions during the oxidation process played a crucial role, as mentioned above. SA2 has a constant amount of oxygen after the acid oxidations. While the O mol%, as desired, increased for G60 after the treatments.

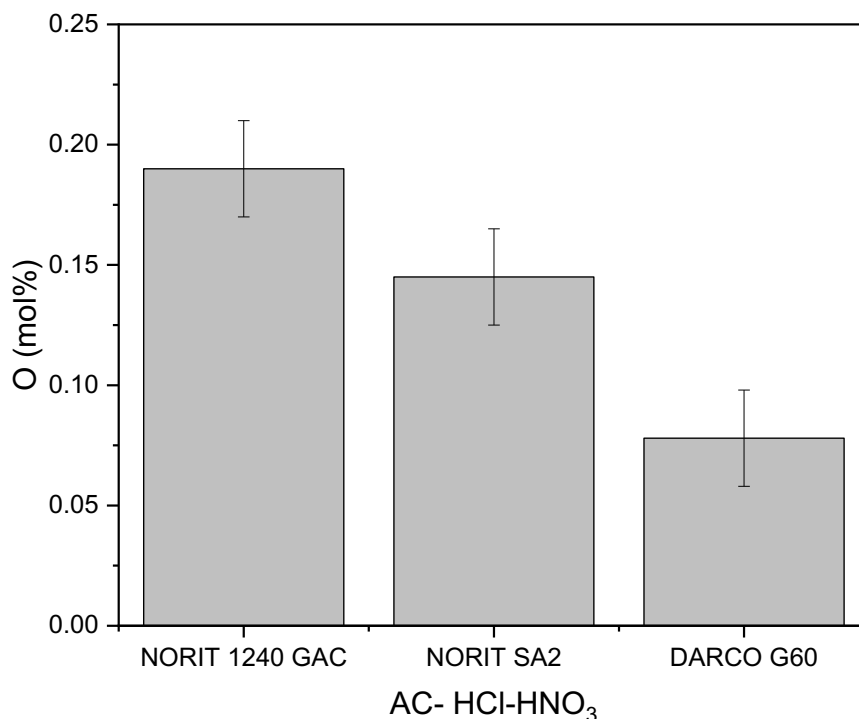


Figure 3.22: Elemental analysis results by mol% for O in the HCl- HNO_3 -AC (GAC, SA2, G60).

D. Catalytic activity, metal leaching and H₂O₂ consumption results for metal-doped HCl-HNO₃-AC

Fe/AC, HCl-HNO₃-AC catalysts for phenol oxidation by CWPO shows that pre-acid treatment of AC by HCl and HNO₃ dramatically dropped the Fe leaching% (from 90-60% to 20%), which was indeed one of the desired targets, thus showing the goodness of our working hypotheses for this parameter (leaching of Fe). However, the catalytic activity decreased from 100% to 80–90% range. Although generally speaking, this is an undesired effect; this is a small decrease in phenol degradation if compared to a much larger decrease in leaching, as a relatively minor 10% loss in catalytic activity by our treatments leads simultaneously to a three-fold reduction (relative to ca. 200%) in leaching.

The residual intermediates% were high with all catalysts, though, implying that the materials retain Fe and degrade phenol but not up to mineralization with catalysts from GAC, SA2, and G60; the consumption of H₂O₂ was 65%, 86%, and 70%, respectively. This means there was consumption of H₂O₂ but not all OH radicals involved in the oxidation process. These results so far support the first hypothesis that HCl pre-treatment of AC is an initial process to eliminate elements and ash from AC but not to affect chemically on the AC. So, to affect chemically on the surface of AC could be done by using an oxidation acid like HNO₃, which was expected to significantly increase the oxygen surface groups increasing the catalytic activity. However, based on these results, both acid pre-treatments for AC was insufficient to increase the catalytic activity and simultaneously prevent the Fe leaching.

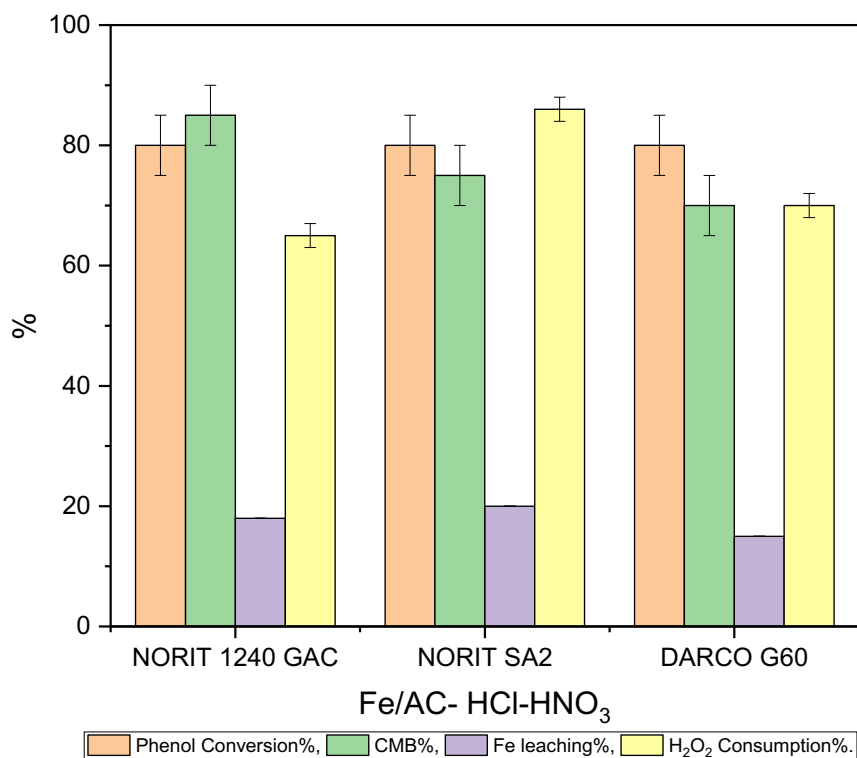


Figure 3.23: Catalytic activity, in terms of phenol conversion, CMB, Fe leaching and H₂O₂ consumption result for phenol oxidation by CWPO, using three types of Fe/AC catalysts prepared by HCl- HNO₃ -AC (GAC, SA2, G60). All catalysts have 12wt% Fe loading (the leaching is a relative leaching% with respect to the total Fe content), 4 h reaction time at 80 °C and 1:100 M:S.

Given this body of data and to reach these goals, all of the materials presented so far were doped with S and N, as will be discussed in the next sections. The rationale of this doping will be explained in detail in section 3.2.

E. Elemental analysis for Fe/AC by HCl-HNO₃-AC

The data in Figure 3.24 show that comparing Fe/AC, HCl-HNO₃-AC and Fe/AC, raw-AC Figure 3.9, O mol% for both GAC and G60 stay steady, but for SA2 decreased. These results were applied to the catalytic activity results.

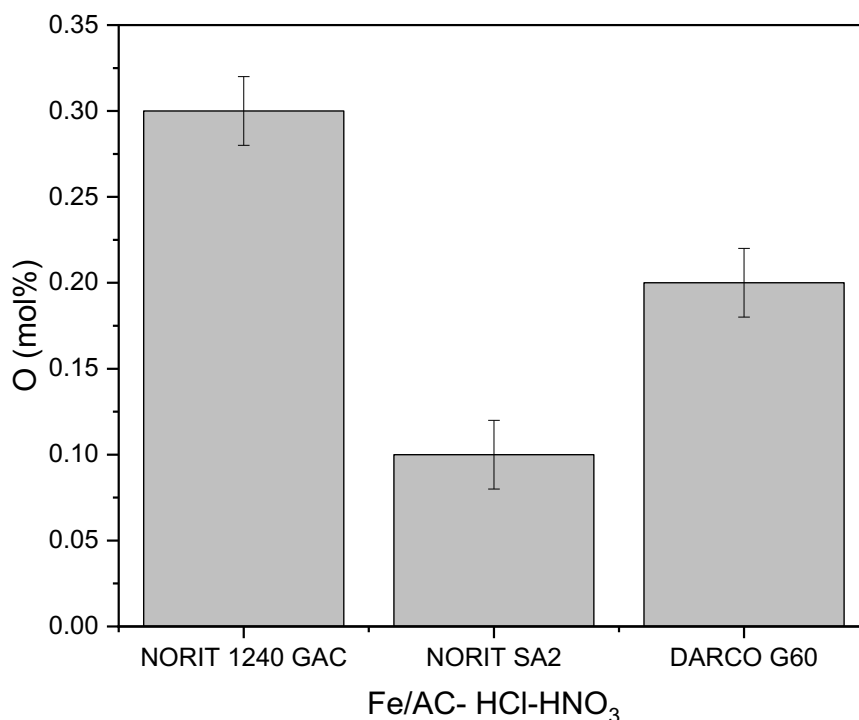


Figure 3.24: Elemental analysis results by mol% for O in the HCl-HNO₃-AC (GAC, SA2, G60) and their catalysts Fe/AC.

Table 3.1: Summary for the phenol adsorption capacity by the three types of AC (GAC, SA2 and G60) and phenol removal (AC+ H₂O₂) at different conditions (untreated AC and pre-acid treated AC).

AC	Mass of AC mg	Fresh AC		HCl-AC		HNO ₃ -AC		HCl-HNO ₃ -AC	
		Phenol adsorption only AC	Phenol removal AC+H ₂ O ₂	Phenol adsorption only AC	Phenol removal AC+H ₂ O ₂	Phenol adsorption only AC	Phenol removal AC+H ₂ O ₂	Phenol adsorption only AC	Phenol removal AC+H ₂ O ₂
GAC	3	4	15	9	11	5	20	5	10
	30	9	26	16	16	13	34	10	22
	60	16	52	27	33	23	53	21	34
SA2	3	5	15	7	11	4	27	4	11
	30	15	23	11	19	9	46	9	25
	60	27	26	18	30	15	50	17	37
G60	3	4	23	8	19	4	27	5	9
	30	8	23	14	25	13	33	10	19
	60	15	33	25	30	20	44	22	31

Table 3.2: Comparison analysis between Fe/AC catalysts prepared at different AC conditions regarding Fe leaching%.

Fe/AC	Fresh AC	HCl-AC	HNO₃-AC	HCl-HNO₃-AC
Fe/GAC	80	19	62	19
Fe/SA2	90	20	62	20
Fe/G60	60	9	63	18

Table 3.3: Comparison analysis between Fe/AC catalysts prepared by different AC conditions in terms of phenol conversion%.

Fe/AC	Fresh AC	HCl-AC	HNO₃-AC	HCl-HNO₃-AC
Fe/GAC	100	58	100	80
Fe/SA2	100	68	100	80
Fe/G60	100	50	100	80

Table 3.4: Comparison analysis between Fe/AC catalysts prepared by different AC conditions in terms of residual intermediates%.

Fe/AC	Fresh AC	HCl-AC	HNO₃-AC	HCl-HNO₃-AC
Fe/GAC	20	100	10	90
Fe/SA2	13	100	17	80
Fe/G60	40	100	19	70

Table 3.5: Comparison analysis between Fe/AC catalysts prepared by different AC conditions in terms of oxygen mol%.

Fe/AC	Fresh AC	HCl-AC	HNO₃-AC	HCl-HNO₃-AC
Fe/GAC	0.29	0.30	0.29	0.30
Fe/SA2	0.30	0.20	0.25	0.10
Fe/G60	0.20	0.20	0.19	0.20

In the summary as can be seen by tables 3.1, 3.2, 3.3, 3.4 and 3.5, all three types of AC without pre-treatment by the control test demonstrate the same phenol adsorption capacity of 5%. In the WHPCO reaction, Fe/AC raw-AC catalysts have high catalytic activity for phenol oxidation; they have full phenol oxidation, but Fe leaching is high, approximately 80%.

The HCl washing process slightly increased the phenol adsorption capacity for all the AC. This pre-acid treatment dramatically decreased the catalytic activity as well as decreased Fe leaching with the WHPCO reaction for phenol. Different kinds of AC react differently with the HCl acid pre-treatment; elemental analysis results indicated a decrease in O mol% for SA2, but not for GAC, or G60. These results confirmed the first hypothesis HCl washing process is essential for any AC to extract metals from AC but not to affect chemically in the AC.

The HNO₃ oxidation for AC finds not to affect the adsorption capacity for phenol at all ACs 5%. The catalytic activity increased for all catalysts by reducing the residual intermediates %, and Fe leaching slightly decreased. However, the elemental analysis did not detect any change in the O mol% inverted what was expected. That could be explained as the conditions that were used during the HNO₃ oxidation were insufficient to increase the oxygen surface groups. However, the increase in the catalytic activity and the decrease in the iron leaching could mean the oxidation by HNO₃ introduce different types of O surface groups that are better binder with Fe without affecting the O mol% content. Based on these results, the second hypothesis doesn't satisfy.

The combination between HCl and HNO₃ pre-acid treatment did not affect the phenol adsorption capacity of the AC, remaining at 5%. These treatments decreased the catalytic activity and Fe leaching. The elemental analysis did not detect a change in the O mol% for GAC and G60 but decreased in the O mol% for SA2. These results failed the third hypothesis.

Fe/AC, HCl-HNO₃-AC catalysts exhibit improvement in terms of Fe leaching, but the catalytic activity needs to enhance at the same time, so, S and N were added for the catalysts Fe-S-N/AC, at different conditions, which will be discussed in the next section.

3.2 S, N and Fe tri-doped activated carbons

3.2.1 Introduction

The rationale for the addition of heteroatoms to our carbons to enhance the catalysis activity and reduce leaching is as follows: in materials science, metallic systems' properties can be significantly enhanced by combining elements in the formation of alloys and intermetallic compounds. Often, alloys improve specific properties through combined influences, and alloys' rich compositions, structures, and properties have led to widespread application in electronics, engineering, and catalysis.⁸⁸ In recent years, there has been increased interest in bimetallic and trimetallic nanoclusters, which are referred to as alloy nanoclusters or nanoalloys, because of their ability to fabricate nanoscale materials with well-defined, controllable properties and structures.⁸⁸

Recent studies demonstrated that the catalytic activity and stability of Fe/AC catalysts were enhanced by N and S doping.⁸⁹⁻⁹² The S and N dopants form S- and N-containing groups on the carbon surface, which are expected to have a favourable effect on catalytic activity. The increased catalytic activity caused by N and S atoms may increase the relative amount of Fe²⁺ on the iron oxide surface and prevent Fe leaching.⁸⁹ It has been reported that dopants of metals and N generate new active sites on carbon surfaces. In this way, donor-acceptor properties are enhanced, thereby improving interfacial electron transfer, which can be beneficial for our reaction.⁹³ N species can improve carbon activity by adjusting their surface acidity. A combination of N and S doping can enhance the hydrophilicity of a final N, S-co-doped porous carbon.⁹⁴ A Fe-S complex on the catalyst surface acts as an active site to promote electron transfer between the oxidant and iron oxide.^{95, 96} It reported that the high performance of the catalyst in the degradation of Acid Red 73 was due to the combined effect of Fe₃-C and Fe₃-N.⁹⁷ In addition, graphite N dispersed in the carbon matrix and FeN species were responsible for higher tetracycline degradation.⁹⁸ Another study reported that, based on DFT calculations, graphitic N and Fe-N₄ complex sites had a higher reactivity in active carbon surrounding sites.⁹⁹

As mentioned above, doping N or S can generate complexes with Fe species and form new active sites on the carbon surface. These sites affect the acidity, hydrophilicity, and electron transfer properties. Nevertheless, there is a lack of research on N, S, and Fe-tri-doped carbon catalysts, and there is no conclusive evidence linking surface species to catalytic activity.⁸⁹

In this work, the Fe/AC catalysts have been modified by doping S and N. Fe-S-N/AC were prepared by a wet impregnation method using three different kinds of AC (GAC , SA2, G60)

under different conditions (raw AC and modifying AC), described in chapter 2. In all catalysts, Fe loading was kept fixed at 12wt%.

Working hypotheses for this section:

- 1- **Doping with S.** The addition of this element into the Fe/AC catalyst is expected to make it more catalytically active by increasing its Fe²⁺ content and preventing Fe leaching. To verify this, we compared Fe/AC and Fe-S-N/AC catalysts in terms of phenol conversion%, residual intermediates%, and Fe leaching%.
- 2- **Doping with N.** Though activated carbons contain some N, to increase its amount, into Fe/AC catalyst is expected to enhance the hydrophilicity of the catalyst surface and promote donor-acceptor properties as an alternative to O. The increase in hydrophilicity led to a strong affinity for H₂O₂. To assist that, it needs to compare H₂O₂ consumption with Fe/AC and Fe-S-N/AC catalysts.
- 3- **Effect of acid pre-treatment in the presence of S and N.** Considering the three hypotheses in the first part of this chapter, it was expected that Fe-N-S/AC (AC washed with HCl and HNO₃) could be the most effective catalyst for phenol removal by the WHPCO reaction in terms of phenol conversion%, residual intermediates%, H₂O₂ consumption% and Fe leaching%.

In order to determine if different preparation methods had an effect on the catalyst structure, both in terms of the effect on the framework and the actual deposition of Fe and in which form, the catalysts, besides the very useful elemental analysis reported so far, were also characterised by an array of tools like BET to evaluate effects on the surface area, XPS to quantify and determine species on the surface of the catalysts, and XRD to gather information on the formation of Fe-oxide clusters and if there were any effects on the structure of the materials, both for carbons and zeolites support (for the latter, see chapters 4, section 4.3.1). Then, if there were an effect on the structure, we were interested in assessing if this also influenced the reaction parameters like phenol conversion, H₂O₂ consumption, and residual intermediates, as well as on the durability of the catalyst by determining the effect of these different synthesis and doping protocols on Fe leaching.

3.2.2 Results and discussion

3.2.2.1 Catalytic test for phenol oxidation by the CWPO using Fe-S-N/AC catalysts prepared by raw-AC

Three sets of Fe-S-N/AC, Fe loading 12wt%, prepared by wetness impregnation method using raw-AC (GAC, SA2, G60) without pre-treatment. These catalysts were applied to phenol oxidation by CWPO reaction.

A. Catalytic activity, metal leaching and H₂O₂ consumption

To assess the catalytic activity for Fe-S-N/AC from raw-GAC (Figure 3.25), it compared with Fe/AC from raw-GAC as shown in Table 3.6, Fe-S-N/AC raw-GAC gives phenol conversion 100% as with Fe/AC raw-GAC. Without doping S and N, a catalyst had a residual intermediates% of 22%, while a catalyst with doping S and N had a residual intermediates % of 30%. The H₂O₂ consumption rate was not significantly different from 75% to 77% after 4 h, Suitable for phenol conversion and residual intermediates results. The amount of Fe leaching decreased by 50% from 80% to 40%. In relative terms, this is a strong improvement as we have reduced the leaching by half, though this is still quite high and still affects the durability of the catalyst.

Table 3.6: Comparative analysis of Fe-S-N/AC raw-GAC and Fe/AC from raw-GAC

	Fe-S-N/AC from raw-GAC	Fe/AC from raw-GAC
Phenol conversion% ± 5	100	100
CMB% ± 5	30	22
H ₂ O ₂ consumption% ± 3	77	75
Fe leaching% ± 1	40	80

To assess the catalytic activity for Fe-S-N/AC from raw-SA2 (Figure 3.25), it compared with Fe/AC from raw-SA2 as shown in Table 3.7, Fe-S-N/AC by SA2 catalysts produced 100% phenol oxidation, the same as with Fe/AC, while 12% of the residual intermediates percentage remained unchanged. As well, the consumption of H₂O₂ remains steady at 75%. Fe leaching remains high at 80%. Based on these results, Fe-S-N/AC and Fe/AC catalysts did not show a significant difference.

Table 3.7: Comparative analysis of Fe-S-N/AC from raw- SA2 and Fe/AC from raw-SA2

	Fe-S-N/ AC from raw-SA2	Fe/AC from raw-SA2
Phenol conversion% ± 5	100	100
CMB% ± 5	12	13
H ₂ O ₂ consumption% ± 3	75	76
Fe leaching% ± 1	80	90

To assess the catalytic activity for Fe-S-N/AC from raw-G60 (Figure 3.25), it compared with Fe/AC from raw- G60 as shown in Table 3.8; the phenol conversion rate decreased slightly from 100% with Fe/AC to 80% with Fe-S-N/AC from raw-G60 catalysts. Additionally, the residual intermediates % increased to 61% from 40%. There was a 65% consumption of H₂O₂ compared to Fe/AC catalysts at 60%; the difference was not significant considering the experimental error 5%. Fe leaching percentage is the same as Fe/AC catalysts at a difference. As a whole these results indicate that raw-G60 Fe-S-N/AC catalysts exhibit the same or a slightly reduced catalytic activity.

Table 3.8: Comparative analysis of Fe-S-N/AC from raw-G60 and Fe/AC from raw-G60

	Fe-S-N/AC from raw-G60	Fe/AC from raw-G60
Phenol conversion% ± 5	83	100
CMB% ± 5	61	40
H ₂ O ₂ consumption% ± 2	65	60
Fe leaching% ± 1	50	60

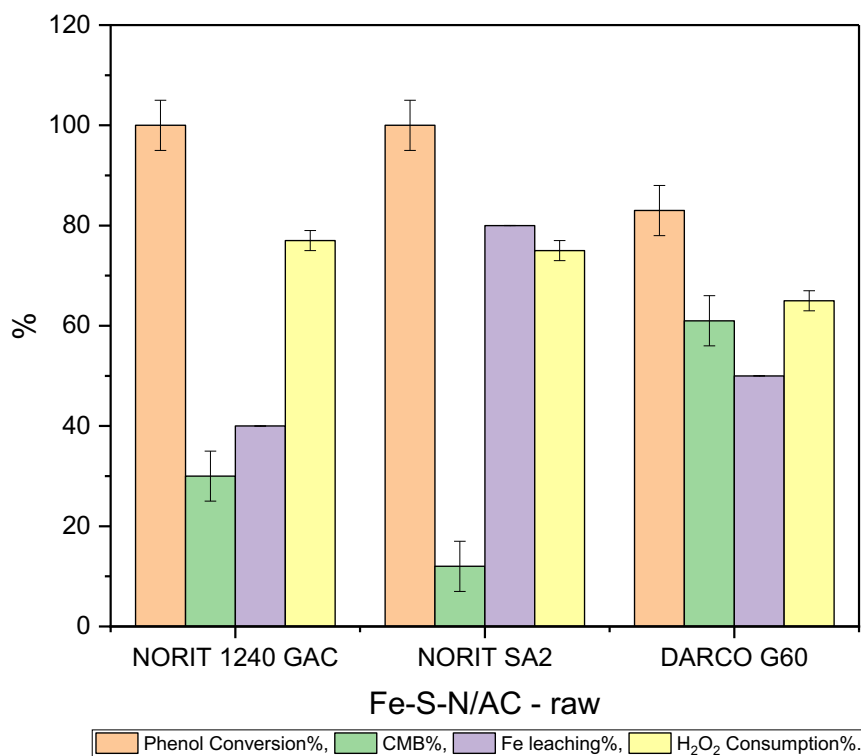


Figure 3.25: Catalytic activity, in terms of phenol conversion, CMB, Fe leaching and H₂O₂ consumption result for phenol oxidation by CWPO, using three types of Fe-S-N/AC, raw-AC (GAC, SA2, G60). All catalysts have 12 wt% Fe loading (the leaching is a relative leaching% with respect to the total Fe content), 4 h reaction time at 80 °C and 1:100 M:S.

B. Elemental analysis for raw-AC and their catalysts

Comparing the raw-AC without doping Fe species, raw- SA2, has the highest S mol% (0.004 mol%), (Figure 3.26) while there was no significant difference between GAC and G60. Doping Fe in the AC by impregnation protocol should not change the S mol% with reference to the raw material. However, that could be explained as different AC batches having different amounts of residual metals in the matrix before washing which causes unexpected behaviours. Some metals can act as catalysts, influencing chemical reactions on the surface of the activated carbon. This can impact the material's performance in applications like catalysis or adsorption of specific substances. Residual metals can affect the adsorption capacity of activated carbon for specific pollutants or substances. The nature of these effects may vary depending on the type and concentration of metals present.

Variability in the amount and type of residual metals can result in batches of activated carbon with different characteristics. These differences may lead to unexpected or inconsistent performance in industrial or environmental applications. For example, in water treatment, activated carbon is often used to remove impurities, and the presence of certain metals may interfere with or enhance its adsorption capabilities. So washing the AC with HCl is an essential process to extract these metals and avoid unexpected behaviour by the catalysts.

The S, N and Fe tri-doped AC catalysts, compared with other catalysts Fe/AC, are expected to have a higher S mol%, with values up to 0.01 mol% whereas starting from nearly zero (Figure 3.26) so expected to prevent Fe leaching more than other catalysts (Fe/AC) and increase the catalytic activity. Tables 3.6, 3.7 and 3.8 show that this is not the case. So, the first hypothesis is that the binding of Fe with S to prevent metal leaching is mostly not satisfied in the case of Fe-S-N/AC catalysts by raw-AC, as they have high iron leaching. The Fe-S-N/AC catalysts prepared by different AC have similar S mol% (0.01 mol%). However, this S mol% of Fe-S-N/AC raw-AC catalysts are more than expected. The calculation to calculate the expected mol of Fe, S and N in the Fe-S-N/AC catalysts, which are 0.002 mol of Fe by the first precursor $\text{Fe}(\text{NO}_3)_3 \cdot (\text{H}_2\text{O})_9$ and 0.002 mol of Fe by the second precursor $(\text{NH}_4)_2\text{Fe} \cdot \text{SO}_4$, and 0.002 mol of S by $(\text{NH}_4)_2\text{Fe} \cdot \text{SO}_4$. So, the ratio between Fe:S was expected to be 2:1, as indicated in the results shown in Table 3.9. This increase in the S mol% could be explained as the raw-AC framework has initially some S.

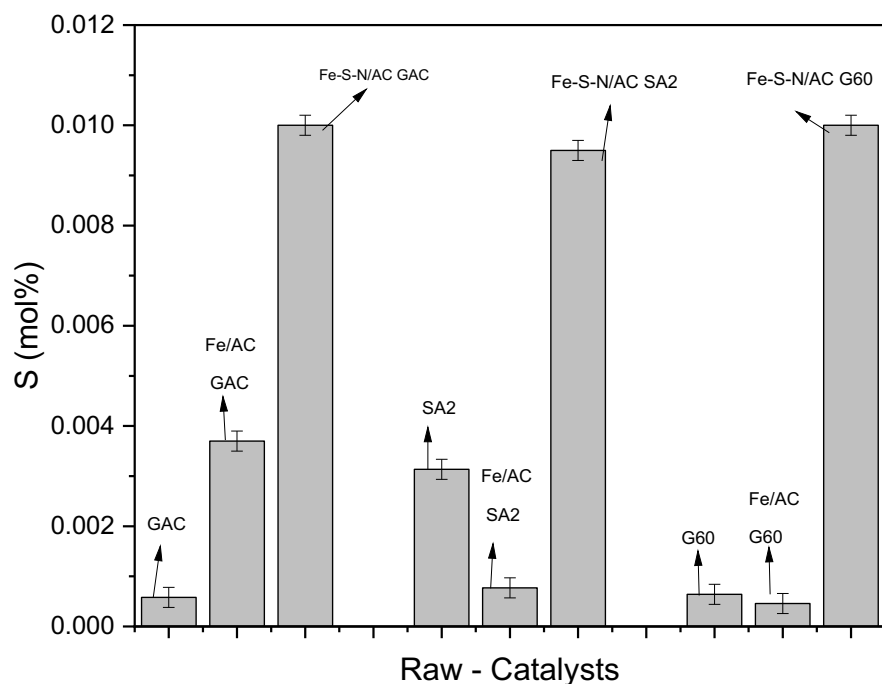


Figure 3.26: Elemental analysis results by mol% for S in the raw-AC (GAC, SA2, G60) and their catalysts Fe/AC and Fe-S-N/AC.

Table 3.9: Comparative analysis of Fe-S-N/AC and Fe/AC from raw-AC catalysts in terms of Fe:S and Fe:O molar ratio

	Fe:S mol	Fe:O mol
Fe/ raw-GAC	18	0.08
Fe/ raw-SA2	32	0.08
Fe/ raw-G60	53	0.03
Fe-S-N/ raw-GAC	2	0.06
Fe-S-N/ raw-SA2	2	0.09
Fe-S-N/ raw-G60	2	0.1

The Fe:S molar ratio for Fe-S-N/AC raw-AC and Fe/AC raw-AC catalysts; it is clear that doping S significantly improve the Fe:S mol% than Fe/AC catalysts (Figure 3.26). The greater the S doping the smaller the ratio, it was decreased to be 2 mol. So, the protocol successfully worked and doped S in the catalysts; these catalysts were supposed to prevent Fe leaching and increase catalytic activity. However, based on the iron leaching results, that was not the case; it was decreased compared with Fe/AC but still, the metal leaching was high, affecting the stability of the catalyst. That could be justified as might not be enough S to bind Fe (Fe:S, 2:1) to form clusters like FeS₂ for example. For the Fe:O ratio, there was no statistical difference comparing the Fe-S-N/AC raw-AC and Fe/AC raw-AC catalysts probably because of the relatively large excess of O with respect to Fe, in all catalysts the molar ratio between the Fe:O was approximately 0.1 mol. On the other hand, this relative large excess of O with respect to Fe, this is expected to contribute to the formation of Fe_xO_y species (as confirmed by XRD sections 3.3.1).

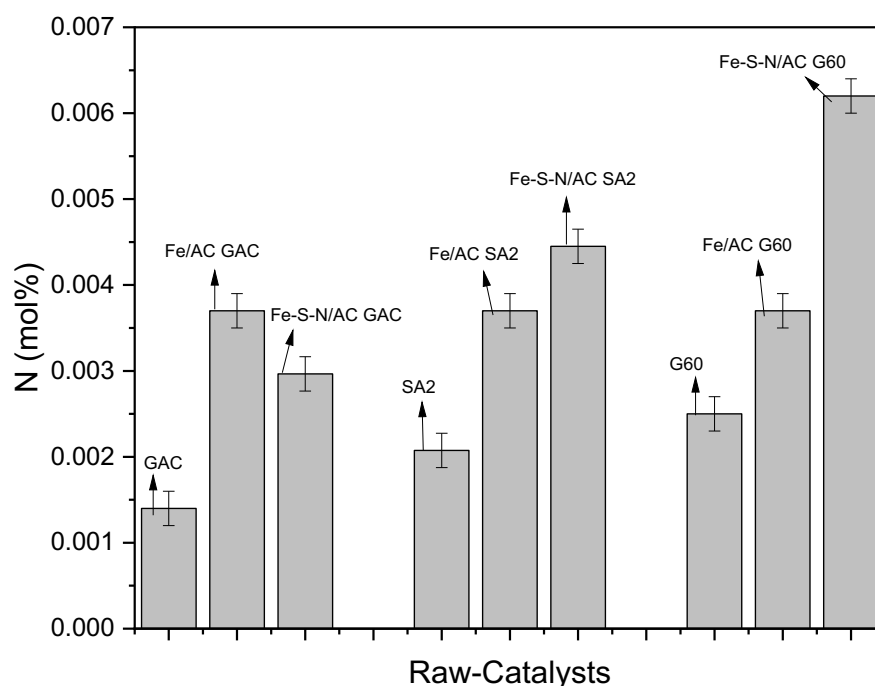


Figure 3.27: Elemental analysis results by mol% for N in the raw-AC (GAC, SA2, G60) and their catalysts Fe-S-N/AC.

Comparing the raw-AC without doping Fe species, raw-GAC has slightly lower N mol% (0.001 mol%). While there was no significant difference between SA2 and G60 (0.002 mol%). Doping N was expected to increase N mol%, as illustrated (Figure 3.27) with Fe-S-N/AC catalysts, except for raw-GAC, was no difference between the Fe-S-N/AC and Fe/AC catalysts in the N mol%. The highest N mol% is with the catalysts Fe-S-N/AC prepared from raw-G60 (0.006 mol %). Then, Fe-S-N/AC was prepared from raw-SA2 (0.005 mol%). The lower N mol% was for catalysts by GAC (0.003 mol%). Also, their catalysts Fe/AC (0.004 mol%) have more N than Fe-S-N/AC (0.003 mol%). See section 3.2.1, the second hypothesis that doping N should increase the hydrophilicity led to a strong affinity for H₂O₂, comparing the H₂O₂ consumption in Tables 3.6, 3.7 and 3.8 shows that this is not the case, though this might be due to the relatively small amount of N that was eventually correlated with a limited or negligible effect due to its small amount and not for any adverse structural considerations due to the carbon.

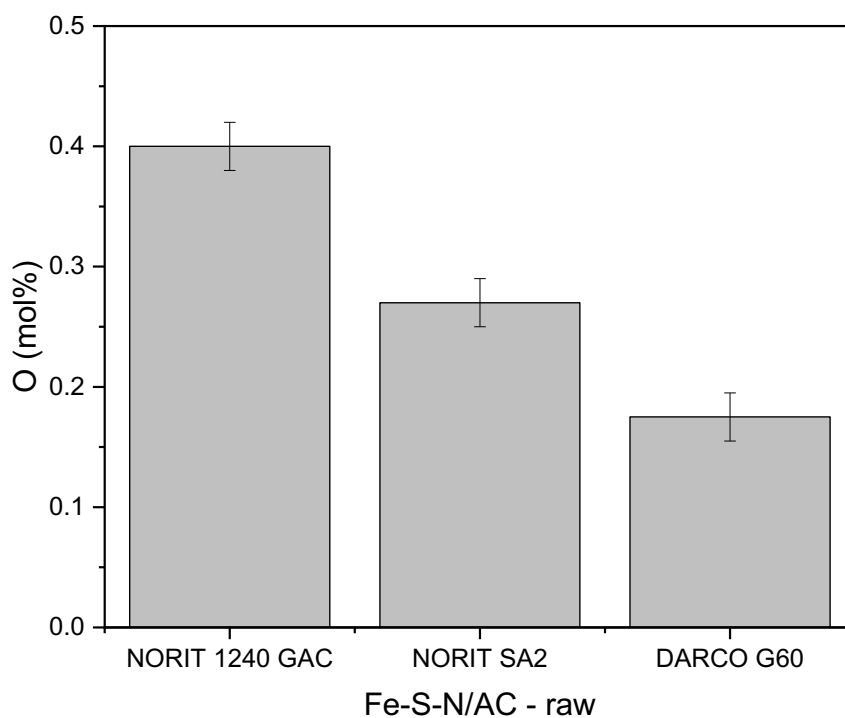


Figure 3.28: Elemental analysis results by mol% for O in the Fe-S-N/AC raw-AC (GAC, SA2, G60) catalysts.

Fe-S-N/AC raw-GAC has the highest O mol% compared with other Fe-S-N/AC catalysts. This result translates to a material preserving high catalytic activity, and at the same time, decreasing metal leaching by 50% (Figure 3.25).

3.2.2.2 Catalytic test for phenol oxidation by the CWPO using Fe-S-N/AC catalysts prepared by HCl-AC

According to the catalytic activity results reported in section 3.1.2.2 D, Figure 3.13. The catalysts were prepared by a washing pre-treatment with HCl, Fe/AC HCl-AC catalysts; their catalytic activity decreased significantly. Accordingly, for the Fe-S-N/AC, HCl-AC catalysts were expected to exhibit decreased catalytic activity as well. Still, when compared Fe-S-N/AC HCl-AC catalysts with Fe/AC, HCl-AC were expected to exhibit higher catalytic activity due to S and N doping. In terms of Fe leaching, it was expected to decrease dramatically by the HCl washing process in addition to S and N doping.

A. Catalytic activity, metal leaching and H₂O₂ consumption

The catalytic activity for Fe-S-N/AC from HCl-GAC (Figure 3.29) was compared with those from Fe-S-N/AC raw-GAC and Fe/AC from HCl-GAC as shown in Table 3.10. For the Fe-S-N/AC HCl-GAC, the phenol conversion slightly decreased from 100% with the Fe-S-N/AC raw-GAC to 88%, but compared with Fe/AC HCl-GAC, where it was 55%, the phenol conversion increased. Residual intermediates % slightly increased from 30% with the Fe-S-N/AC raw-GAC to 57%; however, compared with Fe/AC HCl-GAC, where it was 100% indicated the increase of catalytic activity. In other words, it appears that if the activity (conversion of phenol) decreases, then the residual intermediates increases as a result of the slightly smaller mineralization of CO₂ and H₂O. According to these results, the presence of additional S and N in the carbon matrices was beneficial to an increase in catalytic activity. The H₂O₂ consumption after was 35% for the Fe-S-N/AC HCl-GAC, which was similar to Fe/AC HCl-GAC catalysts; still, the H₂O₂ consumption decreased compared to the raw catalysts Fe-S-N/AC raw-GAC 77% which explained the decrease in the phenol oxidation. The amount of Fe leaching drastically decreased from 40% to 13%.

Table 3.10: Comparative analysis of Fe-S-N/AC raw-GAC, Fe-S-N/AC from HCl-GAC, and Fe/AC from HCl-GAC:

	Fe-S-N/AC from raw- GAC	Fe-S-N/AC from HCl-GAC	Fe/AC from HCl-GAC
Phenol conversion% ± 5	100	88	55
CMB% ± 5	30	57	100
H ₂ O ₂ consumption% ± 3	77	35	34
Fe leaching% ± 1	40	13	15

To assess if the catalytic activity for Fe-S-N/AC from HCl-SA2 (Figure 3.29), compared with the Fe-S-N/AC raw-SA2 and Fe/AC from HCl-SA2 these were compared in Table 3.11. Fe-S-N/AC from HCl-SA2 catalysts produced 40% phenol oxidation, so the catalytic activity significantly decreased compared with Fe-S-N/AC from raw-SA2, where the catalytic activity was 100%. Also, there was a slight difference in the phenol conversion between Fe-S-N/AC from HCl-SA2 catalysts and Fe/AC 66%. With Fe-S-N/AC HCl-SA2 catalysts, the residual intermediates also significantly increased to 66% from 12% with Fe-S-N/AC raw-SA2 catalysts. But compared with Fe/AC HCl-SA2 100%, there was more mineralisation. The consumption of H₂O₂ was 22% with Fe-S-N/AC HCl-SA2 and 32% for Fe/AC from HCl-SA2 catalysts, which is compatible with the catalytic activity results. There was a significant decrease in Fe leaching of 22%, as predicted; as a comparison this was 80% with catalysts using raw carbon. Based on these results, Fe-S-N/AC HCl-SA2 and Fe/AC HCl-SA2 catalysts did not show a significant difference. On the other hand, the lesser the amount of H₂O₂ consumed, the lesser the number of short-chain acids that will eventually lead to CO₂ and H₂O. It might be that these short acids are also playing a role in the leaching of iron species.⁸⁶

Table 3.11: Comparative analysis of Fe-S-N/AC from raw-SA2, Fe-S-N/AC from HCl-SA2, and Fe/AC from HCl-SA2

	Fe-S-N/AC from raw- SA2	Fe-S-N/AC from HCl-SA2	Fe/AC from HCl-SA2
Phenol conversion% ± 5	100	40	66
CMB% ± 5	12	66	100
H ₂ O ₂ consumption% ± 3	75	22	32
Fe leaching% ± 1	80	22	21

To assess if the catalytic activity for Fe-S-N/AC from HCl-G60 (Figure 3.29), compared to the one of Fe-S-N/AC raw-G60 and Fe/AC from HCl-G60 results were reported in Table 3.12. Fe-S-N/AC from HCl-G60 catalyst has a phenol conversion of 71%. There was no significant difference in the phenol conversion between catalysts prepared with Fe-S-N/AC raw-G60, where the conversion reached 83%. With Fe/AC HCl-G60 catalysts, the phenol oxidation was 50%, indicating that doping S and N increased the catalytic activity. Compared to raw and HCl Fe-S-N/AC catalysts, residual intermediates% remained steady at 63%. But decreased from 94% with Fe/AC from HCl-AC catalysts. There was no significant difference in the H₂O₂ consumption between Fe-S-N/AC HCl-G60 and Fe/AC HCl-AC catalysts, but compared to Fe-S-N/AC raw-G60 catalysts was 65%. The relative Fe leaching percentage decreased from 50 to 32% to Fe-S-N/AC raw-G60 and Fe-S-N/AC HCl-G60, respectively. Taken as a whole, these results indicate that there was no significant difference in the catalytic activity between a pre-treated Fe-S-N/AC HCl-G60 and a raw Fe-S-N/AC raw-G60, though iron leaching was reduced as expected, which is still a valuable result from the perspective of catalyst design as decreased leaching translates to increased durability of the catalyst. However, doping with S and N increased the catalytic activity when compared Fe-S-N/AC with undoped Fe/AC HCl-G60 catalysts, thus showing that the combined effect of acid pre-treatment and the incorporation of heteroatoms can indeed lead to higher hydrophilicity and, in turn, reactivity, a higher reproducibility, and lower leaching.

Table 3.12: Comparative analysis of Fe-S-N/AC from raw-G60, Fe-S-N/AC from HCl-G60, and Fe/AC from HCl-G60

	Fe-S-N/AC from raw-G60	Fe-S-N/AC from HCl-G60	Fe/AC from HCl-G60
Phenol conversion% \pm 5	83	71	50
CMB% \pm 5	61	63	94
H ₂ O ₂ consumption% \pm 3	65	22	23
Fe leaching% \pm 1	50	32	5

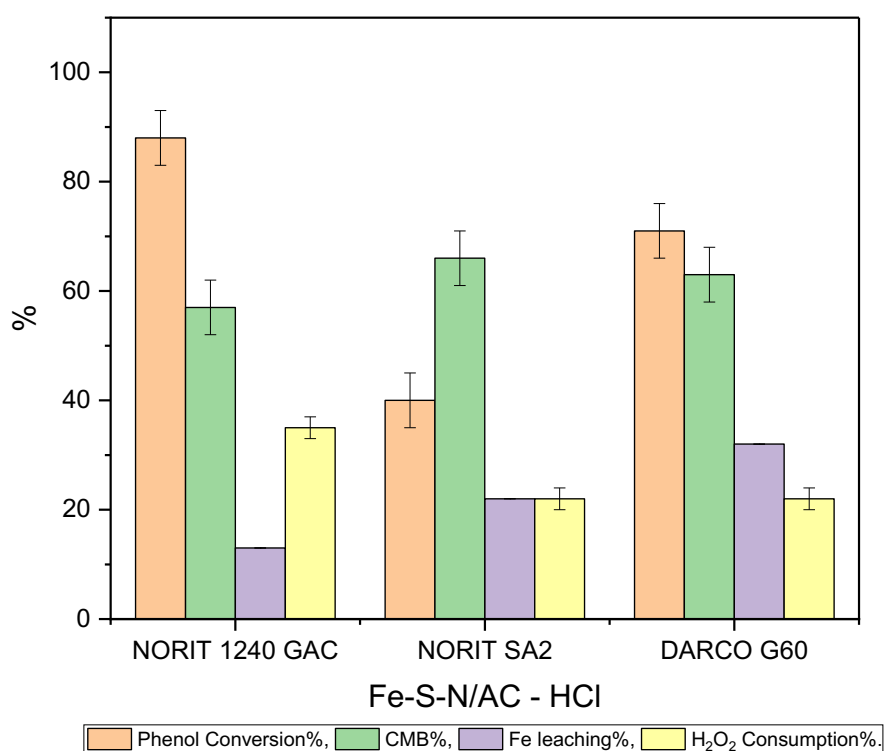


Figure 3.29: Catalytic activity, in terms of phenol conversion, CMB, Fe leaching and H₂O₂ consumption result for phenol oxidation by CWPO, using three types of Fe-S-N/AC catalysts prepared from AC-HCl (GAC, SA2, G60). All catalysts have 12 wt% Fe loading (the leaching is a relative leaching% with respect to the total Fe content), 4 h reaction time at 80 °C and 1:100 M:S.

B. Elemental analysis for HCl-AC

Comparing the HCl-AC without doping Fe species, HCl-GAC has slightly higher S mol% (about 0.002). While there was no significant difference between SA2 and G60 (0.001mol%). Fe doping in AC should not affect S mol%. According to the data shown in Figure 3.30, tri-doped AC catalysts with S, N, and Fe have a significantly higher, about a 5-fold increase, S mol% (0.01, 0.09 and 0.08 mol% for Fe-S-N/AC from GAC, SA2 and G60 respectively) than other Fe/AC catalysts. This should increase catalytic activity while preventing Fe leaching. Tables 3.10, 3.11 and 3.12 show that in the absence of N and S, the leaching was higher, and the catalysts were not as active as in the presence of S and N.

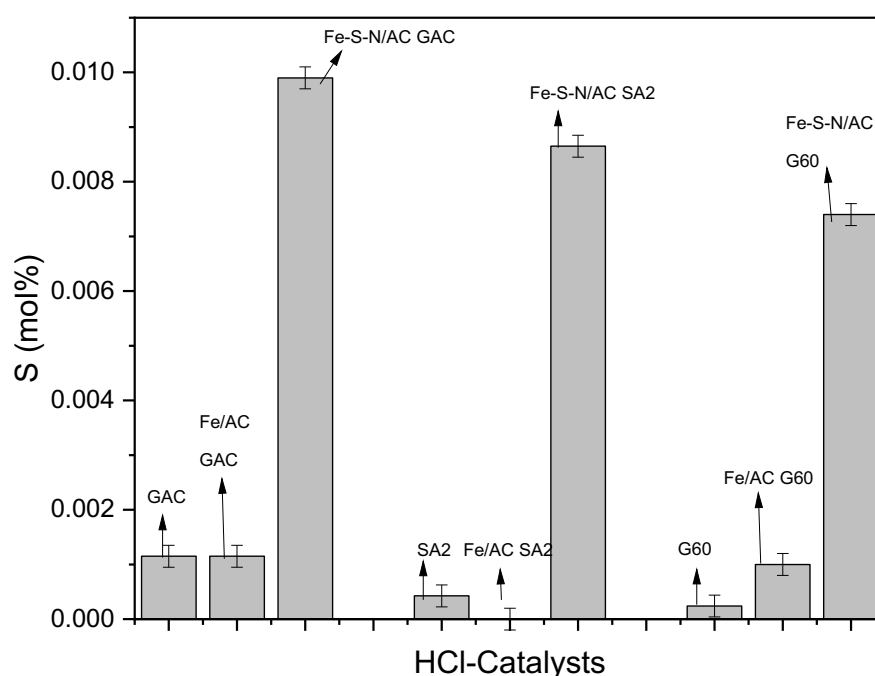


Figure 3.30: Elemental analysis results by mol% for S in the HCl -AC (GAC, SA2, G60) and their catalysts.

Table 3.13: Comparative analysis of Fe-S-N/AC and Fe/AC from HCl-AC catalysts in terms Fe:S and Fe:O molar ratio

	Fe:S mol	Fe:O mol
Fe/ HCl-GAC	17	0.08
Fe/ HCl-SA2	n. a.*	1.8
Fe/ HCl-G60	22	0.1
Fe-S-N/ HCl-GAC	2	0.1
Fe-S-N/ HCl-SA2	2	0.1
Fe-S-N/ HCl-G60	3	0.04

- n. a.= not applicable (no S detected).

Table 3.13 shows the Fe:S molar ratio for Fe-S-N/AC and Fe/AC catalysts; it is clear that doping S significantly improve the Fe:S mol ratio than Fe/AC catalysts, it was decreases from 17 to 2 mol. Accordingly, the protocol is successfully doping S with the AC. It was therefore expected that these catalysts would prevent Fe leaching and increase catalytic activity. However, based on the iron leaching results, that was not the case; it was decreased compared with Fe/AC but still, the metal leaching was high, affecting the stability of the catalyst. In addition, washing the AC with HCl decreased the catalytic activity even with S and N doping catalysts. Regarding the Fe:O ratio, no difference was observed between the Fe-S-N/AC HCl-AC and Fe/AC HCl-AC catalysts in all catalysts. In general, for Fe:O, this is always smaller than 1, so there is a large amount of O to bind Fe. However, it is worth noting that it is not only the amount of O per se that will dictate the final binding of the Fe, its form, and, in turn, its catalytic activity. For example, COOH groups are expected to bind Fe better than OH ones, with the result that the ‘quality’ of these induced oxygen species will also be important and not just their quantity.

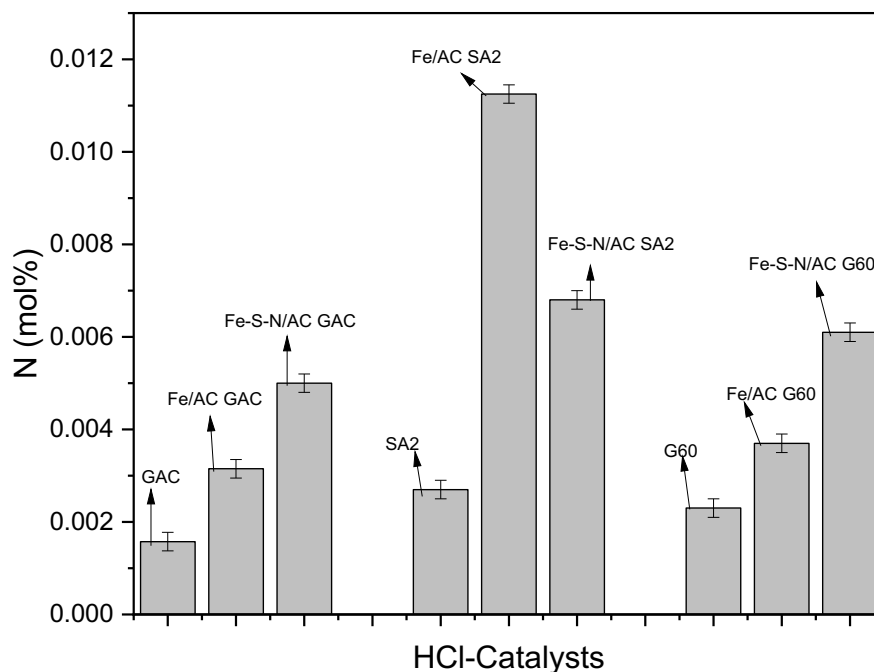


Figure 3.31: Elemental analysis results by mol% for N in the HCl-AC (GAC, SA2, G60) and their catalysts.

HCl-AC is expected to have lower N mol%; comparing these results with Figure 3.27, N mol% for AC without treatment shows no significant change in the N mol% at the majority of HCl-AC and their catalysts. However, the unsteady percentage of N mol% between the HCl-ACs and the catalysts for SA2 could explain as a different batch of the same AC has different metals containing this result detected previously with another sample. In this perspective, although there are many advantages to the use of AC in catalysts listed in section 1.1, a lack of batch reproducibility is a major drawback that will need to be considered with the aim of future catalyst development.

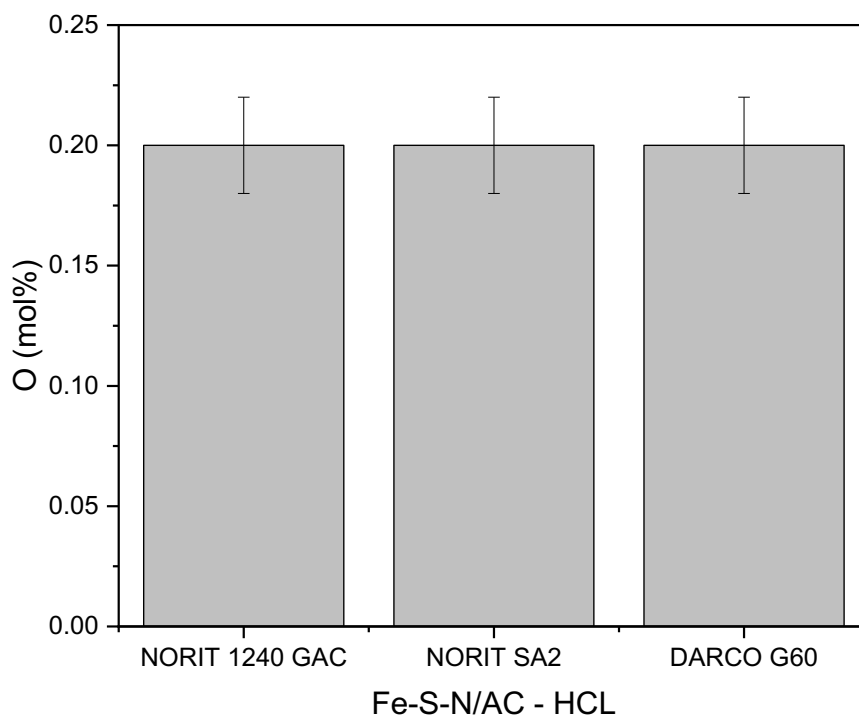


Figure 3.32: Elemental analysis results by mol% for O in the Fe-S-N/AC HCl-AC (GAC, SA2, G60) catalysts.

From Figure 3.32, all Fe-S-N/AC from HCl-AC catalysts have the same O mol% (0.2 mol%). A comparison of the data from Figure 3.32 and Figure 3.28 O mol% at Fe-S-N/AC by raw-ACs, shows that HCl-GAC and HCl-SA2 catalysts decreased O mol% from 0.4 and 0.3 mol% for Fe-S-N/AC from HCl-GAC and HCl-SA2 respectively to 0.2 mol% of O for both, whereas Fe-S-N/AC HCl-G60 catalysts remained constant (see section 3.1.1) the first hypothesis is that washing AC with HCl caused a water molecule to be released, and some loss of oxygen may occur, as confirmed by these results.

3.2.2.3 Catalytic test for phenol oxidation by the CWPO using Fe-S-N/AC catalysts prepared by HNO₃-AC

A. Catalytic activity, metal leaching and H₂O₂ consumption

As shown in Table 3.14, the catalytic activity of Fe-S-N/AC from HNO₃-GAC (Figure 3.33) was compared with Fe-S-N/AC raw-GAC and Fe/AC by HNO₃-GAC. Fe-S-N/AC from HNO₃-GAC has 100% phenol conversion, the same for all catalysts. residual intermediates% was very

low at 11% as with Fe/AC catalysts, which decreased compared with the Fe-S-N/AC raw catalysts indicating the effect of pre-acid treatment by HNO₃. The H₂O₂ consumption rate, 88% after 4h, is compatible with the catalytic activity with no significant difference to raw catalysts having a 77% rate though this is slightly higher than the H₂O₂ consumption rate observed for Fe/AC at 63%. Importantly though, the Fe leaching decreased by 50% by doping S and N for both catalysts raw and HNO₃, according to these results doping S and N decreased Fe leaching but did not affect the catalytic activity, which is still, however, a valuable outcome. The HNO₃ oxidation process slightly increases catalytic activity by decreasing residual intermediates %.

Table 3.14: Comparative analysis of Fe-S-N/AC raw-GAC, Fe-S-N/AC from HNO₃-GAC, and Fe/AC from HNO₃-GAC

	Fe-S-N/AC from raw-GAC	Fe-S-N/AC from HNO₃-GAC	Fe/AC from HNO₃-GAC
Phenol conversion% ± 5	100	100	100
CMB% ± 5	30	11	10
H ₂ O ₂ consumption% ± 3	77	88	63
Fe leaching% ± 1	40	31	63

To assess how the catalytic activity for Fe-S-N/AC from HNO₃-SA2 (Figure 3.33), compared with the Fe-S-N/AC raw-SA2 and Fe/AC from HNO₃-SA2 as shown in Table 3.15, phenol conversion reaches 83%, was slightly decreased compared with the Fe-S-N-AC raw-SA2 and Fe/AC catalysts (100%). Also, residual intermediates % increased from 17% for both Fe-S-N/AC raw- SA2 and Fe/AC from HNO₃-SA2 to 33% for Fe-S-N/AC from HNO₃-SA2. There was no significant difference in the H₂O₂ consumption values. The combination between both treatments doping S and N and pre-acid HNO₃ oxidation, decreased the metal leaching from 60-80% to 28%. Although this is strong and promising progress though more work will be needed to decrease this value further. Therefore, according to these results, the catalytic activity and metal leaching decreased with Fe-S-N/AC from HNO₃.

Table 3.15: Comparative analysis of Fe-S-N/AC from raw-SA2, Fe-S-N/AC from HNO₃-SA2, and Fe/AC from HNO₃-SA2

	Fe-S-N/AC from raw-SA2	Fe-S-N/AC from HNO₃-SA2	Fe/AC from HNO₃- SA2
Phenol conversion% ± 5	100	83	100
CMB% ± 5	12	33	17
H ₂ O ₂ consumption% ± 3	75	70	65
Fe leaching% ± 1	80	28	63

According to the data reported in Table 3.16, we compared the catalytic activity of Fe-S-N/AC from HNO₃-G60 (Figure 3.33) with the Fe-S-N/AC raw-G60 and Fe/AC from HNO₃-G60. As compared to the raw-G60 catalyst, the Fe-S-N/AC from HNO₃-G60 catalyst achieves 100%. A significant reduction in residual intermediates % was also observed when compared with Fe-S-N/AC raw and HNO₃ catalysts from 61% to 15%; in contrast, it was not significant when compared with Fe/AC (19%). These results were in agreement with H₂O₂ consumption values since the stoichiometric amount of H₂O₂ to phenol was used 1:14, the consumption of H₂O₂ ranged between 65, 82 and 71% for Fe-S-N/AC raw-G60, Fe-S-N/AC from HNO₃-G60 and Fe/AC from HNO₃-G60 respectively their phenol conversion reached 100%, but residual intermediates still 15% which is compatible with the H₂O₂ consumption results. as well as for the Fe/AC phenol conversion 80% and residual intermediates 61% which is in agreement with the H₂O₂ results. Approximately 40% of the Fe was leached. As a result of the outcomes, there was no significant difference between Fe-S-N/AC from HNO₃-G60 and Fe/AC from HNO₃-G60, but there was a decrease in the metal leaching rate from 60% to 40%. Compared to raw catalysts, Fe-S-N/AC HNO₃-G60 increased catalytic activity and no difference in the Fe leaching, which results in the way to catalysts with the desired characteristic for this reaction.

Table 3.16: Comparative analysis of Fe-S-N/AC from raw-G60, Fe-S-N/AC from HNO₃-G60, and Fe/AC from HNO₃-G60.

	Fe-S-N/AC from raw-G60	Fe-S-N/AC from HNO ₃ -G60	Fe/AC from HNO ₃ -G60
Phenol conversion% ± 5	83	100	100
CMB% ± 5	61	15	19
H ₂ O ₂ consumption% ± 3	65	82	71
Fe leaching% ± 1	50	40	60

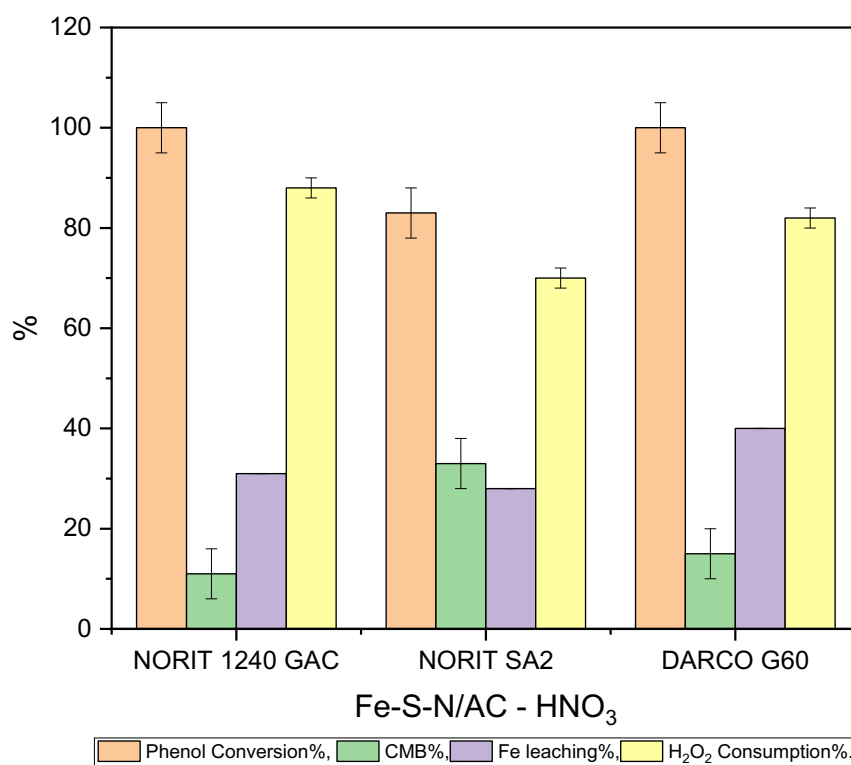


Figure 3.33: Catalytic activity, in terms of phenol conversion, CMB, Fe leaching and H₂O₂ consumption result for phenol oxidation by CWPO, using three types of Fe-S-N/AC catalysts prepared from AC- HNO₃ (GAC, SA2, G60). All catalysts have 12 wt% Fe loading (the leaching is a relative leaching% with respect to the total Fe content), 4 h reaction time at 80 °C and 1:100 M:S.

B. Elemental analysis for HNO₃-AC

Comparing the HNO₃-AC without doping Fe species, HNO₃-GAC, has slightly higher S mol%. While there was no significant difference between SA2 and G60. It should not affect the S mol% if Fe is doped in the AC. As shown in Figure 3.34, tri-doped AC catalysts with S, N, and Fe have dramatically higher S mol% (0.008, 0.01 and 0.009 mol% for Fe-S-N/AC AC1, SA2 and G60, respectively) than other Fe/AC catalysts. This corroborated that the doping of S was successful by our protocol, so they were expected to prevent Fe leaching more than other catalysts (Fe/AC) and increase catalytic activity. These findings are summarised in Tables 3.15, 3.16 and 3.17.

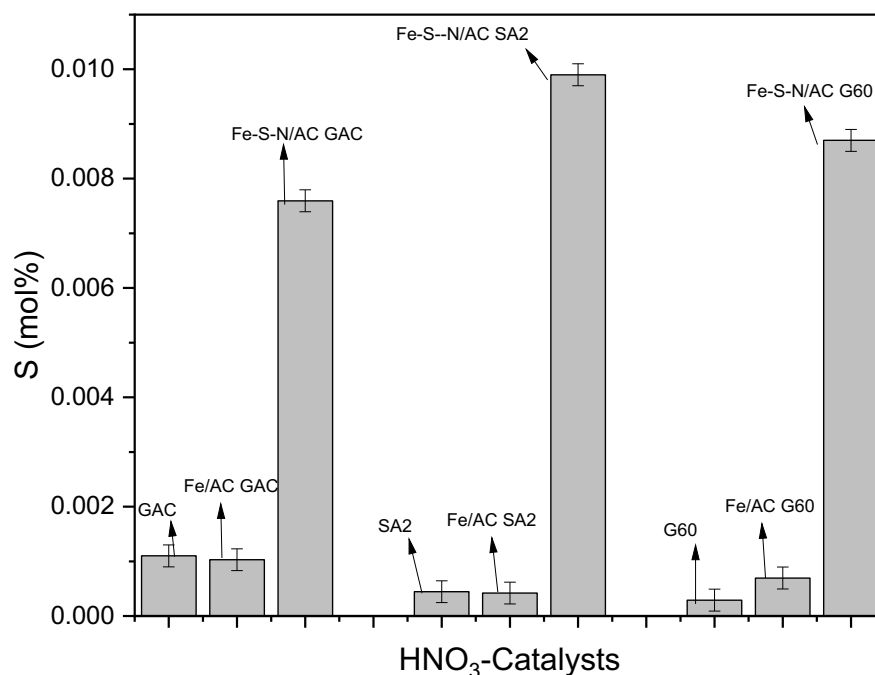


Figure 3.34: Elemental analysis results by mol% for S in the HNO₃-AC (GAC, SA2, G60) and their catalysts.

Table 3.17: Comparative analysis of Fe-S-N/AC and Fe/AC from HNO₃-AC catalysts in terms Fe:S and Fe:O molar ratio

	Fe:S mol	Fe:O mol
Fe/ HNO ₃ -GAC	24	0.08
Fe/ HNO ₃ -SA2	58	0.09
Fe/ HNO ₃ -G60	34	0.1
Fe-S-N/ HNO ₃ -GAC	3	0.15
Fe-S-N/ HNO ₃ -SA2	2	0.04
Fe-S-N/ HNO ₃ -G60	3	0.1

Table 3.17 shows the Fe:S molar ratio for Fe-S-N/AC and Fe/AC catalysts; it is clear that doping S significantly improve the Fe:S mol (2-3 mol) than Fe/AC catalysts (24,58 and 34 mol), as mentioned before this mol ratio was expected to be 2 mol. It was therefore expected that these catalysts would prevent Fe leaching and increase catalytic activity. Based on the results, there were improvements in the catalytic activity, including phenol conversion and residual intermediates; also, iron leaching was decreased compared with Fe/AC but still, the metal leaching was high, affecting the stability of the catalyst. Based on the Fe:S table above, it would seem that despite the amount of S increasing, either: the amount of S is not sufficient to bind all the Fe that would be needed, or the possible Fe-S bridges/bonds are not as strong, under reaction conditions, as originally thought. Also, it seems that when this particular carbon is used, the results are also, in part, AC-dependent. For the Fe:O ratio, there was no static difference comparing the Fe-S-N/AC raw-AC and Fe/AC raw-AC catalysts in all catalysts. for Fe:O, this is always (and by far) smaller than 1, so there is a lot of O to bind Fe (but the aspect of the ‘quality of these O as binder with Fe may cause the leaching).

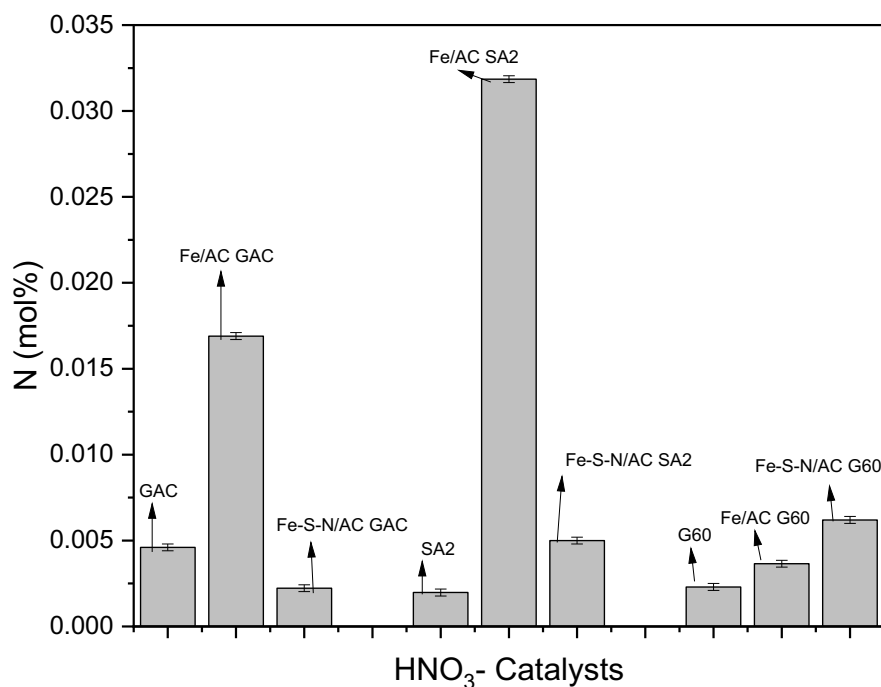


Figure 3.35: Elemental analysis results by mol% for N in the HNO₃-AC (GAC, SA2, G60) and their catalysts.

As anticipated HNO₃-AC is expected to have more N mol%; comparing the results reported in Figure 3.35 with Figure 3.27, N mol% for AC without treatment shows an increase in the N mol% for HNO₃-GAC (from 0.001 to 0.005 mol%) and HNO₃-G60 (from 0.002 to 0.004 mol%), while for HNO₃-SA2 the N mol% stays steady (0.002 mol%). Despite this, the unsteady percentage of N mol% between the HNO₃-ACs and their catalysts Fe/AC and Fe-S-N/AC for GAC and SA2 could explain this because a different batch of the same AC contains different metals that were detected previously for this result. However, with the data gathered so far, there was no evidence to support the second hypothesis of N doping in this study.

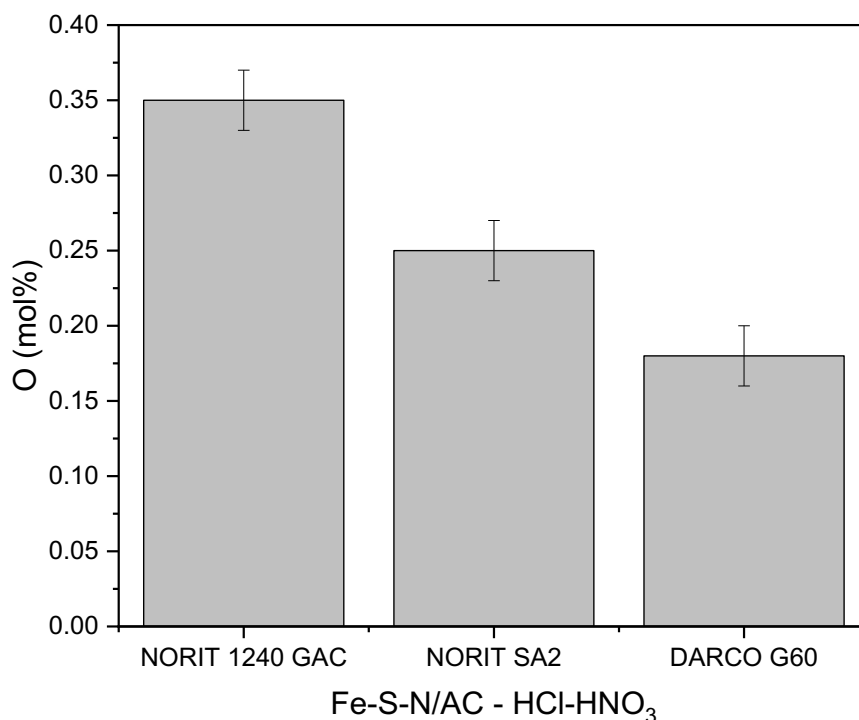


Figure 3.36: Elemental analysis results by mol% for O in the Fe-S-N/AC HNO₃-AC (GAC, SA2, G60) catalysts.

A comparison of the data in Figure 3.36 with those in Figure 3.28 shows that the O mol% for Fe-S-N/AC from raw-ACs, shows no significant difference in the O mol% in contrast to what was expected by HNO₃ treatment to increase the O functional groups. This means that the HNO₃ pre-treatment didn't induce any significant pre-oxidation and, in turn, any appreciable increase in the number of oxygen surface groups. However, not changing the amount of O (which was indeed one of our expected results) doesn't necessarily mean not changing the AC properties. In fact, HNO₃ may not oxidize AC (though this would have been expected, maybe this is due to our treatment conditions). Still, HNO₃ could oxidize C-OH groups to COOH groups, and these are still better binders for Fe. In turn, even if there is no quantitative effect, there might still be a qualitative effect, which could still reduce the leaching, as shown in Tables 3.14, 3.15 and 3.16.

3.2.2.3 Catalytic test for phenol oxidation by the CWPO using Fe-S-N/AC catalysts prepared by HCl-HNO₃-AC

A. Catalytic activity, metal leaching and H₂O₂ consumption

To evaluate the catalytic activity of Fe-S-N/AC from HCl-HNO₃-GAC (Figure 3.37), the results were compared with Fe-S-N/AC raw-GAC and Fe/AC from HCl-HNO₃-GAC reported in Table 3.18. Fe-S-N/AC HCl-HNO₃ catalyst has 100% phenol conversion as the raw catalyst. In comparison to Fe/AC HCl-HNO₃, where phenol conversion was 80%, S and N enhanced catalytic activity. Additionally, residual intermediates results confirmed that S and N doping increased catalytic activity (phenol conversion and residual intermediates), HCl-HNO₃ and raw Fe-S-N/AC did not show a significant difference. However, residual intermediates decreased significantly from 80% with Fe/AC HCl-HNO₃ to 30% with S and N doping. H₂O₂ consumption was compatible with the catalytic activity results and did not differ between Fe-S-N/AC, either raw or pre-treated catalysts (80%), but slightly increased in comparison to Fe/AC (65%). Fe leaching was lowest for Fe-S-N/AC HCl-HNO₃ at 15%, which was significantly lower than raw catalysts at 40%, but there was no difference if compared to Fe/AC catalysts. It should also be noted that the decrease of leaching paired with a decrease in catalyst activity is contrary to Fe-S-N/AC HCl-HNO₃. These results indicated that pre-acid treatment with HCl-HNO₃ and S and N increased catalytic activity and decreased metal leaching.

Table 3.18: Comparative analysis of Fe-S-N/AC raw-GAC Fe-S-N/AC from HCl-HNO₃-GAC, and Fe/AC from HCl-HNO₃-GAC

	Fe-S-N/AC from raw- GAC	Fe-S-N/AC from HCl-HNO₃-GAC	Fe/AC from HCl- HNO₃-GAC
Phenol conversion% ± 5	100	100	80
CMB% ± 5	30	30	85
H ₂ O ₂ consumption% ± 3	77	80	65
Fe leaching% ± 1	40	15	18

The catalytic activity of Fe-S-N/AC from HCl-HNO₃-SA2 (Figure 3.37) was compared with the Fe-S-N/AC raw-SA2 and Fe/AC from HCl-HNO₃-SA2, as shown in Table 3.19. Fe-S-

N/AC from HCl-HNO₃-SA2 has full phenol conversion as the raw catalyst and is compared with the Fe/AC from HCl-HNO₃, where the phenol conversion of 80% confirms the increased catalytic activity when doping S and N. Despite the residual intermediates increase from 12% to 29% for Fe-S-N/AC from HCl-HNO₃ compared with the raw catalysts, it was significantly lower (that is, more mineralization) if compared with catalysts without doping S and N 75%. Compared to Fe/AC, Fe-S-N/AC consumption of H₂O₂ compatible with catalyst activity was not different, whether the catalysts were raw or pre-treated. The Fe leaching for Fe-S-N/AC HCl-HNO₃ was 30%, which was significantly lower than raw catalysts at 80%. Contrary to Fe-S-N/AC HCl-HNO₃, the decrease in Fe leaching at Fe/AC appeared to be paired with a decrease in catalyst activity. In summary the result of the pre-acid treatment with HCl-HNO₃ and S and N, is: an increased catalytic activity followed by a simultaneous decrease of the Fe leaching, which is exactly one of the major aims of this research project.

Table 3.19: Comparative analysis of Fe-S-N/AC from raw-SA2, Fe-S-N/AC from HCl-HNO₃-SA2, and Fe/AC from HCl-HNO₃-SA2

	Fe-S-N/AC from raw-SA2	Fe-S-N/AC from HCl-HNO₃-SA2	Fe/AC from HCl- HNO₃-SA2
Phenol conversion% ± 5	100	100	80
CMB% ± 5	12	29	75
H ₂ O ₂ consumption% ± 3	75	72	86
Fe leaching% ± 1	80	30	20

As a way to assess the catalytic activity of Fe-S-N/AC from HCl-HNO₃-G60 (Figure 3.37), comparisons were made with Fe-S-N/AC raw-G60 and Fe/AC from HCl-HNO₃-G60 as shown in Table 3.20. Fe-S-N/AC from HCl-HNO₃ has 100% phenol conversion, which was increased in comparison with both Fe-S-N/AC raw-G60 and Fe/AC from HCl-HNO₃ catalysts 80%. residual intermediates results were also significantly decreased with Fe-S-N/AC from HCl-HNO₃ catalyst relative to others from 61-70% to 15%. H₂O₂ consumption was compatible with the phenol degradation, and there was no significant difference between all catalysts. Fe leaching dropped to 10% with Fe-S-N/AC from HCl-HNO₃ compared to the raw catalysts 50%, while there was no difference from the Fe/AC from HCl-HNO₃; however, there was a decrease in the leaching and catalytic activity in contrast with the Fe-S-N/AC from HCl-HNO₃ catalyst.

Based on these results, catalytic activity increased, and iron leaching decreased by pre-acid treatment and doping S and N.

Table 3.20: Comparative analysis of Fe-S-N/AC from raw-G60, Fe-S-N/AC from HCl-HNO₃-G60, and Fe/AC from HCl-HNO₃-G60

	Fe-S-N/AC from raw-G60	Fe-S-N/AC from HCl-HNO₃-G60	Fe/AC from HCl-HNO₃-G60
Phenol conversion% ± 5	83	100	80
CMB% ± 5	61	15	70
H ₂ O ₂ consumption% ± 3	65	77	70
Fe leaching% ± 1	50	10	15

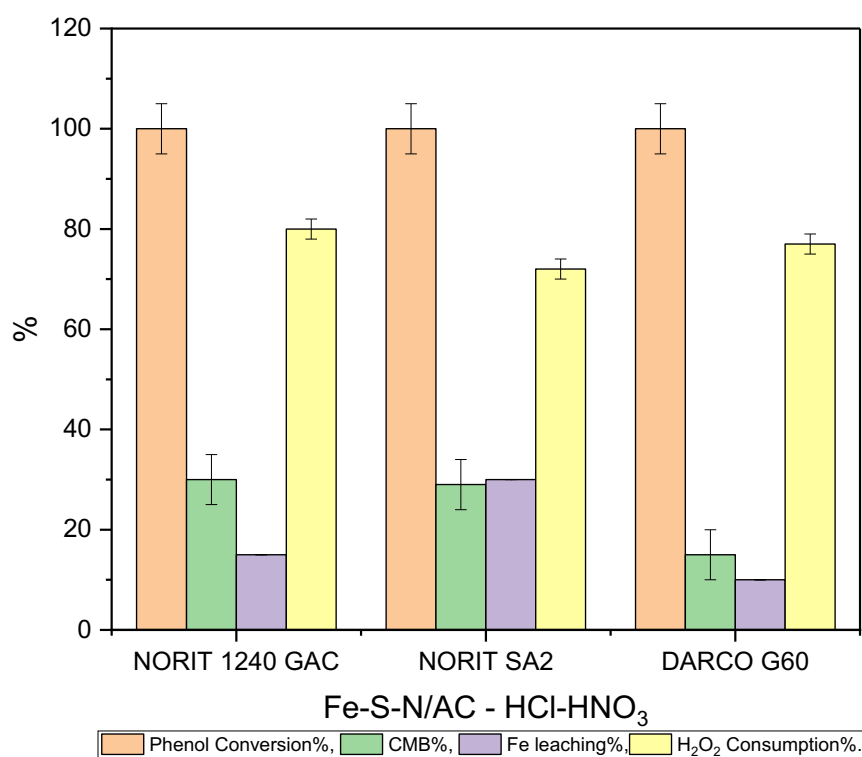


Figure 3.37: Catalytic activity, in terms of phenol conversion, CMB, Fe leaching and H₂O₂ consumption result for phenol oxidation by CWPO, using three types of Fe-S-N/AC catalysts prepared from HCl- HNO₃ -AC (GAC, SA2, G60). All catalysts have 12 wt% Fe loading (the leaching is a relative leaching% with respect to the total Fe content). 4 h reaction time at 80 °C and 1:100 M:S.

B. Elemental analysis for HCl-HNO₃-AC

Comparing the HCl-HNO₃-AC without Fe species doping, there was no significant difference in S mol% between all ACs (0.001 mol%). According to Figure 3.38, tri-doped AC catalysts with S, N, and Fe have significantly higher S mol% than other Fe/AC catalysts, starting from near zero and increasing to 0.01 mol%, so they were expected to prevent Fe leaching more than other catalysts (Fe/AC) and increase catalytic activity. These results validate Tables 3.18, 3.19 and 3.20 results.

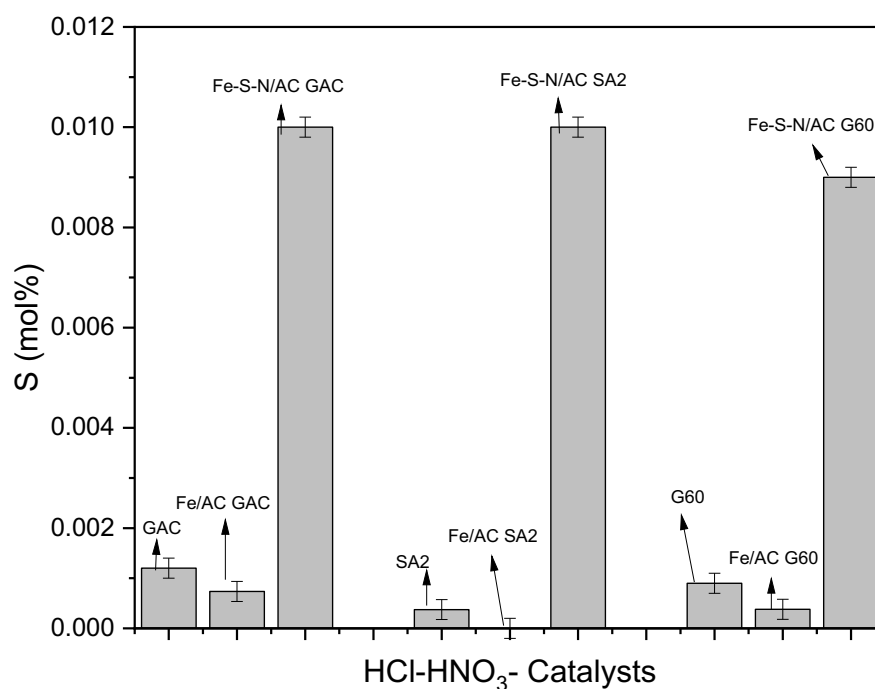


Figure 3.38: Elemental analysis results by mol% for S in the HCl-HNO₃-AC (GAC, SA2, G60) and their catalysts.

Table 3.21: Comparative analysis of Fe-S-N/AC and Fe/AC from HCl-HNO₃-AC catalysts in terms of Fe:S and Fe:O molar ratio

	Fe:S mol	Fe:O mol
Fe/ HCl-HNO ₃ -GAC	34	0.08
Fe/ HCl-HNO ₃ -SA2	n. a.*	0.12
Fe/ HCl-HNO ₃ -G60	34	0.1
Fe-S-N/ HCl-HNO ₃ -GAC	2	0.12
Fe-S-N/ HCl-HNO ₃ -SA2	2	0.03
Fe-S-N/ HCl-HNO ₃ -G60	2	0.18

- n.a. = not applicable (no S detectable).

Table 3.21 shows the Fe:S molar ratio for Fe-S-N/AC and Fe/AC catalysts; it is clear that the doping by S significantly improve the Fe:S mol%, by decreasing the molar ratio, than Fe/AC catalysts (from 34 to 2 mol). The greater the S doping the smaller the ratio. It was therefore expected that these catalysts would prevent Fe leaching and increase catalytic activity. These were approved by the catalytic activity results and iron leaching illustrated above in Tables 3.18, 3.19 and 3.20. On the contrary, for Fe:O, this is always (and by far) smaller than 1, so there is a large excess of O available to bind to Fe.

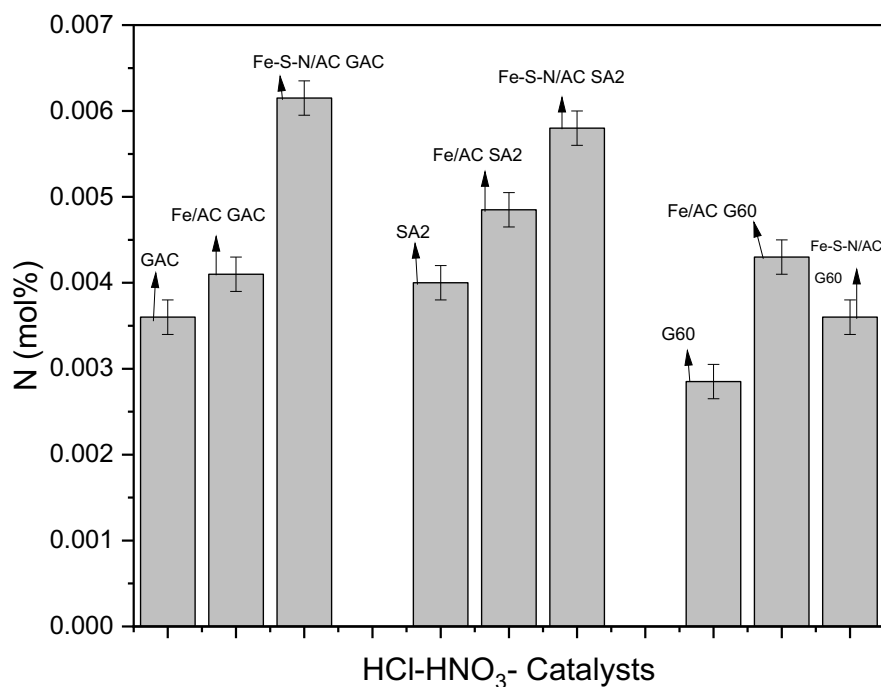


Figure 3.39: Elemental analysis results by mol% for N in the HCl-HNO₃-AC (GAC, SA2, G60) and their catalysts.

Based on these results, the N mol% for all HCl-HNO₃-AC in Figure 3.39 is slightly greater than the N mol% for AC without treatment in Figure 3.27, for GAC-HCl-HNO₃ N mol% raised from 0.001 to 0.0036 mol%, SA2-HCl-HNO₃ from 0.002 to 0.004 mol% and for G60-HCl-HNO₃ from 0.0028 to 0.003 mol%. For Fe-S-N/AC N increased their N mol% for all catalysts; however, Fe/AC and Fe-S-N/AC by G60 showed no significant difference. As explained different batch of the same AC could contain different metals and the raw-AC framework has initially some N that were detected previously for this result, which could explain the unsteady proportion of N mol% between the HCl-HNO₃-ACs and catalysts for G60. In this study, there was no clear trend supporting the second hypothesis of doping N.

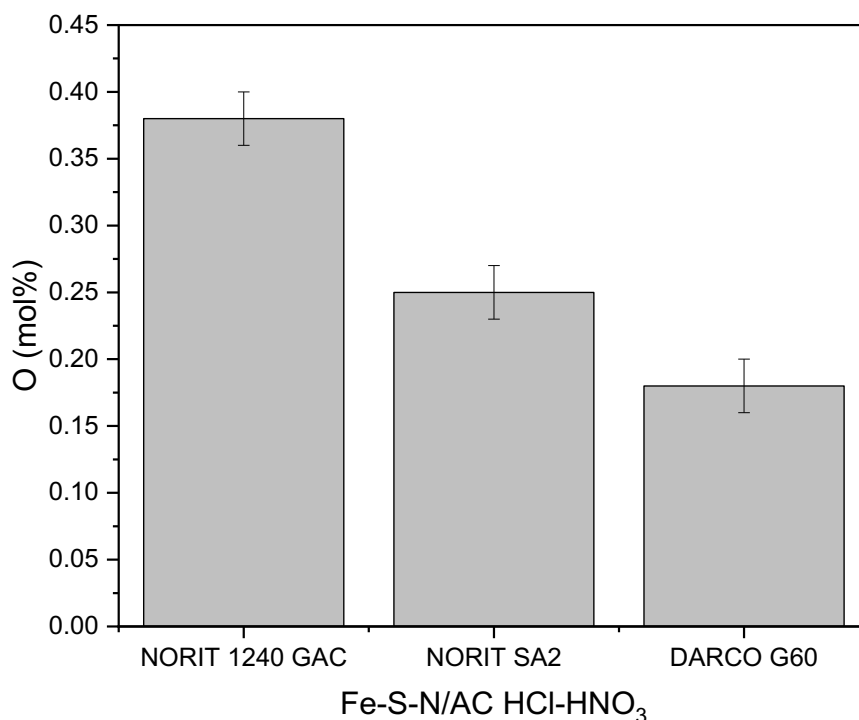


Figure 3.40: Elemental analysis results by mol% for O in the Fe-S-N/AC HCl-HNO₃-AC (GAC, SA2, G60) catalysts.

There is no significant difference in O mol% between the data reported Figure 3.40 and Figure 3.28 at Fe-S-N/ACs from raw-ACs. Accordingly, if the HCl-HNO₃ treatment did not change the amount of O, but leaching decreased, this could indicate the possible formation of CO groups versus OH groups, with CO groups being a better binder (a full COOH would be even better, but in this case, the amount of O also increased).

3.3 Characterization

Different preparation methods were used to determine whether they affected the catalyst structure, both in terms of modifying the framework and in terms of the actual Fe deposition, apart from the elemental analysis reported so far, the catalysts were also characterized with a variety of tools, including BET to measure surface area, XPS to quantify and determine species

on the catalyst surface, and, XRD was used to determine if Fe-oxide clusters were formed and if they affected the structure of the carbon materials.

3.3.1 X-ray diffraction (XRD)

With the aim to gather information on the possible formation of Fe-oxide clusters following our catalyst preparation methods, powder XRD patterns were collected for selected and raw materials of catalysts are shown in Figures (3.41, 3.42, 3.43) for Fe/AC and Fe-S-N/AC catalysts by GAC, SA2 and G60, respectively. The typical diffraction peaks of carbon expected for the graphitic structure were observed at 26.5° from the catalysts. The 2θ angles at about 30.1° , 35.4° , 43.1° , 54.16° , 57.70° and 62.5° , assumed to be 90% of these peaks refer to the characteristic diffraction peaks of iron oxide (Fe_xO_y). These peaks for iron oxide corresponded to both (Fe_3O_4 PDF # 19-0629) and (Fe_2O_3 PDF # 39-1346).¹⁰⁰

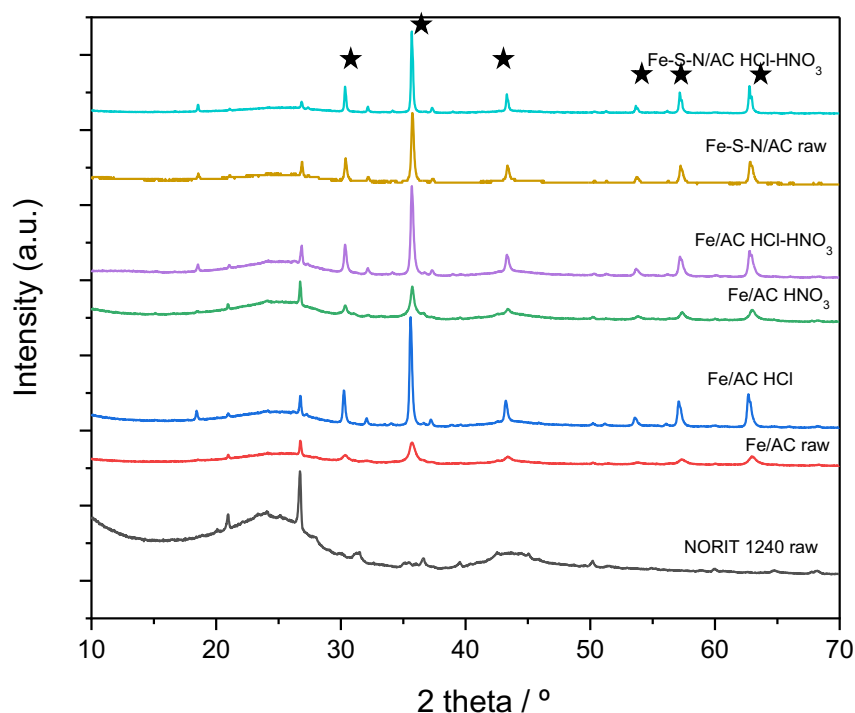


Figure 3.41: XRD patterns of different activated carbon (GAC) catalysts, including the raw material and support. All catalysts have 12 wt% Fe loading. (Where the black star for peaks of Fe-oxide).

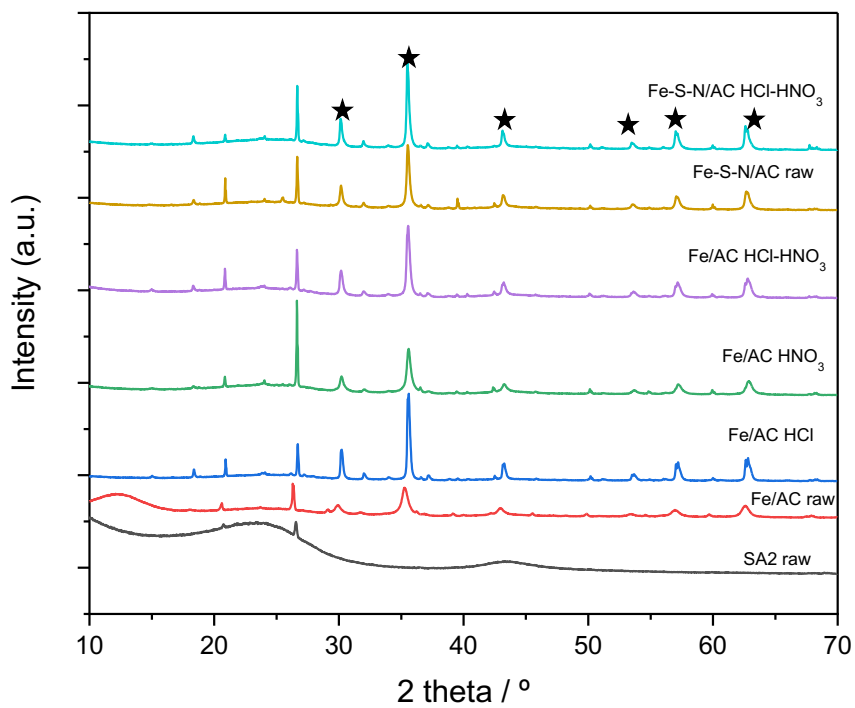


Figure 3.42: XRD patterns of different activated carbon (SA2) catalysts including the raw material and support. Fe loading fixed at 12 wt% for all catalysts. (Where the black star for peaks of Fe-oxide).

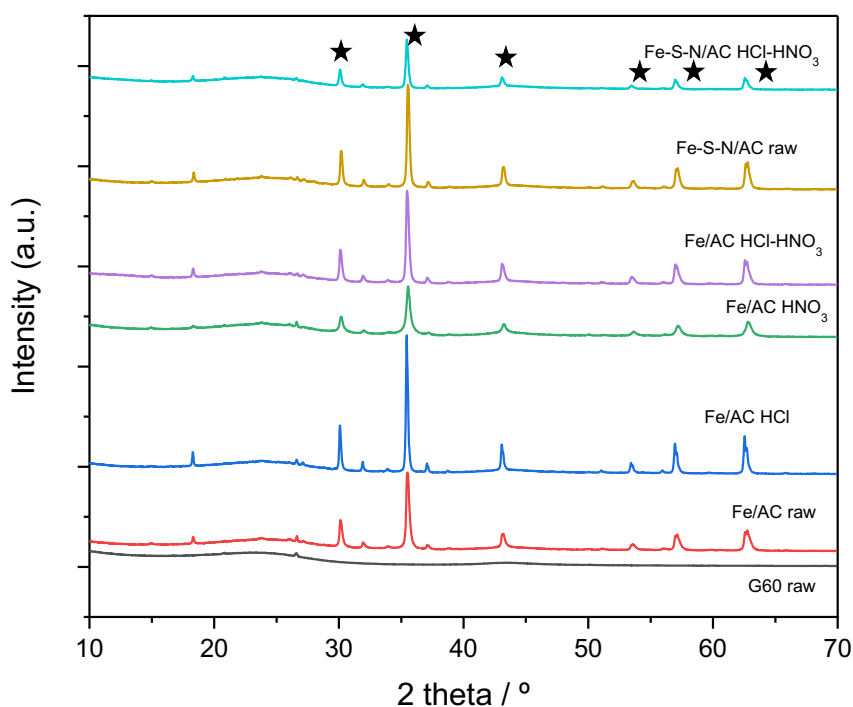


Figure 3.43: XRD patterns of different activated carbon (G60) catalysts including the raw material and support. The loading of Fe is 12wt% with all catalysts. (Where the black star for peaks of Fe-oxide).

According to the data reported in Table 3.22, it is clear that for all cases, the phase present in the higher amount, and probably also the one contributing to the catalytic activity, is Fe_2O_3 . This phase always contributes in excess of 50% of those capable of leading to a diffraction pattern. Then, in the presence of graphitic carbon, which might be naturally present or enhanced by acid treatment, small amounts of Fe_3O_4 in the range of ca. 3% are detected. Then other species that, according to the literature, could have formed, like CFe_3 , FeN , and FeS , are not detected, either meaning they are not present or they are not in a highly crystalline state to lead to a detectable signal. From the elemental analysis data, the first hypothesis is the most probable. For the catalysts prepared by GAC, the weight percentage of Fe_2O_3 ranging between 44 to 69%. Doping Fe in the raw AC (Fe/AC) catalyst has the highest Fe_2O_3 active species at 69%, while the lower active species belongs to Fe/AC catalysts prepared by AC pre-treated with HNO_3 at 44 %. Still, there was no difference in these active particles for other catalysts.

For catalysts prepared by SA2, the amount of Fe_2O_3 active phase ranges between 82% with Fe-S-N/AC (raw-AC) to 32% for Fe/AC by (HNO_3 -AC). The reduction in the percentage of Fe_2O_3 active phase in Fe/AC catalysts prepared by pre-treating AC with HNO_3 in both catalysts GAC and SA2 can be attributed to several factors: surface chemistry changes as HNO_3 is a strong oxidizing agent, and it can modify the surface chemistry of AC by introducing oxygen-containing functional groups (such as carboxyl, hydroxyl, and carbonyl groups) onto its surface. These functional groups can interact with the iron species, possibly leading to the formation of different iron compounds or complexes on the surface of the AC. These new surface groups can compete with the formation of Fe_2O_3 , reducing its percentage. In addition, the pre-treatment with HNO_3 can also alter the surface area and pore structure of the AC. Changes in these properties can affect the dispersion of Fe species on the carbon surface and influence the phase formation. A lower surface area or different pore structure may lead to less favourable conditions for the formation of Fe_2O_3 . Intriguingly, G60 catalysts have significantly higher amounts of Fe_2O_3 active phase than those prepared by other ACs. Active species ranged between 99% and 87%. This is in agreement with the catalytic activity results (see section 3.2.2.4, Figure 3.37) where the Fe-S-N/AC HCl- HNO_3 catalyst has higher catalytic activity in terms of residual intermediates% (15%) than others and simultaneously lower Fe leaching 10%.

Table 3.22: wt% of the phase below in the sample

Catalysts	Fe ₂ O ₃	Fe ₃ O ₄	C-graph	CFe ₃	FeN	FeS
GAC catalysts						
Fe/AC	69	< 1	31	0	0	0
Fe/AC (HCl)	63	2	35	0	0	0
Fe/AC (HNO ₃)	44	1	50	4	0	0
Fe/AC (HCl-HNO ₃)	61	2	37	0	0	0
Fe-S-N/AC	60	2	38	0	0	0
Fe-S-N/AC (HCl-HNO ₃)	65	3	22	0	0	0
SA2 catalysts						
Fe/AC	42	< 1	55	0	2	0
Fe/AC (HCl)	74	4	22	0	0	0
Fe/AC (HNO ₃)	32	< 1	65	0	2	0
Fe/AC (HCl-HNO ₃)	51	< 1	46	0	3	0
Fe-S-N/AC	82	2	12	0	5	0
Fe-S-N/AC (HCl-HNO ₃)	54	2	44	0	< 1	< 1
G60 catalysts						
Fe/AC	87	2.3	9.8	< 1	0	0
Fe/AC (HCl)	91	4.2	4.8	0	0	0
Fe/AC (HNO ₃)	99	1	< 1	0	0	0
Fe/AC (HCl-HNO ₃)	97	3	< 1	0	0	0
Fe-S-N/AC	97	3	< 1	0	0	0
Fe-S-N/AC (HCl-HNO ₃)	97	3	< 1	0	0	0

The lattice parameters obtained from X-ray diffraction (XRD) analysis provide valuable information about the crystal structure of a material, including the likely active species in the catalysts, Fe₂O₃. The lattice parameters provide the dimensions of the unit cell, which is the smallest repeating structural unit of the crystal. These dimensions include the lengths of the cell edges (*a*, *b*, *c*) as shown in the Table 3.23. These values can help determine the volume of the unit cell and the relative positions of the atoms within it. No actual change in crystal lattice parameters for Fe₂O₃ (as well as d-spacing) for all catalysts with different AC was 5 Å, implying no intercalation of hetero species in the Fe₂O₃ lattice.

Table 3.23: lattice parameters unit cell for Fe₂O₃ active phase.

Catalysts	a(Å)	b(Å)	c(Å)	V(Å ³)	d(Å)
GAC					
Fe/AC	8.354	8.354	25.117	1752 ± 2	5.91
Fe/AC (HCl)	8.394	8.394	25.209	1776 ± 2	5.94
Fe/AC (HNO ₃)	8.358	8.358	25.08	1751 ± 2	5.91
Fe/AC (HCl-HNO ₃)	8.39	8.39	25.213	1774 ± 2	5.93
Fe-S-N/AC	8.393	8.393	25.171	1773 ± 2	5.93
Fe-S-N/AC (HCl-HNO ₃)	8.398	8.398	25.205	1777 ± 2	5.94
SA2					
Fe/AC	8.34	8.34	25.126	1747 ± 2	5.90
Fe/AC (HCl)	8.366	8.366	25.187	1762 ± 2	5.92
Fe/AC (HNO ₃)	8.354	8.354	25.112	1752 ± 2	5.91
Fe/AC (HCl-HNO ₃)	8.356	8.356	25.16	1756 ± 2	5.91
Fe-S-N/AC	8.379	8.379	25.166	1766 ± 2	5.92
Fe-S-N/AC (HCl-HNO ₃)	8.389	8.389	25.183	1772 ± 2	5.93
G60					
Fe/AC	8.368	8.368	25.187	1763 ± 2	5.92
Fe/AC (HCl)	8.393	8.393	25.192	1774 ± 2	5.93
Fe/AC (HNO ₃)	8.352	8.352	25.094	1750 ± 2	5.91
Fe/AC (HCl-HNO ₃)	8.383	8.383	25.209	1771 ± 2	5.93
Fe-S-N/AC	8.377	8.377	25.198	1768 ± 2	5.92
Fe-S-N/AC (HCl-HNO ₃)	8.389	8.389	25.189	1772 ± 2	5.93

$$dA = \frac{k \cdot \lambda}{B \cdot \cos \theta} \text{The}$$

Table 3.24: Fe₂O₃ active phase particle size from Scherrer equation.

Catalysts	2- theta(°)	FHW(°)	Inst B(°)	d Å	Diameter(nm)
GAC					
Fe/AC	35	0.5	0.019	167	17
Fe/AC (HCl)	35	0.02	0.019	458	46
Fe/AC (HNO₃)	35	0.4	0.019	205	21
Fe/AC (HCl-HNO₃)	35	0.2	0.019	405	41
Fe-S-N/AC	35	0.1	0.019	745	75
Fe-S-N/AC (HCl-HNO₃)	35	0.1	0.019	878	88
SA2					
Fe/AC	35	0.5	0.019	145	15

Fe/AC (HCl)	35	0.08	0.019	1245	125
Fe/AC (HNO₃)	35	0.3	0.019	274	27
Fe/AC (HCl-HNO₃)	35	0.1	0.019	652	65
Fe-S-N/AC	35	0.2	0.019	366	37
Fe-S-N/AC (HCl-HNO₃)	35	0.2	0.019	316	32
G60					
Fe/AC	35	0.2	0.019	343	34
Fe/AC (HCl)	35	0.1	0.019	609	61
Fe/AC (HNO₃)	35	0.3	0.019	252	25
Fe/AC (HCl-HNO₃)	35	0.2	0.019	411	41
Fe-S-N/AC	35	0.2	0.019	479	48
Fe-S-N/AC (HCl-HNO₃)	35	0.2	0.019	451	45

An analysis of the relationship between the size of the particles and their catalytic activity is presented in the following Figures. Figure 3. 44 a) shows the correlation between phenol conversion and particle size. In general, smaller particles provide higher catalytic activity, as expected. Due to their large surface area, small nano-particles increase catalytic activity. It is possible to observe a broad correlation between Fe₂O₃ particle size and activity. The catalysts are active or more active for an estimated Fe₂O₃ particle size below 40 nm from 15 to 40 nm. Beyond this threshold, they were less active. Also, if below 40 nm, the H₂O₂ consumption does not change significantly (Figure 3. 44 b) show the correlation between H₂O₂ consumption and particles size. However, the residual intermediates does, for much smaller particle that is more mineralization (Figure 3.44 c) show the correlation between the residual intermediates and particle size. This means the leaching was a consequence of either low pH during the reaction or acidic intermediates due to the reaction, and not attack by H₂O₂. From the data in Figure 3.44 d) show the correlation between the Fe leaching and the particle size of catalysts, suggested that, the products of the final catalysts are carbon-dependent after all, means that the type of carbon catalyst used can significantly influence the outcomes or products of a chemical reaction. In our reaction, the choice of activated carbon can be crucial in determining the end result. The least leaching is for the G60 (pH 6.8); that the specific preparation method of the carbon catalyst may not be as critical as the choice of the right type of carbon. This means that regardless of how the catalyst is prepared, if it is G60 with a neutral pH and non-graphitic properties, it is effective in reducing leaching. That is, a neutral and non-graphitic carbon would

seem desirable because from the formation of an active Fe phase perspective. Conversely, as long as the carbon has limited graphite and is not basic, using N and S can reverse the leaching.

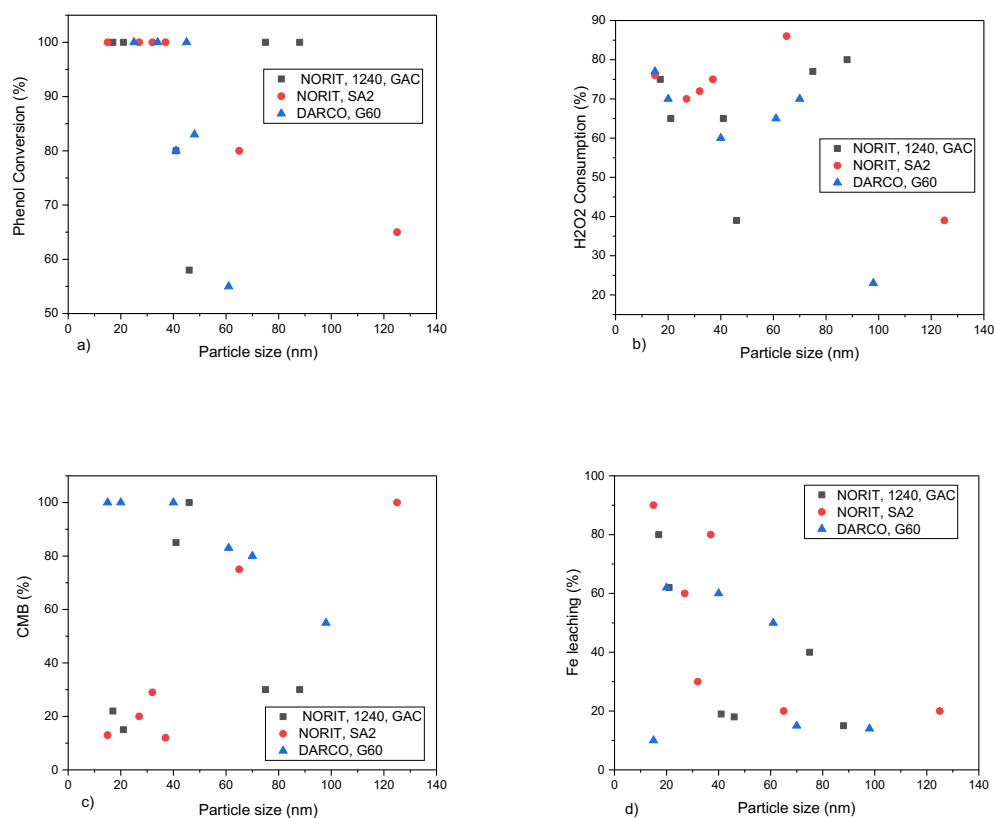


Figure 3. 44: a) The correlation between phenol conversion and the particle size of catalysts prepared by the three types of AC. b) The correlation between the H₂O₂ consumption and the particle size of catalysts. c) The

correlation between the CMB and the particle size of catalysts. d) The correlation between the Fe leaching and the particle size of catalysts.

3.3.2 X-ray photoelectron spectroscopy (XPS)

XPS was also used to gather information on the distribution of Fe species and other possible clusters not datable from XRD. In fact, XRD is a bulk method. This is important because, unless leaching phenomena are present, and in our case in part they are, it is only the metal of the surface of the support that is expected to be reactive and not the one in potentially deeper layers of the support or inside the porous of a microporous material.

From the data in Table 3.25, the samples have a large variation in surface Fe amount (that is Fe that dispersed on the surface of the carbon), which does not seem to correlate with the phenol conversion data in the Figure 3.45 a.

This lack of correlation can still be used for data interpretation. It means that it does not matter where Fe is located if on the surface of the catalyst or inside the pore; both it will react (or not react) in the same manner regardless of their location. This could also imply that the rate determining step of the reaction is the decomposition of H_2O_2 to form $\cdot OH$ radical that will attack phenol and not the attack of the radical to phenol.

It does worth noting though that While some surface iron species may be active for the catalytic conversion of phenol, others might be inert or less active. The nature of these species (Fe_2O_3 , Fe_3O_4 , iron oxides, or iron complexes) and their accessibility to reactants can vary and impact the catalytic activity differently. Even if the total surface iron content varies among samples, the distribution and availability of active catalytic sites on the surface can vary significantly. Some samples may have a higher concentration of accessible active sites, while others may have a lower concentration despite similar overall iron content.

In this context the surface area of the catalyst may vary among samples, affecting the number of active sites available for catalysis. A higher surface area could result in more active sites, leading to better catalytic performance, but this relationship isn't always straightforward. Various factors, including the reaction mechanism, surface interactions, and kinetics, can influence the conversion of phenol. These factors may not be accounted for in the XPS analysis but can impact the phenol conversion. There is also no correlation between surface iron and

leaching of Fe (Figure 3.45 b) still from the XRD data see section 3.3.1, there is correlation with particle size, leaching and activity.

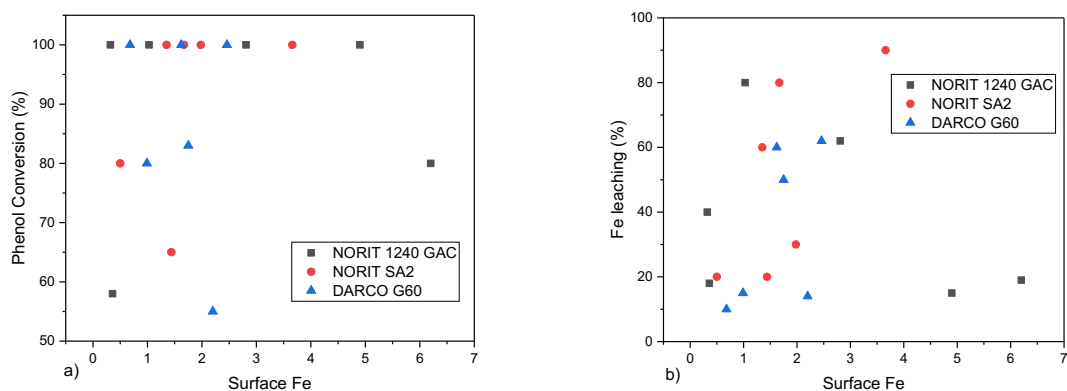


Figure 3. 45: a) XPS correlation between phenol conversion and surface Fe. b) Surface Fe and Fe leaching correlation.

Table 3.25: An XPS measurement of the atomic percentage (at%) of elements on catalyst surfaces.

Catalysts	C 1s	O 1s	Fe 2p	N 1s	S 2p
GAC					
Fe/AC	86	10	1	--	--
Fe/AC (HCl)	88	9	0.3	--	--
Fe/AC (HNO ₃)	83	12	2	--	--
Fe/AC (HCl-HNO ₃)	75	17	6	--	--
Fe-S-N/AC	86	9	0.3	0.4	1
Fe-S-N/AC (HCl)	88	7	0.8	0.5	1.7
Fe-S-N/AC (HNO ₃)	90	6	0.3	0.3	1.7
Fe-S-N/AC (HCl-HNO ₃)	78	13	4	0.8	2
SA2					
Fe/AC	69	21	3	--	--
Fe/AC (HCl)	85	11	1	0.4	--
Fe/AC (HNO ₃)	90	7	1	--	--
Fe/AC (HCl-HNO ₃)	92	6	0.5	0.5	--
Fe-S-N/AC	77	15	1.6	0.5	1.9
Fe-S-N/AC (HCl)	85	9	1.5	1	1.7
Fe-S-N/AC (HNO ₃)	85	10	1.7	0.9	1.5
Fe-S-N/AC (HCl-HNO ₃)	85	9	1.9	0.7	1.8
G60					
Fe/AC	90	7	1	--	--

Fe/AC (HCl)	88	8	2	--	--
Fe/AC (HNO₃)	88	8	2	--	--
Fe/AC (HCl-HNO₃)	91	7	0.9	0.5	--
Fe-S-N/AC	84	10	1.7	1	1.7
Fe-S-N/AC (HCl)	86	8	1	0.8	2
Fe-S-N/AC (HNO₃)	84	11	2	0.2	1.5
Fe-S-N/AC (HCl-HNO₃)	93	5	0.6	0.3	1.4

However, each time the carbon is treated with HCl, the amount of O surface decreases (experimental errors can easily affect this, though). This effect, however, suggests that HCl is actually dehydrating alcoholic groups, resulting in less oxygen and larger Fe₂O₃ particles (which are in line with hypotheses and XRD data), meaning less activity and less leaching. Regarding any effects of HNO₃, they are difficult to detect. From high-resolution data, there is often a tiny peak at 533.2 eV, which could correspond to a R- C = OO- R group as opposed to an R-O-R group. However, as can see from the catalytic data (see section 3.2.1.5), the effect on the reaction is minuscule. As shown in the table above, whenever the Fe-S-N/AC protocol is used, the carbon contains S and N, so the protocol is working however, the effect of this on the catalytic reaction seems to be negligible. It also seems that the catalysts treated with HNO₃ have the smallest Fe₂O₃ clusters, while the catalysts from the Fe-S-N/AC protocol have the least leaching. As a result, S reduces leaching. Therefore, surface S is helping to reduce leaching, but a compromise would be to reduce the carbon before this protocol. Catalysts are definitely low-oxidation Fe when they are prepared, but when they are analysed or used, they are Fe₂O₃.

3.3.3 Measurement of porosity

Table 3.26 displays the results of the textural and chemical properties of the support AC (G60) and the catalysts Fe-S-N/AC by (HCl-HNO₃). S_{BET} is often determined using gas adsorption techniques, such as nitrogen adsorption, and it provides information about the material's external and accessible internal surface area. The parent activated carbon G60 exhibited a high specific surface area (S_{BET}, 781 m².g⁻¹) and micropore surface area, micropores are very small pores with diameters less than 2 nm S_{micro} provides insight into the surface area within these tiny pores, (460 pore volume m².g⁻¹). The external surface area, the surface area of the material that is accessible from the outside, excluding the surface area within pores (321 m².g⁻¹). The total pore volume is (V_t, 0.42 cm³.g⁻¹) and the micropore volume is (0.21 cm³.g⁻¹). It was noted that Fe-S-N/AC catalyst showed a decrease in specific surface area (S_{BET}), micropore surface area (S_{micro}) and total pore volume (V_t) compared to G60. It is likely that these results were

caused by the N and S doping which resulted in blockages of the pores. Other studies have reported similar results.^{89, 104} Further, pre-treatment acids with HCl and HNO₃ for AC could affect both pore and surface areas, suggesting oxygen groups were introduced by modification of the surface.

Table 3.26: Porosimeter data of the Fe-S-N/AC catalysts prepared from G60 pre-treated with both acid HCl and HNO₃.

Sample	S _{BET} (m ² ·g ⁻¹) ^(a)	S _{micro} (m ² ·g ⁻¹) ^(a)	S _{ext} (m ² ·g ⁻¹) ^(a)	V _{tot} (cm ³ ·g ⁻¹) ^(b)	V _{micro} (cm ³ ·g ⁻¹) ^(b)
Raw-G60	781 ± 20	460 ± 22	321 ± 15	0.42 ± 0.05	0.21 ± 0.02
Fe-S-N/AC (G60- HCl/HNO ₃)	758 ± 22	430 ± 21	327 ± 16	0.35 ± 0.03	0.22 ± 0.02

(a) Values obtained from the adoption branch of the adsorption isotherms using Brunauer–Emmett–Teller (BET) theory.

(b) Value obtained at the absorption–desorption point using a Barret–Joyner–Halenda (BJH) method.

3.4 Diffusion control tests

As in heterogeneous catalytic systems, mass transfer limitations may occur, and if so, they are critical to reaction rates, conversion rates, and product (selectivity) formation, it was appropriate to verify whether diffusion (mass transfer) limitations were affecting our measurements or not. Catalysed reactions occur when reactant molecules come into contact with the active sites, which, in our case, are usually located within the pores of the catalyst, but they may also be present on the external surface. Thus, the catalytic reaction occurs when molecules react within a catalyst particle after diffusing through a fluid layer (external diffusion) and then through its pores (internal diffusion).

There are a number of processes that can affect the overall rate of heat and mass transfer between the fluid and the solid or inside the porous solid. Solid-catalyzed reactions are affected by transport limitations in the following ways: firstly, effects of mass transfer region one; external transport occurs when the reactant diffuses through the stagnant boundary layer surrounding a particle. Region two: internal transport, where the reactant diffuses into the pores of the particle. Secondly, the effects of heat transfer. However, in porous catalysts, internal molecule diffusion is highly dependent on the pore network's dimensions. Micropore: < 2 nm; changing the pore size to those typical of AC results in a dramatic decrease in diffusivity.

Furthermore, internal diffusion is more likely to occur with gas. This study does not expect to be affected by heat transfer as the application is in water which has a high heat capacity.¹⁰⁵⁻¹⁰⁸

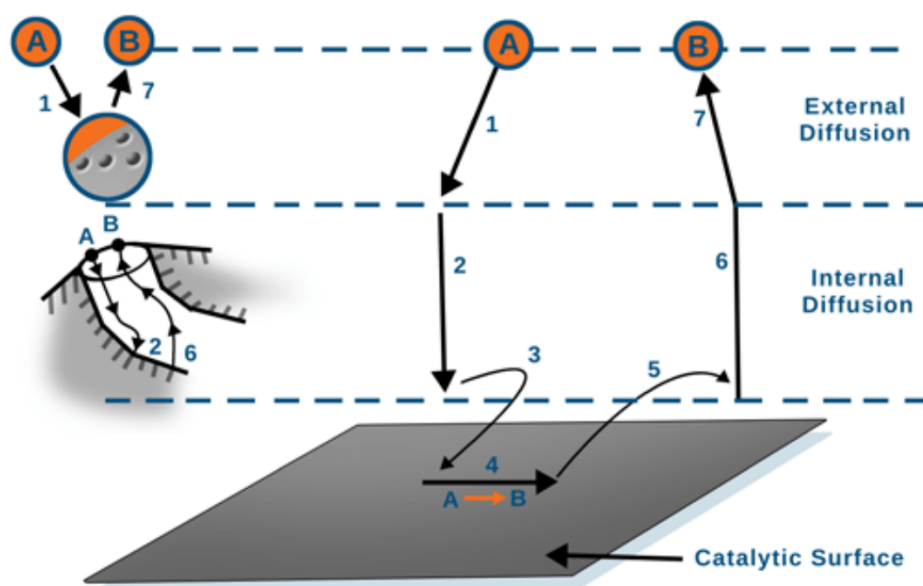


Figure 3.46: Catalytic reactions in heterogeneous systems. 1. The mass transfer (diffusion) of reactant(s) (e.g. species A) from the bulk liquid and a separate liquid film covering each particle of the catalyst to the surface of the catalyst particles. 2. The reactant diffuses from the pore mouth through the pores of the catalyst to the opposite side of the internal surface of the catalyst. 3. The adsorption of reactant A to catalyst surfaces. 4. Reaction on the catalyst surface (e.g. $A \rightarrow B$). 5. Release of the products (e.g. B) from the surface. 6. Diffusion of the products from the pellet interior to the pore mouth at the external surface. 7. Mass transfer of products from external pellet surfaces to bulk fluids.¹⁰⁵

3.4.1 External diffusion tests:

A. Using different stirring rates

There are two possible cases: firstly, the conversion increases per stirring rate increase. As mixing reduces diffusion, the reaction is affected by diffusion limitations (also known as diffusion regimes). Alternatively, diffusion could contribute (or even be) to the rate determining step of the process. Secondly, the conversion doesn't change per stirring rate

change. This means that diffusion phenomena do not apply, and the reaction rate is determined by the reaction at the surface (also known as the kinetic regime).

I. Fe-S-N/AC (AC1) (HCl-HNO₃):

According to Table 3.27, as the stirring rate changed, the conversion did not change. As a result, diffusion phenomena were irrelevant with Fe-S-N/AC from GAC pre-treated with HCl and HNO₃. However, while this doesn't change the conversion (that is, the attack of •OH to phenol), it does slightly change the CMB (that is, selectively). In other words, whereas the attack of •OH is not affected by diffusion, the mineralization is.

Table 3.27: External diffusion tests using the different the stirring rate for the Fe-S-N/AC from GAC pre-treated with HCl and HNO₃:

M:S	RMP/ min	Phenol conversion% ± 5	residual intermediates% ± 5
1:100	0	94	36
1:100	200	96	36
1:100	300	99	8
1:100	500	100	9
1:100	700	98	12

II. Fe-S-N/AC (SA2) (HCl-HNO₃):

According to Table 3.28, as the stirring rate changed, the conversion did not change. In addition, no effect on the residual intermediates. As a result, diffusion phenomena were irrelevant with Fe-S-N/AC from SA2 pre-treated with HCl and HNO₃. It is important to note that the two carbons are different, though; in general, the smaller the grains, the smaller (often) the diffusion limitation effect.

Table 3.28: External diffusion tests using the different the stirring rate for the Fe-S-N/AC from SA2 pre-treated with HCl and HNO₃:

M:S	RMP/ min	Phenol conversion% ± 5	residual intermediates% ± 5
1:100	0	98	15
1:100	200	98	9
1:100	300	99	8
1:100	500	100	2
1:100	700	100	5

III. Fe-S-N/AC (G60) (HCl-HNO₃)

According to Table 3.29, as the stirring rate increased, conversion increased. Mixing reduced diffusion, so diffusion limitation affected the reaction with Fe-S-N/AC from G60 pre-treated with HCl and HNO₃.

Table 3.29: External diffusion tests using the different the stirring rate for the Fe-S-N/AC from G60 pre-treated with HCl and HNO₃:

M:S	RMP/ min	Phenol conversion% ± 5	residual intermediates% ± 5
------------	---------------------	---------------------------------------	--

1:100	0	38	70
1:100	200	47	60
1:100	300	46	62
1:100	500	100	11
1:100	700	38	67

Diffusion phenomena were irrelevant with Fe-S-N/AC from GAC pre-treated with HCl and HNO₃. Although this does not change the conversion, the **residual intermediates** is slightly altered. Also, diffusion phenomena were irrelevant with Fe-S-N/AC from SA2 pre-treated with HCl and HNO₃. However, diffusion limitation influenced the reaction with Fe-S-N/AC by G60 pre-treated with HCl and HNO₃.

B. Using different M:S

There are two cases: firstly: the conversion increases per increase in the amount of catalyst: the reaction will be under a kinetic regime, kinetic laws can be determined, and it will be needed to determine the best amount of catalyst in terms of compromise considering the amount of catalyst and yield of the product. Secondly: the conversion doesn't change with increasing the catalyst amount. There are two possible explanations: (i) there's a diffusion limitation, or (ii) the conversion is already at 100% maximum. In this case, doubling the catalyst amount will not impact the conversion since it's already at maximum.

Fe-S-N/AC (GAC) (HCl-HNO₃):

According to Table 3.30, an increase in conversion is caused by increasing the amount of catalyst: the reaction was under a kinetic regime, kinetics law can be determined, and the best Fe-S-N/AC (GAC) (HCl-HNO₃) catalyst amount is 1:100 taking into account the amount of catalyst and yield of the product, and residual intermediates reached zero.

Table 3.30: External diffusion tests using the different M:S for the Fe-S-N/AC from GAC pre-treated with HCl and HNO₃:

M:S	RMP/ min	Phenol conversion% ± 5	residual intermediates% ± 5
-----	-------------	------------------------------	--------------------------------

0.1:100	500	28	79
0.5:100	500	58	54
1:100	500	100	9
15:100	500	100	0
20:100	500	100	0

II. Fe-S-N/AC (SA2) (HCl-HNO₃):

According to Table 3.31, an increase in conversion is caused by increasing the amount of catalyst: the reaction was under a kinetic regime, kinetics law can be determined, and the best Fe-S-N/AC (SA2) (HCl-HNO₃) catalyst amount is 1:100 taking into account the amount of catalyst and yield of the product also, residual intermediates significantly decreased to zero% considering the experimental error.

Table 3.31: External diffusion tests using the different M:S for the Fe-S-N/AC from SA2 pre-treated with HCl and HNO₃:

M:S	RMP/ min	Phenol conversion% ± 5	residual intermediates% ± 5
0.1:100	500	36	73
0.5:100	500	79	39
1:100	500	100	18
15:100	500	100	5
20:100	500	100	0

III. Fe-S-N/AC (G60) (HCl-HNO₃)

According to Table 3.32, an increase in conversion is caused by increasing the amount of catalyst: the reaction was under a kinetic regime, kinetics law can be determined, and the best Fe-S-N/AC (G60) (HCl-HNO₃) catalyst amount is 1:100 taking into account the amount of catalyst and yield of the product.

Table 3.32: External diffusion tests using the different M:S for the Fe-S-N/AC from G60 pre-treated with HCl and HNO₃:

M:S	RMP/ min	Phenol conversion% ± 5	residual intermediates% ± 5
0.1:100	500	10	90
0.5:100	500	28	75
1:100	500	100	12
15:100	500	97	6
20:100	500	100	0.3

From the interpretation of these data, catalytic tests are not affected by external diffusion limitations. As such, the reported data are validated and can be used.

3.5 Conclusion

Iron-doped activated carbon (Fe/AC) and iron, sulphur and nitrogen-tri-doped activated carbon (Fe-S-N/AC) were prepared using three different kinds of AC at different conditions, characterised and tested as catalysts or support for CWPO of phenol. Doping N and S improved the catalytic activity of activated carbon by increasing electron density on the surface. Besides, N and S dual-doped Fe/AC significantly enhanced its catalytic performance and prevented Fe leaching. With Fe-S-N/AC raw-GAC, phenol oxidation was 100% and 30% residual intermediates and reduced the iron leaching by 50% to 40% compared to Fe/AC raw-GAC. Doping S and N into raw-SA2 (Fe-S-N/AC raw-SA2) gives high catalytic activity at 100%

and 12% for phenol conversion and residual intermediates, respectively. However, compared to Fe/AC raw-SA2, there was no significant difference since the Fe leaching was still high at 80%. With the G60 catalysts adding S and N for Fe/AC raw-G60, the catalyst exhibited slightly reduced catalytic activity (phenol conversion reduced from 100% to 80%, and residual intermediates became 60% while was 40% with Fe/AC). Also, there was no difference in the Fe leaching results. Elemental analysis results for these catalysts show doping S significantly increased S mol% with all Fe-S-N/AC catalysts by different AC. Accordingly, the protocol successfully worked as expected. N mol% for these catalysts increased, but for GAC. However, there was no correlation between N mol% and H₂O₂ consumption, which does not agree with the second hypothesis doping N enhance H₂O₂ attacks (see section 3.2.1).

Pre-acid treatment with HCl, then doping S and N, for Fe-S-N/AC HCl-GAC shows increased catalytic activity than Fe/AC HCl-GAC (phenol oxidation from 55% rise to 88% as well residual intermediates reduced from 100% to 57%). Also, Fe leaching was 13%. HCl-SA2 catalysts did not show an effect by S and N doping. On the other hand, HCl-G60 indicated the enhancement of S and N on the catalytic activity of Fe-S-N/AC HCl-G60 catalysts. However, these catalysts did not reach the target full phenol oxidation and simultaneously maintain stability. Elemental analysis results detected a reduction in the O mol%, which was expected and explained as a dehydration process. The reduction in the catalytic activity, in general, is associated with catalysts prepared by HCl-AC, either Fe/AC or Fe-S-N/AC catalysts, interpreted via XRD results where the particle size of the active species was considerably large compared to others. Again, for these catalysts, S mol% dramatically increased, as N mol%, but for SA2, there was no correlation between H₂O₂ Consumption and N mol%.

Oxidation of AC using HNO₃ for Fe-S-N/AC HNO₃-GAC maintains high activity (full phenol conversion and 11% residual intermediates). Furthermore, it reduced leaching by 50% (from 63% to 50%). Fe-S-N/AC HNO₃-SA2 slightly decreased the activity for phenol conversion (from 100% for Fe/AC HNO₃-SA2 to 83% by Fe-S-N/AC HNO₃-SA2), but the leaching was 50% less (from 60-80% to 28%). Fe-S-N/AC HNO₃-G60 keeps the catalytic activity while dropping the leaching from 60% to 40% compared with Fe/AC HNO₃-G60. Elemental analysis results detected a significant increase in the S mol%, but there was no difference in the O mol%. Nevertheless, keeping the amount of O the same does not mean keeping the surface of the AC the same. Therefore, HNO₃ may not oxidize AC but C-OH to COOH, which appears better to bind Fe.

For all cases, XRD clearly shows that Fe_2O_3 is present in the highest amount and probably contributes to catalytic activity. The contribution of this phase to diffraction patterns is always greater than 50%. Then, when graphic carbon is present, either naturally or as a result of acid treatment, there is a small amount of Fe_3O_4 present in the range of ca. 3%. Furthermore, other species that, based on the literature, could exist, like CFe_3 , FeN , and FeS , have not been detected, suggesting that they are not present or are not crystalline enough to be detected. It appears that the first hypothesis is most likely based on the elemental analysis data. The weight percentage of Fe_2O_3 varies between 44 and 69% for catalysts prepared by GAC. Fe doping in raw AC (Fe/AC) catalyst has the highest Fe_2O_3 active species at 69%, while Fe/AC catalysts prepared by AC pre-treated with HNO_3 have the lowest active species at 44%. The amount of Fe_2O_3 active phase in catalysts prepared by SA2 varies from 82% with Fe-S-N/AC (raw-AC) to 32% with Fe/AC (HNO_3 -AC). G60 catalysts contain significantly more Fe_2O_3 active phase than other ACs. The percentage of active species ranged from 99 to 87%. It is consistent with the catalytic activity results showing that Fe-S-N/AC HCl- HNO_3 has higher catalytic activity (15% residual intermediates) and lower Fe leaching (10%) than others.

For all catalysts with different AC, the lattice parameters obtained from X-ray diffraction (XRD) show no change in crystal lattice parameters (as well as d-spacing) for Fe_2O_3 , indicating no intercalation of hetero species. Furthermore, it is clear that HCl pre-treatment does affect the intrinsic properties of the catalyst. HCl-AC with GAC, SA2 and G60 makes Fe_2O_3 particles larger 46, 125 and 61 nm for Fe/AC. Since no intercalation occurred, this implies that HCl operates a dehydration reaction on carbon, reducing Fe anchoring points and increasing Fe_2O_3 . In light of these results, it is easy to understand why these catalysts prepared by HCl-AC have low activity. HNO_3 had no discernible effect on the XRD pattern.

In the XPS data, the samples have a large variation in surface Fe amount (Fe dispersed on the carbon surface) that does not seem to correlate with phenol conversion. When the carbon is treated with HCl, the amount of O surface decreases. It is likely, however, that HCl dehydrates alcoholic groups, resulting in less oxygen and larger Fe_2O_3 particles (according to hypotheses and XRD data), resulting in less activity and less leaching. In terms of HNO_3 's effects, they are hard to detect. Based on high-resolution data. In spite of this, the catalytic data show that the effect is negligible. When the Fe-S-N/AC protocol is used, S and N are present in the carbon. Catalysts treated with HNO_3 also appear to have the smallest Fe_2O_3 clusters, while catalysts from Fe-S-N/AC have the least leaching. Therefore, S reduces leaching. This way, surface S reduces leaching, but reducing carbon before this protocol would be a compromise. When

catalysts are prepared, they are definitely low-oxidation Fe, but when they are analysed or used, they are Fe₂O₃.

Pre-acid treatments by both acids HCl and HNO₃ and doping S and N, Fe-S-N/AC HCl-HNO₃-AC1 expressed high catalytic activity (phenol conversion 100% and residual intermediates 30%). They reduced Fe leaching to the lowest level (15%) compared to other catalysts by GAC. Fe-S-N/AC HCl-HNO₃-SA2 gives 100% phenol oxidation and 29% residual intermediates and reduces the leaching to 30%. Fe-S-N/AC HCl-HNO₃-G60 confirmed these results, which showed complete phenol oxidation and high mineralization of 15% residual intermediates and only 10% Fe leaching. Consequently, it can be concluded by saying that the doped Fe-S-N/AC prepared by AC pre-acid treatments by HCl and HNO₃ catalysts were quite stable and more active for CWPO of phenol than Fe/AC. N and S atoms enhance catalytic performance. Fe-S-N/AC prepared by AC pre-acid treatments by HCl and HNO₃ catalysts were an effective and stable catalyst in the CWPO of phenol. As a result, it may be useful for treating phenol-containing wastewater.

3.6 References

1. A. Abdullah and K. E. O'Shea, *Journal of Photochemistry and Photobiology A: Chemistry*, 2019, **377**, 130-137.
2. F. C. Moreira, R. A. Boaventura, E. Brillas and V. J. Vilar, *Applied Catalysis B: Environmental*, 2017, **202**, 217-261.
3. Y. Yang, T. Chen, M. Sumona, B. S. Gupta, Y. Sun, Z. Hu and X. Zhan, *Reviews in Environmental Science and Bio/Technology*, 2017, **16**, 289-308.
4. P. Gao, Y. Song, M. Hao, A. Zhu, H. Yang and S. Yang, *Separation and Purification Technology*, 2018, **201**, 238-243.
5. T. W. Leal, L. A. Lourenço, H. d. L. Brandão, A. da Silva, S. M. G. U. de Souza and A. A. U. de Souza, *Journal of hazardous materials*, 2018, **359**, 96-103.
6. H. Li, J. Shang, Z. Yang, W. Shen, Z. Ai and L. Zhang, *Environmental Science & Technology*, 2017, **51**, 5685-5694.
7. P. Nidheesh, *Rsc Advances*, 2015, **5**, 40552-40577.
8. J. Bedia, V. Monsalvo, J. Rodriguez and A. Mohedano, *Chemical Engineering Journal*, 2017, **318**, 224-230.
9. R. S. Ribeiro, A. M. Silva, J. L. Figueiredo, J. L. Faria and H. T. Gomes, *Applied Catalysis B: Environmental*, 2016, **187**, 428-460.
10. M. Munoz, Z. M. De Pedro, J. A. Casas and J. J. Rodriguez, *Applied Catalysis B: Environmental*, 2015, **176**, 249-265.
11. S. Messele, C. Bengoa, F. Stüber, A. Fortuny, A. Fabregat and J. Font, *Desalination and Water Treatment*, 2016, **57**, 5155-5164.
12. M. R. Carrasco-Díaz, E. Castillejos-López, A. Cerpa-Naranjo and M. L. Rojas-Cervantes, *Microporous and Mesoporous Materials*, 2017, **237**, 282-293.
13. M. Munoz, Z. M. de Pedro, N. Menendez, J. A. Casas and J. J. Rodriguez, *Applied Catalysis B: Environmental*, 2013, **136**, 218-224.
14. Y. Yan, S. Jiang and H. Zhang, *Separation and Purification Technology*, 2014, **133**, 365-374.
15. Z. Wan and J. Wang, *Journal of Hazardous Materials*, 2017, **324**, 653-664.

16. L. R. Radovic and F. Rodriguez-Reinoso, *Chemistry & physics of carbon*, 1996, 261-376.
17. F. Rodriguez-Reinoso, *Carbon*, 1998, **36**, 159-175.
18. H. Marsh, E. A. Heintz and F. Rodríguez-Reinoso, *Introduction to carbon technologies*, Publicacions Universitat Alacant, 2018.
19. G. Centi, S. Perathoner, T. Torre and M. G. Verduna, *Catalysis Today*, 2000, **55**, 61-69.
20. M. Ren, X. Qian, M. Fang, D. Yue and Y. Zhao, *Research on Chemical Intermediates*, 2018, **44**, 4103-4117.
21. Z. Li and S. Dai, *Chemistry of materials*, 2005, **17**, 1717-1721.
22. B. Li, F. Dai, Q. Xiao, L. Yang, J. Shen, C. Zhang and M. Cai, *Energy & Environmental Science*, 2016, **9**, 102-106.
23. W. Kiciński, M. Szala and M. Bystrzejewski, *Carbon*, 2014, **68**, 1-32.
24. Y. Zhang and S.-J. Park, *Carbon*, 2017, **122**, 287-297.
25. H. Tamon and M. Okazaki, *Carbon*, 1996, **34**, 741-746.
26. H. P. Boehm, *Carbon*, 2002, **40**, 145-149.
27. P. Vinke, M. Van der Eijk, M. Verbree, A. Voskamp and H. Van Bekkum, *Carbon*, 1994, **32**, 675-686.
28. H. Valdés, M. Sánchez-Polo, J. Rivera-Utrilla and C. Zaror, *Langmuir*, 2002, **18**, 2111-2116.
29. C. A. Toles, W. E. Marshall and M. M. Johns, *Carbon*, 1999, **37**, 1207-1214.
30. D. Prahas, Y. Kartika, N. Indraswati and S. Ismadji, *Chemical Engineering Journal*, 2008, **140**, 32-42.
31. S. Wang and G. M. Lu, *Carbon*, 1998, **36**, 283-292.
32. C. Moreno-Castilla, F. Carrasco-Marin, E. Utrera-Hidalgo and J. Rivera-Utrilla, *Langmuir*, 1993, **9**, 1378-1383.
33. M. V. Lopez-Ramon, F. Stoeckli, C. Moreno-Castilla and F. Carrasco-Marin, *Carbon*, 1999, **37**, 1215-1221.
34. Y. El-Sayed and T. J. Bandoz, *Journal of colloid and interface science*, 2004, **273**, 64-72.
35. C. L. y Leon, J. Solar, V. Calemma and L. R. Radovic, *Carbon*, 1992, **30**, 797-811.
36. H. Boehm, *Carbon*, 1994, **32**, 759-769.
37. M. S. Shafeeyan, W. M. A. W. Daud, A. Houshmand and A. Shamiri, *Journal of Analytical and Applied Pyrolysis*, 2010, **89**, 143-151.

38. R. Arrigo, M. Hävecker, S. Wrabetz, R. Blume, M. Lerch, J. McGregor, E. P. Parrott, J. A. Zeitler, L. F. Gladden and A. Knop-Gericke, *Journal of the American Chemical Society*, 2010, **132**, 9616-9630.
39. E. Auer, A. Freund, J. Pietsch and T. Tacke, *Applied Catalysis A: General*, 1998, **173**, 259-271.
40. C. Prado-Burguete, A. Linares-Solano, F. Rodriguez-Reinoso and C. S.-M. De Lecea, *Journal of Catalysis*, 1989, **115**, 98-106.
41. C. Prado-Burguete, A. Linares-Solano, F. Rodriguez-Reinoso and C. S.-M. De Lecea, *Journal of Catalysis*, 1991, **128**, 397-404.
42. M. Román-Martínez, D. Cazorla-Amorós, A. Linares-Solano and C. S.-M. De Lecea, *Carbon*, 1993, **31**, 895-902.
43. A. Rehman, M. Park and S.-J. Park, *Coatings*, 2019, **9**, 103.
44. A. E. Aksoylu, M. M. A. Freitas and J. L. Figueiredo, *Applied Catalysis A: General*, 2000, **192**, 29-42.
45. W. Wen and S. Sun, *Separation Science and Technology*, 1981, **16**, 1491-1521.
46. A. Lau, D. Furlong, T. Healy and F. Grieser, *Colloids and surfaces*, 1986, **18**, 93-104.
47. K. Kinoshita, *Carbon: electrochemical and physicochemical properties*, Journal of the American Chemical Society, United States, 1988.
48. D. Fuerstenau, J. Rosenbaum and Y. You, *Energy & fuels*, 1988, **2**, 241-245.
49. J. Solar, *Carbon*, 1990, **28**, 369-375.
50. L. CALY and R. LR, *Chemistry and physics of carbon*, 1994, **24**, 213-310.
51. C. Moreno-Castilla, M. Ferro-Garcia, J. Joly, I. Bautista-Toledo, F. Carrasco-Marin and J. Rivera-Utrilla, *Langmuir*, 1995, **11**, 4386-4392.
52. C. Moreno-Castilla, F. Carrasco-Marín and A. Mueden, *Carbon*, 1997, **35**, 1619-1626.
53. C. Moreno-Castilla, F. Carrasco-Marin, F. Maldonado-Hodar and J. Rivera-Utrilla, *Carbon*, 1998, **36**, 145-151.
54. F. Carrasco-Marín, A. Mueden and C. Moreno-Castilla, *The Journal of Physical Chemistry B*, 1998, **102**, 9239-9244.
55. B. Puri, *Chemistry and physics of carbon*, 1970, **6**, 191-282.
56. M. López-Ramón, C. Moreno-Castilla, J. Rivera-Utrilla and R. Hidalgo-Alvarez, *Carbon*, 1993, **31**, 815-819.
57. J. Rivera-Utrilla, A. López-Peinado, C. Moreno-Castilla and J. D. López-Gonzalez, *Fuel*, 1987, **66**, 237-241.

58. J. P. Chen and S. Wu, *Langmuir*, 2004, **20**, 2233-2242.
59. J. Clayden, N. Greeves and S. Warren, *Organic chemistry*, Oxford university press, USA, 2012.
60. A. Tomita, O. Mahajan and P. Walker Jr, *Am Chem Soc Div Fuel Chem Prepr*, 1977, **22**, 4e6.
61. J. Parra, J. D. Sousa, R. C. Bansal, J. Pis and J. Pajares, *Adsorption Science & Technology*, 1995, **12**, 51-66.
62. C. Moreno-Castilla, M. Ferro-García, J. Joly and I. Bautista-Toledo, *Langmuir*, 1995, **11**, 4386-4392.
63. I. Kuzin, *Pascal and Francis Bibliographic Databases*, 1972, **45**, 1128-1130.
64. F. Carrasco-Marin, A. Mueden, T. A. Centeno, F. Stoeckli and C. Moreno-Castilla, *Journal of the Chemical Society, Faraday Transactions*, 1997, **93**, 2211-2215.
65. A. Gil, G. De la Puente and P. Grange, *Microporous Materials*, 1997, **12**, 51-61.
66. J. Choma, M. Jaroniec and W. Burakiewicz-Mortka, *Polish Journal of Chemistry*, 1998, **72**, 860-868.
67. J. Choma and M. Jaroniec, *Adsorption Science & Technology*, 1998, **16**, 295-302.
68. S. Barton, M. Evans, S. Liang and J. MacDonald, *Carbon*, 1996, **34**, 975-982.
69. J. Choma, W. Burakiewicz-Mortka, M. Jaroniec, Z. Li and J. Klinik, *Journal of colloid and interface science*, 1999, **214**, 438-446.
70. Y.-C. Chiang, P.-C. Chiang and E.-E. Chang, *Journal of environmental engineering*, 2001, **127**, 54-62.
71. K. Kinoshita, *Carbon: Electrochemical and Physicochemical Properties*, 1988, 316-350.
72. N. A. Zeid, G. Nakhla, S. Farooq and E. Osei-Twum, *Water Research*, 1995, **29**, 653-660.
73. F. J. DeSilva, *Water Conditioning & Purification*, 2001.
74. K. R. Crincoli, P. K. Jones and S. G. Huling, *Science of The Total Environment*, 2020, **734**, 139435.
75. S. Vanderheyden, R. Van Ammel, K. Sobiech-Matura, K. Vanreppelen, S. Schreurs, W. Schroeyers, J. Yperman and R. Carleer, *Journal of Radioanalytical and Nuclear Chemistry*, 2016, **310**, 301-310.
76. S. PAP, V. Bežanović, M. Novaković, D. Adamović, I. Mihajlović, M. ĐOGO, A. Babić, S. Šarić, J. Radonić and M. T. Sekulić, *Acta Technica Corviniensis-Bulletin of Engineering*, 2017, **10**.

77. M. Elazabi, B. Draskovic, M. Novakovic, I. Mihajlovic and A. Hgeig, *FEB FRESENIUS ENVIRONMENTAL BULLETIN*, 2021, 1030.
78. A. Hgeig, University of Novi Sad (Serbia), 2020.
79. P. Casella, D. Musmarra, S. Dimatteo, S. Chianese, D. Karatza, S. Mehariya and A. Molino, *Chem. Eng. Trans*, 2020, **79**, 295-300.
80. <https://www.chembk.com/en/chem/ACTIVATED%20CARBON%20DARCO%20G-60>, (accessed date March 2023).
81. A. El-Wakil, W. Abou El-Maaty and F. Awad, *J Anal Bioanal Tech*, 2014, **5**, 1-14.
82. P. Rumbach, D. M. Bartels and D. B. Go, *Plasma Sources Science and Technology*, 2018, **27**, 115013.
83. A. Georgi and F.-D. Kopinke, *Applied Catalysis B: Environmental*, 2005, **58**, 9-18.
84. M. Conte, A. F. Carley, C. Heirene, D. J. Willock, P. Johnston, A. A. Herzing, C. J. Kiely and G. J. Hutchings, *Journal of catalysis*, 2007, **250**, 231-239.
85. M. Conte, A. F. Carley and G. J. Hutchings, *Catalysis Letters*, 2008, **124**, 165-167.
86. C. Zhou, PhD thesis, University of Sheffield, 2021.
87. C. A. Wilde, Y. Ryabenkova, I. M. Firth, L. Pratt, J. Railton, M. Bravo-Sanchez, N. Sano, P. J. Cumpson, P. D. Coates and X. Liu, *Applied Catalysis A: General*, 2019, **570**, 271-282.
88. R. Ferrando, J. Jellinek and R. L. Johnston, *Chemical reviews*, 2008, **108**, 845-910.
89. H. Qin, R. Xiao and J. Chen, *Science of the Total Environment*, 2018, **626**, 1414-1420.
90. G. Yang, S. Mo, B. Xing, J. Dong, X. Song, X. Liu and J. Yuan, *Environmental Pollution*, 2020, **258**, 113687.
91. S. Messele, O. Soares, J. Órfão, F. Stüber, C. Bengoa, A. Fortuny, A. Fabregat and J. Font, *Applied Catalysis B: Environmental*, 2014, **154**, 329-338.
92. P. Johnston, N. Carthey and G. J. Hutchings, *Journal of the American Chemical Society*, 2015, **137**, 14548-14557.
93. Y. Yao, H. Chen, C. Lian, F. Wei, D. Zhang, G. Wu, B. Chen and S. Wang, *Journal of hazardous materials*, 2016, **314**, 129-139.
94. H. Tan, J. Liu, G. Huang, Y. Qian, Y. Deng and G. Chen, *ACS Applied Energy Materials*, 2018, **1**, 5599-5608.
95. X. Cheng, H. Guo, Y. Zhang, Y. Liu, H. Liu and Y. Yang, *Journal of colloid and interface science*, 2016, **469**, 277-286.

96. M. Pu, Y. Ma, J. Wan, Y. Wang, M. Huang and Y. Chen, *Journal of colloid and interface science*, 2014, **418**, 330-337.
97. C. Wang, Q. Yang, Z. Li, K.-Y. A. Lin and S. Tong, *Separation and Purification Technology*, 2019, **213**, 447-455.
98. Y. Yang, X. Zhang, Q. Chen, S. Li, H. Chai and Y. Huang, *Acs Omega*, 2018, **3**, 15870-15878.
99. T. Zeng, S. Li, J. Hua, Z. He, X. Zhang, H. Feng and S. Song, *Science of the Total Environment*, 2018, **645**, 550-559.
100. H. Zhao, Y. Wang, Y. Wang, T. Cao and G. Zhao, *Applied Catalysis B: Environmental*, 2012, **125**, 120-127.
101. J. Li, H. Dahn, L. Krause, D.-B. Le and J. Dahn, *Journal of the Electrochemical Society*, 2008, **155**, A812.
102. M. F. Al-Hakkani, G. A. Gouda and S. H. Hassan, *Heliyon*, 2021, **7**.
103. A. Patterson, *Physical review*, 1939, **56**, 978.
104. A. Rey, A. Bahamonde, J. Casas and J. Rodríguez, *Water Science and Technology*, 2010, **61**, 2769-2778.
105. R. Klaewkla, M. Arend and W. F. Hoelderich, *A review of mass transfer controlling the reaction rate in heterogeneous catalytic systems*, INTECH Open Access Publisher Rijeka, 2011.
106. N. L. Smith and N. R. Amundson, *Industrial & Engineering Chemistry*, 1951, **43**, 2156-2167.
107. T. K. Sherwood, *Pure and Applied Chemistry*, 1965, **10**, 595-610.
108. D. Weber, A. J. Sederman, M. D. Mantle, J. Mitchell and L. F. Gladden, *Physical chemistry chemical physics*, 2010, **12**, 2619-2624.

Chapter 4: Iron-doped zeolites ZSM-5 and Y for phenol oxidation via CWPO

4.1 Introduction

The main objective of this part of the project is to produce and improve the well-known Fe-ZSM-5 catalysts to be durable catalysts with high catalytic activity (complete phenol conversion) for phenol oxidation by CWPO reaction. In this context, with reusability and durability, we mean a material that can be reused about 5 times. Although this is not a convention, it is common practice for this and other catalytic studies^{1,2} This chapter moves from activated carbon (AC) as catalyst support for Fe species to zeolites. Both are well-known supports and widely used for water treatment applications.³⁻⁶ ACs are frequently employed as supports for heterogenous, solid catalysts in the CWPO method for phenol oxidation,⁷⁻¹⁰ because of their features, for example, a large surface area ($800-1200 \text{ m}^2 \cdot \text{g}^{-1}$), large pore size around ($0.9-1.3 \text{ mL} \cdot \text{g}^{-1}$) as well as the low cost,¹¹ which have been comprehensively discussed in the present thesis work (see the entire chapter 3). Compared to zeolites, ACs are also cheaper (1 kg of AC costs approximately 60-80 £, while the same amount of zeolite ranges between 500 £ and 700 £). On the other hand, despite the many advantages of AC reported both in this thesis work (Chapter 3) and the specialized literature, zeolites are, generally speaking, more reusable than AC, as they suffer from a much lower batch-to-batch reproducibility during manufacturing, unlike ACs which although undergoing synthetic treatments they all start from natural products caused by varying structures of carbon precursors.¹² As discussed, in part, in Chapter 3, ACs may already contain some metal residue; therefore, if not pre-treated, it is likely that a particular batch of carbon may behave differently, meaning that the batch may perform very well for an application under consideration, while another set may behave differently. In addition, zeolites also have a large surface area, typically between 500 to 800 $\text{m}^2 \cdot \text{g}^{-1}$.¹³ A textual parameter that, generally increases the catalytic activity.¹² By virtue of these properties, under mild working conditions, the system using Fe-ZSM-5 zeolite with MFI structure achieved total elimination of phenol and significant removal of total organic carbon (TOC). Furthermore, Fe-ZSM-5 remains active after repeated runs. Besides that, zeolites have a

microporous structure.¹⁴ A strong acidity is another advantage of zeolites for a large class of reactions; like alkane conversion¹⁵ and fructose dehydration reaction,¹⁶ have Bronsted and Lewis acid sites, typically hydroxyl groups and unsaturated cations, respectively. In some cases, both Bronsted and Lewis acidity can predominate, depending on the chemical reaction, the crystal structure, the post-synthesis treatment, as well as the state of hydroxylation below the reaction circumstance. The acidity properties of zeolites play a crucial role in their catalytic activity for phenol oxidation using CWPO. The catalytic activity of zeolites in this reaction is may dependent on the presence and strength of acid sites within the zeolite framework. Zeolites possess Bronsted acid sites (protonic acid sites) and Lewis acid sites (non-protonic acid sites). These acid sites can act as active centres for the adsorption of phenol and the activation of hydrogen peroxide. The presence of Bronsted acid sites in zeolites can facilitate the activation of H₂O₂, generating [•]OH. In addition, phenol molecules can be adsorbed onto the surface of zeolites through interactions with the acid sites. The adsorbed phenol molecules are then more accessible to the activated hydrogen peroxide species, promoting the phenol oxidation reaction. The type and strength of the acid sites can influence the reaction pathways and selectivity of the phenol oxidation reaction. Different acid sites may lead to the formation of different intermediate species, affecting the overall reaction results. To determine the correlation between zeolites' acidity properties and their catalytic activity, it must provide information about their acidic sites' quantity, nature, location, and strength.¹⁷ Also, hydrophobic and hydrophilic properties can be adjusted by controlling zeolite's Si:Al ratio. For example, high Si:Al zeolites are relatively hydrophilic; these Si-rich zeolites demonstrate excellent performance for carbon dioxide capture in moist atmospheres.¹⁸ The other benefits include their availability and environmentally safe materials.¹⁹ Therefore, thanks to their unique properties, zeolites have received much attention as support or heterogeneous catalysts or as catalysts themselves. Zeolite Y, for instance, plays an essential role in heterogeneous catalysis, like, catalytic cracking.^{20,21} Also, ZSM-5 is a promising catalyst for the wet oxidation of phenol by H₂O₂ in the Fenton reaction.^{14, 22-24}

A zeolite with ten oxygen rings usually has a sizeable crystalline framework which means that it has a relatively large and well-defined structure composed of interconnected tetrahedral units (the zeolite crystals are relatively large in size, which can be advantageous for certain applications. Larger crystals may provide better mechanical stability and ease of handling during industrial processes), exhibiting other essential properties, such as its high activity and hydrothermal stability. From the family of oxygen ring zeolites with 10 members, the MFI type

ZSM-5 zeolite probably has the most significant application.²⁵ Incorporating the ZSM-5 framework with atoms other than Si and Al can significantly alter the catalytic and acid-base properties.²⁶⁻²⁹ In most of these reactions, the reactivity of Fe-ZSM-5 catalysts is caused by the presence of particular extra framework iron-containing cationic species within the micropores of ZSM-5 zeolite or on the external surface of the zeolite crystals.³⁰ In other words, the extra-framework iron species in Fe-ZSM-5 can include: Iron oxides, such as Fe₂O₃ (hematite), can form on the external surface of the zeolite or within its pores. These iron oxides may act as active sites for specific catalytic reactions. Some iron ions may aggregate and form dinuclear iron sites, where two iron ions are in close proximity to each other. These dinuclear iron sites can exhibit unique catalytic properties. Iron oxyhydroxide species, such as FeOOH (goethite) or Fe(OH)₃ (ferrihydrite), may aggregate and form clusters on the zeolite surface. These oxyhydroxide clusters can also contribute to the catalytic activity of Fe-ZSM-5.^{31, 32} However, the nature of the active sites for the different reactions that Fe-ZSM-5 catalyses is still debatable.

As mentioned, transition metal zeolites are among the most efficient CWPO catalysts.³³⁻³⁶ Several studies have examined the properties of ZSM-5 zeolites containing Fe.^{23, 37-42} Over a wide pH range, these catalysts are highly efficient at oxidising organic substrates with hydrogen peroxide. Several studies have shown that Fe improves zeolite's ability to catalyse organic oxidation, and the synthesis procedure of Fe-zeolite can affect its catalytic activity.^{42, 43} According to the literature, Fe-zeolite activity and hydrothermal stability (Hydrothermal stability, in the context of Fe-zeolites, refers to the ability of the material to maintain its structure and performance under high-temperature and high-pressure conditions in the presence of water. A hydrothermally stable Fe-zeolite would demonstrate minimal degradation or structural changes when exposed to elevated temperatures and pressures in the presence of water. The stability is essential for maintaining the catalytic activity of the material over extended periods, as well as for preventing structural collapse or loss of performance during practical applications), these properties are affected by several factors, such as: (i) zeolite topology, (zeolite topology refers to the specific arrangement and connectivity of atoms within the framework structure of a zeolite mineral. Zeolites are crystalline aluminosilicates with a well-defined three-dimensional framework composed of interconnected tetrahedral units, usually involving silicon, aluminum, and oxygen atoms. The arrangement of these tetrahedral units determines the overall structure and porosity of the zeolite, which is critical to its unique properties and applications. It is often described in terms of its framework type, which is

assigned a specific code based on its crystal structure. The International Zeolite Association (IZA) has established a framework type classification system that assigns a three-letter code to each unique zeolite topology. For example, the most common natural zeolite, clinoptilolite, is designated as the framework type "CHA," while synthetic zeolites like ZSM-5 are identified as "MFI."), (ii) the synthesis method, (iii) the amount of metal dopant, and (iv) any post-synthesis treatment (are often performed to modify or enhance the properties of the material for specific applications for example ion exchange is a common post-synthesis treatment used to replace some of the cations within the zeolite framework with other cations). The catalyst may also contain a number of iron species and iron oxide clusters.⁴⁴ However, different iron species in the zeolite structure may have different activities based on their structure, location, and electronic environment.⁴⁵

The objective of this part of the work is to develop and apply zeolite-based catalysts, mainly based on Fe doping over ZSM-5 by:

(i) investigate the effects of different synthesis methods of Fe-ZSM-5 on their catalytic activity using different iron precursors, different forms of ZSM-5 (H-ZSM-5 and NH₄-ZSM-5) and varying iron loading. The criteria for assessment to determine the best catalyst from these changes in synthesis parameters is to compare these catalysts in terms of phenol conversion via CWPO.

(ii) to study the effect of different preparation methods, Fe-ZSM-5 was prepared by two different procedures, incipient wetness impregnation and vacuum impregnation methods. A comparative study of the structural characteristics was made between the two impregnated Fe-ZSM-5 catalysts, especially aimed at enhancing the durability (i.e. limiting leaching effects) of these materials.

(iii) S and N were doped with Fe-Zeolite with the aim of enhancing their stability and durability. In addition, ZSM-5 with different Si:Al molar ratios (23, 50, and 80), Zeolite-Y was also used.

(iv) investigate the role of Ag species as a potential metal dopant for CWPO. Current literature would suggest that Ag could be an efficient promotion of H₂O₂ decomposition to reactive •OH species. Therefore, Ag was added for different zeolite frameworks ZSM-5 with different Si:Al ratios (23, 50, and 80), and considering zeolites of different morphology like Zeolite-Y.

Various catalysts are assessed based on their phenol conversion. Different methods of characterization were used, like XRD, XPS and BET techniques and associated with catalytic efficiency.

4.2 Results and Discussion

4.2.1 The effects of preparing Fe-ZSM-5 with different iron precursors and ZSM-5 counterions, and study the effect of increasing Fe loading 5wt.% Fe/ZSM-5 and 10 wt%Fe-ZSM-5 on CWPO of phenol

The Fe precursor to carrying out the metal doping plays an important role in controlling the distribution of Fe species in the Fe-ZSM-5 catalyst prepared by the wetness impregnation method, the different precursors resulting in different catalytic activities.⁴⁶ Study conducted by Kim and his team to examine the partial oxidation of CH₄ with hydrogen peroxide in water using Fe-ZSM-5. For the preparation of Fe-ZSM-5 catalysts, the effect of Fe precursors on catalytic performance was investigated. Moreover, two preparation methods were used: wet impregnation (WI) and ion exchange (IE). Fe-ZSM-5 derived from FeCl₂ was found to perform better than the Fe-ZSM-5 catalysts derived from FeSO₄, Fe(CH₃CO₂)₂, FeCl₃, Fe₂(SO₄)₃, Fe(C₅H₇O₂)₃, and Fe(NO₃)₃ obtained by the WI method. In Fe-ZSM-5 catalysts prepared by the IE method, low-valent Fe precursors, like FeSO₄, FeCl₂, and Fe(CH₃CO₂)₂, exhibit greater catalytic activity than trivalent Fe precursors, like Fe₂(SO₄)₃, FeCl₃, and Fe(NO₃)₃.⁴⁶

In addition, over the last decade, investigations into the mechanism and kinetics of H₂O₂ decomposition by Fe²⁺ and Fe³⁺ species have been carried out extensively.⁴⁷⁻⁵⁰ In the Fenton process, H₂O₂ reacts with Fe ions to produce active oxygen species, which oxidize organic and inorganic compounds.⁵¹ Reagents that can be involved in the Fenton reaction are H₂O₂, Fe²⁺, Fe³⁺ and organic or inorganic ligands.⁵² As mentioned in Chapter 1, in the Fenton reactions, if the reaction is started using Fe³⁺/H₂O₂ rather than Fe²⁺/H₂O₂, the reaction will be slower because Fe³⁺ should be reduced to Fe²⁺ prior to the production of hydroxyl radicals (see equations chapter 1).⁵³ To investigate this effect, in this study, in the presence of zeolites as a support, two precursors have been selected, Fe(NO₃)₃·9H₂O (Fe³⁺) and FeSO₄·7H₂O (Fe²⁺), to prepare Fe-ZSM-5.

Interestingly to observe a survey conducted by Delahay *et al.*^{54, 55} found that when the Fe loading in the zeolite is low, monoatomic iron-oxo cations are the most common and have high reduction potential (E₀). In contrast, by increasing the Fe loading, binuclear iron-oxo species and iron oxides can form fewer active compounds. Binuclear oxo-complexes are active in SCR

reactions⁵⁶ and the direct decomposition of N_2O .⁵⁷ In light of this, we conducted a study where Fe-ZSM-5 were prepared at various iron loading 1, 5 and 10 wt%. As a first step, though, and similar to how ACs were studied in Chapter 3, homogeneous catalytic tests without the zeolite as a kind of control and blank tests were carried out. The aim was to compare the effect of Fe^{2+} and Fe^{3+} towards the Fenton system and in case of leaching. For these tests 50 mL of the mixture solution containing $1 \text{ g}\cdot\text{L}^{-1}$ of phenol and metal ions (Fe^{3+} from $\text{Fe}(\text{NO}_3)_3$ or Fe^{2+} from FeSO_4) M:S ratio was 1:100, a stoichiometric amount of H_2O_2 to phenol (1:14) was added to the solution to start the reaction 80°C heating degree was used for 4 h. The results showed that in both precursors, phenol conversion reached 100%, and the CMB% was approximately the same with both Fe^{2+} and Fe^{3+} , 46% and 40%, respectively, considering the experimental error of 5%. There is no difference between Fe^{2+} and Fe^{3+} as starting a homogeneous catalyst with our reaction conditions where the reaction continues for 4 h, and the difference between them is negligible.

In view of this result, we have selected $\text{Fe}(\text{NO}_3)_3\cdot 9\text{H}_2\text{O}$ as a main precursor for the synthesis of our catalytic materials and synthesised 1 wt% Fe-ZSM5 using as a support the ammonium NH_4 -ZSM-5 and acidic form H-ZSM-5, and here abbreviated as A-1 and A-2 samples respectively. In addition, we have prepared these same materials by using $\text{FeSO}_4\cdot 7\text{H}_2\text{O}$, here denoted B-1 and B-2 for the ammonium and acidic forms, respectively. All these catalysts were used for phenol oxidation by CWPO. Phenol concentration $1 \text{ g}\cdot\text{L}^{-1}$, M:S was 1:100, and a stoichiometric amount of H_2O_2 to phenol was used at 1:14 at 80°C for 4 h.

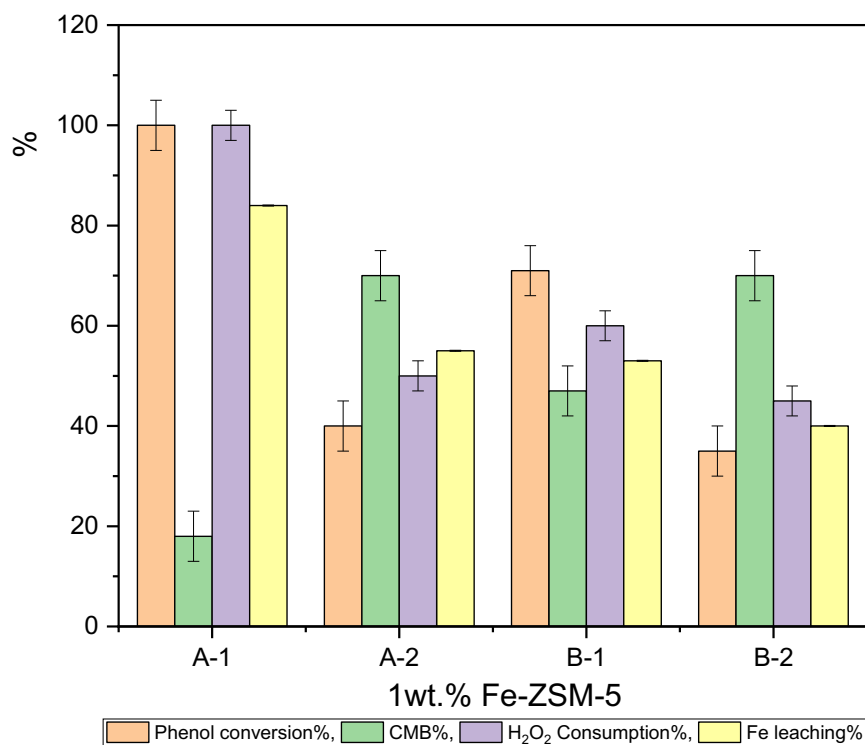


Figure 4.1: Catalytic activity test for phenol oxidation by CWPO using various catalysts: (A-1) 1wt% Fe-ZSM-5 that catalyst synthesized via $\text{Fe}(\text{NO}_3)_3 \cdot 9\text{H}_2\text{O}$ and $\text{NH}_4\text{-ZSM-5}$; (A-2) 1wt% Fe-ZSM-5 that catalyst synthesized via $\text{Fe}(\text{NO}_3)_3 \cdot 9\text{H}_2\text{O}$ and H-ZSM-5; (B-1): 1wt% Fe-ZSM-5 that catalyst synthesized via $\text{FeSO}_4 \cdot 7\text{H}_2\text{O}$ and $\text{NH}_4\text{-ZSM-5}$; (B-2) 1wt% Fe-ZSM-5 catalyst synthesized via $\text{FeSO}_4 \cdot 7\text{H}_2\text{O}$ and H-ZSM-5. All reactions were conducted using 50 ml of phenol, a concentration of $1 \text{ g} \cdot \text{L}^{-1}$, M:S was 1:100, and 1:14 molar ratios of phenol:H₂O₂ at 80 °C for 4 h.

In a comparison of catalysts: 1wt% Fe-ZSM-5 (A-1) and (A-2), despite having the same precursor but a different counterion for the zeolite, NH_4^+ for (A-1) and H^+ for (A-2), it appears that (A-1), gives complete phenol oxidation as well as high mineralization, where the CMB% was 18%. In contrast, the catalytic activity of 1wt% Fe-ZSM-5 (A-2) for phenol conversion and residual intermediates were very low, 40% and 70%, respectively. Also, H₂O₂ consumption confirms these results; it was 100% for 1wt% Fe-ZSM-5 (A-1) but only 50% for the other catalyst where an H^+ counterion was used. Iron leaching is high for both catalysts, though, thus affecting their durability. Still, the leaching with 1wt% Fe-ZSM-5 (A-1) (84%) was much larger than Fe-ZSM-5 (A-2) (55%); these could be a result of an increase in short-chain acids in solution, for example, oxalic acid, which is the main reason for leaching as reported

frequently.^{58, 59} Therefore, when Fe doping in NH₄-ZSM-5 is more active than using H-ZSM-5 for phenol conversion via CWPO reaction.

Comparing 1wt% Fe-ZSM-5 (B-1) that prepared by NH₄-ZSM-5 and FeSO₄.7H₂O and (B-2) produced by H-ZSM-5 and FeSO₄.7H₂O (Figure 4.1), there is a significant difference in the catalytic activity for phenol oxidation and residual intermediates,. 1wt% Fe-ZSM5 (B-1) gives 71% phenol conversion and 47% residual intermediates, while for 1wt% Fe-ZSM-5 (B-2), the catalytic activity dropped to 35% phenol oxidation and 70% residual intermediates. H₂O₂ consumption was 60% and 45% for 1wt% Fe-ZSM-5 (B-1) and 1wt% Fe-ZSM-5 (B-2), respectively compatible with the catalytic activity results, justified that not all H₂O₂ has been decomposed to form •OH other ways more phenol oxidation and mineralization will reach. The results regarding iron leaching show there was no significant difference between both (B-1) and (B-2). Still, both catalysts suffered from high iron leaching. These results were compatible with the above catalysts using iron nitrate precursor, where doping Fe in the form of NH₄-ZSM-5 increased the catalytic activity more than using the form H-ZSM-5. In summary, if the phenol conversion is taken as a parameter to assess these various catalysts, the best is the one prepared by using Fe(NO₃)₃ precursors and zeolite ZSM-5 in the ammonium form.

As previously explained, metal loading can also influence the catalytic activity as it solely affects the metal dispersion, the same materials described in section(4.2.1) were prepared with a metal loading of 5 and 10 wt%. These catalysts (A-1), (A-2), (B-1) and (B-2) applied for phenol conversion by CWPO reaction at the same condition.

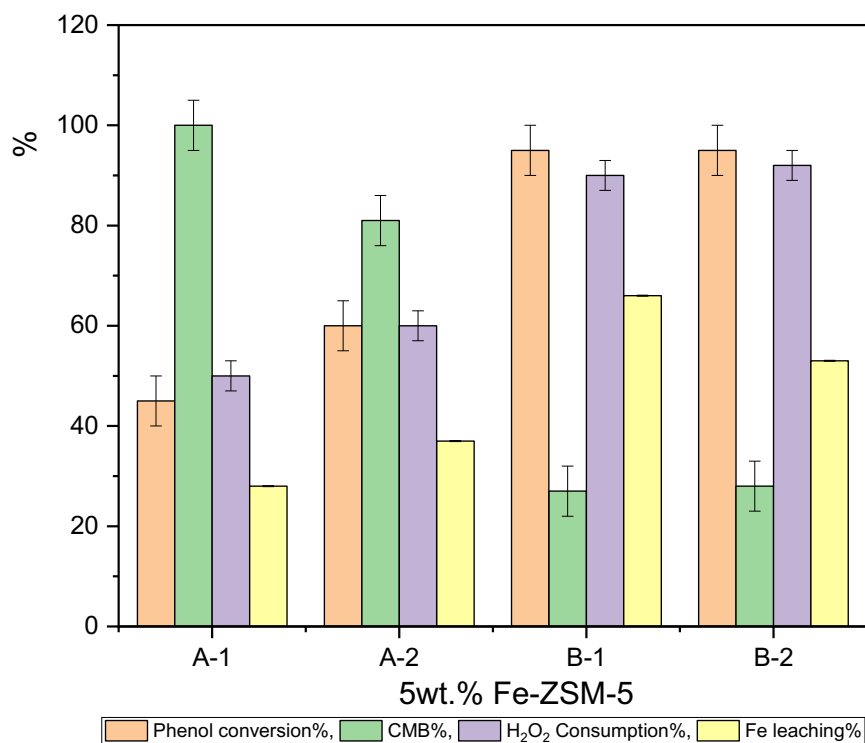


Figure 4.2: Catalytic activity test for phenol oxidation by CWPO using various catalysts. The first catalyst (A-1) 5wt% Fe-ZSM-5 that catalyst synthesized via $\text{Fe}(\text{NO}_3)_3 \cdot 9\text{H}_2\text{O}$ and $\text{NH}_4\text{-ZSM-5}$; (A-2) 5wt% Fe-ZSM-5 that catalyst synthesized via $\text{Fe}(\text{NO}_3)_3 \cdot 9\text{H}_2\text{O}$ and H-ZSM-5; (B-1) 5wt% Fe-ZSM-5 that catalyst synthesized via $\text{FeSO}_4 \cdot 7\text{H}_2\text{O}$ and $\text{NH}_4\text{-ZSM-5}$; (B-2) 5wt% Fe-ZSM-5 catalyst synthesized via $\text{FeSO}_4 \cdot 7\text{H}_2\text{O}$ and H-ZSM-5. All reactions were conducted using the same condition as section 4.2.1.

Comparative analysis between Figure 4.1 and 4.2, when iron loading was increased from 1 to 5 wt% for Fe-ZSM-5 (A-1) catalysts, phenol oxidation activity was significantly decreased from 100 to 45% and mineralization (residual intermediates) was elevated from 18% to 100%. On the other hand, increasing the loading of Fe from 1wt% to 5wt% within (A-2) catalysts do not affect their catalytic activity for phenol oxidation—however, both these catalysts (A-2) either 1wt% or 5wt% Fe loading, has a low activity for phenol conversion (40–60%) and low mineralization (residual intermediates between 70 and 100%). The opposite effect of increasing the Fe doping from 1 to 5wt% was observed for (B-1) and (B-2) catalysts. where the rises in the Fe loading result in higher catalytic activity in both (B-1) and (B-2) to reach approximately full phenol oxidation at 95% and 28% of residual intermediates.

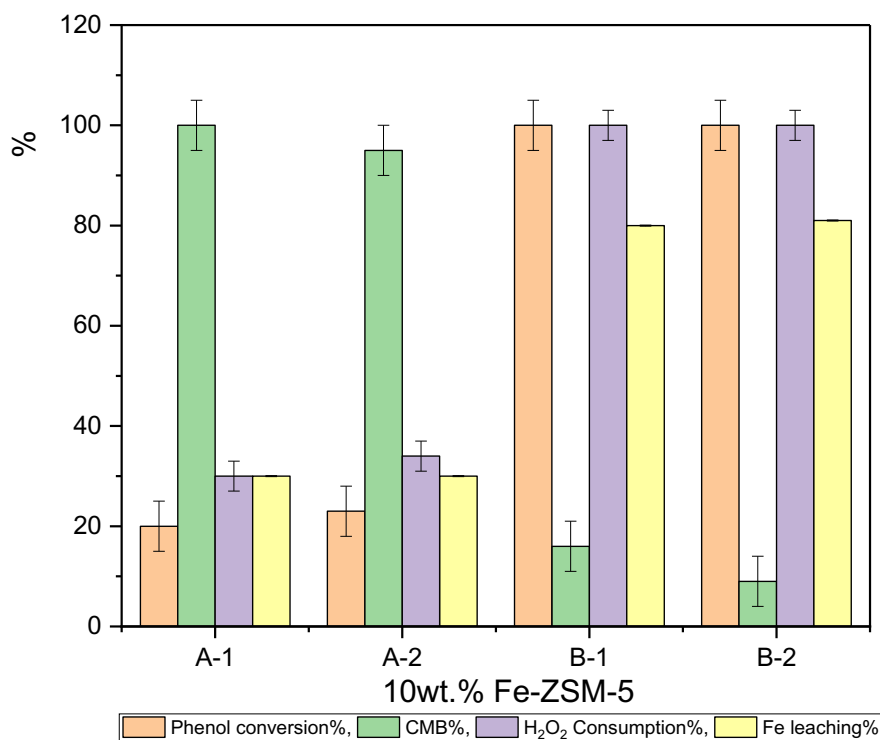


Figure 4.3: Catalytic activity test for phenol oxidation by CWPO using various catalysts. The first catalyst is 10wt% Fe-ZSM-5 (A-1) that catalyst synthesized via $\text{Fe}(\text{NO}_3)_3 \cdot 9\text{H}_2\text{O}$ and $\text{NH}_4\text{-ZSM-5}$, the second catalyst 10wt% Fe-ZSM-5 (A-2) that catalyst synthesized via $\text{Fe}(\text{NO}_3)_3 \cdot 9\text{H}_2\text{O}$ and H-ZSM-5 , the third catalyst 10wt% Fe-ZSM-5 (B-1) that catalyst synthesized via $\text{FeSO}_4 \cdot 7\text{H}_2\text{O}$ and $\text{NH}_4\text{-ZSM-5}$ and the final one 10wt% Fe-ZSM-5 (B-2) that catalyst synthesized via $\text{FeSO}_4 \cdot 7\text{H}_2\text{O}$ and H-ZSM-5 . All reactions were conducted using the same reaction parameters as in section 4.2.1.

The same trend is observed here; increasing the iron loading to 10wt% for catalysts prepared by iron nitrate dramatically dropped the catalytic activity of Fe-ZSM-5 (A-1) and (A-2) for phenol oxidation by CWPO. Phenol conversion from 100% to 20% and residual intermediates from 18% to 100% for 1wt% and 10wt% (A-1) respectively. Additionally, the activity was reduced by 50% (phenol oxidation from 40% to 23% and residual intermediates from 70 to 95%) for 1wt% and 10wt% (A-2) in that order. Alternatively, the opposite effect was noted for the catalysts prepared by the iron sulphate precursors, where the increase in the metal loading caused a substantial increase in activity, resulting in enhanced mineralization from 27% for 5wt% (B-1) and (B-2) to be 16% and 9% for 10wt% (B-1) and (B-2), respectively. In summary, comparing all the 10wt% Fe-ZSM-5 catalysts, (B-1 and B-2) catalysts have higher catalytic activity.

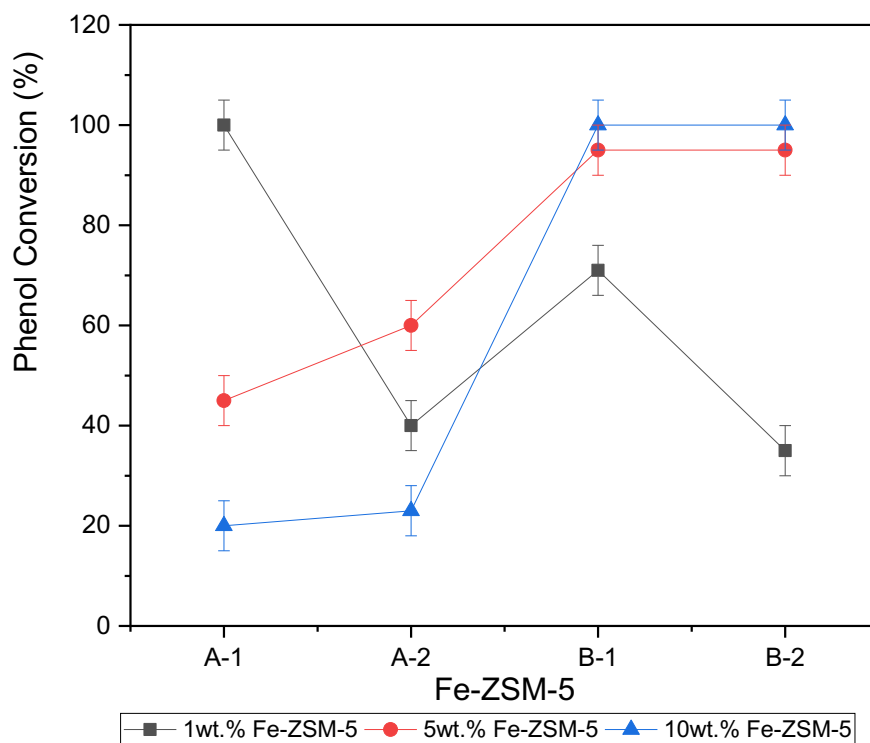


Figure 4.4: Phenol oxidation by CWPO using various catalysts at different Fe loading. The black line is for 1wt% Fe-ZSM-5 (A-1), (A-2), (B-1) and (B-2). The red line is for 5wt% Fe-ZSM-5 (A-1), (A-2), (B-1) and (B-2). The blue line is for 10wt% Fe-ZSM-5 (A-1), (A-2), (B-1) and (B-2). Where (A-1) that catalyst synthesized via $\text{Fe}(\text{NO}_3)_3 \cdot 9\text{H}_2\text{O}$ and $\text{NH}_4\text{-ZSM-5}$, the second catalyst (A-2) that catalyst synthesized via $\text{Fe}(\text{NO}_3)_3 \cdot 9\text{H}_2\text{O}$ and H-ZSM-5, the third catalyst (B-1) that catalyst synthesized via $\text{FeSO}_4 \cdot 7\text{H}_2\text{O}$ and $\text{NH}_4\text{-ZSM-5}$ and the final one (B-2) that catalyst synthesized via $\text{FeSO}_4 \cdot 7\text{H}_2\text{O}$ and H-ZSM-5.

Increasing the iron loading for the Fe-ZSM-5 catalyst prepared by $\text{Fe}(\text{NO}_3)_3 \cdot 9\text{H}_2\text{O}$ precursor decreases the catalytic activity (both phenol conversion and mineralization) for phenol oxidation by CWPO according to the results in Figure 4.4; the best catalyst is 1 wt% Fe-ZSM-5 (A-1) where phenol conversion reaches 100%. On the other hand, increasing the iron loading for Fe-ZSM-5 that is synthesized via $\text{FeSO}_4 \cdot 7\text{H}_2\text{O}$ (10 wt% Fe-ZSM-5 (B-1 and B-2)), catalysts resulted in to increase in the catalytic activity for phenol conversion. That can explain as a result of the Fenton reaction effect, where Fe^{2+} in the $\text{FeSO}_4 \cdot 7\text{H}_2\text{O}$ initiate the reaction immediately, but Fe^{3+} in the $\text{Fe}(\text{NO}_3)_3 \cdot 9\text{H}_2\text{O}$ need to transform to form Fe^{2+} and then start the reaction, so if the iron loading increases, the particles get bigger the exposed fraction gets lower, the total area with the low Fe loading is bigger, so that means less dispersion metal resulting in less capability to do the reaction with less amount of Fe^{2+} . However, $\text{FeSO}_4 \cdot 7\text{H}_2\text{O}$

can initiate the Fenton reaction directly. As a result, it is expected that the higher amount of Fe leads to a higher number of initiator species. Therefore, more iron loading leads to higher activity. Still, these high metal loading catalysts have a limitation due to the limited number of Fe²⁺ species that can decompose with time.

4.2.2 Study the effect of different preparation methods by synthesis of Fe-ZSM-5 under vacuum method

The properties of catalysts prepared by different methods differ, including dispersion and distribution of metals and metal size, which affect their performance in chemical reactions.⁶⁰⁻⁶² Dispersion of a metal dopant, as we have also seen in our own experiments when using ACs, is particularly important. In view of this, we wanted to export and extend these results to the zeolite by using a vacuum impregnation protocol. Based on current literature, a vacuum impregnation method produces highly dispersed active species, which results in an active catalyst. Mandal reported that the vacuum treatment after incipient wetness impregnation appears to enhance the dispersion of cobalt on the SBA-15 catalysts because of the decrease in the metal crystallite size.⁵⁹ Using vacuum impregnation, a pressure difference occurs between the support and the external atmosphere, enhancing both rate of impregnant diffusion and support micropore activity.⁶³ Researchers studied vacuum-impregnated Fischer-Tropsch synthesis (FTS) catalysts to produce light olefins for gasoline and diesel, and Fe/Cu/K/AC (activated carbon) catalysts were prepared. It was found that there was a strong interaction between catalyst precursors and support, as well as higher stability and H₂ adsorption ability.⁶⁴ When AC was impregnated with metal cobalt under vacuum conditions, CO conversion and stability of the catalysts improved compared with catalysts that were prepared under normal conditions.⁶⁵

In view of the literature evidence, Fe-ZSM-5 catalysts were synthesised by vacuum impregnation (VI) and a wetness impregnation (WI) sample for comparison at the same conditions as the (VI) sample but without vacuum.

Iron was doped in the ZSM-5 in two ways wetness impregnation under normal conditions (25 °C and 1 atmospheric pressure), and the other catalyst was prepared by wetness impregnation under vacuum. Iron loading was fixed to be 1wt% for both catalysts. They were applied for phenol conversion by the CWPO reaction using the same reaction conditions of phenol concentration $1 \text{ g}\cdot\text{L}^{-1}$, M:S 1:100 at 40, 60 and 80 °C for 4 h.

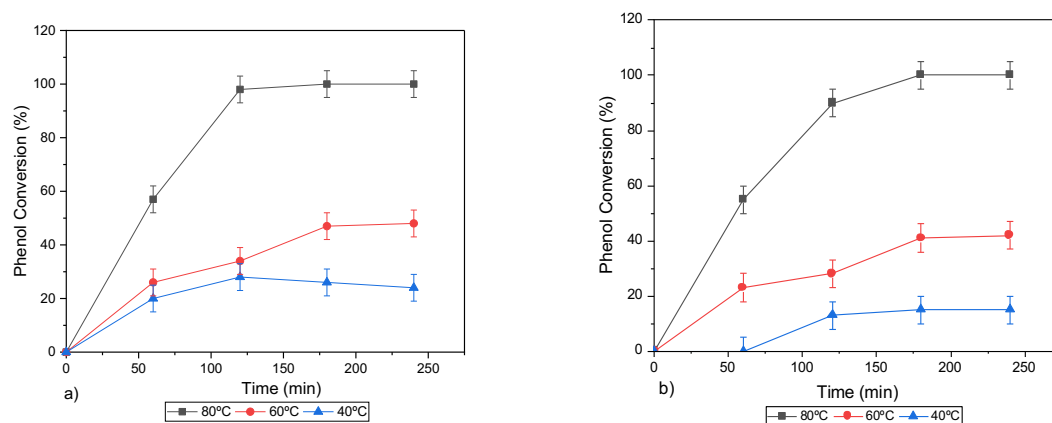


Figure 4.5: Temperature effect on the degradation of phenol by the CWPO reaction using a) 1wt% of Fe-ZSM-5 (WI) and b) 1wt% Fe-ZSM-5 (VI). The black line belongs to the kinetic reaction for the catalyst at 80 °C, the red line for the catalytic activity test at 60 °C and the blue one for the catalytic reaction at 40 °C. Phenol concentration $1 \text{ g}\cdot\text{L}^{-1}$ and M:S 1:100, 1:14 H_2O_2 at 40, 60 and 80 °C for 4 h.

Figure 4.5 illustrates the temperature effect on the catalytic activity of Fe-ZSM-5 (WI) and Fe-ZSM-5 (VI) to phenol oxidation by CWPO reaction. The activity increased by increasing the T as at 80 °C, H_2O_2 started to be consumed by Fe ions to form $\cdot\text{OH}$, thus lowering the activation energy and leading to better phenol oxidation.⁶⁶ Still, there was slight H_2O_2 consumption at lower T, but 80 °C is the optimal heat degree for this reaction. A similar observation was made by Zazo, who found that increasing the temperature of the catalytic oxidation process increased phenol degradation.⁶⁷ Comparing the catalytic activity of both catalysts, the Fe-ZSM-5 (WI) and the Fe-ZSM-5 (VI) for phenol oxidation at 80 °C show there was no significant difference between both catalysts that were prepared by different methods. There was full phenol oxidation after 3h and high mineralization of 10% as well as complete H_2O_2 consumption. In view of this, due to the high differences in catalytic acidity between these two catalysts, the reaction temperature was decreased to 60 °C.

The catalytic activity for both catalysts was identical also at 60 °C. Fe-ZSM-5 (WI) and (VI) oxidized phenol by 48% and 42%, respectively; residual intermediates was 70% with both catalysts and 50% of H₂O₂ was transformed after 4h. However, phenol conversion dramatically decreased by 60% by decreasing the reaction temperature from 80 to 60 °C. That can be explained as the minimum reaction temperature that needs to substantially catalyse H₂O₂ and produce •OH radicals is 80 °C, that compatible with what was reported in many previous studies. On the other hand, to tentatively attempt to discern any difference between the two materials, the reaction temperature was further decreased to 40 °C to confirm this result. After decreasing the reaction temperature to 40 °C. Results show that the conversion by Fe-ZSM-5 (WI) was slightly higher (ca. 25%) activity than Fe-ZSM-5 (VI) (ca. 15%). However, phenol oxidation and mineralization dramatically dropped with the decrease in the reaction temperature from 80 °C to 40 °C. For Fe-ZSM-5 (WI), phenol oxidation was only 24%, and residual intermediates was 81% after 4 h, the consumption of H₂O₂ decreased significantly to 19%. In addition, Fe-ZSM-5 (VI) has low catalytic activity at lower temperatures (40 °C), converting phenol 15%, residual intermediates 19%, and consuming H₂O₂ 14%, respectively.

According to these results, there is no difference in the catalytic activity between the two catalysts Fe-ZSM-5 (WI) and Fe-ZSM-5 (VI) for phenol oxidation by the CWPO reaction. This may also be because of the high activity of the Fe-ZSM-5 catalyst that changing preparation methods did not seem to affect performance. In addition, possibly, this is caused by the generation and existence of equivalent Fe_xO_y species. Overall, it is confirmed that the Fe-ZSM-5 catalysts, irrespective of the preparation methods, had high activity in the CWPO of the phenol reaction.

4.2.3 Adding S and N to Fe-zeolite catalysts

As demonstrated in Chapter 3, and further corroborated by recent studies,^{1,68,69} The deposition of heteroatoms like N and especially S, on activated carbons for Fe doping generally leads to catalysts with enhanced activity and the highest resistance to leaching. N and S doping enhanced Fe/AC catalyst activity and stability. This might be due to the formation of nucleation centres based on Fe²⁺.¹ In addition, improving interfacial electron transfer, which can benefit our reaction.^{70 71, 72}

The zeolite topology has significant effects on the stabilization of cations within the micropores system,⁷³ which may impact the activity.⁷⁴ So, zeolites' activity depends on their properties. Various Si:Al molar ratios produce different morphologies and crystallite sizes in ZSM-5. Furthermore, Si:Al ratio is one of the key factors that control the reactivity of zeolite; the number of charges on zeolites is almost equal to the number of aluminium atoms. A more AlO₄⁻ is a negative charge that needs to be balanced by more positive counterions. These positive ions have a crucial role in the reactivity of zeolites because they are located outside of the Al-O-Si framework. In addition, zeolite acidity is determined by the nature of these cations. For instance, a higher Bronsted acidity of a zeolite can be achieved if the extra framework cation is hydrogen H⁺. Acid site strength and concentration are correlated with zeolite type and Si:Al molar ratio.⁷⁵ The acid site strength and concentration in zeolites can play a significant role in catalytic reactions like our reaction. The zeolite type and Si:Al influence these properties, which, in turn, can impact the reaction kinetics and selectivity. Different zeolites have distinct structures and compositions, leading to variations in their acid site characteristics. For instance, zeolites such as ZSM-5, Beta, and Y have different pore structures and acid site distributions. The choice of zeolite type can influence the accessibility of reactants to the active sites and the strength of the acid sites. The Si:Al molar ratio in a zeolite framework affects its acidity. A higher Si:Al ratio generally leads to a lower concentration of acid sites and weaker acidity, as silicon atoms are less acidic than aluminum atoms. Zeolites with a high Si:Al ratio are often called "non-acidic" zeolites. Conversely, zeolites with a lower Si:Al ratio are more acidic due to aluminum, which can serve as strong Lewis acid sites.⁷⁴

The acidity of zeolites can enhance the catalytic activity in phenol oxidation reactions. Strong acid sites can facilitate the protonation of phenol, making it more reactive with hydrogen peroxide. This can lead to improved reaction rates and higher phenol conversion. Furthermore, a higher concentration of acid sites can increase the number of active sites available for the reaction. This can lead to higher catalytic activity and improved phenol conversion rates.

Different zeolite types may offer varying degrees of selectivity in the phenol oxidation reaction. Some zeolites may promote the desired product formation, while others may favour unwanted by-products. For most applications, zeolites' acidity and basicity play a key role. In spite of this very important practical role, there are still many questions regarding how zeolites behave, with different reactions.⁷⁶ ZSM-5 samples with different Si:Al ratios have different acidity. There is a nonlinear decrease in Brønsted acid sites when the Si:Al ratio rises in ZSM-5.⁷⁷ Moreover, Si:Al ratio strongly influences the zeolite affinity towards water. The higher the Si:Al ratio more hydrophobic the zeolite, while decreasing the Si:Al ratio increases the hydrophilicity of zeolite, which increases its affinity towards water,⁷⁸ which could be beneficial for this reaction water is used as a solvent.

During this part of the project, three different Si:Al ratios (23, 50 and 80) ZSM-5 were used to prepare Fe-S-N-ZSM-5. In addition, Zeolite-Y (5.1) has been used. All catalysts have 1wt% Fe loading and all of them synthesised by wetness impregnation method. These catalysts were applied for phenol oxidation by the CWPO reaction at the same reaction conditions as section 4.2.1.

In section 4.2.2 the Fe-ZSM5 (23) was used for the CWPO reaction to oxidize phenol and resulted in 100% phenol conversion and 7% residual intermediates after 4h. In this case, the deposition of Fe was accompanied by the presence of S and N. It was possible to observe (Figure 4.6) that phenol oxidation by Fe-S-N-ZSM-5 gradually accelerated over time to reach 80% after 4h. Compared with Fe-ZSM5 (23), the catalyst's activity slightly decreased, with phenol conversion from 100 to 80% and residual intermediates from 7 to 30%. Interestingly, doping S and N, as desired, dramatically decreased the iron leaching by 50% from 80% to 40% after 4h with Fe-ZSM-5 and Fe-S-N-ZSM-5 (23), respectively. There was no significant difference in the H₂O₂ consumption between both catalysts. The minor reduction in the catalytic activity could be ignored against increasing the catalyst's durability.

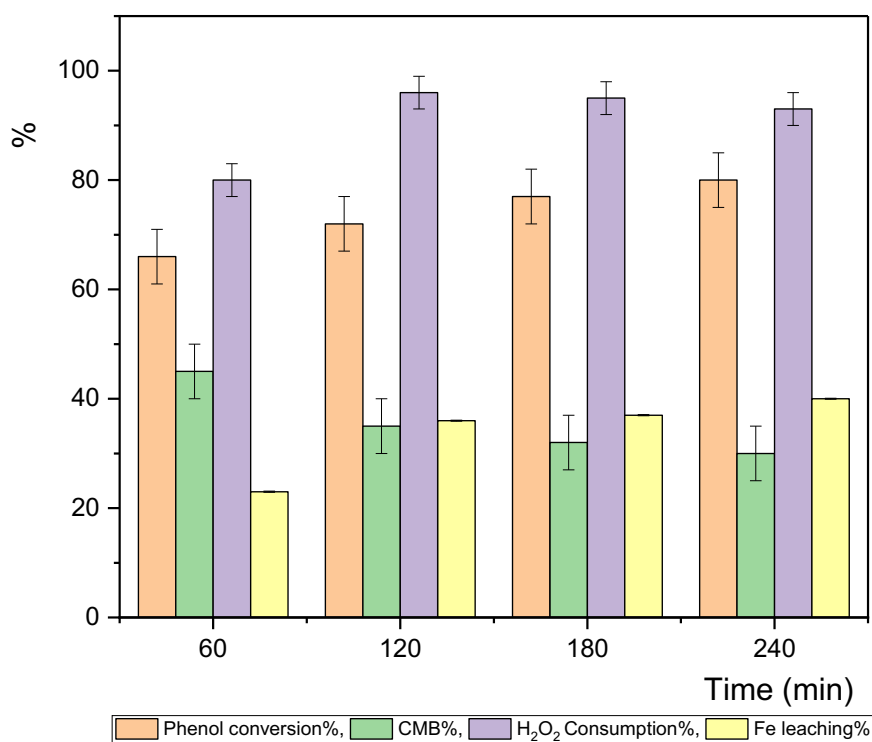


Figure 4.6: Kinetic reaction of the catalytic activity for the Fe-S-N-ZSM-5 (23) at different reaction times for phenol oxidation by CWPO. The catalyst gives 80% phenol oxidation and 40% Fe leaching.

There is no doubt that the total acid sites of ZSM-5 decrease with higher levels of Si:Al molar, zeolites have a well-defined pore structure with acidic sites associated with aluminum (Al) atoms. This can affect the adsorption and activation of reactants on the catalyst surface based on the literature.^{77, 79} However, by increasing the Si:Al molar ratio, the specific surface area and pore volume of ZSM-5 zeolites increase slightly.⁷⁵ still, it well known that the Fenton system is pH-dependent after all. To examine the effect of different zeolite properties, S, N and Fe were doped for ZSM-5 (50) and applied for the reaction, then compared to the performance of Fe-S-N-ZSM-5 (23).

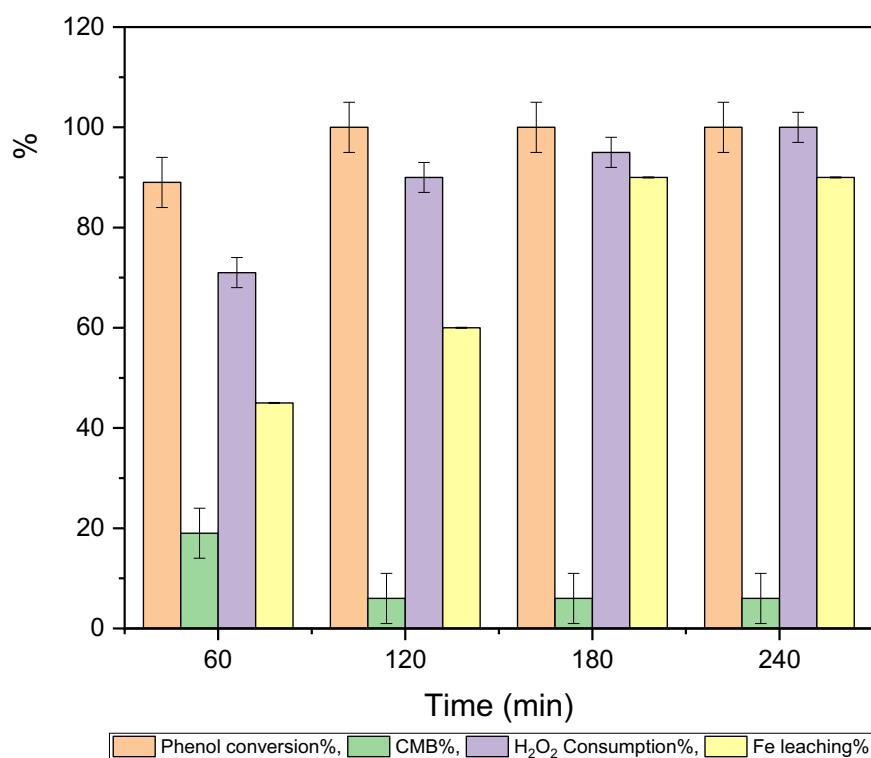


Figure 4.7: Kinetic analysis of Fe-S-N-ZSM-5 (50)'s catalytic activity in the CWPO oxidation of phenol. The reaction was conducted using the same reaction parameters as in section 4.2.1.

As indicated by Figure 4.7, the performance of the catalyst was improved considerably when compared to a catalyst prepared using a lower Si:Al molar ratio (Figure 4.6). By the second hour of the reaction, full phenol conversion had been achieved, along with high mineralization to give 6% residual intermediates. The stability of the catalyst was reduced due to high Iron leaching; for the Fe-S-N-ZSM-5 (23), Iron leaching was 40% while, for the Fe-S-N-ZSM-5 (50) increased to 90% at 4 h. Consequently, a higher Si:Al molar ratio leads to an increase in the catalytic activity of the Fe-S-N-ZSM-5 catalyst; this effect is specific to this case of a reaction.

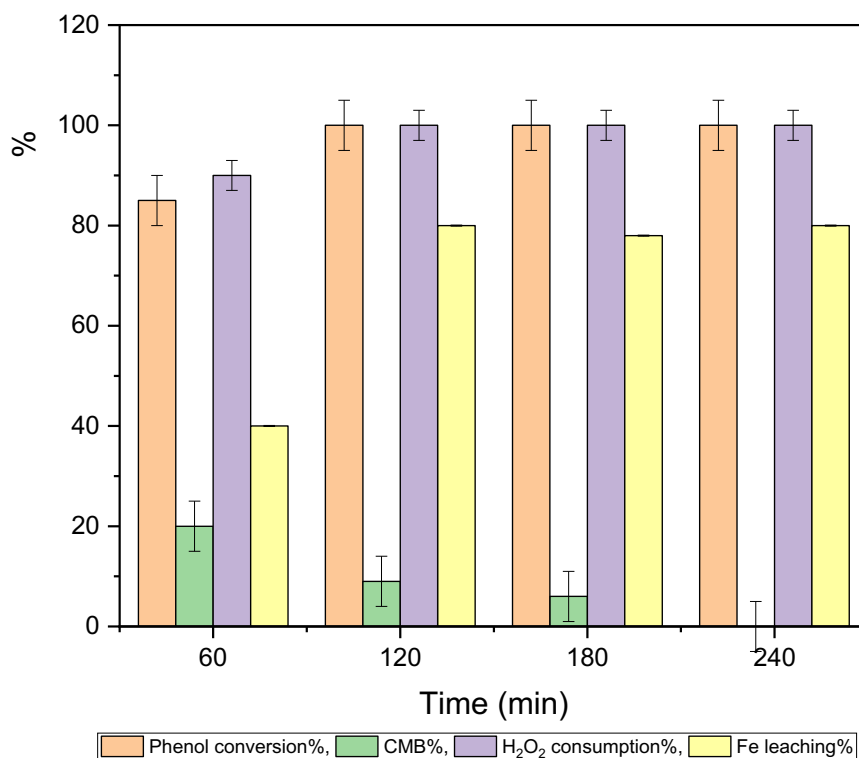


Figure 4.8: Analysis of the kinetic reaction of Fe-S-N-ZSM-5 (80) during CWPO oxidation of phenol. The reaction was applied using 50 ml of mixer solution containing 1 g.L⁻¹ phenol, 1:100, Fe:phenol molar ratio and stoichiometric amount of H₂O₂, 1:14 at 80 °C for 240 min. The catalyst gives 100 % phenol oxidation by 120 min of time reaction.

Comparing Figure 4.7 and 4.8, there was no significant difference in the catalytic activity by increasing the Si:Al ratio from 50 to 80. Both catalysts have high activity for this reaction. At 120 min of the reaction time (Figure 4.8), phenol oxidation reaches 100% and 9% residual intermediates using Fe-S-N-ZSM-5 (80). Furthermore, there was full mineralization after 4h. Still, the catalyst suffers from high metal leaching. Accordingly, it was decided to change the zeolite type to use Zeolite-Y to incorporate Fe, S and N. This zeolite is known to have a large pore size (~7.4 Å), called faujasite.⁸⁰ Thus, it is suitable for applications that involve larger molecules (for example, the MFI pore diameter is 5.5 Å). In terms of their Si:Al ratio, faujasites are classified as X (Si:Al = 1–1.5) and Y (Si:Al >2) despite having the same topological framework.⁸¹ In recent years, zeolite Y has become one of the most widely used molecular sieves,⁸² particularly in the petrochemical, fine chemical industry⁸³⁻⁸⁵ and water treatment due to its high stability and activity.⁸⁶

In our case, we examined this catalyst Fe-S-N-Zeolite-Y to study the effect of different zeolite morphology (bigger pore size) and if that will impact the activity and durability of the catalyst. Their morphology can vary significantly, and it plays a crucial role in their properties and applications. The morphology can affect the size and distribution of the pores within the zeolite structure. Some zeolites have large pores, while others have smaller ones, and this can influence their adsorption and activity properties.

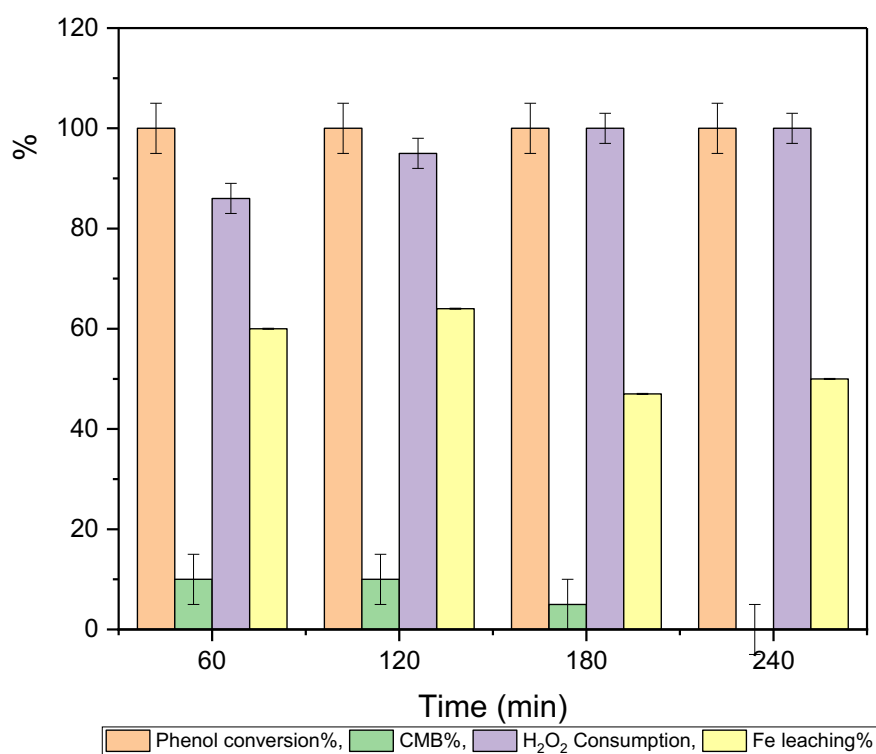


Figure 4.9: The kinetic reaction of the catalytic activity for the Fe-S-N-Zeolite-Y in phenol oxidation by WCPO. The same reaction conditions were used in Figure 4.8. The catalyst reaches full phenol oxidation within 60 min of reaction time.

The Fe-S-N-Zeolite-Y has extremely high activity for the reaction. It gives 100% phenol oxidation for the first 60 min, as well as complete mineralization over time. Interestingly seems to be the bigger pore size of the zeolite impact in a positive way on the catalyst stability, where the iron leaching decreased to 50% compared to 90 and 80% with the MFI catalysts. Possibly, the larger pore size of the support provides more space to be hosted and accommodation for the active metal species reducing the metal leaching. In addition, increasing the accessibility

of the zeolite Y micropores for the organic molecules present in the water. It has been reported that with zeolites, conversion rate and selectivity may be greatly affected by the time the substances remain inside the zeolite crystal.⁸⁷ Even H₂O₂ consumption was 100% since the second hour. Due to these catalytic results, a zeolite-Y framework will also serve as a basis for the oxidation of homologues of phenol (see Chapter 5).

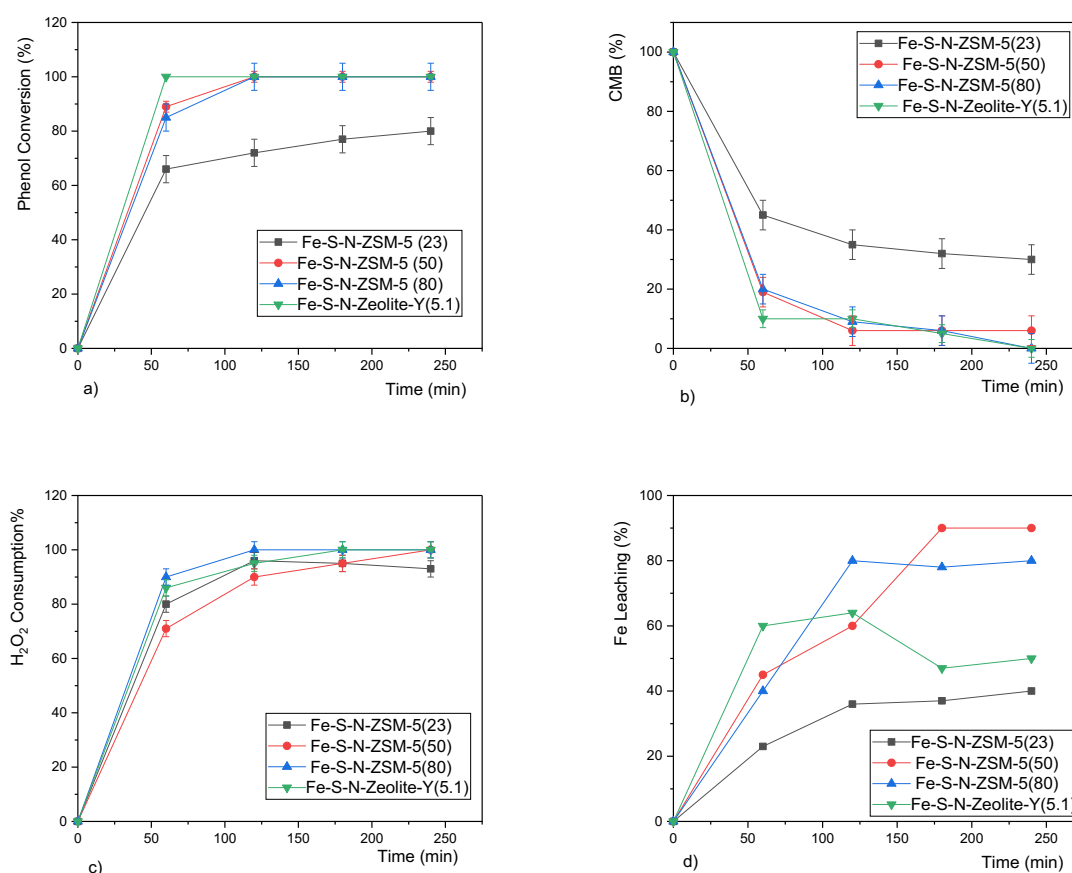


Fig 4.10: Catalytic activity results for different zeolite catalysts Fe-S-N-ZSM5(23, 50 and 80) and Fe-S-N-Zeolite-Y (5.1) for phenol oxidation by the CWPO reaction. a) phenol conversion, b) CMB, c) H₂O₂ consumption and d) Fe leaching. Phenol concentration 1g.L⁻¹ and M:S 1:100, 1:14 H₂O₂ at 80 °C for 4 h.

Comparative analysis for the catalytic activity of these catalysts is demonstrated in Figure 4.10. As discussed above, the catalytic activity for Fe-S-N-ZSM-5 catalysts increased with the increase of the Si:Al molar ratio from 23 to 50 and 80. Phenol conversion increased from 80% to 100% with Fe-S-N-ZSM-5 (23) and Fe-S-N-ZSM-5 (80), respectively. The Fe-S-N-Zeolite-

Y catalyst was found to be the most efficient catalyst for this reaction in terms of full phenol oxidation and mineralization, as well as H₂O₂ consumption; moreover, the leaching of Fe is less (50%) than Fe-S-N-ZSM-5 catalysts (ranging between 80-90%). These results indicate that the zeolite type and the molar ratio of Si:Al influence the performance of the final catalysts.

4.2.4 Fe-Ag-Zeolites

As in the CWPO of phenol reaction, active metal species, which generate free radicals $\cdot\text{OH}$ to decompose pollutants, play an important role in determining a catalyst's performance.⁸⁸ and as recent literature Ag showed that Ag can have some activity in the CWPO process,^{89, 90} we investigate this metal for our model reaction. In fact, a redox cycle such as Ag^+/Ag^0 can also convert H₂O₂ to $\cdot\text{OH}$ radicals,^{89, 91, 92} furthermore, Ag and H₂O₂ have earned their reputation as universal eco-friendly disinfectants for bacteria. Both silver and hydrogen peroxide exhibit broad-spectrum antimicrobial activity, meaning they are effective against a wide variety of bacteria, viruses, fungi, and even some parasites. This versatility makes them valuable for various disinfection applications. One reason why these disinfectants are considered eco-friendly is their minimal environmental impact. When used in appropriate concentrations and under controlled conditions, they break down into harmless by-products, reducing the risk of long-term environmental pollution. Khan and co-workers demonstrated that AgPd/TiO₂ bimetallic catalysts were used to produce H₂O₂ and break it down into reactive oxygen species, they reported that stabilizers and activators are both functions of Ag.⁹³ In addition, there some examples in the use of Ag-Fe-ZSM-5 for the oxidation of volatile organic compounds.⁹⁴⁻⁹⁶

In this part of the work, Fe and Ag-doped zeolite catalysts were prepared by the wetness impregnation (WI) technique as expected that the combination of both active metals will enhance the catalytic activity for phenol conversion and mineralization by reducing the reaction time as well as improve the durability. Various variables were studied, including different Fe loading, different Si:Al ratios with ZSM-5 and different zeolite types Zeolite-Y(5.1). These catalysts were tested for phenol oxidation by CWPO reaction using 1 g·L⁻¹ phenol with an M:S ratio of 1:100 at 80 °C for 4 h.

4.2.4.1 Effect of Fe and Ag loading to CWPO activity

As can be seen in Figure 4.11 the catalyst Ag-Fe-ZSM-5 (1 wt% Fe and 1 wt% Ag loading) has high catalytic activity for the degradation of phenol by H₂O₂. It reached full phenol conversion, mineralization and H₂O₂ consumption within the first 60 min of the reaction time. Iron leaching

decreased by 30% compared to Fe-ZSM-5 (80%). However, these results were shown with the previous catalyst Fe-S-N-Zeolite-Y (Si:Al 5.1). To approve if the Ag-Fe-ZSM-5 catalyst is a better catalyst, we decided to reduce the metal loading to 0.5wt% for both Ag and Fe. So the following catalyst is Ag-Fe-ZSM-5 (Si:Al 23) (0.5wt% Ag, 0.5wt% Fe loading).

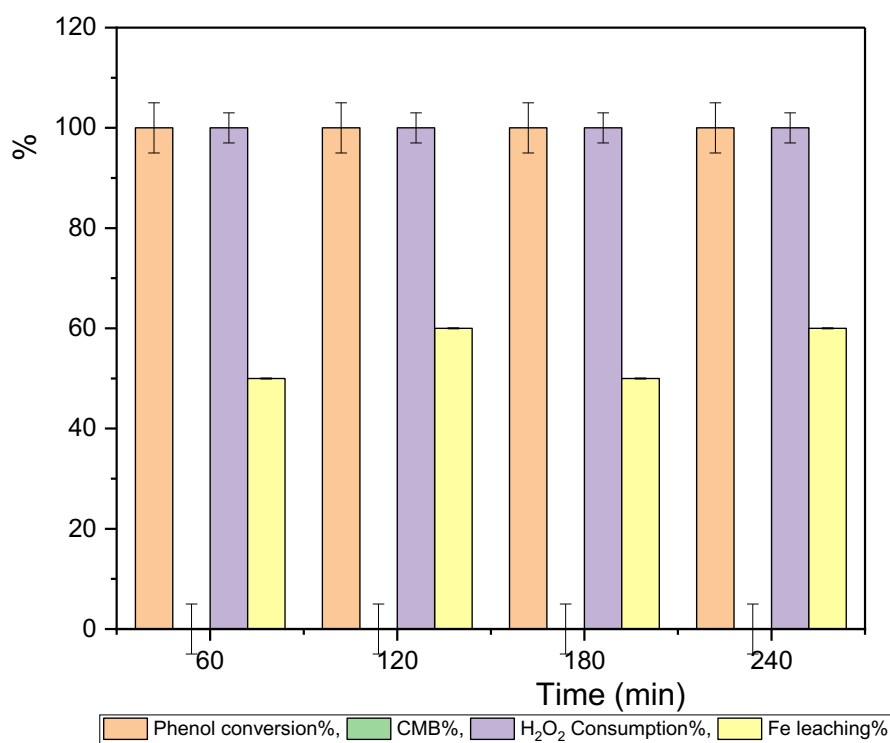


Figure 4.11: Kinetic reaction for the catalytic activity tests of Fe-Ag-ZSM-5 catalysts at 1wt.% Fe and Ag loading. Phenol concentration $1\text{g}\cdot\text{L}^{-1}$ at 50 ml reaction mixture, M:S 1:100, 1:14 H₂O₂ at 80 °C for 4 h. By 60 minutes of reaction time, 1 wt% Fe-Ag-ZSM-5 catalyst converts 100% of the phenol.

Doping Ag with Fe bimetallic nanoparticles has been approved to significantly increased catalytic activity, including complete phenol conversion, low residual intermediates as well as full H₂O₂ consumption, even with less amount of metal loading (0.5 wt%) as seen in Figure 4.12 Furthermore, dramatically prevented Fe from leaching; only 30% of the Fe was leaching over the reaction time. To correlate the metals loading with the catalytic activity Fe-Ag -ZSM-5 (23) with (2wt% Fe and 2 wt% Ag loading) was prepared and applied for the phenol oxidation Figure 4.13.

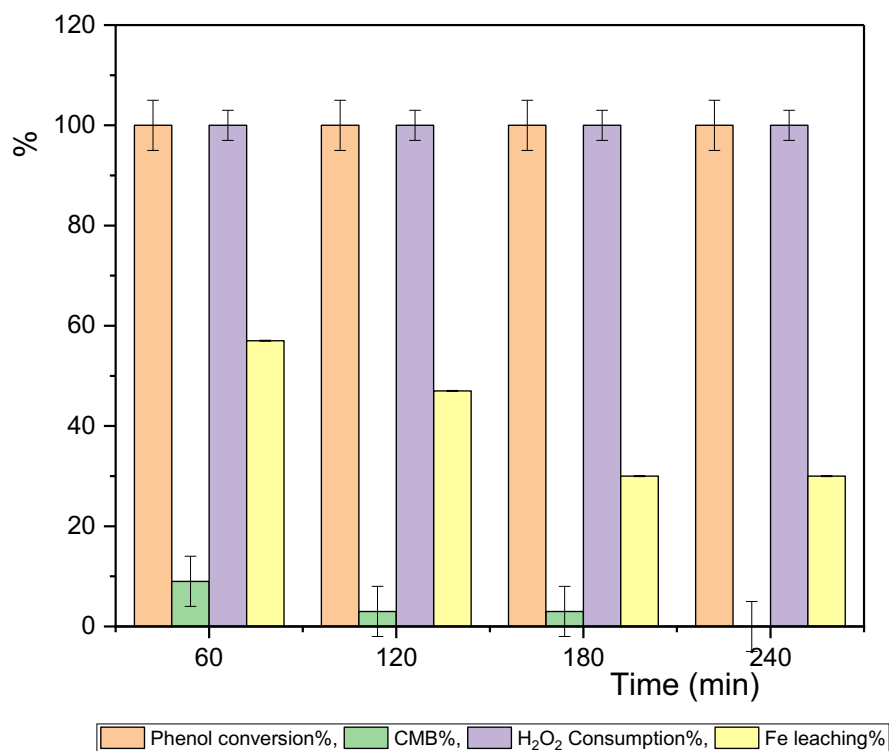


Figure 4.12: Reaction kinetics studies of Fe-Ag-ZSM-5 catalysts at 0.5wt% Fe and Ag loading. The same reaction conditions were used in Figure 4.11. After 60 minutes of reaction time, the Fe-Ag-ZSM-5 catalyst converts 100% phenol.

As can be seen in Figure 4.13, phenol conversion reached 100% as well as full mineralization and H₂O₂ consumption by the reaction over time; also, the metal leaching remained steady at 30%, emphasizing the stabilization properties of the Ag. However, increasing the iron loading to 2 wt% decreased the catalytic activity in terms of the reaction time, where the full mineralization and phenol conversion reached after 4 h, compared to the lower metal loading catalysts, where they reduced the reaction time to 60 min, this means reducing the consumption of energy and the cost of the whole process as a result.

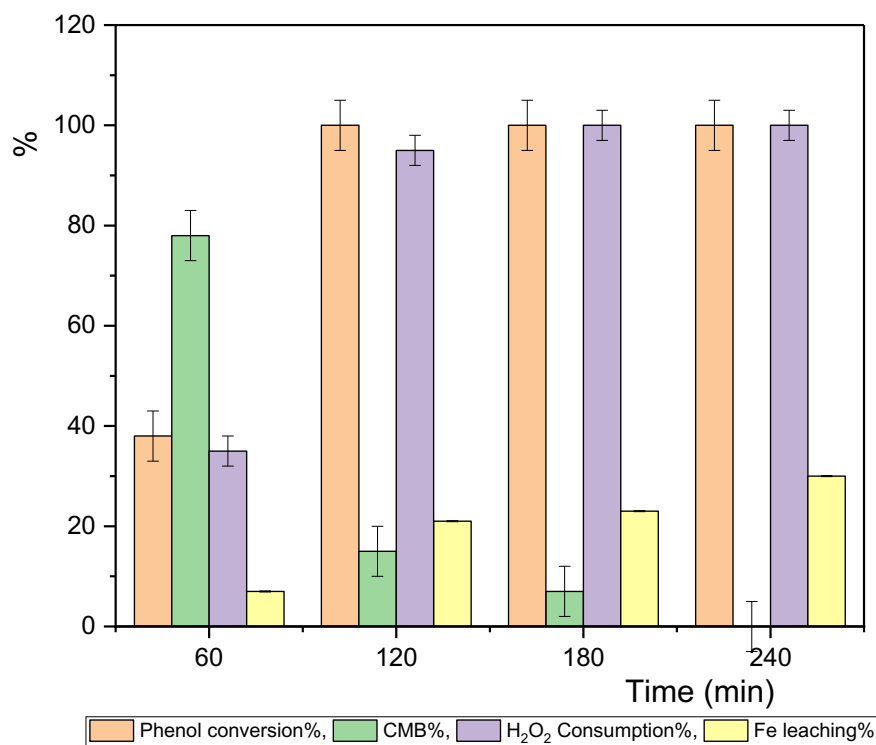


Figure 4.13: An analysis of the kinetics used in the catalytic activity tests of Fe-Ag-ZSM-5 catalysts at 2wt% Fe and Ag loading. Using the same reaction parameters as Figure 4.11. The catalytic activity of Fe-Ag-ZSM-5 was reduced by increasing the loading of the catalyst from 0.5 to 2 wt% for both metals Ag and Fe.

It is observed in Figures above 4.11, 4.12 and 4.13, that combined Fe and Ag in the ZSM-5 extremely enhance the catalytic activity irrespective of the metals loading (the loading of metal changed but the M:S ratio kept constant at 1:100). For all Fe-Ag-ZSM-5 catalysts, complete phenol oxidation, mineralization and H₂O₂ consumption were reached. The highest Fe loss was 60% after 240 min for 1wt% Fe-Ag-ZSM-5, implying the poor stability of the catalysts. While 0.5 wt% and 2wt% Fe-Ag-ZSM-5 are more durable catalysts with 30% iron loss after 240 min. Meanwhile, the Fe concentrations determined in the reaction mixture over 0.5 wt% Fe-Ag-ZSM-5 catalyst went down gradually with reaction time after 1 h owing to the re-adsorption of Fe ions onto the zeolite support. In general, to explain these similarities in the iron loss for all three mentioned catalysts, we speculate that the Fe species on the Fe-Ag-ZSM-5 catalysts prepared by the WI method are mainly extra-framework rather than intra-framework Fe.⁸⁸

Due to its high catalytic activity and durability, as well as its ability to reduce the reaction time to only one hour, 0.5wt% Fe-Ag-ZSM-5 was selected as the best catalyst in terms of effect of a low metal loading for this reaction.

4.2.4.2 Effect of different Si:Al ratios on the activity of 0.5wt% Fe- 0.5wt% Ag doped zeolites ZSM-5 and Y

Given, however, the effect that changes in Si:Al ratios may have on the CWPO reaction (see sections 4.2.3), we have invented the most promising catalyst so far, 0.5wt% Fe-Ag-ZSM-5, by evaluating the effect of changes in Si:Al ratios. As demonstrated with previous catalysts, Fe-S-N-ZSM-5, increasing the Si:Al ratio improved the catalytic activity for this reaction which could be as the lowering in the relatively hydrophilicity of the catalyst leading to protection of the catalyst from deactivation by the water. However, as different doping metals can respond differently to these kind of effects, different Si:Al ratios were tested towards Fe and Ag.

By comparing Ag-Fe-ZSM-5 Si:Al 23 with Si:Al 50 (Figure 4.14), there was no noticeable difference in the activity results. Even with the higher Si:Al ratio, the catalyst has high catalytic activity for the reaction, achieving complete phenol oxidation and mineralization, as well as H₂O₂ consumption over the reaction time. However, increasing the Si:Al ratio negatively impacts the catalyst durability and increases the iron loss from 30% to 90% with Ag-Fe-ZSM-5 Si:Al 23 and Ag-Fe-ZSM-5 Si:Al 50, respectively. This trend is difficult to interpret and it might relate to the circumstance of Fe and Ag competing for a lower number of binding sites in the zeolite material in the assumption that these binding sites are next to Al³⁺ centres.⁹⁷ When the Si:Al ratio was further increased to 80 it was also giving 100% phenol oxidation (Figure 4.14). Consequently, the catalysts have high catalytic activity for this reaction, irrespective of the array Si:Al ratios. Still, the more Si:Al catalysts exhibit greater metal leaching, affecting its stability.

The same changes in Si:Al ratio were considered for zeolite Y doped with Ag and Fe. Baek *et al.*⁹⁸ studied Mn, Fe, Co, Ni, Cu, Zn and Ag over Zeolite-Y for catalytic oxidation of toluene and methyl ethyl ketone; their results show that Ag gives the best activity. Based on that, the combination of Ag and Fe in the Zeolite-Y is supposed to be very active for phenol oxidation.

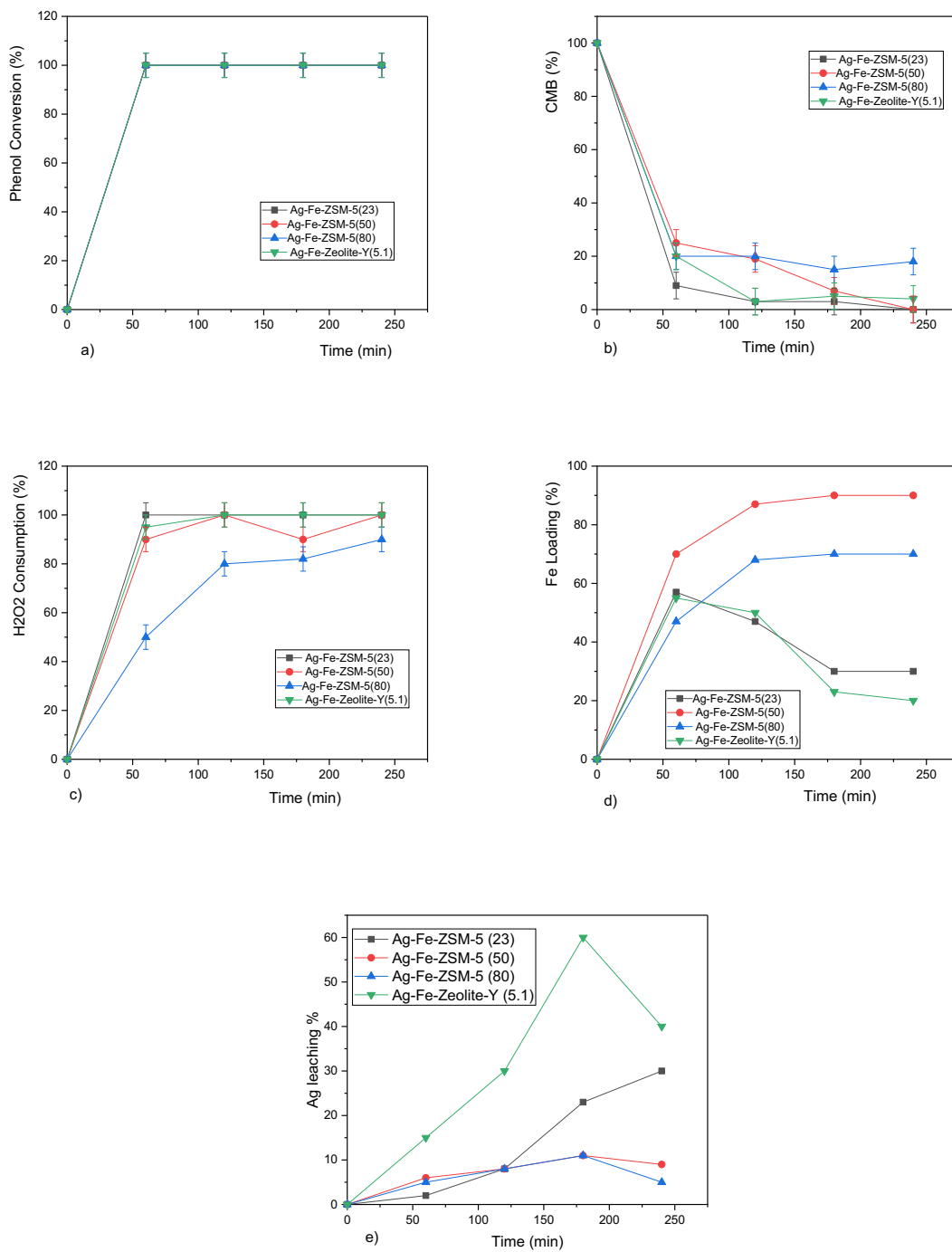


Fig 4.14: Catalytic activity results for different zeolite catalysts Ag-Fe-ZSM-5(23, 50 and 80) and Ag-Fe - Zeolite-Y (5.1) for phenol oxidation by the CWPO reaction. a) phenol conversion%, b) CMB%, c) H₂O₂ consumption%, d) Fe leaching%, and e) Ag leaching%. Phenol concentration 1g.L⁻¹ and M:S 1:100, 1:14 H₂O₂ at 80 °C for 4 h.

An overview of these data (Figure 4.14) shows the extreme activity of bimetallic Ag-Fe-Zeolite catalysts for phenol oxidation by the CWPO reaction regardless of Si:Al ratios or Zeolite types. Figure 4.14a) illustrates full phenol conversion for all catalysts, b) extensive mineralization with all catalysts, furthermore, residual intermediates reached 0% with most catalysts Ag-Fe-ZSM-5 (23, 50) and Ag-Fe-Zeolite-Y(5.1). In addition, 4.14c) shows the complete H₂O₂ consumption for the majority of the catalysts except for Ag-Fe-ZSM-5 (80), which is a bit lower than others (90%). On the other hand, a significant difference was shown by the iron leaching Figure d), where Ag-Fe-ZSM-5 (50) was less durability based on the high Fe loss (90%), then, Ag-Fe-ZSM-5 (80) was suffering as well from less stability (70%). While both Ag-Fe-ZSM-5 (23) and Ag-Fe-Zeolite-Y (5.1) are more stable, 30% and 20%, respectively. Ag leaching% in 4.14e) the highest Ag losing was with Ag-Fe-Zeolite-Y 40%, but more Si:Al increased the Ag stability to be the Ag leaching less than 10% for Ag-Fe-ZSM-5 (50) and (80). The catalytic activity of the catalyst is not affected by changing the morphology of the zeolite from ZSM-5 to Zeolite-Y (Figure 4.14). Zeolite-Y increased the durability and stability of the catalyst (20% iron leaching) while maintaining high catalytic activity.

For investigating whether the extreme activity of Ag-Fe-Zeolite catalysts comes from a synergistic effect of the two metals Ag and Fe on the support or if these are independent, 1wt% Ag-ZSM-5 Si:Al 23 catalyst was prepared under similar conditions and used in the reaction, as physical mixtures of the two zeolites were prepared and tested.

4.2.4.3 Ag-ZSM-5 1wt% metal loading

It was observed that sole Ag-ZSM-5 had no activity for the conversion of phenol (Figure 4.15) After 4 h, phenol oxidation was 24% and residual intermediates 81% also, low H₂O₂ consumption was 26%. These results. Compared with the results of using Fe-ZSM-5 which gives 100% phenol removal and 18% residual intermediates (see section 4.2.1), this confirms a synergistic effect between Ag and Fe.

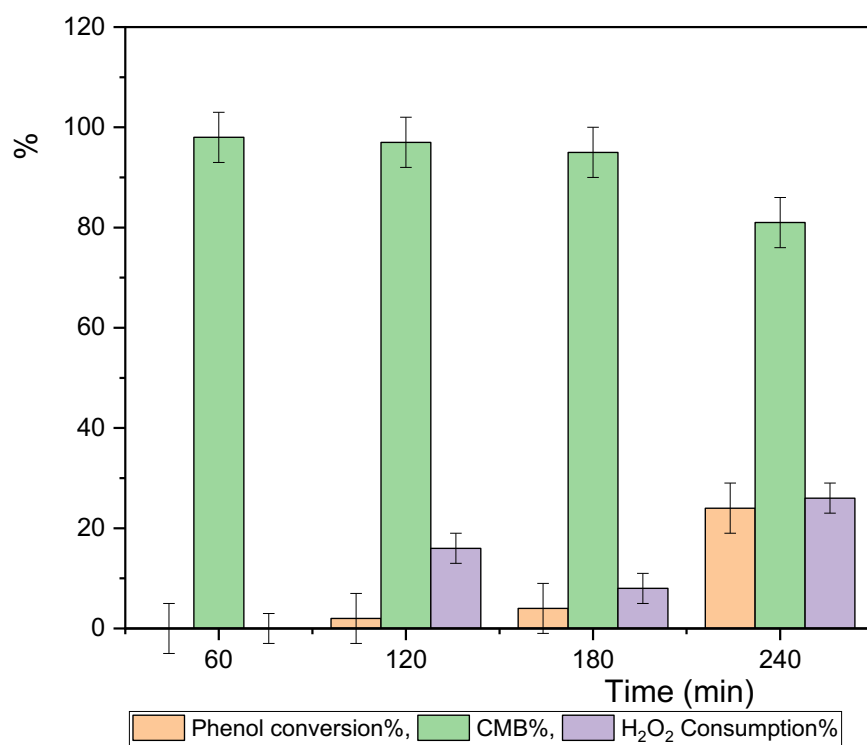


Fig 4.15: A CWPO reaction using Ag-ZSM-5 to oxidise phenol. The reaction was carried out in a 50 ml reaction vessel, with a solution containing 1 g.L⁻¹ phenol concentration and a catalyst concentration of 1:100. A molar ratio of 1:14 of H₂O₂ was used at 80 °C for 240 minutes. The catalyst has no activity in oxidizing phenol; after 240 minutes, only 24% of the phenol was oxidized.

To further corroborate these results a physical mixture of Fe-ZSM-5 and Ag-ZSM-5 was prepared and tested.

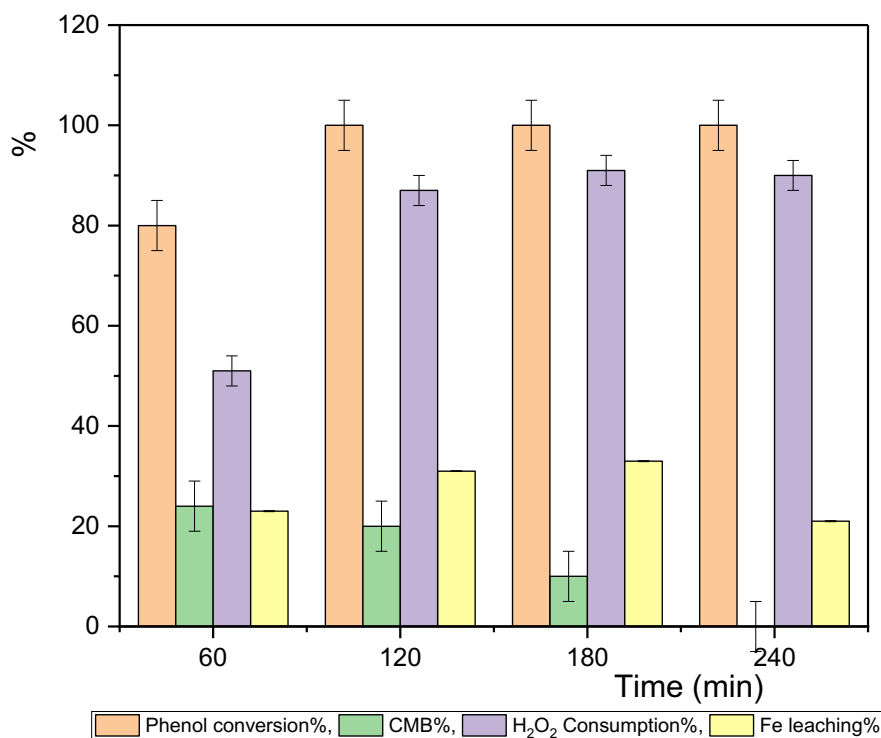


Figure 4.16: This is a kinetic reaction by which phenol is oxidized through the CWPO reaction, and this reaction is performed using a physical mix of both catalysts 1 wt% Fe-ZSM-5 (23) and 1 wt% Ag-ZSM-5 (23).

This mixture gives full phenol conversion and mineralization after 4h (Figure 4.16) with results similar to those of Fe-ZSM-5 catalysts only (see section 4.2.1) and concerning the activity of these materials. However, the leaching of Fe was as high as 84% with Fe-ZSM-5 catalysts, whereas now, this is reduced to about 24%. This result is counterintuitive as in a physical mixture Fe and Ag are not in contact. On the other hand, it may suggest that tint the presence of the two metals Ag⁺ may be attacked faster than Fe³⁺. That said, the most active material is the one when both Ag and Fe are simultaneously supported, though if these data are combined with the peck mixture data, it would also suggest that these two metals, when simultaneously present, are also segregated and behave independently with respect to each other.⁹⁹ Furthermore, it prevented Fe from leaching (30%).

4.3 Characterisation of the catalysts

4.3.1 X-ray diffraction (XRD)

As a way to characterize the crystalline structure of the prepared catalysts, XRD patterns were collected for different metals-doped zeolite catalysts. The similar XRD patterns of the pure $\text{NH}_4\text{-ZSM-5}$ support and the different catalysts in Figure 4.17 and 4.18 also pure Zeolite-Y and their catalysts in Figure 4.19 and 4.20 indicate that the original structure of $\text{NH}_4\text{-ZSM-5}$ and Zeolite-Y did not distort during the wetness impregnation process. In the Fe-Ag-ZSM-5 catalysts, patterns are attributed only to zeolite structure; mainly, no iron and silver species were detected, and XRD patterns did not differ significantly from $\text{NH}_4\text{-ZSM-5}$ support in Figure 4.17. However, it was expected to detect two peaks of iron oxide at (1 0 4) and (1 1 0) planes at 2θ of 33.0° and 35.6° respectively.²³ The silver oxide phase was expected at $2\theta = 32.28^\circ$.¹⁰⁰ As stated in Li's report,¹⁰¹ the intensity of XRD peaks depends on crystal size and dispersion on supports. A number of previous studies also found that a weak peak of crystalline phase could be attributed to good dispersion of the crystalline phase accompanied by a small crystal size.^{102, 103} It can be concluded from this that the Iron and Ag particles dispersed over the zeolite during preparation were well distributed.

ZSM-5 support and Fe-ZSM-5 catalysts are illustrated in Figure: 3.18. In all samples, diffraction peaks were observed at 2θ of $7\text{-}9^\circ$ and $23\text{-}25^\circ$, in agreement with ZSM-5's standard pattern.¹⁰⁴ For the Fe-ZSM-5 catalyst, There is a decrease in peak intensity of the Fe-ZSM-5 catalyst that may be related to increased X-ray absorption caused by Fe cations and decreases in zeolite crystal size.²³ X-ray analyses of all Fe-zeolites catalysts (Figure 4.18, 4.19 and 4.20) did not show patterns associated with iron oxide clusters. It is possible that iron oxide particles, greater than 3–5 nm in size, do not exist on Fe-ZSM-5, F-S-N-Zeolite and Fe-Ag-Zeolite catalysts. There are no discernible reflections of any extra element or its oxide; so in case any Fe_2O_3 or Ag_2O are present, they have to be rather small (less than 5 nm). However, unlike activated carbons, zeolites have tens of reflections, which also overlap with the expected positions for Fe_2O_2 and Ag_2O . Overall, the preparation did not significantly affect the lattice parameters, nor did any metal dopant if present in the form of small particulate (Table 4.1).

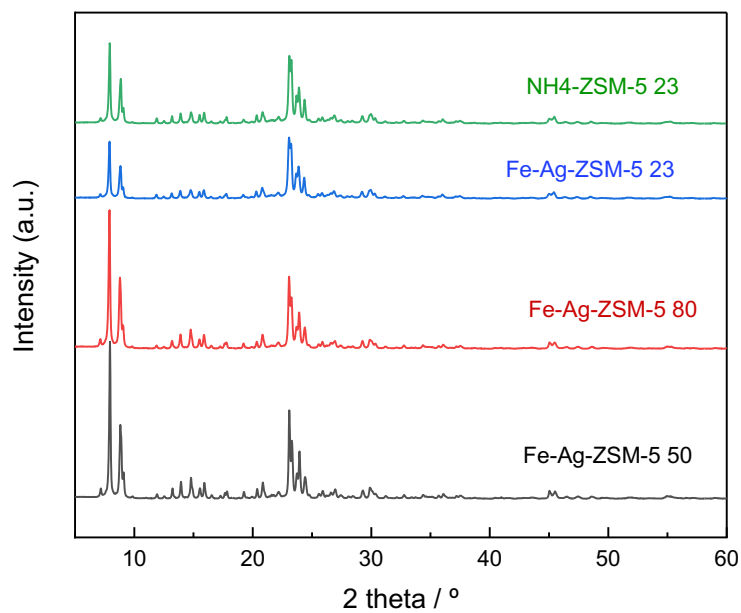


Figure 4.17: X-ray diffraction patterns of different Fe-Ag-ZSM-5 catalysts with various Si:Al ratios (23, 50 and 80) and pure NH₄-ZSM-5. All catalysts were compatible with the ZSM-5 patterns. Doping metals did not affect the zeolite crystal structure.

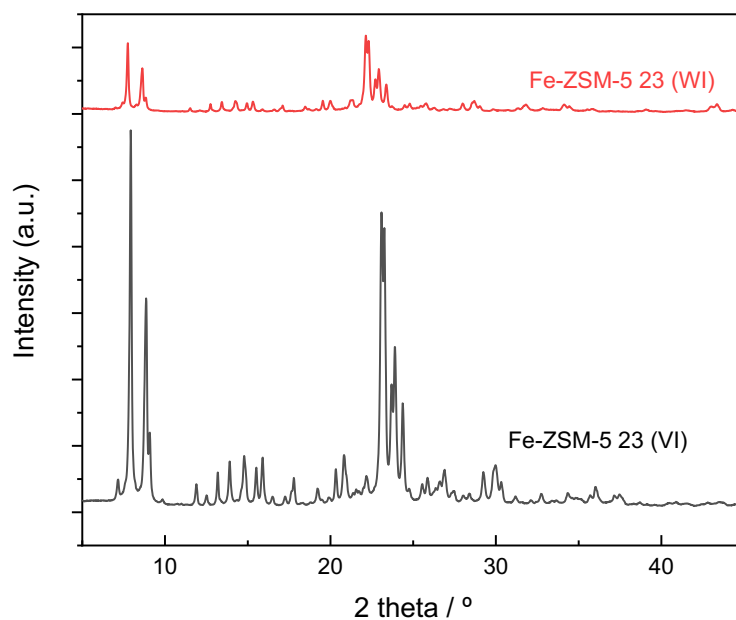


Figure 4.18: XRD patterns for Fe-ZSM-5 catalysts prepared by vacuum wetness impregnation and the second one via wetness impregnation method.

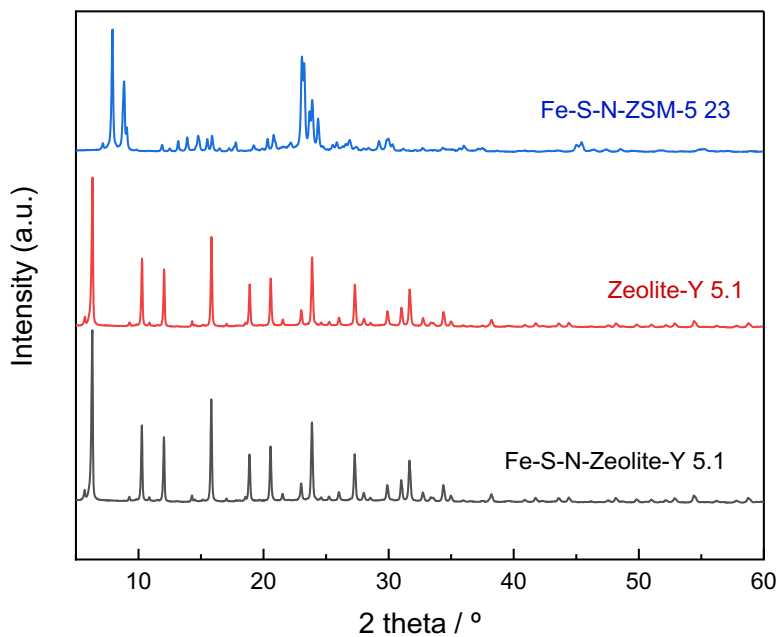


Figure 4.19: XRD patterns for Fe-S-N-Zeolite catalysts using both ZSM-5 and Zeolite-Y, in compaction with blank Zeolite-Y.

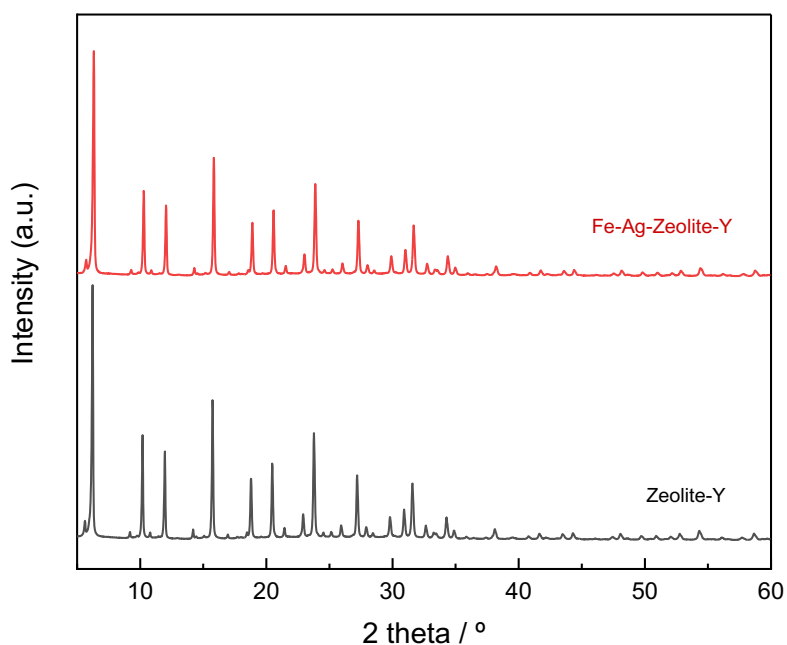


Figure 4.20: XRD patterns for Fe-Ag-Zeolite-Y and the pure zeolite-Y without doping metals. They are identical, indicating that all the patterns are linked to the Zeolite-Y framework, and there was no pattern to Fe_2O_3 or Ag_2O .

Table 4.1: Parameters of a unit cell of the Fe-doped zeolite catalysts, compared to undoped ZSM-5 and Zeolite-Y.

Catalysts	Unit cell parameters			
	a	b	c	V
Zeolite-Y (5.1)	24.511± 0.004	24.511 ± 0.004	24.511 ± 0.004	14725 ± 5
Fe-Ag-Zeolite-Y(5.1)	24.507 ± 0.003	24.507 ± 0.003	24.507 ± 0.003	14718 ± 3
Fe-S-N-Zeolite-Y(5.1)	24.496 ± 0.004	24.496 ± 0.004	24.496 ± 0.004	14700 ± 4
ZSM-5 (23)	20.104 ± 0.008	19.940 ± 0.008	13.430 ± 0.006	5384 ± 4
Fe-Ag-ZSM-5(23)	20.132 ± 0.007	19.957 ± 0.007	13.444 ± 0.006	5401 ± 3
Fe-Ag-ZSM-5 (50)	20.121 ± 0.002	19.919 ± 0.002	13.404 ± 0.002	5372 ± 1
Fe-Ag-ZSM-5 (80)	20.096 ± 0.003	19.909 ± 0.002	13.392 ± 0.002	5358 ± 1
Fe-S-N-ZSM-5 (23)	20.125± 0.005	19.944 ± 0.004	13.430 ± 0.004	5391 ± 2
Fe-ZSM-5 (23) VI	20.122 ± 0.004	19.945 ± 0.004	13.433 ± 0.004	5391 ± 2
Fe-ZSM-5 (23) WI	20.127 ± 0.013	19.952 ± 0.012	13.427 ± 0.010	5392 ± 6

a, b, c in Angstroms, *V* in Å³ all angles constrained to be 90°.

4.3.2 Porosimetry

The catalyst preparation protocol does not affect much the total surface area see Table 4.2. Regarding the protocol used, there is, however, a significant difference between the use of zeolite ZSM-5 and zeolite-Y. When the impregnation protocols are applied over zeolite ZSM-5, there is a strong decrease in the microporous surface and practically a collapse of the microporous volume. This would imply that most of the deposited metal is inside the pores of the zeolite. For zeolite-Y, instead, the trend is the opposite, and most of the dopants are associated with the external textural properties of the zeolite, thus suggesting that of this material, Fe deposition is on the other side of the zeolite crystals.

Table 4.2: Porosimetry data of the Fe-ZSM-5, Fe-Ag-ZSM-5, Fe-S-N-ZSM-5 and Fe-S-N-Zeolite-Y catalysts prepared by wetness impregnation method

Samples	S_{BET} ($\text{m}^2 \cdot \text{g}^{-1}$) ^(a)	S_{micro} ($\text{m}^2 \cdot \text{g}^{-1}$) ^(a)	S_{ext} ($\text{m}^2 \cdot \text{g}^{-1}$) ^(a)	V_{tot} ($\text{cm}^3 \cdot \text{g}^{-1}$) ^(b)	V_{micro} ($\text{cm}^3 \cdot \text{g}^{-1}$) ^(b)
H-ZSM-5	408 ± 12	275 ± 14	133 ± 7	0.19 ± 0.01	0.15 ± 0.01
Fe-Ag-ZSM-5 (Fe 0.5 wt%)	438 ± 13	67 ± 4	371 ± 19	0.31 ± 0.02	0.03 ± 0.01
Fe-S-N-ZSM-5 (Fe 1wt%)	433 ± 12	162 ± 8	271 ± 13	0.20 ± 0.01	0.08 ± 0.01
Zeolite-Y	797 ± 24	297 ± 15	500 ± 24	0.34 ± 0.02	0.26 ± 0.02
Fe-S-N-Zeolite-Y (Fe 1wt%)	727 ± 22	345 ± 12	382 ± 19	0.30 ± 0.02	0.16 ± 0.01

(a) Values obtained from the adoption branch of the adsorption isotherms using Brunauer–Emmett–Teller (BET) theory. (b) Value obtained at the absorption–desorption point using a Barret–Joyner–Halenda (BJH) method.

4.4 Diffusion test

As reported in Chapter 3, mass transfer limitations may occur in heterogeneous catalytic systems, affecting reactions and conversions. A verification of diffusion limitations (mass transfer) was necessary. Due to the fact that diffusion depends on the support and that different metals in the same support will not influence diffusion, two catalysts were examined Fe-ZSM-5 and Fe-S-N-Zeolite-Y.

4.4.1 External diffusion tests

A. Varying the stirring rate

Two possible scenarios exist: First, a higher stirring rate increases conversion. Since mixing reduces diffusion, diffusion limitations affect the reaction. As a result, diffusion may contribute to the process rate-determining step. Second, the stirring rate does not affect conversion. Therefore, diffusion phenomena do not exist, and the reaction at the surface determines the reaction rate. As shown in Table 4.4, the phenol conversion and residual intermediates did not change with the stirring rate for Fe-ZSM-5. Thus, mass transfer limitation did not take place when using Fe-ZSM-5.

Table 4.3: External diffusion tests using the different the stirring rate for the Fe-ZSM-5:

M:S	RMP/ Min	Phenol conversion% ± 5	residual intermediates% ± 5
1:100	0	100	1
1:100	200	100	7
1:100	300	100	8
1:100	500	100	7
1:100	700	100	8

The same can be concluded for Fe-S-N-Zeolite-Y (Table 4.4).

Table 4.4: External diffusion tests using the different the stirring rate for the Fe-S-N-Zeolite-Y:

M:S	RMP/ min	Phenol conversion% ± 5	residual intermediates% ± 5
1:100	0	100	10
1:100	200	100	9
1:100	300	100	8
1:100	500	100	3
1:100	700	100	5

B. Implementing different M:S

There are two possible cases that by changing M:S ratios may affect the conversion of a reaction: firstly: as the amount of catalyst increases, and the conversion also increases: this implies a kinetic regime during the reaction and thus negligible diffusion; secondly: as the catalyst amount increases, the conversion does not change. In this case, there are two further possibilities: (i) there is a diffusion limit, or (ii) conversion has already reached 100% conversion or the maximum conversion compatible with the thermodynamics of the reaction if this is an equilibrium one. Consequently, double catalyst amounts have no effect on conversion as it is already at maximum (although it should shorten the time it takes to detect 100% conversion). The M:S ratio changed by changing the amount of catalyst only.

For Fe-ZSM-5 (Table 4.5), the reaction followed a kinetic regime; that is, the observed kinetics or decay of phenol is due to the catalyst activity and not to diffusion. Moreover, considering the experimental error, residual intermediates decreased to zero within the experimental error, which is a highly valuable result.

Table 4.5: External diffusion tests using the different M:S for the Fe-ZSM-5

M:S	RMP/ Min	Phenol conversion% ± 5	residual intermediates% ± 5
0.1:100	500	4	94
0.5:100	500	13	88
1:100	500	100	7
15:100	500	100	4
20:100	500	100	3

Similar considerations can be done also for Fe-S-N-Zeolite-Y.

Table 4.6: External diffusion tests using the different M:S for the Fe-S-N-Zeolite-Y:

M:S	RMP/ min	Phenol conversion% ± 5	residual intermediates% ± 5
0.1:100	500	40	75
0.5:100	500	80	40
1:100	500	100	0
15:100	500	100	0
20:100	500	100	0

Based on these data, external diffusion limitations did not affect our catalytic tests. Thus, the reported data are validated.

4.5 Conclusion

Fe-ZSM-5 was prepared using various iron precursors and ZSM-5 frameworks (H-ZSM-5 and NH₄-ZSM-5) with differing Fe loading. Fe-ZSM-5 by FeNO₃.9H₂O and NH₄-ZSM-5 at 1 wt.% iron doping results in higher activity. This catalyst also has high catalytic activity for phenol oxidation by the CWPO reaction regardless of the preparation methods studied, that is there was no significant difference between wetness impregnation either under normal conditions or under vacuum. Then, doping S and N with Fe-Zeolite significantly enhances the catalytic activity and stability of this reaction, resulting in 100% phenol conversion and 0% residual intermediates within 60 minutes, while Fe-ZSM-5 gives 100% and 20% residual intermediates in 4 hours. In addition, the durability of the catalyst improved by 50%. Iron leaching was 80% for Fe-ZSM-5 and dropped to 40% with Fe-S-N-ZSM-5. Increasing Si:Al ratios increase the catalytic activity. Moreover, Fe-S-N-Zeolite-Y was found to be an active and durable catalyst. Finally, material preparing by containing simultaneously Ag and Fe, and as such to be classed as bimetallic zeolites, presented multiple features. the coexistence of the two metals reduced the reaction time from 4h to 1h, leading to a reduction in the cost and energy consumption of the process. In addition, good stability is another feature associated with these catalysts 20% and 30% Fe leaching for Fe-Ag-Zeolite-Y and Fe-Ag-ZSM-5 Si:Al 23 respectively.

For characterizing the crystalline structure of zeolite catalysts, XRD patterns have been collected from zeolite catalysts doped with various metals. It appears from the XRD patterns of pure NH₄-ZSM-5 support and the different catalysts, as well as pure Zeolite-Y and their catalysts, suggesting that their original structures did not alter during wetness impregnation. In the Fe-Ag-ZSM-5 catalysts, only zeolite structures are responsible for the patterns; in particular, no iron or silver species were detected, and XRD patterns were not significantly different from NH₄-ZSM-5 support. Crystal size and dispersion on the support affect the intensity of XRD peaks. In previous studies, good dispersion of crystalline phase accompanied by a small crystal size was also found to be related to weak peaks of crystalline phase. This indicates that the iron and silver particles dispersed over the zeolite during preparation were highly distributed.

Iron oxide clusters were not detected in any of the Fe-zeolites catalysts analysed with X-rays. It is possible that Fe-ZSM-5, F-S-N-Zeolite, and Fe-Ag-Zeolite catalysts do not contain iron oxide particles larger than 3–5 nm. There are no discernible reflections of any extra elements

or their oxides; so in case any Fe_2O_3 or Ag_2O are present, they have to be rather small (less than 5 nm). Zeolites, however, have tens of reflections, which overlap with Fe_2O_2 and Ag_2O 's expected positions, unlike activated carbons. In general, neither the preparation nor a metal dopant presents as small particles affected the lattice parameters.

These catalysts provide excellent results and reach the target full phenol oxidation and mineralization. The stability of these catalysts was enhanced significantly by adding the S, N and Ag. However, still these catalysts suffer from metals leaching affecting their durability. More efforts are required to solve this challenge. Accordingly, these results become a motivation to apply selected of the best catalysts for another phenolic compound oxidation, as will be studied in the next chapter.

4.6 References

1. H. Qin, R. Xiao and J. Chen, *Science of the Total Environment*, 2018, **626**, 1414-1420.
2. A. Aziz and K. S. Kim, *Journal of hazardous materials*, 2017, **340**, 351-359.
3. H. M. S. Munir, N. Feroze, N. Ramzan, M. Sagir, M. Babar, M. S. Tahir, J. Shamshad, M. Mubashir and K. S. Khoo, *Chemosphere*, 2022, **297**, 134031.
4. T. X. H. Le, M. Drobek, M. Bechelany, J. Motuzas, A. Julbe and M. Cretin, *Microporous and Mesoporous Materials*, 2019, **278**, 64-69.
5. X. Hu, L. Lei, H. P. Chu and P. L. Yue, *Carbon*, 1999, **37**, 631-637.
6. A. Bhatnagar, W. Hogland, M. Marques and M. Sillanpää, *Chemical Engineering Journal*, 2013, **219**, 499-511.
7. A. Rey, M. Faraldos, J. Casas, J. Zazo, A. Bahamonde and J. Rodríguez, *Applied Catalysis B: Environmental*, 2009, **86**, 69-77.
8. R.-M. Liou and S.-H. Chen, *Journal of Hazardous Materials*, 2009, **172**, 498-506.
9. A. Quintanilla, J. Casas and J. Rodriguez, *Applied Catalysis B: Environmental*, 2010, **93**, 339-345.
10. C. M. Domínguez, A. Quintanilla, J. A. Casas and J. J. Rodríguez, *Chemical Engineering Journal*, 2014, **253**, 486-492.
11. S. Messele, F. Stüber, C. Bengoa, A. Fortuny, A. Fabregat and J. Font, *Procedia Engineering*, 2012, **42**, 1373-1377.
12. E. Auer, A. Freund, J. Pietsch and T. Tacke, *Applied Catalysis A: General*, 1998, **173**, 259-271.
13. C. N. Satterfield, *Heterogeneous catalysis in practice*, McGraw-Hill Companies, 1980.
14. K. Fajerweg and H. Debellefontaine, *Applied Catalysis B: Environmental*, 1996, **10**, L229-L235.
15. P. Wang, S. Wang, Y. Yue, T. Wang and X. Bao, *Microporous and Mesoporous Materials*, 2020, **292**, 109748.
16. V. Rac, V. Rakić, D. Stošić, O. Otman and A. Auroux, *Microporous and mesoporous materials*, 2014, **194**, 126-134.
17. A. Corma, S. Zones and J. Cejka, *Zeolites and catalysis: synthesis, reactions and applications*, John Wiley & Sons, 2010.
18. R. P. Lively, R. R. Chance and W. J. Koros, *Industrial & Engineering Chemistry Research*, 2010, **49**, 7550-7562.

19. P. Misaelides, *Microporous and Mesoporous Materials*, 2011, **144**, 15-18.
20. J. Weitkamp, *Solid state ionics*, 2000, **131**, 175-188.
21. K. Li, J. Valla and J. Garcia-Martinez, *ChemCatChem*, 2014, **6**, 46-66.
22. D. He, H. Zhang and Y. Yan, *Royal Society open science*, 2018, **5**, 172364.
23. Y. Yan, S. Jiang and H. Zhang, *Separation and Purification Technology*, 2014, **133**, 365-374.
24. O. P. Taran, A. N. Zagoruiko, A. B. Ayusheev, S. A. Yashnik, R. V. Prihod'ko, Z. R. Ismagilov, V. V. Goncharuk and V. N. Parmon, *Chemical Engineering Journal*, 2015, **282**, 108-115.
25. M. M. Mohamed, I. O. Ali and N. Eissa, *Microporous and Mesoporous Materials*, 2005, **87**, 93-102.
26. A. Ribera, I. Arends, S. De Vries, J. Pérez-Ramírez and R. Sheldon, *Journal of Catalysis*, 2000, **195**, 287-297.
27. J. B. Taboada, A. R. Overweg, P. J. Kooyman, I. W. Arends and G. Mul, *Journal of Catalysis*, 2005, **231**, 56-66.
28. J. Pérez-Ramírez, G. Mul, F. Kapteijn, J. Moulijn, A. Overweg, A. Doménech, A. Ribera and I. Arends, *Journal of Catalysis*, 2002, **207**, 113-126.
29. M. Schwidder, M. S. Kumar, K. Klementiev, M. M. Pohl, A. Brückner and W. Grünert, *Journal of Catalysis*, 2005, **231**, 314-330.
30. G. Li, E. A. Pidko, R. A. van Santen, C. Li and E. J. Hensen, *The Journal of Physical Chemistry C*, 2013, **117**, 413-426.
31. J. Pérez-Ramírez, *Journal of Catalysis*, 2004, **227**, 512-522.
32. E. Hensen, Q. Zhu, M. Hendrix, A. Overweg, P. Kooyman, M. Sychev and R. Van Santen, *Journal of Catalysis*, 2004, **221**, 560-574.
33. G. Centi, S. Perathoner, T. Torre and M. G. Verduna, *Catalysis Today*, 2000, **55**, 61-69.
34. O. Makhotkina, E. Kuznetsova and S. Preis, *Applied Catalysis B: Environmental*, 2006, **68**, 85-91.
35. K. M. Valkaj, A. Katovic and S. Zrnčević, *Industrial & Engineering Chemistry Research*, 2011, **50**, 4390-4397.
36. M. Dükkançı, G. Gündüz, S. Yılmaz and R. Prihod'ko, *Journal of hazardous materials*, 2010, **181**, 343-350.
37. E. Kuznetsova, E. Savinov, L. Vostrikova and V. Parmon, *Applied Catalysis B: Environmental*, 2004, **51**, 165-170.

38. O. P. Pestunova, G. L. Elizarova, Z. R. Ismagilov, M. A. Kerzhentsev and V. N. Parmon, *Catalysis today*, 2002, **75**, 219-225.
39. N. H. Phu, T. T. K. Hoa, N. Van Tan, H. V. Thang and P. Le Ha, *Applied Catalysis B: Environmental*, 2001, **34**, 267-275.
40. E. Parkhomchuk, M. Vanina and S. Preis, *Catalysis Communications*, 2008, **9**, 381-385.
41. I. Stolyarova, I. Kovban', R. Prikhod'ko, A. Kushko, M. Sychev and V. Goncharuk, *Russian Journal of Applied Chemistry*, 2007, **80**, 746-753.
42. M. Romero-Sáez, D. Divakar, A. Aranzabal, J. González-Velasco and J. González-Marcos, *Applied Catalysis B: Environmental*, 2016, **180**, 210-218.
43. D. Divakar, M. Romero-Sáez, B. Pereda-Ayo, A. Aranzabal, J. A. González-Marcos and J. R. González-Velasco, *Catalysis today*, 2011, **176**, 357-360.
44. S. Brandenberger, O. Kröcher, A. Tissler and R. Althoff, *Catalysis Reviews*, 2008, **50**, 492-531.
45. A. Zecchina, M. Rivallan, G. Berlier, C. Lamberti and G. Ricchiardi, *Physical chemistry chemical physics*, 2007, **9**, 3483-3499.
46. M. S. Kim and E. D. Park, *Microporous and Mesoporous Materials*, 2021, **324**, 111278.
47. H. J. H. Fenton, *Journal of the Chemical Society, Transactions*, 1894, **65**, 899-910.
48. W. Barb, *Nature*, 1949, **163**, 692-694.
49. J. De Laat and H. Gallard, *Environmental science & technology*, 1999, **33**, 2726-2732.
50. C. Walling and M. Cleary, *International Journal of Chemical Kinetics*, 1977, **9**, 595-601.
51. V. Sarria, S. Kenfack, O. Guillod and C. Pulgarin, *Journal of Photochemistry and Photobiology A: Chemistry*, 2003, **159**, 89-99.
52. E. E. Kiss, J. G. Ranogajec, R. P. Marinković-Nedučin and T. J. Vulić, *Reaction Kinetics and Catalysis Letters*, 2003, **80**, 255-260.
53. J. Sotelo, G. Ovejero, F. Martinez, J. Melero and A. Milieni, *Applied Catalysis B: Environmental*, 2004, **47**, 281-294.
54. G. Delahay, M. Mauvezin, B. Coq and S. Kieger, *Journal of Catalysis*, 2001, **202**, 156-162.
55. G. Delahay, M. Mauvezin, A. Guzman-Vargas and B. Coq, *Catalysis Communications*, 2002, **3**, 385-389.
56. H.-Y. Chen, T. Voskoboinikov and W. M. Sachtler, *Journal of Catalysis*, 1998, **180**, 171-183.

57. E.-M. El-Malki, R. Van Santen and W. Sachtler, *Journal of Catalysis*, 2000, **196**, 212-223.
58. S. O. Lee, T. Tran, Y. Y. Park, S. J. Kim and M. J. Kim, *International Journal of Mineral Processing*, 2006, **80**, 144-152.
59. S. Mandal and P. C. Banerjee, *International Journal of Mineral Processing*, 2004, **74**, 263-270.
60. Y.-J. Huang, J. Schwarz, J. Diehl and J. Baltrus, *Applied catalysis*, 1988, **36**, 163-175.
61. A. Infantes-Molina, C. Moreno-León, B. Pawelec, J. Fierro, E. Rodríguez-Castellón and A. Jiménez-López, *Applied Catalysis B: Environmental*, 2012, **113**, 87-99.
62. G. Lee, Y. Jeong, B.-G. Kim, J. S. Han, H. Jeong, H. B. Na and J. C. Jung, *Catalysis Communications*, 2015, **67**, 40-44.
63. Y. Wang, *Nonlinear Analysis: Theory, Methods & Applications*, 2007, **67**, 103-125.
64. X. Zhou, Q. Chen, Y. Tao and H. Weng, *Journal of natural gas chemistry*, 2011, **20**, 350-355.
65. J. Mao, B. Wan, F. Wu, R. Wang and S. Lu, *Journal of Molecular Catalysis-A-Chemical*, 2005, **232**, 9-12.
66. J. Guo and M. Al-Dahhan, *Industrial & engineering chemistry research*, 2003, **42**, 2450-2460.
67. J. Zazo, J. Casas, A. Mohedano and J. Rodríguez, *Applied Catalysis B: Environmental*, 2006, **65**, 261-268.
68. G. Yang, S. Mo, B. Xing, J. Dong, X. Song, X. Liu and J. Yuan, *Environmental Pollution*, 2020, **258**, 113687.
69. S. Messele, O. Soares, J. Órfão, F. Stüber, C. Bengoa, A. Fortuny, A. Fabregat and J. Font, *Applied Catalysis B: Environmental*, 2014, **154**, 329-338.
70. Y. Yao, H. Chen, C. Lian, F. Wei, D. Zhang, G. Wu, B. Chen and S. Wang, *Journal of hazardous materials*, 2016, **314**, 129-139.
71. X. Cheng, H. Guo, Y. Zhang, Y. Liu, H. Liu and Y. Yang, *Journal of colloid and interface science*, 2016, **469**, 277-286.
72. M. Pu, Y. Ma, J. Wan, Y. Wang, M. Huang and Y. Chen, *Journal of colloid and interface science*, 2014, **418**, 330-337.
73. A. Corma, *Chemical reviews*, 1995, **95**, 559-614.
74. M. Mauvezin, G. Delahay, F. Kisslich, B. Coq and S. Kieger, *Catalysis letters*, 1999, **62**, 41-44.

75. C. Kalamaras, D. Palomas, R. Bos, A. Horton, M. Crimmin and K. Hellgardt, *Catalysis Letters*, 2016, **146**, 483-492.
76. G. Busca, *Microporous and Mesoporous Materials*, 2017, **254**, 3-16.
77. C. Costa, I. Dzikh, J. M. Lopes, F. Lemos and F. R. Ribeiro, *Journal of Molecular Catalysis A: Chemical*, 2000, **154**, 193-201.
78. T. Okuhara, *Chemical reviews*, 2002, **102**, 3641-3666.
79. L. Shirazi, E. Jamshidi and M. Ghasemi, *Crystal Research and Technology: Journal of Experimental and Industrial Crystallography*, 2008, **43**, 1300-1306.
80. R. Szostak, *Handbook of molecular sieves: structures*. Springer Science & Business Medi, New York, 1992.
81. V. Nikolakis, G. Xomeritakis, A. Abibi, M. Dickson, M. Tsapatsis and D. G. Vlachos, *Journal of Membrane Science*, 2001, **184**, 209-219.
82. D. Verboekend, N. Nuttens, R. Locus, J. Van Aelst, P. Verolme, J. Groen, J. Pérez-Ramírez and B. F. Sels, *Chemical Society Reviews*, 2016, **45**, 3331-3352.
83. T. Li, H. Liu, Y. Fan, P. Yuan, G. Shi, X. T. Bi and X. Bao, *Green chemistry*, 2012, **14**, 3255-3259.
84. O. Travkina, M. Agliullin, N. Filippova, A. Khazipova, I. Danilova, N. Grigor'Eva, N. Narender, M. Pavlov and B. Kutepov, *RSC advances*, 2017, **7**, 32581-32590.
85. J. Jin, C. Peng, J. Wang, H. Liu, X. Gao, H. Liu and C. Xu, *Industrial & Engineering Chemistry Research*, 2014, **53**, 3406-3411.
86. H. Hassan and B. Hameed, *Desalination*, 2011, **276**, 45-52.
87. S. Van Donk, A. H. Janssen, J. H. Bitter and K. P. de Jong, *Catalysis Reviews*, 2003, **45**, 297-319.
88. C. Zhou, PhD, thesis, University of Sheffield, 2021.
89. E. Aneggi, A. Trovarelli and D. Goi, *Journal of environmental chemical engineering*, 2017, **5**, 1159-1165.
90. J. Carriazo, E. Guélou, J. Barrault, J.-M. Tatibouët, R. Molina and S. Moreno, *Water research*, 2005, **39**, 3891-3899.
91. F. Tomul, F. T. Basoglu and H. Canbay, *Applied Surface Science*, 2016, **360**, 579-593.
92. G. Zhao, H. Liang, H. Xu, C. Li, Q. Tan and D. Zhang, *RSC advances*, 2021, **11**, 15959-15968.
93. Z. Khan, N. F. Dummer and J. K. Edwards, *Philosophical Transactions of the Royal Society A: Mathematical, Physical and Engineering Sciences*, 2018, **376**, 20170058.

94. A. Jodaei, A. Niaei and D. Salari, *Korean Journal of Chemical Engineering*, 2011, **28**, 1665-1671.
95. B. Izadkhah, S. Nabavi, A. Niaei, D. Salari, T. M. Badiki and N. Çaylak, *Journal of Industrial and Engineering Chemistry*, 2012, **18**, 2083-2091.
96. N. Delibaş, *Journal of Industrial and Engineering Chemistry*, 2012, **18**, 2083-2091.
97. E. Morra, M. Signorile, E. Salvadori, S. Bordiga, E. Giamello and M. Chiesa, *Angewandte Chemie*, 2019, **131**, 12528-12533.
98. S.-W. Baek, J.-R. Kim and S.-K. Ihm, *Catalysis Today*, 2004, **93**, 575-581.
99. O. Kubaschewski, *Iron—Binary phase diagrams*, Springer Science & Business Media, 2013.
100. A. Jodaei, D. Salari, A. Niaei, M. Khatamian and N. Caylak, *Environmental technology*, 2011, **32**, 395-406.
101. X. Li, L. Wang, Q. Xia, Z. Liu and Z. Li, *Catalysis Communications*, 2011, **14**, 15-19.
102. Z.-Q. Zou, M. Meng, L.-H. Guo and Y.-Q. Zha, *Journal of hazardous materials*, 2009, **163**, 835-842.
103. J.-L. Cao, Y. Wang, T.-Y. Zhang, S.-H. Wu and Z.-Y. Yuan, *Applied Catalysis B: Environmental*, 2008, **78**, 120-128.
104. O. Levenspiel, *Chemical reaction engineering*, John wiley & sons, 1998.

Chapter 5: Oxidation of phenolic compounds and homologues

5.1 Introduction

The results obtained so far and described in chapters 3 and 4 prompted us to apply the most promising activated carbon and zeolite based iron catalysts for the oxidation of phenolic compounds. This is with the aim of expanding the applicability of our materials and gathering structural information on which kinds of phenolic based compounds can be better degraded by using an approach based on the catalytic wet peroxide decomposition.

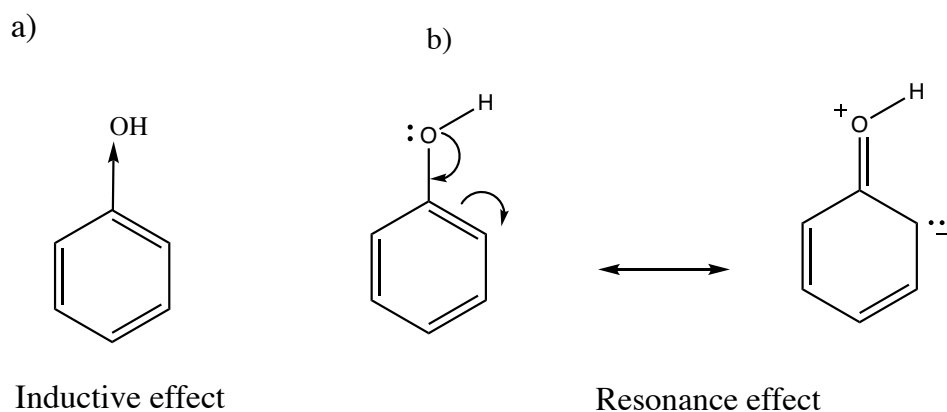
It is well known that the composition of industrial organic wastewater is extremely complex, so the chemical structure of pollutants plays a crucial role to the efficiency of the degradation process. Furthermore, for the selection of advanced oxidation processes, the cooperative effect of different active oxygen species such as hydroxyl radical ($\cdot\text{OH}$), or ozone (O_3), the catalysts used can also change the degradation mechanism. As a result, different conclusions will be obtained based on different starting reaction mixture's compositions.¹

It has been reported that the electron-interaction between benzene rings and their substituents influences the resistance to degradation in many organic compounds.² In phenolic compounds, substituent number, position and the types of substituent group either donating or withdrawing electrons have a significant impact on reactivity.³ For example, in the case of substituted phenols, degradation rates of phenols that contain *ortho* or *para* substituent take a long time because of steric hindrance.^{4, 5} The degradation rates of phenols with *ortho*-substituents can indeed be influenced by steric hindrance, but whether the substituents donate or withdraw electrons can also play a significant role. Both factors steric hindrance and electronic effects can impact the reactivity of *ortho* and *para*-substituted phenols in degradation reactions. *Ortho*-substituents on phenolic compounds can lead to steric hindrance, which hinders the approach of reactants (such as oxidants or other molecules involved in degradation reactions) to the reactive sites on the phenol ring. This may slow down the reaction rate and result in longer degradation times. The electronic nature of the substituents also influences the degradation rates. *Ortho*-substituents can be classified as electron-donating or electron-withdrawing based on their effect on the phenol ring's electron density. These electronic effects impact the stability of the phenol's intermediate radicals during oxidation reactions. Electron-donating substituents (e.g., $\cdot\text{OH}$) can stabilize radicals and enhance reactivity, potentially counteracting the steric hindrance effects. On the other hand, electron-withdrawing substituents (e.g., $-\text{NO}_2$) can interfere with radicals and pending the nature of the attacking radical species, either slow down

or accelerate a reaction. Therefore, the combined influence of steric hindrance and electronic effects can lead to varied degradation rates for *ortho* and *para*-substituted phenols, depending on the specific substituent and reaction conditions. In some cases, the steric hindrance effect will dominate, thus resulting in slower degradation rates regardless of whether the substituent donates or withdraws electrons. In other cases, the electronic effects will outweigh steric hindrance, leading to more complex reactivity patterns. Regarding the number of substituents, with a higher electron-withdrawing group number, the degradation rate decreases. On the other hand, as $\cdot\text{OH}$ radical is electron deficient and as such practically bearing like-if bearing a small positive charge, it would be expected that degradation rates would increase with the presence of electron donating groups.⁶ The same expectation applies to *para*-substituted phenols.⁷⁻⁹

The electronic structures of the target molecules are expected to influence the reaction. In the case of our reaction, $\cdot\text{OH}$ usually attacks aromatic compounds by an electrophilic-like substitution meaning that $\cdot\text{OH}$ will mainly attack directly the aromatic ring. In this assumption, the decomposition rate is determined by this same step,¹⁰ which also occur to be the first step in the radical oxidation reaction mechanism.¹¹ As a consequence, substitutions on the ring will be able to induce a control of the position of $\cdot\text{OH}$ addition, with *ortho*- and *para*-hydroxylation usually predominating due to the electrophilic nature of $\cdot\text{OH}$.^{12, 13} An additional oxidation in the dihydroxy compound occurs by removing a hydrogen atom, resulting in benzoquinones; aliphatic acids can then be formed by cleaving the ring.¹⁴

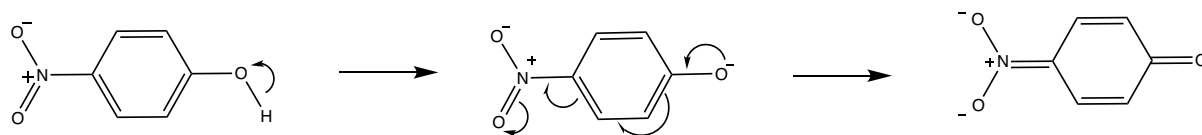
As mentioned above, the electron-donating or electron-withdrawing effect of a substituent in an aromatic ring plays a significant role in controlling the reactivity of phenolic compounds towards the catalyst.¹⁵⁻¹⁸ However, an atom or functional group within a compound may exhibit electronic effects known as resonance or inductive effect. Electronegativity determines the inductive effect of an atom or functional group. An atom or functional group that is electronegative compared to H such as the halogens, oxygen and nitrogen. The term resonance refers to the bonding or sharing of electrons between more than two atoms (nuclei).¹⁹ Scheme 5.1 show that phenol can withdraw electron density via the inductive effect (a) and donate electrons via the resonance effect (b).



Scheme 5.1: The electron density of phenol can be withdrawn by its inductive effect (a) as well as donated by its resonance effect (b).

Two groups of phenolic derivatives were determined according to their ability to accept or give electrons from or to the aromatic ring: (a) These include phenols with electron-donating substituents. Since electronic delocalisation in the ring is favoured, they are expected to be more easily oxidised.²⁰ (b) Other phenol derivatives that are electron-withdrawing and they are expected to be more complicated to oxidise.²¹ Electron donors contain at least one pair of non-bonded electrons on the atom participating in resonance (-OH, -OR, -NR₂, -SR). Therefore, donating electrons promote reactions.

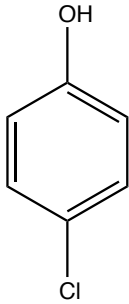
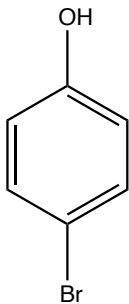
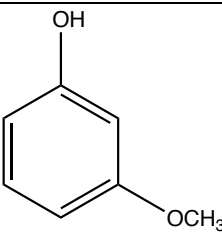
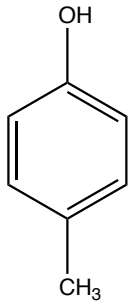
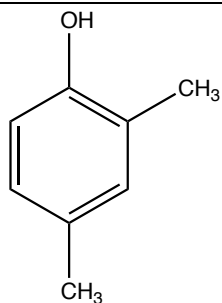
Electron-withdrawing groups consist of atoms or functional groups that possess a higher electronegativity compared to the surrounding atoms in a molecule. These groups tend to pull electron density away from the rest of the molecule, particularly from conjugated systems like aromatic rings. As a result, they exhibit a deactivating effect on the reactivity of the aromatic ring. The following examples Scheme 5.2 illustrate this:



Scheme 5.2: Electron withdrawing groups, consist of atoms lacking electrons attached to a conjugation site. That deactivated reactivity on the aromatic ring.

Five phenol derivatives were chosen for discussion of the influence of the structure of phenolic compounds on degradation performance and possible expand the applicability range of our catalysts. Table 5.1, show the formula of these phenolic compounds, they are mainly industrial chemicals and pharmaceuticals found in wastewater.²²

Table 5.1: The five phenolic compounds involved in this study.

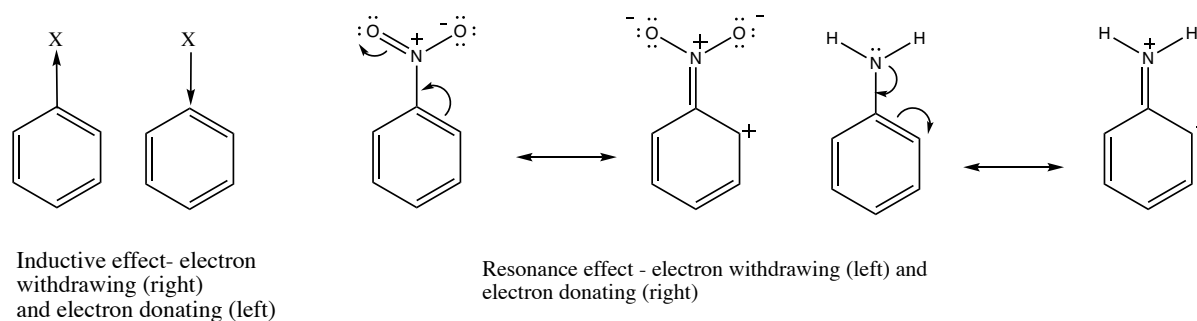
Phenolic compounds	Chemical formulas
4-chlorophenol (4CP)	 <chem>Oc1ccc(Cl)cc1</chem>
4-bromophenol (4BrP)	 <chem>Oc1ccc(Br)cc1</chem>
3-methoxyphenol (3MOP)	 <chem>Oc1cccc(OC)c1</chem>
4-Cresol (4MP)	 <chem>Cc1ccc(O)cc1</chem>
2,4 di methyl-phenol (DMP)	 <chem>Cc1c(O)cccc1C</chem>

Their reactivity is predicted by the following factors:

- I. The 4-chlorophenol (**4CP**) is expected to exhibit five effects: (i) chlorine is withdrawing-electron group by inductive effect since Cl more electronegative than C which is expected to negatively impact on the oxidation rate. (ii) On the other hands though, chlorine is at the same time a donating-electron functional group via resonance affect, since it could share electron with conjugation (in an electronic configuration, the bonds alternate between single bonds and double bonds pi bonds), which is expected to enhance the degradation process. However, (iii) chlorination may involve for the reaction by generation Cl^{\bullet} radicals which has very high oxidation potential, which could increase the reaction's rate. (iv) a scavenger function by Cl^{\bullet} radicals, according to some literature studies Cl^{\bullet} radicals could prevent the oxidation by scavenge $\bullet\text{OH}$ radicals.²³⁻²⁶ Consequently, inhibit the degradation of 4CP. In addition, (v) the effect of the substituent position, as mentioned above, para substituted phenols are supposed to be difficult to oxidise as the provided position for electrophilic attack will be limited.
- II. In 4-bromophenol (**4BrP**), the same five factors (i)-(v) described for 4CP are present. Bromine is withdrawing electron group by inductive effect so could negatively impact on the oxidation of 4BrP. However, bromine is donating electron to aromatic ring via resonance that promotes the oxidation. Still, a debromination step is one of the possible mechanisms may occur during the oxidation of 4BrP. Br^{\bullet} radicals could play role in the oxidation process increasing the efficiency of the 4BrP conversion. On the other hand, as for Cl^{\bullet} , these free Br^{\bullet} radicals may be scavenger of hydroxyl radicals effecting on both Br^{\bullet} free radicals' sufficient amount to oxidation reaction and $\bullet\text{OH}$ radicals that need to attack the target. Finally; the position of Br substituent is important and para are not preferable.
- III. The 3-methoxyphenol (**3MOP**) oxidation procedure is influenced by four variables: firstly; 3MOP could be considered as a withdrawing functional group by inductive effect That will decrease the oxidation rate. Meanwhile, 3MOP could behave as a donating-electrons to the phenolic ring enhancing the degradation that by resonance. The third possibility; $\bullet\text{OCH}_3$ could enhance the oxidation of 3MOP as another oxidising agent. Moreover, the impact of meta position which expected to increase the rate of oxidation by providing more electrophilic sites on the ring.

- IV.** 4-methylphenol (**4MP**), for this species, oxidation may be influenced by two factors. First; the presence of the phenolic ring suggests the possibility of resonance effects. However, the methyl group (CH_3) attached to the ring does not participate in resonance due to the sp^3 hybridization of the carbon atom. In 4-methylphenol, the methyl group (CH_3) is electron-donating due to its inductive effect, which means it donates some electron density to the rest of the molecule. This makes the electrons in the ring more accessible, and the aromatic system becomes more electron-rich. As a result, makes phenols more susceptible to oxidation.
- V.** 2,4 dimethylphenol (**DMP**) in this compound only one position will be available to electrophilic attacks. Steric hindrance occurs when large substituents obstruct the approach of other molecules or groups. Due to the arrangement of the methyl groups, the electrophilic attack on the phenolic ring becomes challenging. On the other hands, the methyl groups ($-\text{CH}_3$) at the 2 and 4 positions are electron-donating in nature due to their inductive effect. This means they donate electron density to the aromatic ring. The presence of the electron-rich system increases the potential for electrophilic attacks, as the ring is more capable of sharing its electron density.
- VI.** It is important to note that the residual intermediates calculation was estimated for these phenolic compounds based on the calibration curves of phenol's intermediates.

The inductive and resonance effects are essential in explaining the behaviour of phenolic compounds degradation. The study report in this thesis work delves into the intricate between these effects produced by electron-donating and electron-withdrawing groups. An example explaining these effects is shown in Scheme 5.3.



Scheme 5.3: Inductive and resonance effects by either electron donating or electron withdrawing groups.

Due to the array of factors involved in the degradation process, some promoting the oxidation process and some impeding it, no clear prediction will be possible unless only one of these factors is largely dominant with respect to the others. It is also due to this, that despite many studies aiming to enhance the removal of hazardous organic compounds, degradation mechanisms remain unknown due to their inner complexities.²⁷

5.2 Characterization of phenolic compounds

In analogy to the methodological approach described for phenol (Chapter 2), these phenolic compounds were analysed at the first optimal wavelength for the characterization of these various compounds, and the identification of their retention times by means of standards was carried out (Table 5.2).

Table 5.2: Peak position and the optimal wavelength for the maximum absorption of phenolic compounds separated by HPLC:

Compound	Abbreviation	Wave length (λ) / nm	Retention time / min
3-methoxyphenol	3MOP	274	16.8
4-Cresol	4MP	273	18.3
4-chlorophenol	4CP	281	19.4
4-bromophenol	4BrP	281	19.7
2,6 di methyl-phenol	DMP	271	20.3

Reversed-phase chromatography was used, the stationary phase is non-polar (*n*-octyldecyl (C₁₈) hydrocarbon chain), and the mobile phase is polar (acetonitrile), so the molecules that are

polar will elute first elution order from shorter to longer retention time as reported in Table 5.2 is:



3MOP has a methoxy group (-OCH₃) in the meta position to the phenolic -OH group, whereas 4MP has a methyl group (-CH₃) in the para position to the -OH group. The methoxy group in 3MOP is more polar than the methyl group in 4MP, which makes 3MOP less retained on the non-polar stationary phase, resulting in a shorter retention time. Then, 4CP and 4BrP, halogens are more electronegative than carbon, and their presence in an analyte molecule can increase its overall polarity. In a reversed-phase system, compounds with higher polarity tend to interact less strongly with the non-polar stationary phase, resulting in shorter retention times. So, 4CP and 4BrP elute earlier than DMP. Halogens, have significant dipole moments due to their electronegativity. This can lead to electric dipole-dipole interactions with polar functional groups in the stationary phase, further affecting retention times. Compounds with halogens may exhibit stronger or weaker interactions depending on the specific conditions. If the analyte contains halogens with a negative charge (e.g., chloride ions), they might interact with positively charged groups in the stationary phase, potentially affecting retention times. This is less common but can be a factor in some cases. Lastly, DMP has two non-polar groups that interact more strongly with the non-polar stationary face, prolonging their retention.

It is well known that electronic transitions in the UV involve n , δ and π molecular orbitals. The transition of an electron from $\delta \rightarrow \delta^*$ need $\lambda < 200$ nm, for example, C-C, C-H. $n \rightarrow \delta^*$ use λ between 160 - 260 nm ex: CH₃OH, CH₃Cl. $\pi \rightarrow \pi^*$ used λ from 200 to 500 nm, such as: C=C, C=O. $n \rightarrow \pi^*$ their λ from 250 to 600 nm like for C=O and C=N. So, Cl and Br will induce a shift λ to 281 nm for 4CP and 4BrP, then 3MOP at 274 nm because of the OCH₃. Flowing by 4MP and DMP at 273 and 271 nm, respectively.

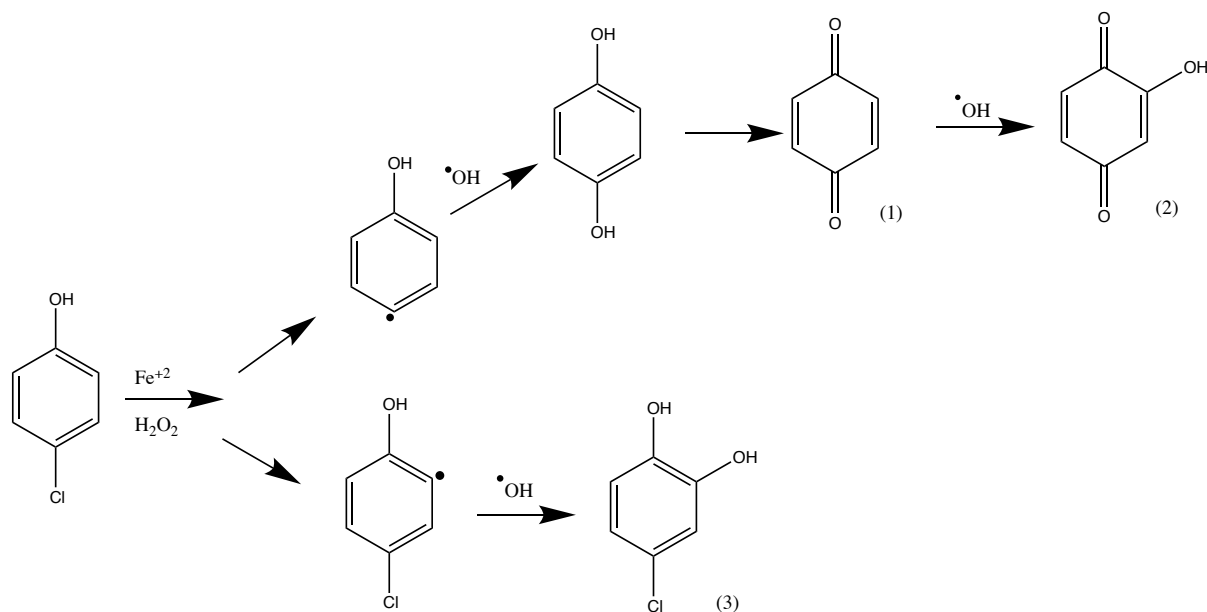
5.3 Oxidation of phenolic compounds by selected AC and zeolite based catalysts

5.3.1 Chlorophenol (4CP) decomposition

Chlorophenols (CPs) are extremely toxic, non-biodegradable, and most of them have carcinogenic properties.²⁸ There is evidence that the intermediates of such compounds are more toxic and refractory than their parent compounds.²⁹ Among all CPs, (4CP) has been chosen to serve as a model substrate as it is one of the most widely used agrochemicals worldwide. 4CP,

used in pesticides, disinfectant agents, wood preservatives and dyes.^{30, 31} Because of their extensive use and resistance to degradation, these compounds accumulate extensively in soil and water.^{32, 33} Consequently, these compounds pose a serious threat to human health as they pass through the food chain and eventually enter the human body.^{34, 35}

It is important to establish a degradation mechanism model in order to understand the degradation reaction better.³⁶ Based on many studies, there is a strong correlation between $\cdot\text{OH}$ concentration and pollutant degradation in an aqueous Fenton system.³⁷⁻³⁹ The most direct pathway for 4CP degradation is through hydroxylation, which will then lead to a ring opening, and mineralisation afterwards if to completion to the most thermodynamically stable products. The expected oxidation mechanism of 4CP is illustrated in Scheme 5.4.⁴⁰ Fenton's oxidation of 4CP produced benzoquinones and hydroxyquinone as intermediates (compounds (1) and (2) in Scheme 5.4).^{41, 42} The formation of non-chlorinated compounds confirms that the chlorine group does not inhibit $\cdot\text{OH}$ interaction with the ring. However, $\cdot\text{OH}$ attacks occurred more readily at positions without chlorine groups because de-chlorination occurs via a different mechanism, such as hydrogenolysis. In the presence of a hydrogen source (such as molecular hydrogen or hydrogen gas), de-chlorination can occur through a hydrogenolysis mechanism. The hydrogen reacts with the chlorine atom, breaking the carbon-chlorine bond and forming hydrogen chloride (HCl) as a by-product. This process replaces the chlorine atom with a hydrogen atom; perhaps this reaction is less efficient than non-dechlorinating reactions.⁴³ Evidence shows that benzoquinones can accelerate iron's redox cycle.^{44, 45} As the reaction progresses, aromatic rings open and decompose to shorter chains, and organic acids, including muconic, oxalic and acetic acid, are formed.¹⁴ Noteworthy to this project, it has been noted that there might be a detrimental role from these acids; as they could deactivate iron by forming stable complexes with it.^{43, 46-48}



Scheme 5.4: The proposed reaction pathway of 4CP oxidation with Fenton's reagent system by CWPO reaction. (1) Hydroquinone and (2) benzoquinone are the main intermediates; by the reaction time, the aromatic ring (not shown) will then open to produce acid groups.⁴⁰

The conversion of 4CP in the Fenton system by CWPO reaction was investigated in an aqueous solution in Figure 5.1. For this purpose, nine novel heterogenous catalysts were applied and labelled as that the first group is three zeolite catalysts A, B and C. (A) for 1 wt% Fe-ZSM-5, (B) for 0.5 wt% Fe loading, Fe-Ag-ZSM-5, (C) for 1 wt% Fe loading, Fe-S-N-Zeolite-Y. The second group of catalysts Fe/AC, 12 wt% iron doping three different kind of activated carbons, D, E and F. (D) for Fe/AC raw-GAC, (E) for Fe/AC raw-SA2, (F) for Fe/AC raw-G60. The third group of catalysts 12 wt% Fe doping, Fe-S-N/AC, G, H and I. (G) for Fe-S-N/AC HCl-HNO₃-GAC, (H) for Fe-S-N/AC HCl-HNO₃-SA2 and (I) for Fe-S-N-AC HCl-HNO₃-G60. Using 1 g.L⁻¹ of 4CP in 50 mL solution, 1:27 molar ratio 4CP to H₂O₂ for 4 h at 80 °C.

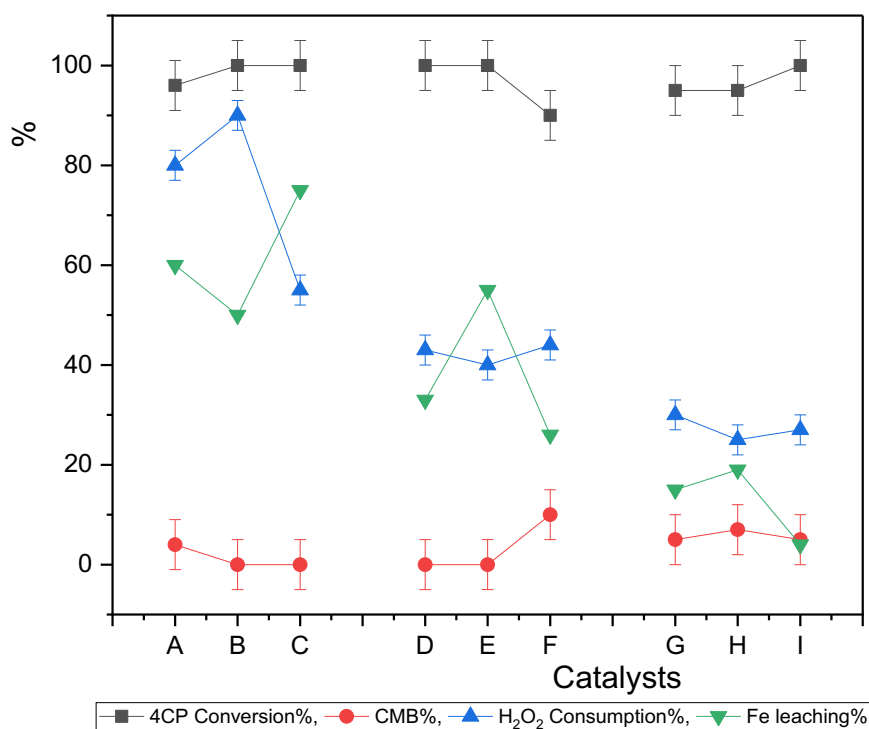


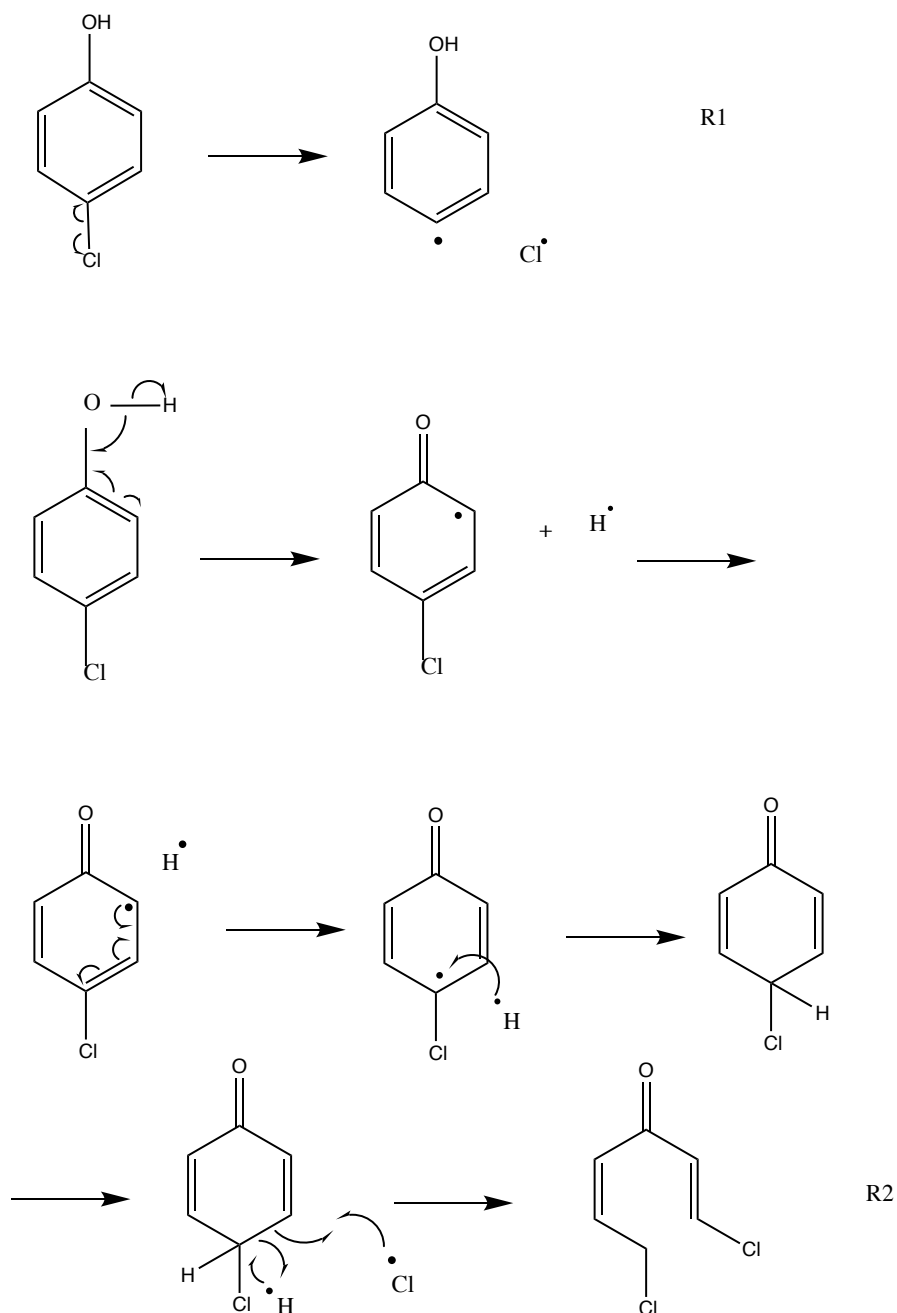
Figure 5.1: Catalytic activity results for 4CP conversion by the WCPO reaction using multiple catalysts the first group of catalysts, zeolite catalysts (A) for Fe-ZSM-5, (B) for Fe-Ag-ZSM-5, (C) for Fe-S-N-Zeolite-Y. The second group of catalysts, iron-doped different AC, (D) for Fe/AC raw-GAC, (E) for Fe/AC raw-SA2, (F) for Fe/AC raw-G60. The third group of catalysts (G) for Fe-S-N/AC HCl-HNO₃-GAC, (H) for Fe-S-N/AC HCl-HNO₃-SA2 and (I) for Fe-S-N-AC HCl-HNO₃-G60. Using 1 g.L⁻¹ of 4CP in 50 mL solution, 1:27 molar ratio 4CP to H₂O₂ for 4h at 80 °C.

The catalytic activity for all these catalysts shows extremely high activity for 4CP oxidation. The results give almost full 4CP conversion at 100% but with catalyst (F) Fe/AC raw-G60, 90%. Also, complete mineralisation of organic compounds was observed for most of the catalysts. In terms of H₂O₂ consumption, almost with all catalysts, there was no complete H₂O₂ consumption, it was found that the [•]OH had a significant degradation effect on the oxidation of 4CP, but there are possible other effects that might be taking part in the process. For example: Cl[•] could contribute to the oxidation of 4CP when it remains high 100% even with low H₂O₂ consumption. though it is expected to be [•]OH to play a major role in the oxidation of 4CP. Furthermore, as for all the Fenton based processes, the reaction follows a pH dependence and

is most efficient in the pH range of 2-3, for this reaction a lower pH could either be obtained from the formation of organic acids or the formation of HCl from H-abstraction reactions by Cl^\bullet .⁴³ It had been reported that chlorine accelerated the decomposition of phenol, and evidence for this was found when phenolic compounds were oxidised by $\cdot\text{OH}$ over clay-based catalysts. The degradation of phenol with Cl^\bullet has been confirmed through analytical methods such as mass spectroscopy MS suggesting that the rate-limiting step has been accelerated with Cl^\bullet present.⁴⁹ This observation has been confirmed by several studies. María reported that under high salinity conditions, the photo-Fenton reaction has been tested for its ability to oxidize imidacloprid and methomyl as commercial formulations. Contrary to what is described in some literature though, the halogen radicals has been shown to enhance pesticide degradation.^{50, 51} A study by Naresh investigating the addition of simple additives like salt (NaCl) and carbon tetrachloride showed an increase of process intensification to reduce the treatment times and, in turn, operating costs. It has been observed that the phenol degradation process is accelerated.⁵¹ The degradation of phenolic compounds may be enhanced by Cl^\bullet by forming chlorinated intermediates that act as electron carriers.^{42, 52} Micó and co-workers explained an enhancement in phenol derivatives degradation by the participation of Cl^\bullet in the reaction, whose activity for the reaction is comparable to that of $\cdot\text{OH}$.⁵⁰ In contrast, a study by Mahamuni and Pandit reported that NaCl was transferring the phenol to an organic/water interface (phase transfer process), promoted by the salting out effect and did not participate in the chemical reaction.⁵¹ In view of these data, there is no doubt that Cl-species plays a complex role in the CWPO reaction of phenol, although their mechanism is not fully understood, probably in part due to the coexistence of different radical species in solution.⁴⁹

Based on these findings, a mechanism including Cl^\bullet as a promoter for the decomposition of phenol derivatives is proposed in Scheme 5.5. The oxidation reaction of 4CP by chlorine involves de-chlorination of Cl atom in the para position of the phenolic ring. In this reaction, chlorine acts as the oxidizing agent. The mechanism of this reaction involves several steps: starting with an initiation the reaction is initiated by a Cl radical abstraction. This forms a phenoxyl carbon centred radical intermediate. Then follows a canonical pattern involving propagation and termination, with a propagation, where 4CP reacts with another Cl^\bullet that can indeed lead to the opening of the phenolic ring followed by termination: eventually, two radicals may combine to form Cl_2 which unless it is dissociated would stop the reaction. According to the residual intermediates results (0%) there was complete mineralisation to CO_2 and H_2O which meaning that either HCl or Cl_2 are the most possible products could form at

the end of the reaction (residual intermediates was estimated based on the phenol's intermediates).



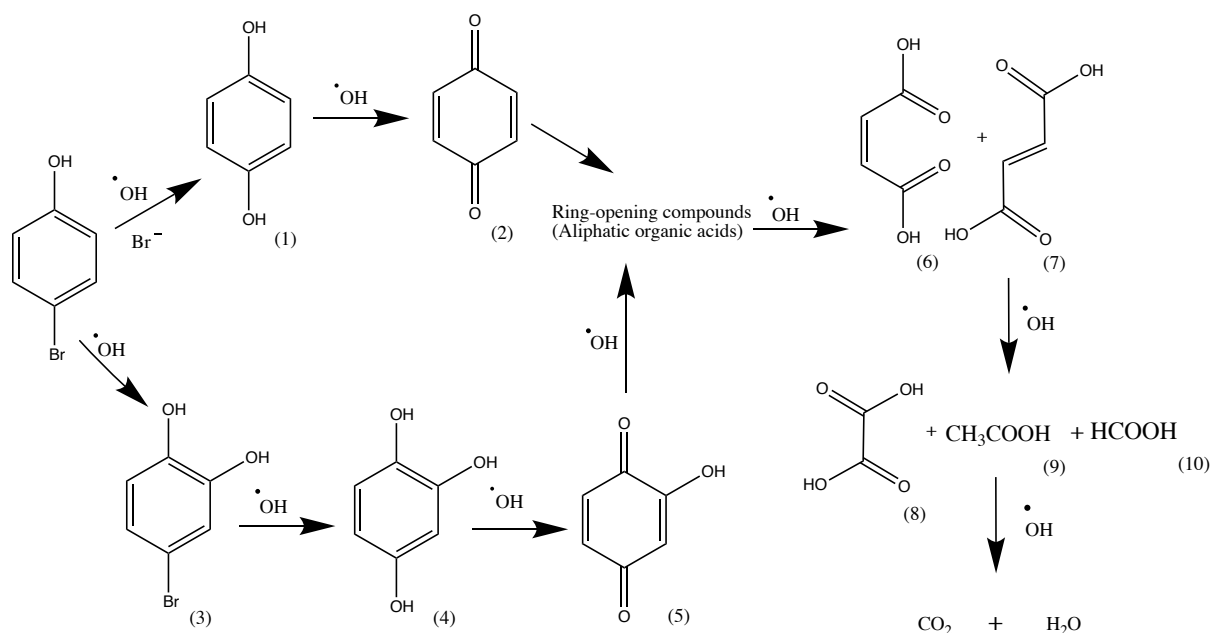
Scheme 5.5: Oxidation of 4CP by chlorin radicals. the first step contains de-chlorination from 4-chlorophenol to form phenoxy radicals. Then Cl[•] attack 4CP in the para position. The phenolic ring will break down forming chlorinated products. The migration of H was not shown or implicitly assumed, and we are giving weight to the product in meta. Note: R1 is only an initiating step and that the reaction is not balanced because the aromatic residue from R1 can take part in a number of other reactions or decomposition pathways.

Regarding the stability of the catalysts, the results show Fe-Ag-ZSM-5 and Fe-S-N-Zeolite-Y are less durable and have higher Fe leaching at 50% and 70%, respectively, compared to the results reported in chapter 4, when these same materials were applied for phenol oxidation and leaching in the range of 30% and 50% respectively were detected. This higher leaching could be the result of a pH variation associated with acid released (HCl formation) or the formation of Fe-chlorinated species.⁵³ Still, Fe-S-N/AC catalysts are more stable than others, particularly Fe-S-N/AC HCl-HNO₃, G60, which has 0.4% Fe leaching.

5.3.2 Bromophenol (4BrP) decomposition

The majority of bromophenols (BrPs) are toxic and non-biodegradable substances. Due to their genotoxic, mutagenic, and carcinogenic properties, they are considered major pollutants and their abatement a priority.⁵⁴ As stated by both the United States Environmental Protection Agency (EPA) and the European Union (EU),^{55,56} there is widespread use of BrPs as pesticides in agriculture and as a precursor to resorcinol.⁵⁷ In addition a waste stream from electronic waste can also release these compounds into the environment.⁵⁸ Because of the extreme toxicity of these compounds, they have been chosen as further target substrates for CWPO by using our catalysts, as well as from the promising results obtained in the degradation of 4CP.

Scheme 5.6 shows one of the currently postulated mechanisms for the oxidation of 4BrP,⁵⁹ where a *para*-substituted bromo phenol can be degraded via either of two pathways. A first route involves the formation of 4-hydroquinone and benzoquinone; a second way, instead, the formation of 4-bromocatechol by $\cdot\text{OH}$ attack.⁶⁰ Due to a stronger *para*-directing from the -OH and -Br substituents the $\cdot\text{OH}$ radical can attack the *para* position of 4BrP, releasing bromide ions and forming 4-hydroquinone. 4BrP then oxidises to 4-benzoquinone.⁶¹ The 4-benzoquinone further reacts with $\cdot\text{OH}$ to undergo opening of the aromatic ring to form various short-chain aliphatic acids, which can further degrade to smaller chain organic acids, including malonic acid, maleic, oxalic, acetic, formic and finally CO₂.^{62,63}



Scheme 5.6: The possible reaction pathways for the degradation of 4-bromophenol by CWPO reaction. The first pathway formation of (1) 4-hydroquinone and (2) 4-benzoquinone. The second pathway formation of (3) bromocatechol, (4) hydroxyl hydroquinone and (5) 4-hydroxybenzoquinone through the $\cdot\text{OH}$ attack. The degradation continues into shorter-chain organic acids, including (6) maleic acid, (7) malic acid, (8) oxalic acid, (9) acetic acid and (10) formic acid.⁵⁹

Similarly, to 4CP, there are a few factors contributing to the degradation of 4BrP. By inductive effect, bromine would withdraw electrons, which could negatively affect 4BrP's oxidation. In contrast, bromine donates electrons to aromatic rings via resonance, which promotes the oxidation/degradation. It is possible that debromination happens during 4BrP oxidation. The $\text{Br}\cdot$ radicals could contribute to the abatement of the compound, thus enhancing 4BrP conversion or conversely could work as scavenger for $\cdot\text{OH}$ which could then inhibit the reaction.

Figure 5.2 shows the catalytic activity for 4BrP degradation via the CWPO method, by using nine novel heterogenous catalysts were applied and labelled as that the first group is three zeolite catalysts A, B and C. (A) for 1 wt% Fe-ZSM-5, (B) for 0.5 wt% Fe loading, Fe-Ag-ZSM-5, (C) for 1 wt% Fe loading, Fe-S-N-Zeolite-Y. The second group of catalysts Fe/AC, 12 wt% iron doping three different kind of activated carbons, D, E and F. (D) for Fe/AC raw-GAC, (E) for Fe/AC raw-SA2, (F) for Fe/AC raw-G60. The third group of catalysts 12 wt% Fe doping, Fe-S-N/AC, G, H and I. (G) for Fe-S-N/AC HCl-HNO₃-GAC, (H) for Fe-S-N/AC

HCl-HNO₃-SA2 and (I) for Fe-S-N-AC HCl-HNO₃-G60. At the same reaction conditions reported in Section 5.2.1, using 1 g.L⁻¹ of 4BrP and 1:27 4BrP to H₂O₂.

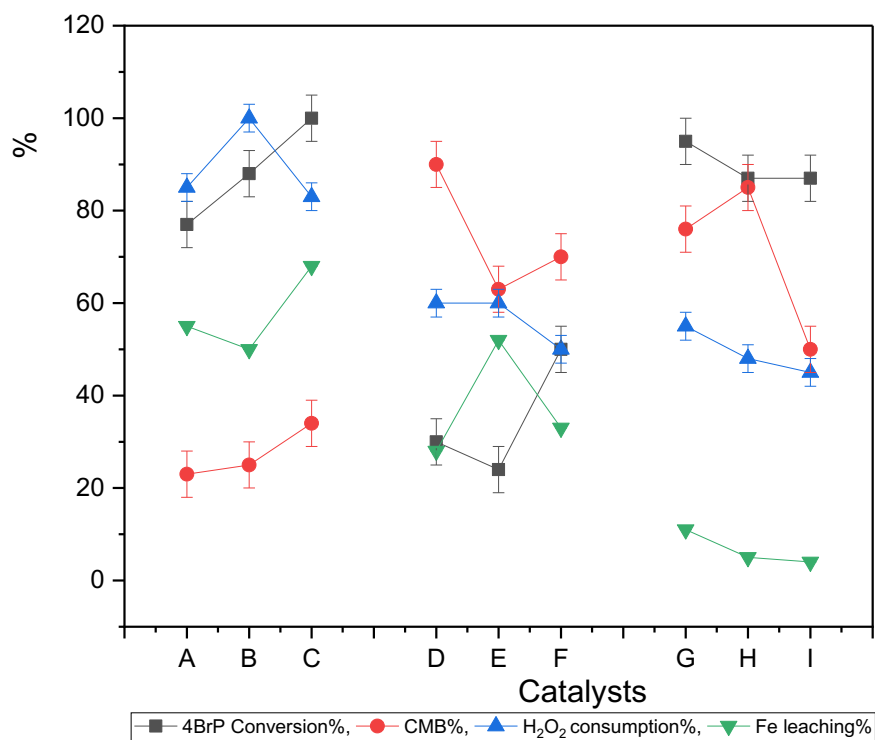


Figure 5.2: The analysis of the catalytic activity for multiple catalysts was used to convert 4BrP the first group of catalysts, zeolite catalysts (A) for Fe-ZSM-5, (B) for Fe-Ag-ZSM-5, (C) for Fe-S-N-Zeolite-Y. The second group of catalysts, iron-doped different AC, (D) for Fe/AC raw-GAC, (E) for Fe/AC raw-SA2, (F) for Fe/AC raw-G60. The third group of catalysts (G) for Fe-S-N/AC HCl-HNO₃-GAC, (H) for Fe-S-N/AC HCl-HNO₃-SA2 and (I) for Fe-S-N-AC HCl-HNO₃-G60. Using 1 g.L⁻¹ of 4BrP in 50 mL solution, 1:27 4BrP to H₂O₂ for 4h at 80 °C.

As shown in Figure 5.2 the oxidation include conversion and mineralization of 4BrP is lower than that of 4CP at the same reaction conditions, using the same catalysts. With Fe-doped zeolite catalysts, catalyst (A) Fe-ZSM-5 gives 80% of 4BrP conversion, (B) Fe-Ag-ZSM-5 raised the conversion to 90% and (C) Fe-S-N-Zeolite-Y enhanced the conversion of 4BrP to reached 100%. In addition, the estimated residual intermediates was almost equivalent for both A and B catalysts at 25% while slightly higher for C at 35%. The consumption of H₂O₂ was high and compatible with results between 85-100%. A second trend regarding 4BrP abatement is for Fe/AC catalysts, where the conversion was poor at 30% with both (D) Fe/AC by raw-

GAC and (E) Fe/AC raw-SA2 and 50% for (F) Fe/AC raw-G60. Moreover, the mineralisation with these catalysts was low; the estimated residual intermediates detected roughly in the range of 70% for these catalysts. The consumption of hydrogen peroxide was 60%, 50%, and 55% for D, E, and F, respectively. In the case of Fe-S-N/AC HCl-HNO₃ catalysts, the results show that a high oxidation for 4BrP reached 95% with G, H and I (Fe-S-N/AC) catalysts. Thus, implying that the doping by S and N enhances the catalytic activity of Fe/AC for oxidation of 4BrP from 30-50% to 95%. In spite of this, the catalysts exhibit poor mineralisation, 75%, 85% and 50% residual intermediates, for G, H and I catalysts, respectively, which could, in principle lead to the generation of toxic brominated by-products.⁶⁴

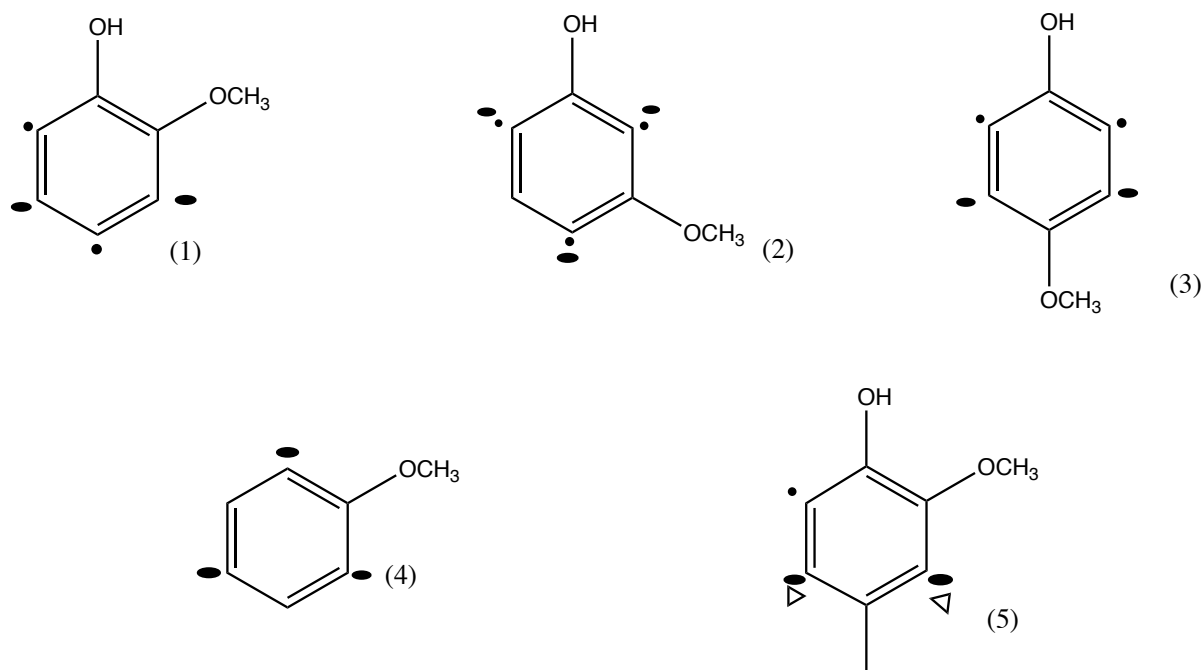
In this wider context, the assessment of the toxicity of the major transformation products of debromination degradation, which may be higher than that of the original molecule, is essential.⁶⁵ This because there are only a few reports available regarding the toxicity of the intermediates generated during BrP degradation.⁶⁶ The same low hydrogen peroxide consumption here with almost 50% consumption which is clearly compatible with the catalytic activity results as the fact that half the amount of $\cdot\text{OH}$ has been used to partly oxidise the 4BrP. However, these processes were inhibited, as there was no complete oxidation of the high aromatic intermediate based on the estimated residual intermediates results. These results could be explained by a lower H-abstraction capability from Br \cdot compared to Cl \cdot . Bromine is larger than chlorine due to its higher atomic number and a greater number of electron shells. The larger atomic radius of bromine means that the hydrogen atom bonded to it is relatively farther away from the bromine radical compared to the hydrogen bonded to a chlorine radical. This greater distance results in a weaker hydrogen-bromine bond compared to the hydrogen-chlorine bond. As a result, chlorine radicals are generally more reactive than bromine radicals due to their smaller size and higher electronegativity. Chlorine radicals have a stronger tendency to abstract hydrogen atoms from other molecules, making them more aggressive in radical reactions like our reaction condition hydrogen abstraction. However, as for Cl \cdot , free Br \cdot radicals may also scavenge hydroxyl radicals, thus preventing or inhibiting the oxidation process. Also, the presence of a bromine atom in the ortho- or para-position of the phenolic ring may negatively influence the reactivity of 4-bromophenol. The bromine substituent can stabilize the phenoxy radical formed during the Fenton reaction, making it less susceptible to further oxidation. As a result, the rate of degradation may be slower compared to other phenolic compounds without bromine substituents in the para position. However, to confirm this other position for 4BrP have to be tested.

Regarding the catalyst's stability and durability based on the Fe leaching results by ICP-MS, it appears that the zeolite catalysts A, B and C have higher metal leaching at 55%, 50% and 68%, respectively. Nonetheless, the Fe/AC catalysts have a metal loss about 30%, and ultimately, the Fe-S-N/AC catalysts show greater durability at 11%, 5%, and 4% metal leaching. The best catalyst's performance for 4BrP oxidation is Fe-S-N-Zeolite-Y with 100% conversion and 30% residual intermediates. Even so, the toxicity of intermediate compounds negatively affects the degradation of 4BP like (4-Bromocatechol, 4-Bromoresorcinol, 4-Bromoquinone can be an intermediate if the oxidation process continues and 4-Bromobenzoquinone) particularly for poor mineralisation, which is confirmed by the high estimated residual intermediates results (60% to 90% for AC's catalysts), although with a high 4BrP conversion in the range of 85-100%.

5.3.3 Decomposition of 3-methoxy phenol (3MOP)

Methoxyphenols represent a substantial proportion of emissions from biomass burning caused by natural fires, human-initiated vegetation burning, and residential wood burning.⁶⁷⁻⁶⁹ The study conducted by Tourneur was concerned with the reaction of $\cdot\text{OH}$ radicals with 2-methoxy phenol and other related compounds, such as 3-methoxy phenol, 4-methoxy phenol, 2-methoxy-4-methyl phenol, and methoxybenzene, their outcomes find that the meta isomers, 3-methyl phenol and 1,3-dimethylbenzene, are the most reactive of the methyl phenols and dimethyl benzenes, respectively.⁷⁰ The explanation for these matters of fact is based on the number of aromatic ring sites that are activated toward the electrophilic addition of $\cdot\text{OH}$.

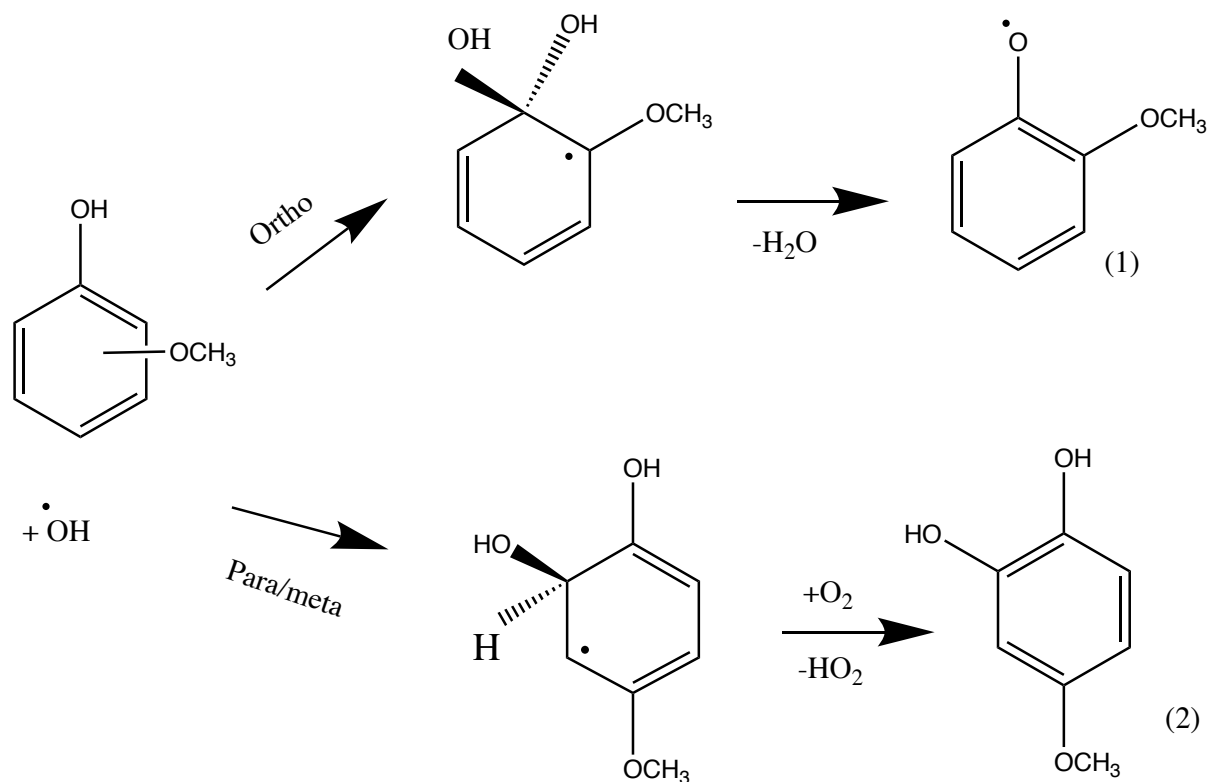
Figure 5.3 illustrates the activation sites of the $-\text{OH}$ and $-\text{OCH}_3$ groups in methoxyphenol isomers. Electron density is transferred to both ortho and para positions by both substituents. In 3-methoxy phenol, three positions on the aromatic ring are activated by both the $-\text{OH}$ and $-\text{OCH}_3$ groups, thus being doubly activated, while the other two isomers, 2- and 4-methoxy phenol, contain four singly activated positions. Consequently, for other disubstituted aromatics, meta isomer, that is, 3-methoxy phenol, is the one expected to be the most reactive. In spite of the fact that the experimental data support this hypothesis, there is only a relatively small difference between 3-methoxy phenol and 4-methoxy phenol in terms of reactivity, suggesting that reactivity may also be influenced by other factors, such as steric effects.⁷⁰



Scheme 5.7: Methoxy aromatics, the sites that are activated by the hydroxyl (•), methoxy (●), and methyl (Δ) groups to attract electrophiles.⁷⁰ (1) 2-methoxyphenol, (2) 3-methoxyphenol, (3) 4-methoxyphenol, (4) methoxybenzene and (5) 2-methoxy-4-methylphenol.

According to this, 3MOP has been chosen as a further model for CWPO reaction by multiple heterogeneous catalysts at the same experimental conditions as reported in the sections above. Furthermore, given the reason explained in section 5.1 about substituent effects it was expected for our catalysts to be highly active for this substrate.

The proposed reaction mechanism for methoxy phenol oxidation by $\cdot\text{OH}$ radicals is reported in Scheme 5.8.⁷¹ An important reaction pathway for ortho position involves adding $\cdot\text{OH}$ to a carbon atom with an attached OH group, followed by the formation of phenoxy species after H_2O elimination. That said, for *ortho*-methoxy phenols, there may be two different H-abstraction pathways. The first is H-abstraction from the OH group, resulting in phenoxy radical intermediates. The other route is H-abstraction from the methoxy group. This pathway generates phenoxy radicals. For meta- and *para*-methoxy phenols, instead, $\cdot\text{OH}$ addition will form catechol species and, still for *meta*- and *para*-methoxy phenols, it was found that only the H-abstraction pathway from the OH group is probably to occur. These differences can be explained by the steric hindrance effect and/or the intramolecular hydrogen bond due to ortho-methoxy substitutions.⁷¹



Scheme 5.8: The overview of the proposed major reactions involving $\cdot\text{OH}$ radicals and methoxylated phenols. For clarity, the para-species are shown in the lower line. In this reaction, the dominant step is the addition of $\cdot\text{OH}$ to the carbon position with an attached OH group, resulting in the formation of phenoxy species (1). For *meta*- and *para*-methoxylated phenols, $\cdot\text{OH}$ -addition occurs at the carbon position next to the $\cdot\text{OH}$ group, forming catechol species (2).⁷¹ The migration of H was not shown or implicitly assumed, and we are giving weight to the product in meta.

The catalytic activity results for the 3MOP oxidation by CWPO reaction using 9 different heterogenous catalysts are shown in Figure 5.4. The first group is three zeolite catalysts A, B and C. (A) for 1 wt% Fe-ZSM-5, (B) for 0.5 wt% Fe loading, Fe-Ag-ZSM-5, (C) for 1 wt% Fe loading, Fe-S-N-Zeolite-Y. The second group of catalysts Fe/AC, 12 wt% iron doping three different kind of activated carbons, D, E and F. (D) for Fe/AC raw-GAC, (E) for Fe/AC raw-SA2, (F) for Fe/AC raw-G60. The third group of catalysts 12 wt.% Fe doping, Fe-S-N/AC, G, H and I. (G) for Fe-S-N/AC HCl-HNO₃-GAC, (H) for Fe-S-N/AC HCl-HNO₃-SA2 and (I) for Fe-S-N-AC HCl-HNO₃-G60. At the same reaction conditions reported in section 5.2.1, using 1 g.L⁻¹ of 3MOP and 1:20 3MOP to H₂O₂.

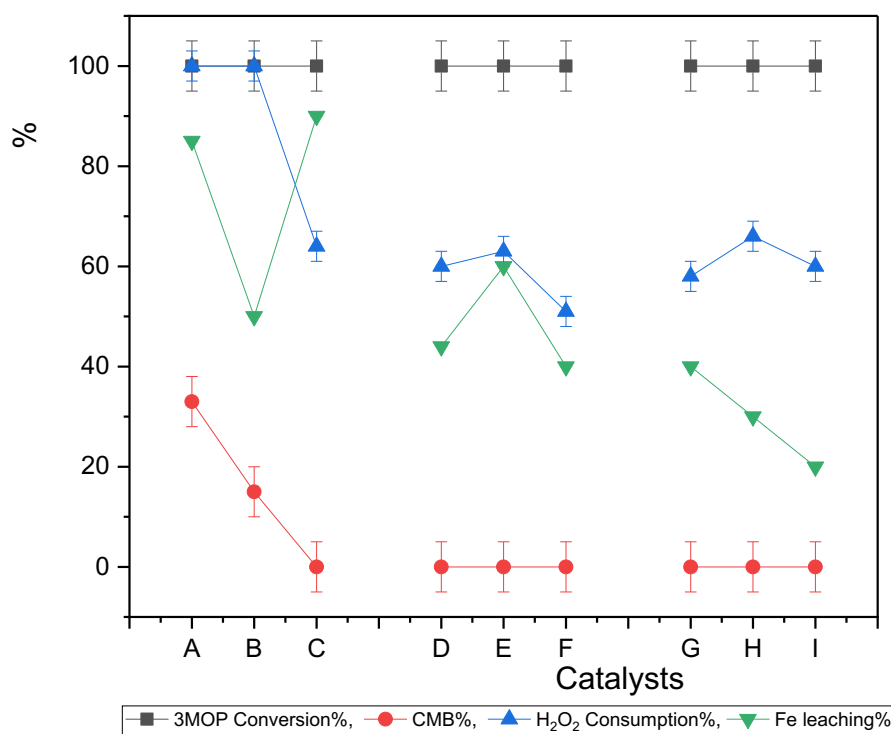
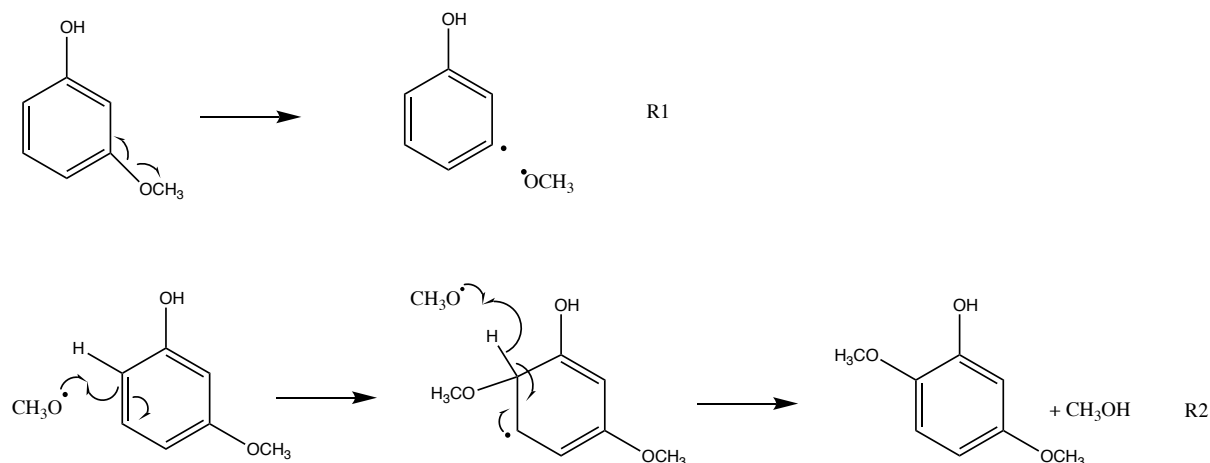


Figure 5.4: The analysis of the catalytic activity for multiple catalysts was used to convert 3MOP. the first group of catalysts, zeolite catalysts (A) for Fe-ZSM-5, (B) for Fe-Ag-ZSM-5, (C) for Fe-S-N-Zeolite-Y. The second group of catalysts, iron-doped different AC, (D) for Fe/AC raw-GAC, (E) for Fe/AC raw-SA2, (F) for Fe/AC raw-G60. The third group of catalysts (G) for Fe-S-N/AC HCl-HNO₃-GAC, (H) for Fe-S-N/AC HCl-HNO₃-SA2 and (I) for Fe-S-N-AC HCl-HNO₃-G60. Using 1g.L⁻¹ of 3MOP in 50 mL solution, 1:20 3MOP to H₂O₂ for 4 h at 80 °C.

As expected, with the catalyst are very active towards this substrate and can complete 3MOP oxidation up to 100% conversion for all catalysts and mineralisation except for catalysts Fe-ZSM-5 (A) and Fe-Ag-ZSM-5 (B) were 33% and 15%, respectively. The consumption of H₂O₂ was 100% for both A and B catalysts and 60% for the rest. •OH radicals play an essential role in pollutant oxidation and mineralisation. However, the full 3MOP oxidation, including conversion and mineralisation in the case of 60% H₂O₂ consumption, could be explained as there was another oxidant in the solution involved in the reaction, which in the case of 3MOP oxidation, could be •OCH₃ species. Scheme 5.9 shows this possible oxidation path way by •OCH₃ radicals. The methoxy radical •OCH₃ abstracts a hydrogen atom from the 2-methoxyphenol molecule to form a phenoxyl radical and a methanol molecule. Then the phenoxyl radical can then react with molecular oxygen •OH to regenerate the methoxy radical

and form various products, including quinones and other aromatic compounds. This chain reaction continues as long as there are 2-methoxyphenol and methoxy radicals present.⁷²



Scheme 5.9: Possible oxidation path way of 3MOP by $\cdot\text{OCH}_3$ radicals. First step include remove $\cdot\text{OCH}_3$ from the phenol ring. Then in the second reaction step this $\cdot\text{OCH}_3$ radical attack ortho position to form 3,5 di methoxyphenol. The migration of H was not shown or implicitly assumed, and we are giving weight to the product in meta. Note: R1 is only an initiating step in both cases and that the reaction is not balanced because the aromatic residue from R1 can take part in a number of other reactions or decomposition pathways.

The durability of catalysts is the same trend that was observed previously, Zeolite catalysts are the lesser stable catalysts compared to others. The Fe leaching was 85%, 50% and 90% for (A) Fe-ZSM-5, (B) Fe-Ag-ZSM-5 and (C) Fe-S-N-Zeolite-Y, respectively. The second trend was for Fe/AC catalysts ranging between 40% to 60%; finally, Fe-S-N/AC they more durable catalysts at 40% to 20%; still, these catalysts become less stable compared with other phenolic compounds such as 4CP (~0.4%).

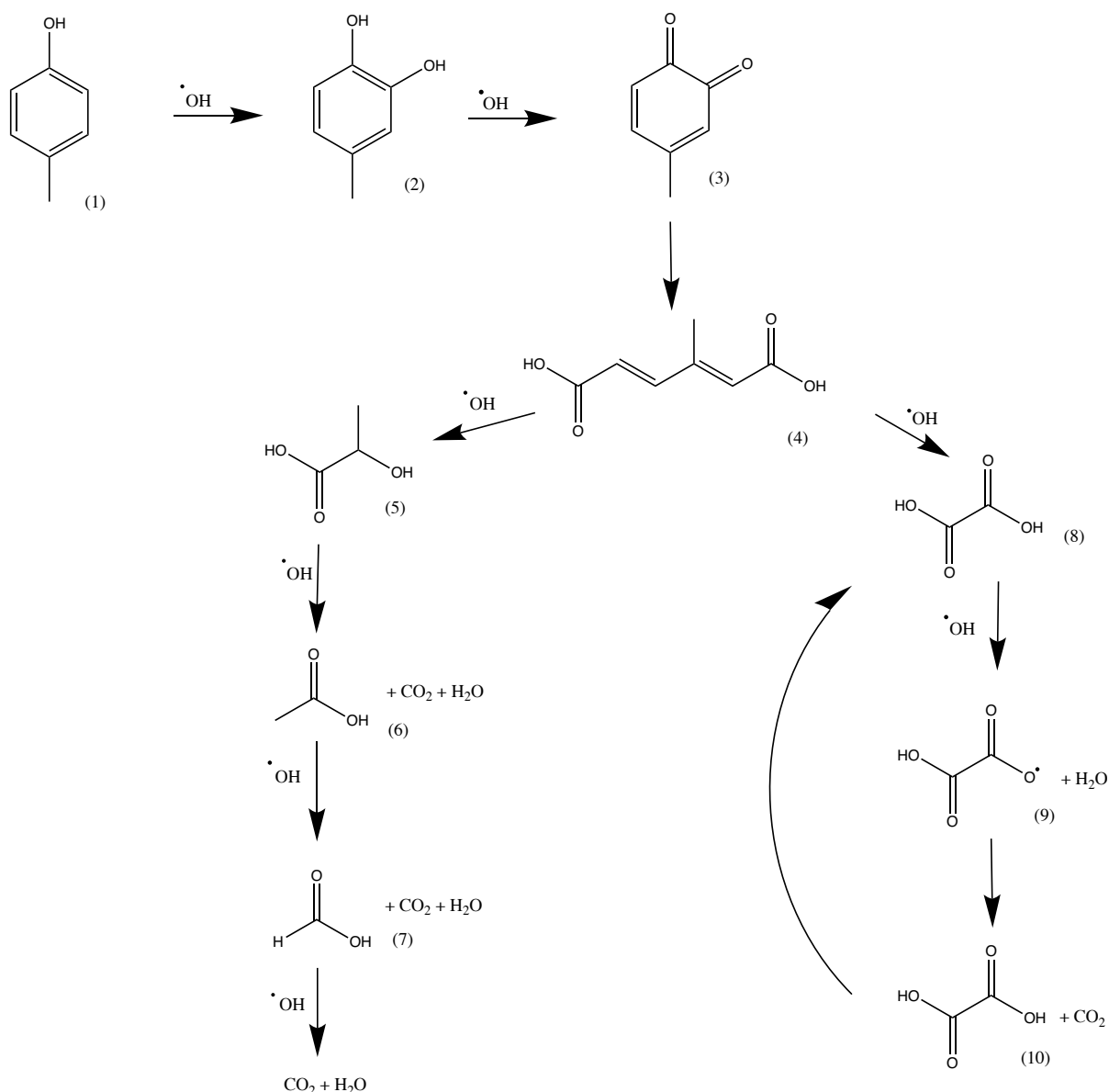
These catalytic results match an expected enhanced reactivity when a substrate like 3MOP is used due to the enhanced reactivity by the contribution form $\cdot\text{OCH}_3$ radicals, to propagate the reaction, and if in meta position.^{70, 71, 73}

5.3.4 Cresol (4MP) decomposition

Cresol is often used as a model for studying water purification from phenol compounds.⁷⁴⁻⁷⁶ *p*-cresol was chosen because, although *p*-cresol is not commonly found in wastewater effluent,

its chemical structure and reactivity with $\cdot\text{OH}$ are similar to that of *p*-nonylphenol, an endocrine disruptor frequently found in wastewater.⁷⁷ Alkylphenols are surfactants that are non-ionic and utilised to produce, like cleaning agents, dyes, dispersants, pesticides, and greases.⁷⁸ This compound is present in surface waters,^{79, 80} groundwater,⁸¹ and industrial wastewater,⁸² and marine sediments.⁸³ In addition, the most frequently identified substance, *p*-nonylphenol, promotes breast cancer cell growth,⁸⁴ and disrupts endocrine function.⁸⁵ Due to this, a full oxidation of these compounds and their removal from the wastewater is very important.

A model for the oxidation of *p*-cresol by $\cdot\text{OH}$ is presented in Scheme 5.10.⁷⁷ First, $\cdot\text{OH}$ radicals are added to the ring to form 4-methylcatechol.^{13, 86} The hydroxylation can be explained by two different pathways. $\cdot\text{OH}$ radicals attack phenolic rings, producing a cyclohexadienyl radical, followed by the production of 4-methylcatechol. Alternatively, $\cdot\text{OH}$ radicals attack phenolic rings and abstracted H atom, creating a phenoxyl radical capable of reacting with another $\cdot\text{OH}$ radical. Even so, the H abstraction reaction of a methyl H atom⁸⁷ is much slower compared to the one of a hydroxyl group and as such the generation of a cyclohexadienyl radical, although possible in principle is practically disfavoured kinetically.⁸⁸ It is possible to convert 4-methylcatechol to the intermediates by further hydroxylation; nevertheless, a small yield is obtained.¹⁴ There are two steps involved in the oxidation of 4-methylcatechol to 4-methylbenzoquinone: 4-methylcatechol semi-quinone is formed by the attack of the $\cdot\text{OH}$ radical⁸⁹, and 4-methylbenzoquinone is formed by oxidising the semi-quinone radical.⁹⁰ Upon forming 4-methyl-benzoquinone, the ring is forced to fission by ring tension and oxidising agents. During the chain reaction, the C-C bond between oxygen atoms and carbons in the ring is cleaved, giving out 3-methyl-muconic acid.⁹¹ Then, since α -hydrogen adjacent to the double bond has a higher acidity, it can more easily be abstracted by the $\cdot\text{OH}$ radical, thus promoting the oxidation process.^{92, 93} From this point on the oxidation carries on like in the previous case by producing organic acids with low molecular weights, including lactic, oxalic acids acetic and formic acids.⁹⁴ Ultimately, as described in the previous sections, acetic acid, formic acid, and oxalic acid are oxidised by $\cdot\text{OH}$ radicals into CO_2 .^{95, 96}



Scheme 5.10: The proposed reaction pathway for oxidising of *p*-cresol by hydroxyl radicals (WCPO).

(1) *p*-Cresol, (2) 4-methylcatechol, (3) 4-methylbenzoquinone, (4) 3-methyl-muconic acid, (5) lactic acid, (6) acetic acid, (7) formic acid, (8,10) oxalic acid, (9) oxalate radical.⁷⁷

Figure 5.5 shows the catalytic activity results for 9 heterogeneous catalysts for MP oxidation by CWPO reactions. The first group is three zeolite catalysts A, B and C. (A) for 1 wt% Fe-ZSM-5, (B) for 0.5 wt% Fe loading, Fe-Ag-ZSM-5, (C) for 1 wt% Fe loading, Fe-S-N-Zeolite-Y. The second group of catalysts Fe/AC, 12 wt% iron doping three different kind of activated carbons, D, E and F. (D) for Fe/AC raw-GAC, (E) for Fe/AC raw-SA2, (F) for Fe/AC raw-G60. The third group of catalysts 12 wt% Fe doping, Fe-S-N/AC, G, H and I. (G) for Fe-S-N/AC HCl-HNO₃-GAC, (H) for Fe-S-N/AC HCl-HNO₃-SA2 and (I) for Fe-S-N-AC HCl-

HNO₃-G60. At the same experimental conditions as used with previous phenolic compounds see 5.2.1 in the above sections and with the same catalysts, 1 g.L⁻¹ of 4MP and 1:17 4MP to H₂O₂.

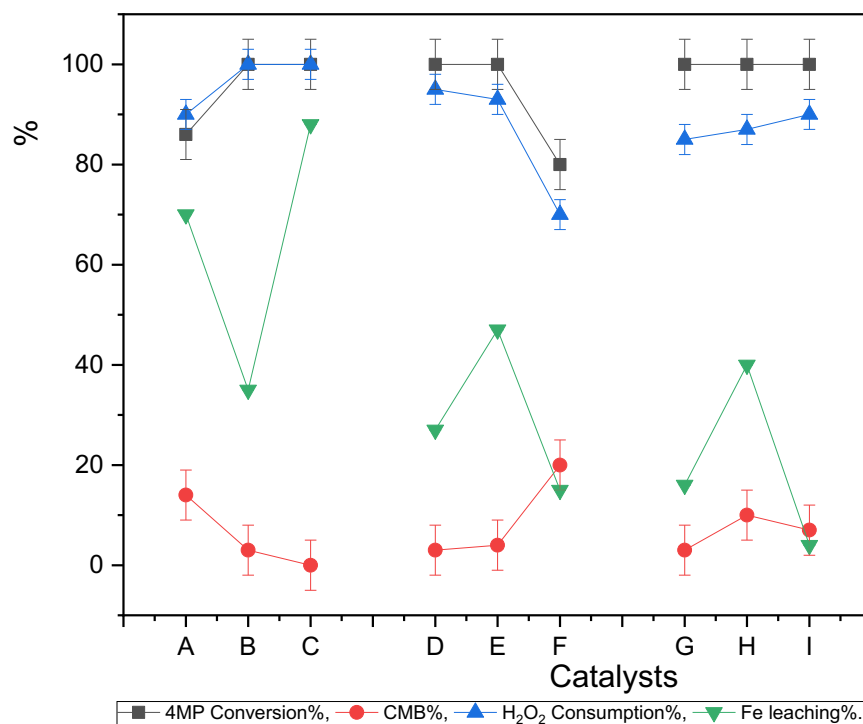


Figure 5.5: Catalytic activity for multiple catalysts was used to convert 4MP. the first group of catalysts, zeolite catalysts (A) for Fe-ZSM-5, (B) for Fe-Ag-ZSM-5, (C) for Fe-S-N-Zeolite-Y. The second group of catalysts, iron-doped different AC, (D) for Fe/AC raw-GAC, (E) for Fe/AC raw-SA2, (F) for Fe/AC raw-G60. The third group of catalysts (G) for Fe-S-N/AC HCl-HNO₃-GAC, (H) for Fe-S-N/AC HCl-HNO₃-SA2 and (I) for Fe-S-N-AC HCl-HNO₃-G60. Using 1 g.L⁻¹ of MP in 50 mL solution, 1:17 4MP to H₂O₂ for 4 h at 80 °C.

For zeolite catalysts (A) Fe-ZSM-5, (B) Fe-Ag-ASM-5 and (C) Fe-S-N-Zeolite-Y, 4MP conversion was 100% for B and C but 80% for A. Also, the residual intermediates was 0% for B and C, while 14% for A catalyst. These results confirm the modification that has been done for the Fe-ZSM-5, either by doping Ag for catalyst (B) or doping S and N for catalyst (C), that enhances the catalytic activity, including conversion and mineralisation. For Fe/AC catalysts D, E and F, the oxidation of 4MP was 100% with both D and E but slightly decreased to 80% for the F catalyst. Moreover, complete mineralisation for their intermediates with D and E while the estimated residual intermediates was 20% for the F catalysts. Accordingly, Fe/AC by

raw-G60 is a slightly lower activity for 4MP oxidation than the other Fe/AC catalysts. For the last three catalysts, for all Fe-S-N/AC HCl-HNO₃ catalysts, 4MP conversion reached 100%, and residual intermediates was 3%, 10% and 7% for G, H and I, respectively. These outcomes confirm the enhancement in the catalytic activity compared to Fe/AC catalysts because of the doping of S and N and the pre-acid treatments of the AC. The overview indicates the high H₂O₂ consumption between 85% to 100%. These results are similar to those of 4MP oxidation where nearly complete conversion and mineralisation were observed, but not a complete H₂O₂ consumption. For example, it was 70% with F catalyst (Fe/AC raw-G60); as a result, there was no complete oxidation at 80%, and residual intermediates was 20%.

The Fe leaching results show that the zeolites catalysts have lower stability of 70% and 88% iron leaching for A and C catalysts, respectively; still, doping Ag significantly decrease the metal leaching to 35% for B (Fe-Ag-ZSM-5). The second trend is for Fe/AC. However, these catalysts suffer from leaching affecting their durability metal leaching at 27%, 47% and 15% for D, E and F, respectively. Fe-S-N/AC catalysts, as they are usually more durable catalysts, the leaching decreased dramatically for these catalysts to 16% and 4% for G, and I still high 40% for H catalyst.

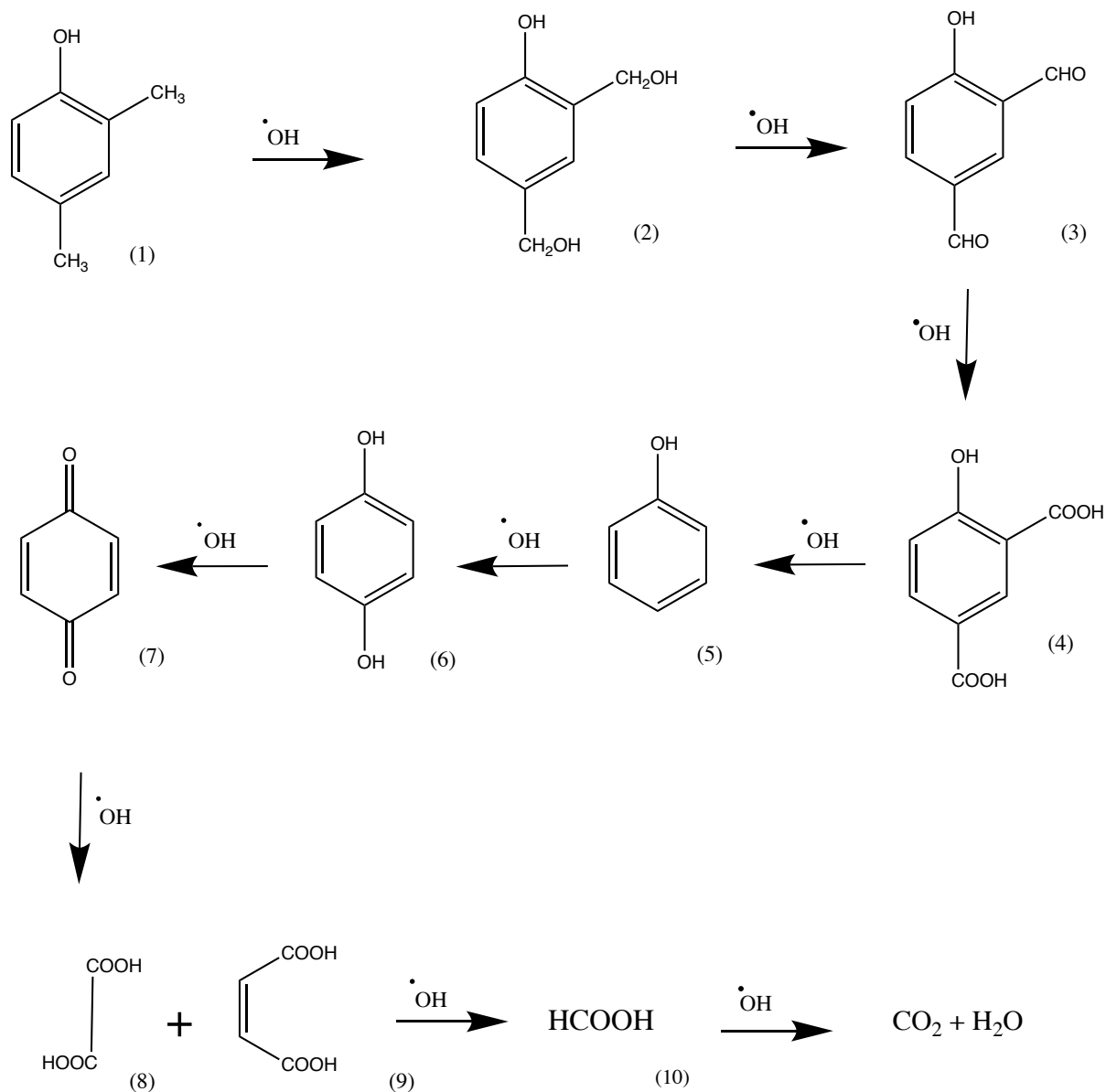
The most probable reason for the high oxidation rate of 4-methyl phenol by hydroxyl radicals could be the electron-donating effect; the methyl group in 4-methyl phenol donates electrons to the phenolic ring, making the phenolic hydrogen more labile and facilitates hydrogen atom abstraction by hydroxyl radicals.

5.3.5 Decomposition of 2,4 dimethylphenol (DMP)

Wastes from agriculture and urban areas contain alkyl dimethylphenols, which are toxic pollutants.⁹⁷ Due to its extensive use in pesticides, treating obesity, dyes, wood preservatives, and phytochemicals and explosives, 2,4-dimethylphenol (DMP) is considered significant.^{98, 99} Despite this, DMP's practical applications face challenges due to persistent secondary pollution, which is a health hazard that is non-biodegradable. Therefore, DMP pollution of water resources must be eliminated.^{100, 101}

The proposed degradation mechanism of DMP is reported in Scheme 5.11.¹⁰² The para and ortho positions of the phenolic ring are attacked by hydroxyl radicals, resulting in 2,4 dihydroxymethyl phenol. More oxidation by $\cdot\text{OH}$ radicals produce 2-hydroxy-5-

formylbenzaldehyde and 4-hydroxy isophthalic acid then phenol. The following steps are the same as discussed above for *p*-cresol section 5.2.4.



Scheme 5.11: The proposed reaction pathway for oxidising of DMP by hydroxyl radicals (CWPO). (1) 2,4-DMP, (2) 2,4 di hydroxymethyl phenol, (3) 2-hydroxy-5-formylbenzaldehyde, (4) 4-hydroxyisophthalic acid, (5) phenol, (6) hydroquinone, (7) benzoquinone, (8) oxalic acid, (9) maleic acid and (10) formic acid.¹⁰² Note: the $\cdot\text{OH}$ is not reported in a stoichiometric amount in this scheme.

Results showing the catalytic activity of the nine selected heterogeneous catalysts are reported in Figure 5.6. The first group is three zeolite catalysts A, B and C. (A) for 1 wt% Fe-ZSM-5, (B) for 0.5 wt% Fe loading, Fe-Ag-ZSM-5, (C) for 1 wt% Fe loading, Fe-S-N-Zeolite-Y. The second group of catalysts Fe/AC, 12 wt% iron doping three different kind of activated carbons, D, E and F. (D) for Fe/AC raw-GAC, (E) for Fe/AC raw-SA2, (F) for Fe/AC raw-G60. The third group of catalysts 12 wt% Fe doping, Fe-S-N/AC, G, H and I. (G) for Fe-S-N/AC HCl-HNO₃-GAC, (H) for Fe-S-N/AC HCl-HNO₃-SA2 and (I) for Fe-S-N-AC HCl-HNO₃-G60. At the same experimental conditions as used with previous phenolic compounds see 5.2.1 in the above sections and with the same catalysts, 1 g.L⁻¹ of DMP and 1:20 DMP to H₂O₂.

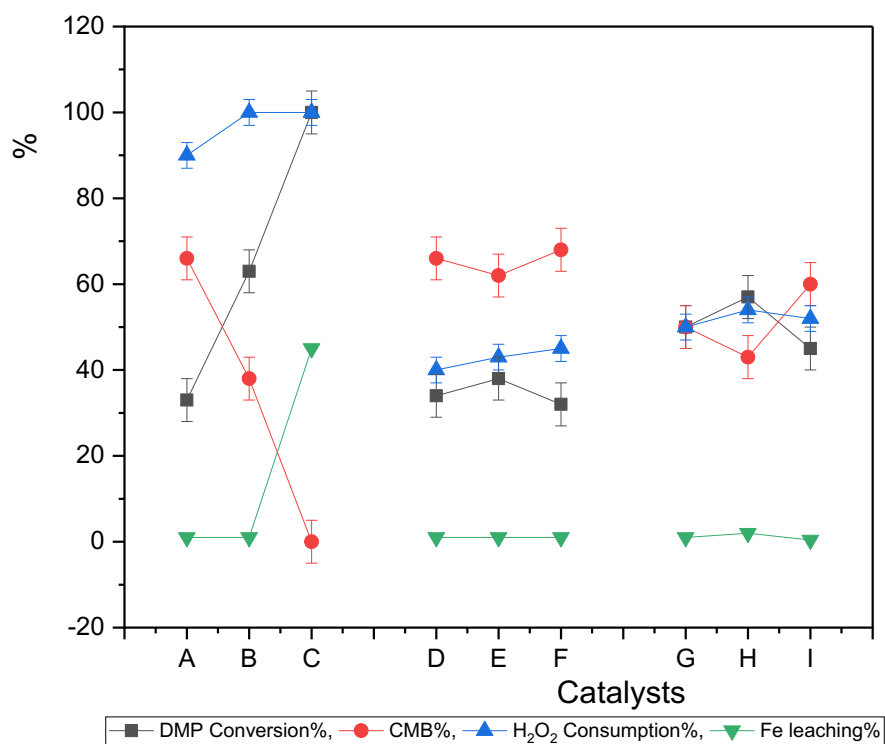


Figure 5.6: The catalytic activity of various catalysts was analysed for DMP conversion the first group of catalysts, zeolite catalysts (A) for Fe-ZSM-5, (B) for Fe-Ag-ZSM-5, (C) for Fe-S-N-Zeolite-Y. The second group of catalysts, iron-doped different AC, (D) for Fe/AC raw-GAC, (E) for Fe/AC raw-SA2, (F) for Fe/AC raw-G60. The third group of catalysts (G) for Fe-S-N/AC HCl-HNO₃-GAC, (H) for Fe-S-N/AC HCl-HNO₃-SA2 and (I) for Fe-S-N-AC HCl-HNO₃-G60. Using 1 g.L⁻¹ of DMP in 50 mL solution, 1:20 DMP to H₂O₂ for 4h at 80 °C.

Firstly, in zeolite catalysts, with the conventional Fe-ZSM-5 (A), the oxidation of DMP was low at 33% and 66% residual intermediates. Doping Ag for these catalysts increases their catalytic activity for DMP by about 50% to be the conversion 63% and 38% residual intermediates. Notably, Fe-S-N-Zeolite-Y was capable of complete oxidation and mineralisation. Further, A, B, and C catalysts consumed high levels of H₂O₂ at high levels between 90% and 100%. In the case of A and B catalysts, the low catalytic activity results could be explained due to the steric hindrance effect of these two alkyl groups as expected to prevent the •OH radicals from attacking the target pollution.

In the second group of catalyst those supported on AC, Fe doping, three different types of AC; D, E and F (Fe/AC), the DMP conversion was in the range of 35%, and residual intermediates was roughly 65%. H₂O₂ consumption was approximately matching these conversions and there aren't extra species that contribute to oxidation. As supposed, adding S and N for these Fe/AC catalysts enhanced their performance. Still, there was a poor level of both DMP conversion and residual intermediates, which was almost 60% and 40%, respectively.

It is important to note that all these catalysts applied for DMP oxidation express high stability where the Fe leaching is almost less than 2% but 45% for the Fe-S-N-Zeolite-Y, which gives significant results that may be a because of the high mineralisation for intermediates which is at some points of the reaction form small chain acidic groups such as oxalic acid causing a high metal leaching.

In summary, the steric hindrance caused by the two methyl groups in the ortho and para positions can make the phenolic hydrogen less accessible to hydroxyl radical attack. In addition, the bulkiness of the methyl groups can hinder the approach of the hydroxyl radical to the phenolic hydrogen, thus reducing the reaction rate. However, Fe-S-N-Zeolite-Y gives extreme results for DMP oxidation by the CWPO reaction. Zeolite-Y, are known for their acidic properties. The presence of acidic sites on the Fe-S-N-Zeolite-Y surface can enhance the adsorption of 2,4-dimethylphenol and facilitate its reaction with hydroxyl radicals, leading to improved catalytic activity.

5.4 Conclusion

The CWPO reaction was applied to an array of phenolic compounds, including: 2,4 DMP, 4MP, 4CP, 4BrP and 3MOP, by using a series of catalyst labelled as that the first group is three zeolite catalysts A, B and C. (A) for Fe-ZSM-5, (B) for Fe-Ag-ZSM-5, (C) for Fe-S-N-Zeolite-Y. The second group of catalysts Fe/AC, iron doping three different kind of activated carbons, D, E and F. (D) for Fe/AC raw-GAC, (E) for Fe/AC raw-SA2, (F) for Fe/AC raw-G60. The third group of catalysts Fe-S-N/AC, G, H and I. (G) for Fe-S-N/AC HCl-HNO₃-GAC, (H) for Fe-S-N/AC HCl-HNO₃-SA2 and (I) for Fe-S-N-AC HCl-HNO₃-G60. The use of these materials and methodology, applied to these substrates is showing some promise for the degradation of these pollutants.

For 4CP interestingly though, despite a complete degradation of the substrate, there was incomplete consumption for H₂O₂. This apparently counterintuitive trend could be explained Cl[•] could be another hydrogen abstractor involved in the degradation process. The results confirm that the donating-electron functional group for chlorine via resonance affect is the dominate which enhance the degradation process.

When 4BrP was used as a substrate, instead, the catalytic activity of zeolite catalysts was higher than that of AC catalysts. Zeolite catalysts converted between 80% and 100%, while AC catalysts converted between 50% and 60% of 4BrP. residual intermediates with zeolite catalysts has a 30%, but 50-90% with AC catalysts. The best catalyst for 4BrP oxidation is Fe-S-N-Zeolite-Y, which gives 100% and 30% conversion and residual intermediates, respectively. The combination of Fe, S, and zeolite components in Fe-S-N-Zeolite-Y creates a synergistic effect that enhances the catalytic activity for 4BrP oxidation. The presence of multiple active components contributes to a more efficient and effective oxidative process. However, there are several factors that could contribute to the poor oxidation of 4-BrP with the other catalysts. It is important to note that for the bromine atom is situated in the para-position of the phenolic ring significantly affects the reactivity of the 4-bromophenol. It is possible for the bromine substituent to stabilize the phenoxyl radical formed, preventing further oxidation. In this way, they may degrade more slowly than other phenolic compounds. Also, the electron-withdrawing effect of bromine on the phenolic ring by inductive, seems to be the controlling affect. This effect reduces the electron density at the reaction site, making it less favourable for the attack of [•]OH. Br[•] radicals as previously mentioned can act as scavengers for [•]OH, prevents further degradation of the substances.

For 3MOP oxidation, all the catalysts show extreme activity in full conversion and mineralisation for their intermediates. H_2O_2 consumption in some cases does not reach 100%, which could be justified as there is another oxidant than hydroxyl radicals to play a role in the oxidation process, in this case, $\cdot\text{OCH}_3$. The most significant results can be explained by the reasons given above, where $-\text{OH}$ and $-\text{OCH}_3$ activated twice three sites on the aromatic ring on 3MOP.

The process of oxidation and mineralization of 4MP is almost always complete in all catalysts. It was complete consumption for the H_2O_2 , which corresponds to the catalytic activity results. The possible reason for the high oxidation rate of 4MP by $\cdot\text{OH}$ maybe because it provides an electron-donating effect.

When moving to DMP, this substrate was expected to be difficult to oxidise as the methyl substituents in this aromatic compound are located in the ortho, para position (2,4 di methyl phenol), which is not optimal for an electrophilic attack mechanism. That was confirmed by the detection of a conversion - less than 60% - for most catalysts and poor mineralisation residual intermediates 40% to 70%. It was observed that for all catalytic activity results, the H_2O_2 consumption value was always higher than the conversion results, which could mean there were sufficient $\cdot\text{OH}$ radicals but could not attack the target due to steric effects and the type and locations of these alkyl groups. However, Fe-S-N-Zeolite-Y was capable of 100% and 0% conversion and residual intermediates, respectively.

In light of the results obtained, phenol substitutes' position and their types either (electron-donation or electron-withdrawing groups) both give significant results with these selected catalysts especially modified novel catalysts (Fe-Ag-ZSM-5 1 wt% Fe loading, Fe-S-N-Zeolite-Y 0.5 wt% Fe loading and Fe-S-N/AC 12 wt% Fe loading). Moreover, metal leaching depends on reaction time and mineralisation of intermediates. In other words, a high level of mineralisation and acids group formation, including oxalic acid, which is the main cause of metal leaching, decreases the stability of catalysts and vice versa. Fe-S-N/AC (G60-HCl- HNO_3) has shown good stability and reusability in all phenolic oxidation reactions (Fe leaching < 4%). Its structural integrity and active sites can be maintained through multiple reaction cycles, making it a possible and practical catalyst for scale up and in turn pollutant degradation.

5.5 References

1. M. Ren, S. Sun, Y. Wu, Y. Shi, Z.-j. Wang, H. Cao and Y. Xie, *Chemosphere*, 2022, **296**, 134071.
2. T. M. Krygowski, K. Ejsmont, B. T. Stepień, M. K. Cyrański, J. Poater and M. Sola, *The Journal of Organic Chemistry*, 2004, **69**, 6634-6640.
3. L. G. C. Villegas, N. Mashhadi, M. Chen, D. Mukherjee, K. E. Taylor and N. Biswas, *Current Pollution Reports*, 2016, **2**, 157-167.
4. C. Karunakaran and R. Dhanalakshmi, *International Journal of Chemical Kinetics*, 2009, **41**, 275-283.
5. D. Juretic, H. Kusic, D. D. Dionysiou and A. L. Bozic, *Journal of hazardous materials*, 2013, **262**, 377-386.
6. A. T. Nguyen, C.-T. Hsieh and R.-S. Juang, *Journal of the Taiwan Institute of Chemical Engineers*, 2016, **62**, 68-75.
7. C. Bougheloum and A. Messalhi, *Physics Procedia*, 2009, **2**, 1055-1058.
8. C. G. Silva and J. L. Faria, *Applied Catalysis B: Environmental*, 2010, **101**, 81-89.
9. L. Yulianti, S. C. Lee and H. O. Lintang, *Materials Today: Proceedings*, 2019, **7**, 697-703.
10. M. Anbar, D. Meyerstein and P. Neta, *The Journal of Physical Chemistry*, 1966, **70**, 2660-2662.
11. L. Wojnárovits, G. Földiák, M. D'Angelantonio and S. Emmi, *Research on chemical intermediates*, 2002, **28**, 373-386.
12. K. Omura and T. Matsuura, *Tetrahedron*, 1968, **24**, 3475-3487.
13. T. Matsuura and K. Omura, *Synthesis*, 1974, **3**, 173-184.
14. C. K. Scheck and F. H. Frimmel, *Water Research*, 1995, **29**, 2346-2352.
15. F. Nawaz, Y. Xie, J. Xiao, H. Cao, Z. A. Ghazi, Z. Guo and Y. Chen, *Catalysis Science & Technology*, 2016, **6**, 7875-7884.
16. O. Gimeno, M. Carbajo, M. J. López, J. A. Melero, F. Beltrán and F. J. Rivas, *Water research*, 2007, **41**, 4672-4684.
17. R. C. Martins and R. M. Quinta-Ferreira, *Applied Catalysis B: Environmental*, 2009, **90**, 268-277.
18. G. Palmisano, M. Addamo, V. Augugliaro, T. Caronna, E. García-López, V. Loddo and L. Palmisano, *Chemical communications*, 2006, **9**, 1012-1014.

19. J. DeRuiter, *Amides*, downloaded from the internet at " [www. auburn. edu/~deruija/pdal-amides. pdf](http://www.auburn.edu/~deruija/pdal-amides.pdf)" on Sep, 2014, **22**.
20. M. J. Sampaio, C. G. Silva, A. M. Silva, V. J. Vilar, R. A. Boaventura and J. L. Faria, *Chemical Engineering Journal*, 2013, **224**, 32-38.
21. A. Tolosana-Moranchel, D. Ovejero, B. Barco, A. Bahamonde, E. Díaz and M. Faraldos, *Journal of Environmental Chemical Engineering*, 2019, **7**, 103051.
22. M. T. Pérez-Prior, R. Gómez-Bombarelli, M. I. González-Sánchez and E. Valero, *Journal of hazardous materials*, 2012, **241**, 207-215.
23. J. E. Grebel, J. J. Pignatello and W. A. Mitch, *Environmental science & technology*, 2010, **44**, 6822-6828.
24. Y. Yang, J. J. Pignatello, J. Ma and W. A. Mitch, *Environmental science & technology*, 2014, **48**, 2344-2351.
25. Z. Wang, Y. Shao, N. Gao and N. An, *Separation and Purification Technology*, 2018, **195**, 92-100.
26. Z. Wang, M. Feng, C. Fang, Y. Huang, L. Ai, F. Yang, Y. Xue, W. Liu and J. Liu, *RSC advances*, 2017, **7**, 12318-12321.
27. S. Fukuchi, R. Nishimoto, M. Fukushima and Q. Zhu, *Applied Catalysis B: Environmental*, 2014, **147**, 411-419.
28. T. Mathialagan and T. Viraraghavan, *Environmental technology*, 2005, **26**, 571-580.
29. S. Esplugas, P. Yue and M. I. Pervez, *Water Research*, 1994, **28**, 1323-1328.
30. A. O. Olaniran and E. O. Igbinsosa, *Chemosphere*, 2011, **83**, 1297-1306.
31. P. K. Arora and H. Bae, *Microbial Cell Factories*, 2014, **13**, 1-17.
32. J. Gao, L. Liu, X. Liu, H. Zhou, S. Huang and Z. Wang, *Chemosphere*, 2008, **71**, 1181-1187.
33. W.-J. Sim, S.-H. Lee, I.-S. Lee, S.-D. Choi and J.-E. Oh, *Chemosphere*, 2009, **77**, 552-558.
34. E. O. Igbinsosa, E. E. Odjadjare, V. N. Chigor, I. H. Igbinsosa, A. O. Emoghene, F. O. Ekhaise, N. O. Igiehon and O. G. Idemudia, *The Scientific World Journal*, 2013, **2013**.
35. J. Pumarega, M. Gasull, D.-H. Lee, T. López and M. Porta, *PloS one*, 2016, **11**, e0160432.
36. Y. Guo, J. Zhou, X. Lou, R. Liu, D. Xiao, C. Fang, Z. Wang and J. Liu, *Chemical Engineering Journal*, 2014, **254**, 538-544.
37. E. Lipczynska-Kochany, G. Sprah and S. Harms, *Chemosphere*, 1995, **30**, 9-20.
38. G. Fu, G. Xu and C. Zhu, *Environmental Science and Management*, 2006, **31**, 133-135.

39. B. G. Kwon, D. S. Lee, N. Kang and J. Yoon, *Water Research*, 1999, **33**, 2110-2118.
40. J. Liu, J.-Y. Wu, C.-L. Kang, F. Peng, H.-F. Liu, T. Yang, L. Shi and H.-L. Wang, *Journal of hazardous materials*, 2013, **261**, 500-511.
41. A. J. Pandell, *The journal of organic chemistry*, 1976, **41**, 3992-3996.
42. R. Chen and J. J. Pignatello, *Environmental science & technology*, 1997, **31**, 2399-2406.
43. D. L. Sedlak and A. W. Andren, *Environmental Science & Technology*, 1991, **25**, 777-782.
44. S. Tamagaki, K. Suzuki and W. Tagaki, *Bulletin of the Chemical Society of Japan*, 1989, **62**, 148-152.
45. S. Tamagaki, M. Sasaki and W. Tagaki, *Bulletin of the Chemical Society of Japan*, 1989, **62**, 153-158.
46. A. Martell and R. Smith, *New York, NY.[Google Scholar]*, 1977.
47. Y. Zuo and J. Hoigne, *Environmental Science & Technology*, 1992, **26**, 1014-1022.
48. C. Zhou, PhD thesis, University of Sheffield, 2021.
49. S. Zhou, C. Zhang, R. Xu, C. Gu, Z. Song and M. Xu, *Water Science and Technology*, 2016, **73**, 1025-1032.
50. M. M. Micó, J. Bacardit, J. Malfeito and C. Sans, *Applied Catalysis B: Environmental*, 2013, **132**, 162-169.
51. N. N. Mahamuni and A. B. Pandit, *Ultrasonics Sonochemistry*, 2006, **13**, 165-174.
52. Y. Du, M. Zhou and L. Lei, *Journal of Hazardous Materials*, 2006, **136**, 859-865.
53. C.-C. Kuan, S.-Y. Chang and S. L. Schroeder, *Industrial & Engineering Chemistry Research*, 2015, **54**, 8122-8129.
54. W.-S. Zou, Y.-J. Ji, X.-F. Wang, Q.-C. Zhao, J. Zhang, Q. Shao, J. Liu, F. Wang and Y.-Q. Wang, *Chemical Engineering Journal*, 2016, **294**, 323-332.
55. L. Keith and W. Telliard, *Sci. Technol*, 1979, **13**, 416423.
56. D. C. Muir and P. H. Howard, *Environmental science & technology*, 2006, **40**, 7157-7166.
57. J. Bursey and E. Pellizzari, *NTIS, SPRINGFIELD, VA(USA). 1983.*, 1983.
58. Y. Zhuang, S. Ahn and R. G. Luthy, *Environmental science & technology*, 2010, **44**, 8236-8242.
59. A. Sharma and R. K. Dutta, *Journal of Cleaner Production*, 2018, **185**, 464-475.
60. X. Li, J. W. Cabbage, T. A. Tetzlaff and W. S. Jenks, *The Journal of Organic Chemistry*, 1999, **64**, 8509-8524.

61. A. Sobczykński, Ł. Duczmal and W. Zmudziński, *Journal of molecular catalysis A: chemical*, 2004, **213**, 225-230.
62. J.-M. Herrmann, *Catalysis today*, 1999, **53**, 115-129.
63. W. Bian, X. Song, D. Liu, J. Zhang and X. Chen, *Journal of Hazardous Materials*, 2011, **192**, 1330-1339.
64. A. De Luca, X. He, D. D. Dionysiou, R. F. Dantas and S. Esplugas, *Chemical Engineering Journal*, 2017, **318**, 206-213.
65. D. Lambropoulou, E. Evgenidou, V. Saliverou, C. Kosma and I. Konstantinou, *Journal of hazardous materials*, 2017, **323**, 513-526.
66. D. Xu, X. Song, W. Qi, H. Wang and Z. Bian, *Chemical Engineering Journal*, 2018, **333**, 477-485.
67. J. D. McDonald, B. Zielinska, E. M. Fujita, J. C. Sagebiel, J. C. Chow and J. G. Watson, *Environmental Science & Technology*, 2000, **34**, 2080-2091.
68. J. J. Schauer, M. J. Kleeman, G. R. Cass and B. R. Simoneit, *Environmental science & technology*, 2001, **35**, 1716-1728.
69. M. D. Hays, C. D. Geron, K. J. Linna, N. D. Smith and J. J. Schauer, *Environmental Science & Technology*, 2002, **36**, 2281-2295.
70. C. Coeur-Tourneur, A. Cassez and J. C. Wenger, *The Journal of Physical Chemistry A*, 2010, **114**, 11645-11650.
71. L. He, T. Schaefer, T. Otto, A. Kroflic and H. Herrmann, *The Journal of Physical Chemistry A*, 2019, **123**, 7828-7838.
72. J. Clayden, N. Greeves and S. Warren, *Organic chemistry*, Oxford University Press, USA, 2012.
73. A. Lauraguais, I. Bejan, I. Barnes, P. Wiesen and C. Coeur, *The Journal of Physical Chemistry A*, 2015, **119**, 6179-6187.
74. E. Land and M. Ebert, *Transactions of the Faraday Society*, 1967, **63**, 1181-1190.
75. O. Saveleva, N. Vysotskaya and L. Shevchuk, *Zhurnal Organicheskoi Khimii*, 1972, **8**, 283-+.
76. M. Roder, L. Wojnarovits, G. Földiák, S. Emmi, G. Beggiato and M. D'Angelantonio, *Radiation Physics and Chemistry*, 1999, **54**, 475-479.
77. T. Zhang, L. Cheng, L. Ma, F. Meng, R. G. Arnold and A. E. Sáez, *Chemosphere*, 2016, **161**, 349-357.
78. P. M. Nagarnaik and B. Boulanger, *Chemosphere*, 2011, **85**, 854-860.

79. S. D. Scullion, M. R. Clench, M. Cooke and A. E. Ashcroft, *Journal of Chromatography a*, 1996, **733**, 207-216.
80. B. Dong, A. Kahl, L. Cheng, H. Vo, S. Ruehl, T. Zhang, S. Snyder, A. E. Sáez, D. Quanrud and R. G. Arnold, *Science of the Total Environment*, 2015, **518**, 479-490.
81. C. H. Swartz, S. Reddy, M. J. Benotti, H. Yin, L. B. Barber, B. J. Brownawell and R. A. Rudel, *Environmental science & technology*, 2006, **40**, 4894-4902.
82. J. E. Loyo-Rosales, C. P. Rice and A. Torrents, *Environmental science & technology*, 2007, **41**, 6815-6821.
83. C. Lye, C. Frid, M. Gill, D. Cooper and D. Jones, *Environmental Science & Technology*, 1999, **33**, 1009-1014.
84. A. M. Soto, H. Justicia, J. W. Wray and C. Sonnenschein, *Environmental health perspectives*, 1991, **92**, 167-173.
85. P.-C. Lee and W. Lee, *Bulletin of Environmental Contamination and Toxicology*, 1996, **57**, 341-348.
86. R. I. Olariu, B. Klotz, I. Barnes, K. H. Becker and R. Mocanu, *Atmospheric Environment*, 2002, **36**, 3685-3697.
87. K.-h. Wang, Y.-h. Hsieh and L.-j. Chen, *Journal of Hazardous materials*, 1998, **59**, 251-260.
88. K. Sehested, H. Corfitzen, H. Christensen and E. Hart, *The Journal of Physical Chemistry*, 1975, **79**, 310-315.
89. M. Gohn and N. Getoff, *Journal of the Chemical Society, Faraday Transactions 1: Physical Chemistry in Condensed Phases*, 1977, **73**, 1207-1215.
90. M. S. Davies, B. Mile, C. C. Rowlands and M. D. Barratt, *Magnetic Resonance in Chemistry*, 1995, **33**, 15-19.
91. J. Pospisil, V. Ettl and V. Skola, *Chem. Prum.(Prague)*, 1957, **7**, 244-248.
92. F. Jin, H. Zhong, J. Cao, J. Cao, K. Kawasaki, A. Kishita, T. Matsumoto, K. Tohji and H. Enomoto, *Bioresource technology*, 2010, **101**, 7624-7634.
93. D. Huang, X. Zhang, Z. Chen, Y. Zhao and X. Shen, *Atmospheric Chemistry and Physics*, 2011, **11**, 7399-7415.
94. N. Boonrattanakij, M.-C. Lu and J. Anotai, *Journal of hazardous materials*, 2009, **172**, 952-957.
95. K. Sehested, N. Getoff, F. Schwoerer, V. Markovic and S. O. Nielsen, *Journal of Physical Chemistry*, 1971, **75**, 749-755.
96. N. K. V. Leitner and M. Doré, *Water Research*, 1997, **6**, 1383-1397.

97. H.-L. Wang, W.-Z. Liang, Q. Zhang and W.-F. Jiang, *Chemical Engineering Journal*, 2010, **164**, 115-120.
98. V. Kavitha and K. Palanivelu, *Journal of Photochemistry and Photobiology A: Chemistry*, 2005, **170**, 83-95.
99. S. S. Shukla, K. L. Dorris and B. V. Chikkaveeraiah, *Journal of hazardous materials*, 2009, **164**, 310-314.
100. A. Romero, A. Santos and F. Vicente, *Journal of Hazardous Materials*, 2009, **162**, 785-790.
101. M. K. Nazal, D. Rao and N. Abuzaid, *Journal of Water Supply: Research and Technology—AQUA*, 2020, **69**, 438-452.
102. A. A. P. Khan, P. Singh, P. Raizada, A. Khan, A. M. Asiri and M. M. Alotaibi, *Chemosphere*, 2023, **316**, 137839.

Chapter 6: Conclusions and future work

6.1: Conclusions

Recently, wastewater compounds containing phenol or phenol derivatives have attracted increasing attention due to their toxic effects and nowadays ubiquitous presence in the environment as restudies from building blocks for the polymer sector.^{1,2} It is one of the most common contaminants found in wastewater. There are several traditional approaches for treating wastewater, namely physical, biological, and chemical processes, that are not always effective, particularly in the case of highly concentrated and non-biodegradable organic substances like phenolic compounds. In addition, most of these methods used large amounts of chemicals, creating an excessive consumption of chemicals. In addition, these technologies are expensive, adding to their disadvantages. Due to this, they are not widely used to remove phenolics. Treatments for phenolic compounds in wastewater, wet air oxidation (WAO) as well as catalytic wet air oxidation (CWAO) have been used in recent years. Nevertheless, high pressure (20 - 200 bar) and high temperatures (200 – 320 C°) are required, which increases the cost of the abatement treatment.

Alternatively, in order to lower the costs of these reactions, hydrogen peroxide H₂O₂ is used as the oxidizing agent, referred to as catalytic wet hydrogen peroxide oxidation (CWPO).³ This methodology exploits the principles of the Fenton chemistry, where iron species, like Fe²⁺, but also Fe³⁺ can break down H₂O₂ to generate hydroxyl radicals as powerful oxidants for organic compounds. In principle, the Fenton's process is a promising technique to wastewater treatment, due to the availability of Fe, it is a relatively safe process to run, cost-effective, and importantly it allows to be scaled up and in turn to be applicable for large scale applications like those expected in water purification. Furthermore, the final decomposition of H₂O₂ produces water and oxygen, both safe and environmentally friendly. Numerous studies have shown that Fenton's oxidation method is the most economical wastewater treatment method due to its ease of installation and mild operation.⁴ Still, it has some shortcomings due to the high H₂O₂ consumption and Fe contamination, requiring removal after treatment, adding to the overall costs of the treatment. Heterogeneous catalysts can overcome these drawbacks, also known as Fenton heterogeneous catalysts. A variety of transition metals, primarily iron, have been used in porous matrices such as activated carbon,^{5,6} clay-based,^{7,8} metal oxides,^{9,10} and zeolites.^{11,12} A supported catalysts in CWPO help to uniformly distribute and stabilize metal active species at the surface, eliminating agglomeration and enhancing thermal and chemical

stability, thus accelerating pollutant elimination, as well as promoting its recovery. However, in general, the main issue associated with heterogenous catalysts is metal leaching, affecting the catalyst's durability and raising the contamination by metals.

6.1.1 Supported Fe activated carbons and zeolites for CWPO

This thesis work contributes to the advancement of science and technology into the water purification by catalytic oxidation of phenolic compounds using wet hydrogen peroxide oxidation reactions involving heterogeneous catalysts (CWPO). During this research project, a comprehensive study on the synthesis and develop novel catalysts to meet the requirements for full phenolic compounds conversion and complete mineralization simultaneously while maintaining their stability. Two supported catalysts been involved in this study activated carbon and zeolites. Due to their unique properties, they have been selected. Large surface areas are characteristic of zeolites,¹³ roughly between 500 to 800 m²·g⁻¹.¹⁴ Zeolites are ideal for adsorption and catalysis because of their porous structure.¹⁵ By exerting steric influence on the reaction, shape-selective pores control reactant and product access. Besides modifying the geometry of the pores, it is also possible to fine-tune zeolites by modifying the Si:Al ratio and the cation composition through ion exchange. The specific properties of zeolites are, partly, responsible for their catalytic activity, with different properties being obtained by altering their composition and structure. Several types of zeolites have been investigated in CWPO of phenol, including natural and synthetic ones.¹⁶ For this work ZSM-5 at different Si:Al molar ratios 23, 50 and 80, also Zeolite-Y have been used as a supported catalyst for Fe active species.

6.1.2 AC and N/S doping and effect of pre-acid treatments

Recently, the CWAO introduced activated carbon-based catalysts with encouraging results.¹⁷ ¹⁸ Particularly, AC is widely used as catalyst support for phenol oxidation via CWPO.^{3, 5, 19, 20} The most notable features of activated carbons (AC) are the large surface area and porous nature in comparison to other supports like Al₂O₃, TiO₂, and CeO₂, plus oxygen groups on their surfaces, which may contribute to catalysis.²¹ ACs have a large surface area, ranging from 800 to 1200 m²·g⁻¹.²² Various functional groups can be introduced on the surface of AC, such as -COOH, -OH, or -NH₂, by pre-acid treatments improving its catalytic activity. Stability in both acidic and basic environments is another essential characteristic.²³

The catalysts were based on activated carbon in this work, expressed various modifications were made to enhance their performance for phenol oxidation. Three different kinds of AC been used: NORIT 1240 GAC, NORIT SA2 and DARCO G60, they were labelled as GAC,

SA2 and G60, respectively. The main findings and key points of this part of study are as follows:

There were three types AC used to prepare iron-doped activated carbon (Fe/AC) and iron, sulphur, and nitrogen-tri-doped activated carbon (Fe-S-N/AC), which were characterized and tested as catalysts for CWPO of phenol. Adding N and S to activated carbon increased its catalytic activity by increasing its electron density. Furthermore, Fe/AC dual-doped with N and S significantly enhanced its catalytic performance. With Fe-S-N/AC raw-GAC, phenol oxidation was 100 % and 30 % residual intermediates and reduced the iron leaching by 50 % to 40 % compared to Fe/AC raw-GAC. Doping S and N into raw-SA2 (Fe-S-N/AC raw-SA2) results in high catalytic activity of 100 % and 12 % in phenol conversion and residual intermediates, respectively. Since Fe leaching was still high at 80 %, there was no significant difference between Fe/AC raw-SA2 and Fe/AC raw-SA2. G60 catalysts that contain S and N for Fe/AC raw-G60 exhibited a slight decrease in catalytic activity (phenol conversion reduced from 100 % to 80 %, and residual intermediates became 60 % while was 40 % with Fe/AC). Leaching results for Fe were also similar. Using different ACs, all Fe-S-N/AC catalysts showed significant increases in S mol% following S doping. Therefore, the protocol worked successfully. There was a slight increase in N mol% for these catalysts but not for GAC. N mol% was unrelated to H₂O₂ consumption, contradicting the second hypothesis that doping N enhances H₂O₂ degradation of the pollutant.

Pre-acid treatment with HCl, then doping S and N, for Fe-S-N/AC HCl-GAC exhibits higher catalytic activity than Fe/AC HCl-GAC (phenol oxidation from 55 % rise to 88 % as well residual intermediates reduced from 100 % to 57 %). The leaching of Fe was also 13 %. The doping of S and N did not affect HCl-SA2 catalysts. In contrast, Fe-S-N/AC HCl-G60 showed enhanced catalytic activity with S and N. However, both stability and full phenol oxidation were not achieved with these catalysts. Based on the results of the elemental analysis, there was a reduction in the O mol%, consistent with dehydration. The decreased catalytic activity is generally associated with catalysts prepared by HCl-AC, either Fe/AC or Fe-S-N/AC catalysts, indicated by XRD results where the particle size of the active species was considerably larger than other catalysts.

Pre-treatment of AC via HNO₃ oxidation then doped metals leads to high activity. Fe-S-N/AC HNO₃-GAC showed complete phenol conversion and 11% residual intermediates. Additionally, leaching was reduced by 50% from 63% to 50%. The second catalyst, Fe-S-N/AC

HNO₃-SA2 slightly decreased the activity for phenol conversion comparing to Fe/AC HNO₃-SA2, from 100% to 83%, but the leaching was 50% less from 60-80% to 28%. The third catalyst, compared with Fe/AC HNO₃-G60, Fe/S-N/AC HNO₃-G60 keeps the catalytic activity while reducing leaching from 60% to 40%. Results of the elemental analysis showed a significant increase in S mol% but no difference in O mol%. However, keeping the amount of O the same does not mean keeping the AC's surface the same. Therefore, HNO₃ may not oxidize AC, but C-OH to COOH, which appears to bind Fe better.

Using both acids HCl and HNO₃ as pre-acid treatments and doping both S and N. For GAC, high catalytic activity was demonstrated phenol conversion of 100% and residual intermediates conversion of 30%. They reduced Fe leaching to the lowest level 15% compared to other catalysts by GAC. Fe-S-N/AC HCl-HNO₃-SA2 produces 100% phenol oxidation and 29% residual intermediates and reduces the leaching to 30%. Then for Fe-S-N/AC HCl-HNO₃-G60 supported these results, demonstrating complete phenol oxidation and high mineralization of 15% residual intermediates and only 10% Fe leaching. Therefore, doped Fe-S-N/AC prepared by AC pre-acid treatments by HCl and HNO₃ catalysts were quite stable and more active for CWPO of phenol than Fe/AC. Catalytic performance is enhanced by N and S atoms. In the CWPO of phenol, Fe-S-N/AC prepared by AC pre-acid treatments by HCl and HNO₃ catalysts was an effective and stable catalyst. Consequently, it may be useful in the treatment of wastewater containing phenol.

XRD analysis shows that for all catalysts Fe₂O₃ contributes the most to catalytic activity. This phase contributes more than 50% to diffraction patterns. In addition, other species that could exist based on the literature, such as CFe₃, FeN, and FeS, were not present, indicating that they either do not exist or are not crystallized enough to be detected. Based on the elemental analysis data, the first hypothesis seems most likely. All catalysts with different ACs show the same lattice parameters (and d-spacing) for Fe₂O₃, indicating that hetero species are not intercalated. In addition, the intrinsic properties of the catalyst are affected by HCl pre-treatment. HCl-AC with GAC, SA2 and G60 makes Fe₂O₃ particles larger at 46, 125 and 61 nm for Fe/AC. No intercalation occurred, so HCl dehydrates carbon, reducing Fe anchoring points and increasing Fe₂O₃. HCl-AC catalysts have low activity based on these results. In terms of the XRD pattern, HNO₃ had no discernible effect.

Based on the XPS analysis, there is a large variation in surface Fe of samples (Fe dispersed on the carbon surface) independent of phenol conversion. The O surface of carbon decreases when

it is treated with HCl. Based on hypotheses and XRD data, it is likely that HCl dehydrates alcoholic groups, resulting in less oxygen and larger Fe_2O_3 particles, which result in decreased activity and leaching. Regarding HNO_3 's effects, there are no noticeable effects. Catalytic data indicate that the effect is negligible. HNO_3 -treated catalysts also appear to have the most minor Fe_2O_3 clusters, whereas Fe-S-N/AC catalysts have the least leaching. As a result, S reduces leaching. Surface S reduces leaching, but reducing carbon before this protocol would be a compromise. Catalysts are low-oxidation Fe when they are prepared, but Fe_2O_3 when they are analysed or used.

6.1.3 Fe and Ag- doped zeolites for CWPO

Zeolite material with iron incorporated into its framework is a well-known catalyst. Fe-ZSM-5 demonstrated significant catalytic activity for the oxidation of phenol compounds, but the high Fe leaching affected their durability. For meeting the required complete phenol oxidation and maintaining the catalyst's stability, variable techniques were considered. These are the following outcomes:

Various forms of ZSM-5 zeolite catalysts and their performance in phenol conversion using different iron precursors were studied. It was found that Fe-ZSM-5 (A-1) prepared by NH_4 -ZSM-5 and $\text{Fe}(\text{NO}_3)_3 \cdot 9\text{H}_2\text{O}$ achieved 100% phenol conversion. Fe-ZSM-5 (A-2) produced from H-ZSM-5 and $\text{Fe}(\text{NO}_3)_3 \cdot 9\text{H}_2\text{O}$ converted 40% of the phenol. Fe-ZSM-5 (B-1) obtained by NH_4 -ZSM-5 and $\text{FeSO}_4 \cdot 7\text{H}_2\text{O}$ gives 70% phenol conversion. Fe-ZSM-5 (B-2) prepared by H-ZSM-5 and $\text{FeSO}_4 \cdot 7\text{H}_2\text{O}$ gives 30% phenol conversion, all these catalysts have 1 wt% Fe loading. These results suggest that the choice of support (NH_4 -ZSM-5 or H-ZSM-5) and the iron precursor ($\text{Fe}(\text{NO}_3)_3 \cdot 9\text{H}_2\text{O}$ or $\text{FeSO}_4 \cdot 7\text{H}_2\text{O}$) significantly influence the catalytic performance of the Fe-ZSM-5 catalysts in phenol conversion.

This study also demonstrated the significant influence of iron loading and precursor choice on the catalytic activity of Fe-ZSM-5 catalysts in phenol conversion. 1 wt% iron loading Fe-ZSM-5 catalysts prepared by $\text{Fe}(\text{NO}_3)_3 \cdot 9\text{H}_2\text{O}$ precursor obtained 100% phenol conversion. Increasing the iron loading to 5 wt% Fe-ZSM-5 dramatically reduce the phenol conversion to be 40%. As well as 10 wt% Fe-ZSM-5 produced 20 % phenol conversion. In this case, it is observed that as the iron loading increases, the catalytic activity of the Fe-ZSM-5 catalyst decreases. The highest phenol conversion is achieved with 1 wt% Fe-ZSM-5, indicating that lower iron loading is more effective for this specific precursor. In contrast, Fe-ZSM-5 catalysts prepared by $\text{FeSO}_4 \cdot 7\text{H}_2\text{O}$ precursor: 1 wt% Fe-ZSM-5 gives 70% phenol conversion, while,

increasing the iron loading for Fe-ZSM-5 increased the catalytic activity to 98% and 100% phenol conversion for 5wt% and 10wt% Fe-ZSM-5, respectively. when using $\text{FeSO}_4 \cdot 7\text{H}_2\text{O}$ as the precursor, increasing the iron loading leads to an improvement in catalytic activity. The highest phenol conversion is achieved with 10 wt% Fe-ZSM-5, suggesting that higher iron loading is more beneficial.

The comparison between Fe-ZSM-5 prepared by wetness impregnation (WI) and Fe-ZSM-5 (VI) prepared by wetness impregnation under vacuum was investigated; there is no difference in the catalytic activity between the two catalysts for phenol oxidation by the CWPO reaction at an array of reaction's temperatures 40, 60 and 80 °C. Changing preparation methods seems not to have affected the performance of Fe-ZSM-5 due to its high activity. It is confirmed that Fe-ZSM-5 catalysts had high activity in the CWPO of the phenol reaction, regardless of the preparation method.

The present study delves into the synthesis and characterization of Fe-S-N-ZSM-5 catalysts, specifically focusing on the influence of Si:Al (23, 50, and 80) molar ratios and the incorporation of Zeolite-Y (5.1). All catalysts contain 1wt.% Fe loading and were synthesized by wetness impregnation. The objective of this study is twofold: first, to assess the impact of Si:Al ratios on the catalytic performance of Fe-S-N-ZSM-5 catalysts, and second, to evaluate the catalytic potential of Fe-S-N-ZSM-5 in comparison to Zeolite-Y (5.1) under similar conditions. The catalytic activity of Fe-S-N-ZSM-5 catalysts increased with increasing Si:Al molar ratios. Phenol conversion improved from 80% to 100% with Fe-S-N-ZSM-5 (23) and Fe-S-N-ZSM-5 (80), respectively. The Fe-S-N-Zeolite-Y catalyst was found to be the most efficient catalyst for this reaction, both in terms of full phenol oxidation and mineralization (100% and 0% for phenol conversion and residual intermediates, respectively). Furthermore, Fe leaching is lower (50%) than Fe-S-N-ZSM-5 (between 80 and 90%). According to the results, zeolite type and Si:Al molar ratio influence the final Fe-S-N-Zeolite catalyst performance.

Fe and Ag-doped zeolite catalysts were prepared using wet impregnation method, different Fe loadings, Si:Al ratios with ZSM-5, and zeolite types Zeolite-Y (5.1) were studied. There was extreme activity for bimetallic Ag-Fe-Zeolite catalysts in CWPO oxidation of phenol irrespective of Si:Al ratios or Zeolite types. Still, Fe-Ag-ZSM-5 (Si:Al, 23) with 0.5 wt% Fe loading appeared to be the most effective catalyst for this reaction that considering its high catalytic activity and durability, along with the ability to reduce reaction time to only one hour,

Overall, with full phenol oxidation and 0% residual intermediates. Also, these catalysts have good stability (30% Fe leaching).

XRD patterns collected from zeolite catalysts doped with various metals have been used to characterize the crystalline structure of zeolite catalysts. The XRD patterns of pure $\text{NH}_4\text{-ZSM-5}$ support and its catalysts, and of pure Zeolite-Y and their catalysts, indicate that their original structures did not change during wetness impregnation. In the Fe-Ag-ZSM-5 catalysts, only zeolite structures are responsible for the pattern; no iron or silver species were detected, and the XRD patterns did not differ significantly from those of $\text{NH}_4\text{-ZSM5}$. The intensity of XRD peaks is affected by crystal size and dispersion on the support. Weak peaks of crystalline phase are also related to good dispersion of crystalline phase accompanied by small crystal sizes, according to previous studies. As a result, the iron and silver particles dispersed over the zeolite during preparation were highly dispersed. X-ray analyses of Fe-zeolites catalysts did not reveal iron oxide clusters. There is a possibility that Fe-ZSM-5, F-S-N-Zeolite, and Fe-Ag-Zeolite catalysts do not contain iron oxide particles larger than 3-5 nm. There is no discernible reflection of any extra elements or their oxides; hence, if Fe_2O_3 or Ag_2O exist, they must be small (less than 5 nm). However, unlike activated carbon, zeolites have tens of reflections that overlap with Fe_2O_2 and Ag_2O 's expected positions. Overall, neither the preparation nor the metal dopant in the form of small particles affected the lattice parameters.

6.1.4 Extension of catalytic properties of our materials to phenol homologues

This study expanded the application of the selected modified heterogeneous catalysts for the oxidation of phenolic compounds; the following key findings have been established: Modifying heterogeneous catalysts is pivotal in enhancing their catalytic performance for phenolic compound oxidation. Introducing specific elements, such as sulphur (S), nitrogen (N), silver (Ag) and iron, led to active sites facilitating the oxidation process. The modified catalysts like Fe-S-N-ZSM-5, Fe-Ag-ZSM-5, and Fe-S-N/AC prepared via the pre-acid treatment of AC by HCl- HNO_3 exhibited improved oxidation efficiency compared to their unmodified counterparts like Fe-ZSM-5 and Fe/AC. The synergistic effects of different modifications contributed to enhanced phenolic compounds conversion and mineralization, offering promising solutions for tackling phenolic pollutants. In this work, the CWPO reaction was applied to a variety of phenolic compounds, which included 4-chlorophenol (4CP), 4-bromophenol (4BrP), 3-methoxyphenol (3MOP), 4-cresol (4MP) and 2,4 dimethylphenol (DMP).

In the case of (4CP) oxidation, significant results are obtained with complete oxidation of 4CP and its intermediates. It is interesting to note that only partial oxidation of H_2O_2 occurred, suggesting that Cl^{\cdot} may be another oxidant involved. This outcome confirms that chlorine has a dominant donating-electron functional group through the resonance effect, which enhances degradation. For oxidising of (4BrP), the catalytic activity of zeolite catalysts is higher than AC catalysts. Zeolite catalysts (Fe-ZSM-5, Fe-Ag-ZSM-5 and Fe-S-N-Zeolite-Y) converted 80% to 100% of 4BrP, while AC (Fe/AC and Fe-S-N/AC, HCl-HNO₃) catalysts converted 50% to 60%. residual intermediates with zeolite catalysts has a 30 %, but 50-90 % with AC catalysts. Fe-S-N-Zeolite-Y is the best catalyst for oxidizing 4BrP, achieving 100% conversion and 30% residual intermediates.

In the case of (3MOP) oxidation, all catalysts are highly active in full conversion and mineralization of their intermediates. In some cases, H_2O_2 consumption does not reach 100%, indicating that another oxidant, in this case $^{\cdot}OCH_3$, might be involved in the oxidation process. Activation of three aromatic ring sites on 3MOP by both -OH and -OCH₃ accounts for the most significant results. For (4MP) is almost always oxidized and mineralized completely by all catalysts. The H_2O_2 was consumed completely as well, consistent with the catalytic activity. 4MP's high oxidation rate by $^{\cdot}OH$ can be attributed to the electron-donating effect. Finally; (DMP) found to be difficult to oxidize due to its ortho, para position, which does not favour electrophilic attack. In most catalysts, conversion was less than 60%, and mineralization was between 40% and 70%. Meanwhile, Fe-S-N-Zeolite-Y achieved significant results of 100% and 0% for DMP oxidation and residual intermediates, respectively.

Considering the results obtained, all the selected phenolic compounds yield significant results with these selected catalysts, especially modified novel catalysts (Fe-Ag-ZSM-5, Fe-S-N-Zeolite-Y and Fe-S-N/AC). In addition, the rate of metal leaching depends on the reaction time and the mineralization of intermediates. Therefore, the stability of catalysts is decreased when there is high mineralisation and formation of acids groups, including oxalic acid, which is the main cause of metal leaching. Fe-S-N/AC (G60-HCl-HNO₃) showed good stability and reusability (Fe leaching < 0.4 mg·L⁻¹). This catalyst's active sites and structural integrity can be maintained through multiple reaction cycles, making it an effective and sustainable pollutant-degrading catalyst.

6.2 Future research directions:

This study can serve as a foundation for future research endeavours. Further investigations could delve into the mechanistic understanding of the catalytic oxidation process and the optimization of modification methods. These potential research directions include:

- I. **Reaction mechanism studies.** In the pursuit of comprehending the intricacies of the oxidation mechanism for various phenolic compounds, a fundamental requirement emerges to identify their intermediates for each phenolic compound. In this study, this was done for phenol and their intermediates but it could be enhanced and studied in detail for other phenolic compounds, including 4CP, 4BrP, 3MOP, 4MP and DMP, by means of kinetic studies, also considering the use of inhibitors to slow down some of the reaction steps and as such to allow to better monitor them by using techniques like HPLC. In addition to analysing the intermediates qualitatively, quantitative analysis is crucial for determining the catalytic activity regarding phenolic conversion and the selectivity for intermediates, especially in this thesis work, which indirectly quantifies CO₂ by carbon mass balance (CMB) determination. This could involve, for example the monitor of CO₂ on gas phase by IR methods to be complemented with trapping like carbonates in the liquid phase.

- II. **Characterization of the zeolites.** The promising results obtained with Fe-S-N-Zeolite catalysts open up several avenues for future research and exploration. To understand the underlying mechanisms of the enhanced catalytic activity and stability of Fe-S-N-Zeolite catalysts, it has to investigate the interactions between Fe, S, and N species and their roles in promoting the reaction. This could involve characterization techniques such as infrared (IR) spectroscopy. When IR is applied to Fe-S-N-Zeolite catalysts it can reveal the presence of specific functional groups within the Fe-S-N-Zeolite catalysts. For example, different peaks in the IR spectrum correspond to characteristic vibrational modes of bonds, such as C-H, N-H, S-H, and metal-oxygen bonds. This helps identify the types of species and chemical groups present on the catalyst surface. IR spectroscopy can detect metal-oxygen bonding, which is particularly relevant for Fe-S-N-Zeolite catalysts. Peaks associated with metal-oxygen vibrations can indicate the coordination of iron (Fe) with the zeolite framework or other species. Also, it can reveal the presence of sulphur species, including sulphur-containing functional groups like thiol (-SH) and sulphide (-S-) bonds. Changes in sulphur bonding patterns can

provide insights into the interaction of sulphur with iron and the zeolite framework. Furthermore, it can identify nitrogen-containing functional groups, such as amine ($-\text{NH}_2$) and nitrile ($-\text{C}\equiv\text{N}$). This can help determine the incorporation of nitrogen into the catalyst and its potential role in catalytic activity. In addition, IR spectra can provide information about the zeolite framework itself, including vibrations related to Si-O-Si and Si-O-Al bonds. Changes in these vibrations could indicate alterations in the zeolite structure due to the incorporation of Fe, S, and N species. Overall, this characterization technique offers a wealth of information about the surface chemistry, active sites, and interactions within Fe-S-N-Zeolite catalysts. By analysing the IR spectra, it can gain a deeper understanding of the catalyst's composition and behaviour, contributing to the optimization of catalytic processes and catalyst design.

- III. **Reusability tests.** Performing a reusability test for a catalyst involves subjecting it to multiple reaction cycles and evaluating its performance over time. After the first cycle, regenerating the catalyst is necessary. Regeneration methods might include washing, calcination, or other treatments to restore the catalyst's activity. Reusability tests provide insight into the catalyst's stability and durability over multiple reaction cycles. This helps identify catalyst deactivation mechanisms and predict its lifetime under practical conditions. For economic considerations determining if a catalyst can be reused without significant activity loss is crucial for cost-effective processes. Reusing catalysts reduces the need for frequent replacement, saving both material and operational costs. It helps develop effective catalyst regeneration strategies. In addition, monitoring changes in catalyst behaviour over time can provide insights into reaction mechanisms, intermediate formation, and kinetic profiles. For example; Fe-Ag-ZSM-5, which demonstrated extrema catalytic activity, there is a possibility of silver (Ag) leaching from the catalyst into the reaction medium over multiple cycles. This could lead to a decrease in catalytic activity and changes in selectivity. Monitoring Ag leaching and its impact on catalytic performance is essential. The activity of Fe-Ag-ZSM-5 may evolve over time due to changes in the distribution of active sites, the formation of intermediates, and potential catalyst deactivation. This could influence the types and amounts of products formed.
- IV. **Alternative metal centres.** Search for other catalysts that could be used in the CWPO process for phenolic compound oxidation to achieve both high activity for phenolic

compounds oxidation and avoiding high metal leaching, in other words, high stability. For example, applying different metals rather than Fe with Ag-ZSM-5 to find an optimal catalyst for the oxidation of phenolic compounds by the WCPO reaction. Oxides of the first transition metal series provide a good possibility that could be investigated (V, Cr, Mn, Co, Ni, Cu and Zn). The choice of metal can significantly influence catalytic activity, selectivity, and stability. Different metals have varying catalytic properties, and their choice can directly impact the overall activity of the catalyst. Some metals may exhibit higher catalytic activity than others due to their ability to facilitate specific reaction pathways or to activate peroxide molecules effectively. The mechanism of the CWPO process can be influenced by the type of metal used. Different metals may promote distinct reaction pathways, leading to variations in intermediate species and final products that could be beneficial in the case of 4BrP oxidation, for example, when was poor mineralization with most of the catalysts. In the context of this study, applying different metals to Ag-ZSM-5 for phenolic compound oxidation is a logical step. Conducting comparative studies with various metals, investigating their effects on reaction kinetics, selectivity, and stability, and understanding the mechanistic insights behind their performance can provide valuable insights for designing efficient and sustainable catalytic systems.

- V. Expanding the application of Fe-S-N-ZSM-5 and Fe-Ag-Zeolite-Y catalysts to other phenolic compound pollutants, such as 2-chlorophenol (2CP), 3-chlorophenol (3CP), 2,4,6 tri chlorophenol (2,4,6 CIP), and 3-bromophenol (3BrP), can provide valuable insights into the catalytic performance and mechanisms of these catalysts for a broader range of phenolic compounds. Furthermore, these specific phenolic compounds selected to understand the effect of substituent position and numbers on phenolic compound oxidation by comparing with this study outcomes (4CP and 4BrP oxidation).
- VI. **Scale-up.** Liaising with process chemists or chemical engineers to test our materials under other reaction conditions, for example, by first exploring the kinetics of plug-flow reactors or a continuous stirred tank reactor as it would be expected in a non-laboratory water treatment context. As a consequence, besides changes in reaction parameters, the catalyst's activity, stability and leaching behaviour under diverse conditions would also need to be assessed.

6.3 References:

1. S. Perathoner and G. Centi, *Topics in Catalysis*, 2005, **33**, 207-224.
2. W. W. Anku, M. A. Mamo and P. P. Govender, *Phenolic compounds-natural sources, importance and applications*, 2017, 419-443.
3. J. Zazo, J. Casas, A. Mohedano and J. Rodríguez, *Applied Catalysis B: Environmental*, 2006, **65**, 261-268.
4. K. Fajerwerg and H. Debellefontaine, *Applied Catalysis B: Environmental*, 1996, **10**, L229-L235.
5. A. Rey, M. Faraldos, J. Casas, J. Zazo, A. Bahamonde and J. Rodríguez, *Applied Catalysis B: Environmental*, 2009, **86**, 69-77.
6. A. Quintanilla, A. Fraile, J. Casas and J. Rodríguez, *Journal of Hazardous Materials*, 2007, **146**, 582-588.
7. J. Carriazo, E. Guelou, J. Barrault, J. Tatibouët and S. Moreno, *Applied Clay Science*, 2003, **22**, 303-308.
8. M. Timofeeva, S. T. Khankhasaeva, E. Talsi, V. Panchenko, A. Golovin, E. T. Dashinamzhilova and S. Tsybulya, *Applied Catalysis B: Environmental*, 2009, **90**, 618-627.
9. S. R. Pouran, A. A. A. Raman and W. M. A. W. Daud, *Journal of Cleaner Production*, 2014, **64**, 24-35.
10. K.-H. Kim, J.-R. Kim and S.-K. Ihm, *Journal of hazardous materials*, 2009, **167**, 1158-1162.
11. G. Ovejero, J. L. Sotelo, F. Martínez, J. A. Melero and L. Gordo, *Industrial & engineering chemistry research*, 2001, **40**, 3921-3928.
12. S. S. Sable, A. Georgi, S. Contreras and F. Medina, *Water-Energy Nexus*, 2021, **4**, 95-102.
13. E. Auer, A. Freund, J. Pietsch and T. Tacke, *Applied Catalysis A: General*, 1998, **173**, 259-271.
14. C. N. Satterfield, M. Modell and J. A. Wilkens, *Industrial & Engineering Chemistry Process Design and Development*, 1980, **19**, 154-160.
15. R. Carvalho, F. Lemos, M. Lemos, J. Cabral and F. R. Ribeiro, *Journal of Molecular Catalysis A: Chemical*, 2006, **248**, 48-52.
16. G. Calleja, J. A. Melero, F. Martinez and R. Molina, *Water Research*, 2005, **39**, 1741-1750.

17. V. Tukač and J. Hanika, *Collection of Czechoslovak chemical communications*, 1996, **61**, 1010-1017.
18. F. Stüber, J. Font, A. Fortuny, C. Bengoa, A. Eftaxias and A. Fabregat, *Topics in Catalysis*, 2005, **33**, 3-50.
19. M. Santiago, F. Stüber, A. Fortuny, A. Fabregat and J. Font, *Carbon*, 2005, **43**, 2134-2145.
20. A. Quintanilla, J. Casas and J. Rodriguez, *Applied Catalysis B: Environmental*, 2010, **93**, 339-345.
21. F. Rodriguez-Reinoso, *Carbon*, 1998, **36**, 159-175.
22. W. Reimerink, *ChemInform*, 1999, **30**, 24.
23. A. E. Aksoylu, M. M. A. Freitas and J. L. Figueiredo, *Applied Catalysis A: General*, 2000, **192**, 29-42.